Genetic Analysis of RadB, a Paralogue of the Archaeal Rad51/RecA Homologue, RadA

Samuel Thomas Haldenby, BSc.

Thesis submitted to the University of Nottingham
for the degree of Doctor of Philosophy,
September 2007

Table of Contents

Abstract

The integrity of all genomes is under constant threat, with DNA double strand breaks being particularly dangerous. Double strand breaks can be repaired by homologous recombination, a process catalysed by recombinase proteins of the RecA family.

The archaeal recombinase, RadA, is homologous to eukaryotic and bacterial Rad51/RecA. Euryarchaea encode an additional Rad51/RecA homologue, RadB. RadB shares homology with the core domain of RadA and has been shown to bind both single and double stranded DNA, binds ATP and possesses a very weak ATPase activity. However, RadB does not catalyse strand exchange. RadB has been shown to interact with RadA, a Holliday junction resolvase (Hjc) and a DNA polymerase (PolD), suggesting a role in recombination.

In this study, *radB* was deleted from the halophilic archaeon, *Haloferax volcanii.* Δ*radB* strains were slow growing, sensitive to mitomycin C and UV irradiation, and deficient for both crossover and non-crossover recombination. Deletion of *radA* results in similar phenotypic characteristics, and complete abrogation of recombination. Strains deleted for both *radA* and *radB* are equally defective as Δ*radA* strains, demonstrating that RadA is epistatic to RadB.

A suppressor of Δ*radB* was isolated and identified as a mutation in the polymerisation domain of RadA (RadA-A196V). *radA-A196V* suppresses the slow growth, crossover and non-crossover recombination defects associated with Δ*radB*, as well as UV and mitomycin C sensitivity phenotypes. On account of the nature of this suppressor, the observed interaction between RadA and RadB, and the epistatic relationship between RadA and RadB, a role for RadB as a recombination mediator protein is proposed.

Finally, strains were deleted for *hjc*. Δ*hjc* strains exhibit no growth, crossover and non-crossover recombination defects and no UV and mitomycin C sensitivity. This suggests that another, as yet unidentified, Holliday junction resolvase is encoded by *Haloferax volcanii*.

Acknowledgements

I would like to thank Thorsten Allers for giving me the opportunity to carry out this research under his supervision. I would especially like to thank him for his patience, wisdom and support. I consider myself very fortunate to have had the opportunity to work with him.

Thankyou to Ed, Belinda, Lee, Michelle, Amy, Andy, Colin and to the other members of the lab for their advice, assistance, and for making my time studying a pleasure. I would especially like to thank Stéphane, for his useful discussions, suggestions and his friendship. I would also like to express my thanks to Amanda Brindley, David Walsh, Geoff Briggs and Martin Warren for their collaboration.

I would like to thank my family for their support and encouragement, and my friends for their understanding and for reminding me that life exists outside work.

Finally, I would especially like to thank Helen for her love, encouragement and patience. I can not imagine I would have been able to complete this work without her support and I look forward to spending many happy years with her.

Abbreviations

5-FOA	5-fluoroorotic Acid
Amp	ampicillin
ATP	adenosine 5' –triphosphate
BER	base excision repair
BIR	break induced replication
bp	base pair
BSA	bovine serum albumin
DMSO	dimethyl sulfoxide
DNA	deoxyribose nucleic acid
DSB	double strand break
DSBR	double strand break repair
dsDNA	double-stranded DNA
dNTP	deoxynucleotide
EDTA	ethylenediaminetetraacetic acid
HJ	Holliday junction
HR	homologous recombination
kb	kilobase pair
Leu	leucine
mb	megabase pair
NER	nucleotide excision repair
NHEJ	non-homologous end joining
RNA	ribonucleic acid
SDS	sodium dodecyl sulphate
SDSA	synthesis dependent strand annealing
SSA	single strand annealing
SSPE	saline sodium phosphate EDTA
ssDNA	single-stranded deoxyribose nucleic acid
Tet	tetracycline
Thy	thymidine
Trp	tryptophan
Ura	uracil
UV	ultraviolet light
v/v	volume per volume
w/v	weight per volume

Chapter 1: Introduction

1.1 Archaea – The Third Domain

Prior to DNA sequencing, organisms were classified by fossil records and/or morphology. Though this system appeared to be accurate for the classification of multicellular organisms where evolutionary traits were visually traceable, the method was not easily used for microorganisms. Initially, life was categorised into two kingdoms, plants and animals. In 1938, Chatton proposed a method of segregating life based on the cellular organisation of organisms (Woese et al., 1990). Chatton's classifications led to life being divided into two domains, eukaryotes and prokaryotes. This division was based on the presence of organelles. Eukaryotes were classified as organisms with membrane enclosed nuclei, cell organelles and cell cytoskeletons. Prokaryotes were classified based on the lack of these features. Subsequent revisions led to a total of five kingdoms of life: Animalia, Plantae, Fungi, Protista and Monera (Whittaker, 1959; Whittaker and Margulis, 1978) (Figure 1.1).

These classifications of life into 5 kingdoms and prokaryotes/eukaryotes were challenged at the advent of DNA sequencing techniques. By analysing the structure and sequence of 16S rRNA, a ubiquitous ribosomal subunit, it was elucidated that not all bacteria were as closely related, as originally suggested. Based on 16S rRNA sequence, a sub-set of bacteria consisting primarily of methanogens was shown to be as diverged from traditional bacteria as bacteria are from eukaryotes (Woese and Fox, 1977). This distinction led Woese and Fox to propose a three-kingdom phylogeny (urkingdom) categorisation of life: eubacteria, eukaryotes and archaebacteria. This phylogeny was supported by several additional observations. Archaebacterial lipids differed from those found in eubacteria and eukaryotes, with archaebacterial lipids containing ether links rather than ester links. Additionally, lipids forming the hydrophobic core of the archaeal cell membrane are composed of isoprenoid side-chains that are ether linked to sn-glycerol-phosphate. These unusual lipids are unique to archaea, further dividing bacteria and archaea (Boucher et al., 2004). Furthermore, antibiotics that are effective against eubacteria by inhibiting transcription were not effective against archaebacteria, i.e. streptolydigin and rifampicin (Prangishvilli et al., 1982; Zillig et al., 1979). Additionally, the biological generation of methane, methanogenesis, was not observed in eubacteria and was found to be exclusive to archaeabacteria, which encoded a variety of unique-coenzymes (Noll and Wolfe, 1986). Finally, it was observed that the core components of the archaeal and eukaryotic RNA polymerase (RNA polymerase II) are more closely related to each other than to the bacterial version (Huet et al., 1983). This observation predated sequencing technology.

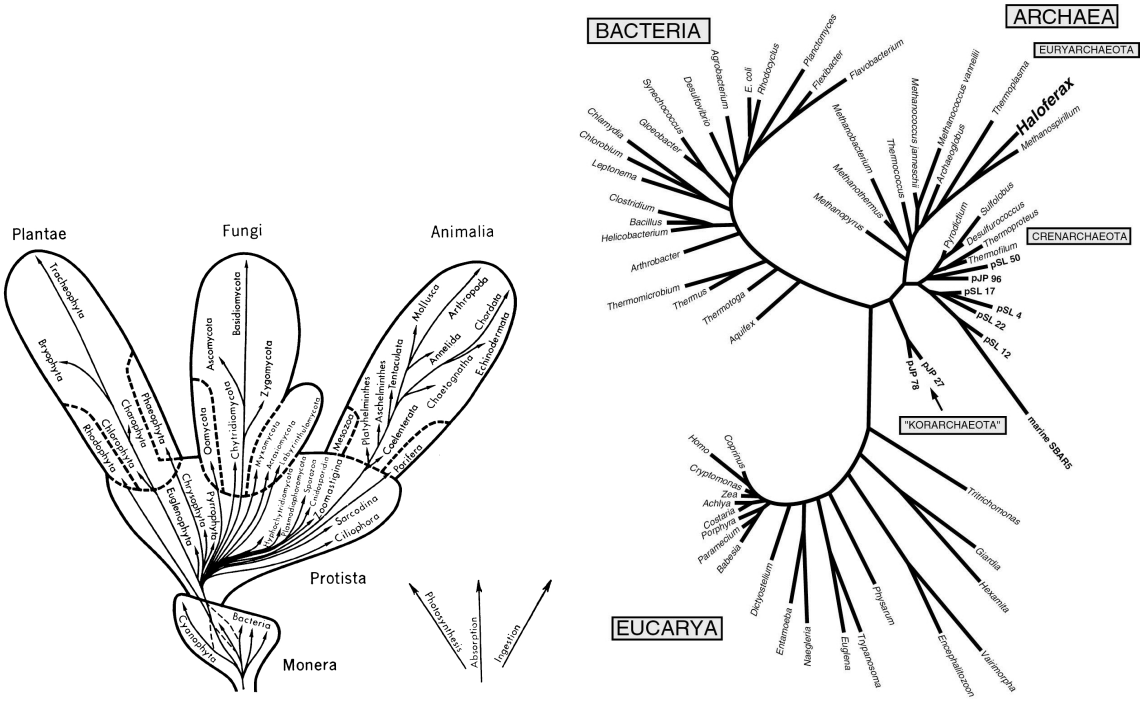

Figure 1.1 Left: Five kingdom tree of life proposed by (Whittaker, 1959), showing suggested evolutionary relationship between Plantae, Fungi, Animalia, Protista and Monera. **Right:** Universal unrooted phylogenetic tree, showing evolutionary relationship between the three domains of life, Eukarya, Bacteria and Archaea (Barns et al, 1996).

16s rRNA sequencing could not directly elucidate the last universal common ancestor (LUCA) (Schmid and Bock, 1981). However this method showed that archaebacteria are more closely related to eubacteria and eukaryotes than they are to each other. Furthermore, the majority of archaebacteria inhabit extreme environments, i.e. extremely high temperatures and low/zero oxygen environments, that are likely to mirror conditions on early Earth. Therefore, archaebacteria were considered more primitive than the other two 'urkingdoms' and closer to the LUCA (discussed in Woese, 1987).

As more sequence data became available, more differences between eubacteria and archaebacteria became apparent. At the same time, similarities between archaebacteria and eukaryotes were elucidated. Transcription was seen to be more similar to the eukaryotic system than the eubacterial system. Archaebacterial RNA polymerase subunits were closely related to eukaryotic RNA polymerase II and III (Puhler et al., 1989). Furthermore, archaebacterial RNA polymerases were significantly more diverged and complex than the eubacterial polymerases (Schnabel et al., 1983). Introns, which were only previously seen in eukaryotes and not bacteria, were discovered in genes encoding tRNA in the archaebacterium *Sulfolobus*

solfataricus (Kaine et al., 1983). Also, where no histone-like proteins are observed in eubacteria, they were isolated from the archaebacterial species *Thermoplasma acidophilum* (DeLange et al., 1981).

In 1990, due to the divergence of conserved protein sequences, Woese *et al* proposed that eubacteria should be separated from the other two kingdoms, eukaryotes and archaebacteria. Also, Woese *et al* proposed that the urkingdoms be renamed as domains. Thus, the present day view of life is separated into three domains: Bacteria, Eukarya and Archaea. Further to this division, analysis of 16s rRNA uncovered two distinct clades of archaea (Woese and Olsen, 1986). These groups were named Euryarchaeota and Crenarchaeota (Woese et al., 1990). This tripartite scheme of classifying life was met with opposition (Woese et al., 1990). Arguments were put forward that classifying the phylogeny of organisms based on the sequence differences of a single molecule was flawed and that the traditional differences in cellular organisation provided a more accurate method of classification. Thus, sceptics held to the traditional prokaryotic/eukaryotic division of organisms with archaea being a subdivision of the prokaryota. Additionally, this notion was supported by phylogenetic data showing that archaea showed similarities to Gram-positive bacteria (Golub et al., 1998). Although the tripartite classification of organisms is more accepted today, some scepticism remains, due to conflicting data depending on the proteins used to construct the phylogenetic tree (Golub et al., 1998). Thus, a variety of models have been proposed in an attempt to elucidate the true relationship between the three domains of life. Three major proposals are outlined here.

1.1.1 The Eocyte Tree

Analysis of an 11 amino acid insertion of EF-1β genes and independent analysis of rRNA sequences led to the proposal of the eocyte tree (Lake, 1988). The crenarchaea were described as direct ancestors of eukaryotes, i.e. eocytes, and the euryarchaea were separated into another clade further down the branch, more closely related to the bacterial clade (Figure 1.2) (Lake, 1988). This proposal has not gained much support as analysis of other protein sequences has shown that euryarchaea and crenarchaea are more closely related than either are to bacteria (Brown and Doolittle, 1997).

1.1.2 The Eukaryotic Chimera Model

It has been suggested that eukaryotic nuclear genomes were formed by the fusion of at least two different and distinct ‘prokaryotic’ genomes. This is by virtue of eukaryotic genomes being a myriad of bacterial and archaeal genes, with other genes being exclusive to eukaryotes. Thus, the fussion of an archaeon and bacterium, by engulfment of one into the other, could explain this. Subsequent gene loss and gene transfer was proposed to result in the reduction in

the endosymbiont chromosome (Doolittle, 1998), leading to the current eukaryotic genome. As archaeal replication, transcription and translation closely resemble the eukaryotic systems, it was proposed that an early archaeal organism provided the eukaryotic nuclear genome (Figure 1.2). Another suggestion was that the archaeal genome was formed as a fusion of bacterial and eukaryotic genes (Koonin et al, 1997).

1.1.3 The Eukaryotic Ancestor Model

This model predicted that the universal tree of life should be rooted with the eukaryotic branch and that eukarya, bacteria and archaea resulted from the simplification of a genome from a eukaryotic-like ancestor (Forterre and Philippe, 1999). Thus, the LUCA was a complex organism that underwent reductive evolution.

1.1.4 The Viral Ancestor Model

It has been proposed that viral species played a key role in the evolution of the information processing machinery in the three domains of life (Forterre, 2006). Forterre suggests that the LUCA was a group of RNA-based cells and that DNA and its processing machinery evolved in viruses. Three distinct, isolated transformations of RNA cells by viruses are proposed to have generated the ancestry for archaea, eukaryotes and bacteria (Figure 1.2).

1.1.5 Horizontal Gene Transfer (HGT) Model

In the defence of the original rRNA phylogeny proposed to define the three domains of life, it has been proposed that inconsistencies in the analysis of individual proteins is due to horizontal, or lateral, gene transfer. It was proposed that the LUCA was a collection of primitive but diverse cells, called progenotes (Woese and Fox, 1977). Progenotes were proposed to have a high mutation rate and mutations that improved the fidelity of information processing were quickly fixed in the population through HGT. As information processing mechanisms became more complex, they also became harder to replace by HGT and the evolution of these processes decreases (Woese, 1998). However, metabolic constraints were not as tight as information processing, Thus, HGT was still prominent for metabolic components. This reinforces the idea that analysis of information processing protein genes provides more accurate phylogenetic data than analysis of metabolic protein genes.

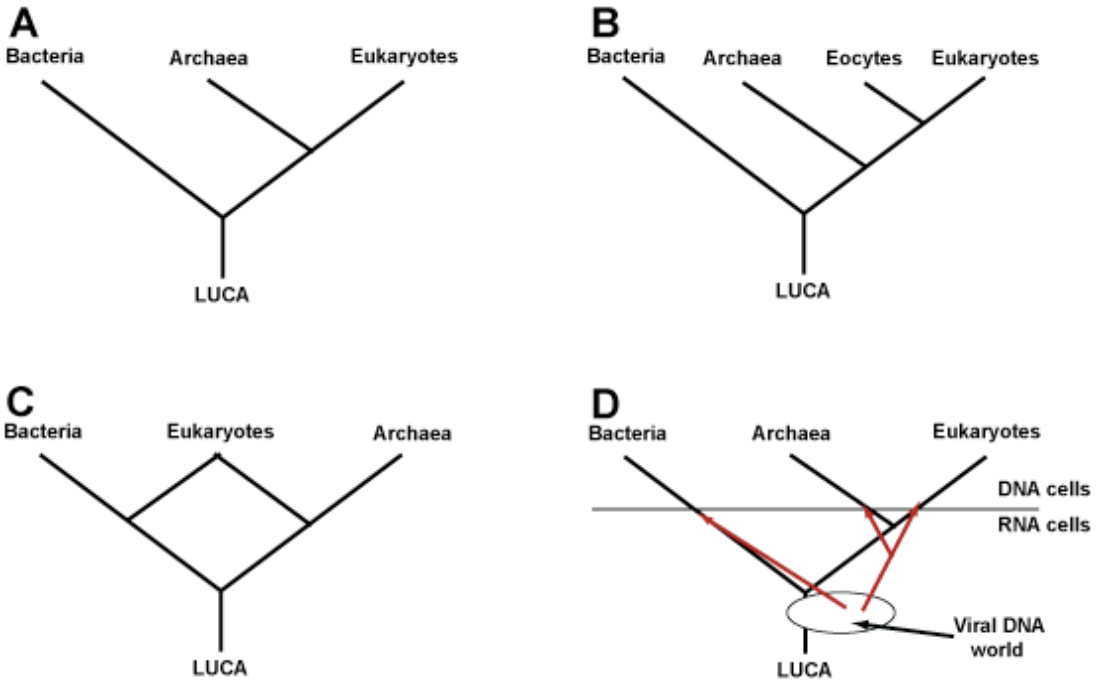

Figure 1.2 Models of early evolution. **A** – Classical rooting of the universal tree based on 16S rRNA sequences. The LUCA is a population of diverse progenote cells readily exchanging genetic material by HGT. When information-processing mechanisms were sufficiently complex, HGT slowed and vertical gene transfer predominated for processing mechanisms. **B** – The Eocyte tree. Crenarchaea are eocytes and are more closely related to eukaryotes than euryarchaeotes, which are suggested to have diverged earlier on the archaeal, eukaryotic branch. **C** – Chimeric theory. Eukaryotes are formed from the engulfment of an archaeal species by a bacterial species, followed by merging of genome components. **D** – DNA cells were produced by transformation of RNA cells by viruses, conferring DNA information processing mechanisms. Transformation of eukaryotes and archaea by related viruses reflects the similarity between the information processing mechanisms of these two domains.

While it is unknown which, if any, of the described models are true, several statements can be made with confidence. Firstly, archaea possess information processing mechanisms more closely related to eukaryotes than bacteria (Allers & Mevarech, 2005). Secondly, archaea possess metabolic mechanisms more closely related to bacteria than eukaryotes. Finally, both bacteria and archaea are less complex than eukaryotes in terms of cellular morphology. In the following section, a comparison of bacterial, eukaryal and archaeal information processing and metabolism is presented, followed by a discussion of homologous recombination in the three domains of life.

1.1.6 DNA replication and genome organisation

Both bacterial and archaeal genomes are comprised of circular DNA molecules while eukaryotic genomes consist of multiple (or a single) linear chromosomes. The organisation of archaeal genomes is more similar to bacterial genomes than eukaryotic ones, with operons being present in both bacteria and archaea but not eukaryotes. However, the machinery that is used for DNA replication differs significantly from bacterial systems (Bell et al, 2002), instead being more similar to eukaryotic systems, but less complex. Eukaryotic organisms encode six ORC (Origin recognition complex) proteins that bind origins of replication. In many eukaryotes, ORC remains bound throughout the cell cycle, whereas DnaA, the bacterial analogue is released upon commencement of replication. Most archaeal species to date contain at least one gene with similarity to Orc1 (Barry and Bell, 2006). In fact, most archaeal genomes encode from one to nine Orc/Cdc6 genes. In bacteria, the replicative helicase is DnaB, and in eukaryotes, it is MCM (minichromosome maintenance complex). All archaeal species sequenced to date encode a homologue of MCM, again reinforcing the significant similarity between archaea and eukaryotes. Furthermore, eukaryotes and archaea both possess similar single stranded binding proteins (RPA) more closely related to each other than to bacterial SSB.

1.1.7 Chromatin

Eukaryotes encode proteins for an octomeric nucleosome, consisting of two copies of the histones H2A, H2B, H3 and H4. Bacteria do not encode histones, but John Reeve reported that the methanogenic archaeaon *Methanothermus fervidus* contains a homologue of eukaryotic histones showing that euryarchaea, but not crenarchaea, where histones are absent, are more closely related to eukaryotes than bacteria in terms DNA compaction (Bell et al, 2002). Archaeal histones are less complex than the eukaryotic counterparts and lack the N- and C-terminal tails that are sites of post-translational modification, suggesting that archaeal chromatin remodelling does not represent a means of transcriptional regulation (Reeve, 2003). In contrast, crenarchaea encode nucleoid proteins such as Alba, which undergo post-translational modification, modulating gene transcription (Bell and Jackson, 2001).

1.1.8 Transcription and translation

Core components of eukaryal and archaeal DNA-dependent RNA polymerases are more closely related to each other than to the bacterial proteins. Furthermore, archaeal RNA polymerase requires basal factors for promoter recognition including TATA-box binding protein (TBP) and transcription factor B (TFB), analogous to eukaryotes (Bell and Jackson, 2001). However, unlike eukaryotes, archaea contain multiple homologues of TBP and/or TFB that may possess different roles in transcription (Thompson et al, 1999). Furthermore, genome analysis has

revealed that archaea possess homologues of bacterial transcription regulators, suggesting that they might employ a bacterial mode of transcriptional regulation, whereby binding of repressors to operator sites interferes with the initiation of transcription (Aravind and Koonin, 1999). Translation in archaea has not been studied to the same extent as transcription. The core component of rRNA is eukaryotic in nature, as are the levels of complexity (Lake, 1988)

1.1.9 Metabolism and energy conservation

Many archaeal operational genes are likely to be bacterial in origin (Lake, 1988). Others, such as those responsible for methanogenesis are not present in bacteria. A significant number of heterotrophic archaea can metabolise sugars. These archaea possess several enzymes that are significantly different to those found in bacteria and eukaryotes, suggesting independent, convergent evolution (Lake, 1988).

1.2 Homologous recombination

Over the years, the accepted model for the process of homologous recombination has changed a number of times to reflect changes and new discoveries in the field.

1.2.1 The Advent of modern genetics

In 1866, Gregor Mendel observed that how characteristics of pea plants were passed from parent to offspring. An important observation that Mendel made was that parental characteristics were not combined in the offspring but were instead transmitted intact,. Half of the observed hereditary features were transmitted to the offspring from each parent with some features displaying dominance over others. The heritable characteristics that Mendel described were the products of genes and his observations were the first known recorded demonstrating that genes are discrete packages of information that remain discrete in diploid of polyploidy offspring. Mendel's studies illustrated the basis of the laws of segregation, whereby a parental cell with heterozygous alleles (AA x aa) will produce haploid gametes with a 2:2 ratio (A:A:a:a). This became the basis of modern genetics.

1.2.2 Gene Conversion and the first model of homologous recombination

Whilst Mendel's studies held true in part, later studies showed that this 2:2 ratio of alleles in gametes from heterozygous parental cells did not always occur, with rare aberrant 3:1 ratios being observed (A:A:A:a). Many years later in 1930, Hans Winkler, a German botanist, also known for coining the word genome in 1920 (Gregory, 2005) (gene + chromosome = genome), defined this rare occurrence as gene conversion, the transfer of information from one allele to another, effectively converting it. It was not until years later that a model for gene conversion was proposed by Robin Holliday, in 1964 (Holliday, 1964) (Liu and West, 2004). Holliday's

proposal provided the first model for homologous recombination that provided a molecular basis for both gene conversion and crossovers between chromosomes. This first model of recombination suggested that following the replication of a chromosome, single strand nicks were introduced into the DNA at the same locus of two DNA molecules, allowing single strands to anneal to the homologous sequences and ligate to the other molecule. This mechanism would effectively switch the strands between chromosomes and if allelic differences were present at this site, a region of heteroduplex DNA would be generated where mismatched nucleotides are present. Holliday proposed that these mechanisms must exist to repair these DNA mismatches and depending on which strand was used as the template for repair, the resulting allelic ratio could be maintained as the classical 2:2, or changed to a 3:1 ratio as was sometimes observed. (Figure 1.3)

As well as switching a region of DNA between two chromosomes, the two DNA molecules would be physically linked together. This four-way branched DNA structure at the point of crossing over was later termed a Holliday junction. It was proposed that this junction could migrate along the length of DNA, generating larger patches of heteroduplex DNA. The second important feature proposed in Holliday's model was that the Holliday junction would then be cut in one of two different orientations, owing to the symmetrical nature of the structure. Either the single strands complementary to the initial nick could be cleaved to cross over the arms that flank the Holliday junction or alternatively, cleavage of the other pair of strands would result in a non-crossover product (Figure 1.3).

In 1971, it was demonstrated that a Holliday junction structure was physically possible, that all the bases in the two double helices would remain paired and that the four strands participating in the exchange are regarded as equivalent (Sigal and Alberts, 1971). This reinforced the Holliday model of recombination. However, inconsistencies in the model became apparent. Following postmeiotic replication, diploid cells contain eight-spored asci (in *Ascolobus*, *Neurospora* and *Sordoria*) or sectored-spore clones (in *Saccharomyces* and *Schizomsaccharomyces*). Examination of these spores allows the determination of the genetic markers present on each of the single strands during meiosis. This analysis is called tetrad analysis and has been used to disprove the Holliday model of recombination.

1.2.3 Problems with the Holliday Model

As shown, the Holliday model was capable of giving rise to both 2:2 and 3:1 (1:3) ratios of alleles observed in gametes through gene conversion. In tetrad analysis, these would equate to normal 4:4 and 6:2 ratios (Figure 1.4). If a parent cell undergoes no recombination events and enters meiosis to generate a total of four haploid daughters, the allelic ratio will be 2:2. After

mitosis, tetrad analysis would show a ratio of 4:4 (Figure 1.4). This is a standard 4:4 ratio. If however, a recombinogenic event occurred in the original AA:aa parent cell, and no correction of alleles through gene conversion occurred, the observed ratio would be 4:4, but an aberrant 4:4 (ab4:4) (Figure 1.4). In *Saccharomyces cerevisiae,* the ordering of tetrads can be achieved by observing external markers. Therefore, the Holliday model would predict the presence of ab4:4 ratios. However, this pattern was not observed in yeast (Fogel and Mortimer, 1970; Fogel and Mortimer, 1974). This was initially explained to be due to the high fidelity of mismatch repair in yeast, therefore no aberrant 4:4 ratios would be expected. However, if mismatch repair, and therefore gene conversion, was efficient, it would be expected that all alleles would be corrected, generating either 6:2 or 2:6 ratios every time (Figure 1.4). This is not the case, as 5:3 and 3:5 ratios were observed, which are characteristic of the repair of only one allele, with the other remaining unrepaired (Figure 1.4). For this reason, it was thought unlikely that reciprocal exchange of DNA markers occurred, as described in the Holliday model, and that non-reciprocal, asymmetric events must be occurring instead.

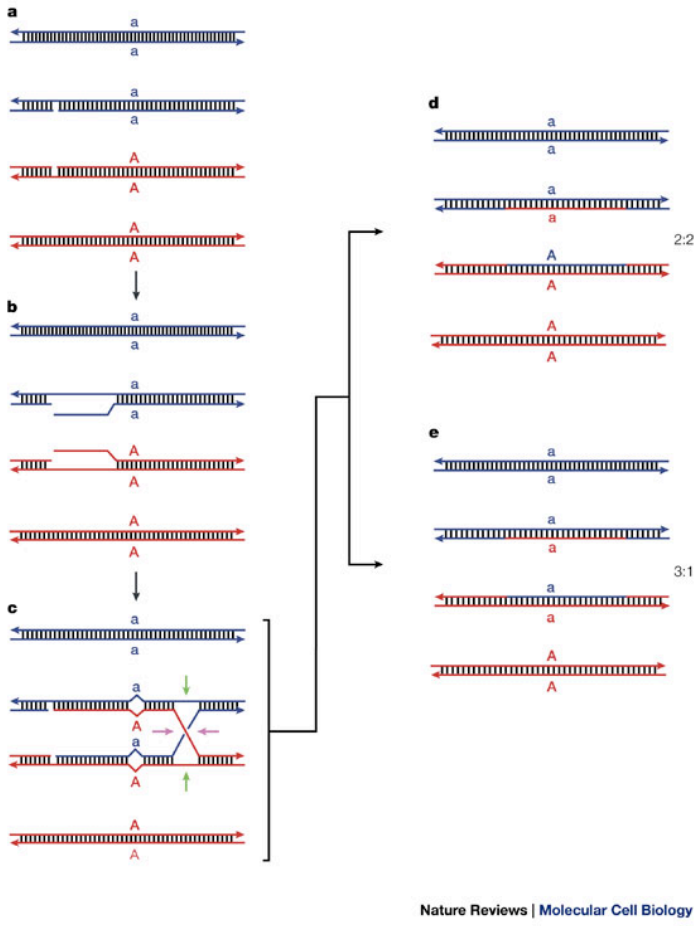

Figure 1.3 The Holliday model, proposed in 1964. Figure from (Liu and West, 2004) **(a)** Following DNA replication, nicks are introduced into the same site of homologous chromosomes. **(b)** Single stranded DNA from each chromosome is exchanged and base pairs with the opposing strand on the opposing chromosome. **(c)** If differences in sequence exist between each chromosome at this region, heteroduplex DNA with mismatches results. The structure at the point of the DNA crossover is a Holliday junction and can be resolved in one of two ways, either by cleavage at the purple arrows to generate **(d)**, a non-crossover product or by cleavage at the green arrows to generate **(e)**, a crossover product where the flanking DNA arms are exchanged. Generation of the either product and subsequent mismatch repair can generate either a 2:2 or 3:1 ratio of alleles in haploid gametes

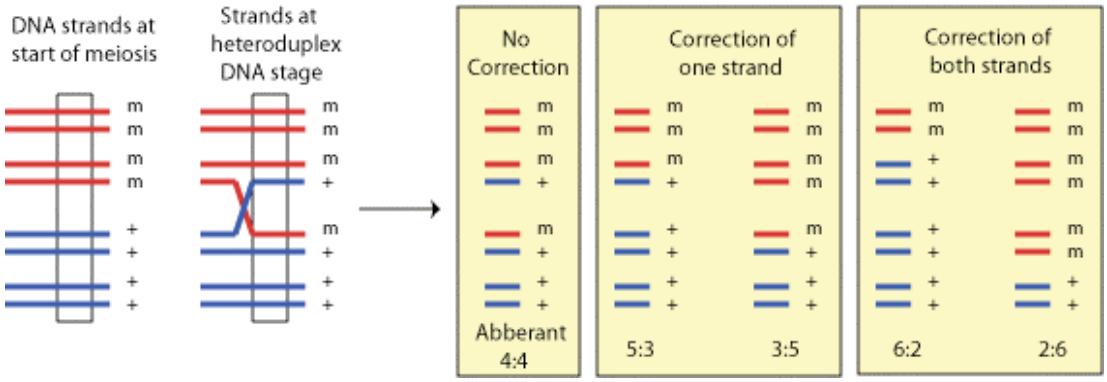

Figure 1.4 Possible outcomes following symmetrical exchange, as predicted by the Holliday model. Following strand exchange and resolution, three main possible outcomes are possible. If no correction of alleles occurs by mismatch repair, an aberrant 4:4 pattern would be observed in gametes (as opposed to a normal 4:4 as is shown in DNA before strand exchange (far left) or if no exchange occurs. Alternatively, correction of one allele can occur, leading to a 5:3, or 3:5 ratio in gametes. If both strands are repaired, 6:2 or 2:6 ratios would be observed. 5:3 ratios but not aberrant 4:4 ratios are observed. As the Holliday model predicts aberrant 4:4s, it was unlikely that the model was correct and that symmetrical exchange did not occur.

1.2.4 The Meselson and Radding Model

In 1974, in an attempt to explain the lack of aberrant 4:4s and the occurrence of 5:3s, Meselson and Radding proposed a modified model that could account for recombination initiated by asymmetric single-strand transfers which could potentially lead to a two-strand (symmetric) exchange thus explaining the observed tetrad analyses (Meselson and Radding, 1974). In this model, many of the features of the original Holliday model remain. Recombination is still suggested to occur from nicked DNA, albeit from a single nick rather than opposing nicks on homologous chromosomes. The generation of a Holliday junction structure is also proposed as an intermediary structure, as is the generation of heteroduplex DNA and subsequent correction to drive gene conversion, except in the Meselson and Radding model, heteroduplex DNA can either result on one chromosome or both.

The model begins with a nick on one of the strands of a DNA molecule. DNA synthesis is primed from this nick, displacing single stranded DNA. This single stranded flap pairs with the complementary sequences on another DNA molecule forming a D-loop structure, which is excised resulting in heteroduplex DNA flanked by nicks. Ligation between the free DNA ends generates a Holliday junction. If branch migration of the junction occurs, this can generate heteroduplex DNA on the second DNA molecule also, following resolution. If the junction is resolved before branch migration, heteroduplex DNA will be present on one DNA molecule

with the other remaining entirely parental. The heteroduplex DNA present on the donor strand could then be corrected by mismatch repair (Figure 1.5). The Meselson and Radding model of recombination was able to answer some of the questions that the original Holliday model was not. It was able to explain the low incidence of aberrant 4:4 tetrads in yeast asci, by suggesting that non-reciprocal exchange between duplexes occurred, i.e. single strand invasion events rather than one strand from each duplex invading the other duplex. Thus, the updated model could also explain the occurrence of 5:3 tetrads in the absence of any aberrant 4:4 tetrads.

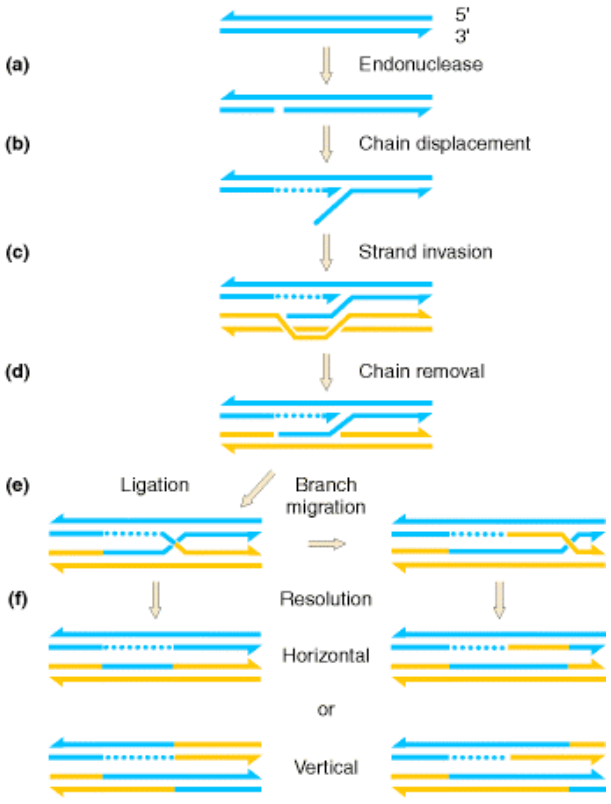

Figure 1.5 The Meselson and Radding model of recombination. Diagram from (Stahl, 1994). **(a)** DNA is nicked on one strand. **(b)** DNA replication displaces one strand. **(c)** The resulting flap displaces its counterpart on a homologous duplex, generating heteroduplex DNA, and a D-loop. **(d)** The D-loop is excised. **(e)** Ligation results in the formation of a Holliday junction. If the junction migrates, heteroduplex DNA can arise on both duplexes. **(f)** Resolution of the junction occurs as in the Holliday model.

1.2.5 Szostak model of recombination: The Double-Strand-Break Repair Model

Nearly ten years after Meselson and Radding proposed their model of recombination that could account for both reciprocal and one-sided strand invasion events, Szostak *et al* proposed another model for recombination. (Szostak et al., 1983). The model differed from both the original Holliday model and Meselson and Radding model, where recombination was proposed to initiate from a nick in a DNA duplex. In the Szostak model, recombination was proposed to initiate from double strand DNA breaks instead, thus it was named the 'double-strand-break repair model for recombination'. Today, Szostak's model is still held as the paradigm with modifications being made to it over the years that will be discussed later in this chapter.

Szostak *et al* had observed that the frequency of recombination between a plasmid and chromosome increased 1000-fold if a double strand break was first introduced into the donor plasmid. Prior to this, it had been suggested that the repair of double strand breaks by homologous recombination was a theoretical possibility, (Resnick, 1976). This was tested further and shown to be true (Neitz and Carbon, 1987; Szostak et al., 1983). Furthermore, the Messelson Radding model predicted that the invaded DNA would be converted, generating heteroduplex DNA. However, cut plasmid by chromosome recombination studies had shown that the cut plasmid was the recipient of gene conversion, and not the donor. These observations led to an update in the recombination model (Figure 1.6).

The proposed double strand break repair (DSBR) model consists of three stages, pre-synapsis, synapsis and post-synapsis. During pre-synapsis, when the recombination/repair process initiates, exonucleases resect the double stranded ends of the DNA break in a 5' to 3' orientation (Figure 1.6). This results in the formation of two 3' single-stranded tails. These ssDNA structures then become coated by a polymer of recombinase (Rad51) in the form of a nucleoprotein filament. During synapsis, a homologous duplex is required and one of the two 3' ends invades this duplex at regions of homology, generating a D-loop structure (Figure 1.6) During post-synapsis, the new D-loop is then utilised to prime DNA synthesis from the invading strand using the intact duplex as a template,. DNA synthesis extends the D-loop structure until it encompasses a region of homology present on the opposing side of the resected double strand break. At this point, the second 3' tail is captured by the D-loop through the annealing of homologous sequences and this permits a second round of DNA synthesis to be primed (Figure 1.6). Following DNA synthesis on both strands, the sequence lost through the processing of the original DSB is restored, and two Holliday junction structures are generated. Like the other models of recombination, Szostak's model explains the occurrence of the two recombination products, crossover and non-crossover, by the orientation in which the Holliday junction intermediates are resolved. If both junctions are cleaved in the same

orientation, the resulting product will be non-crossover and if the junctions are cleaved in opposite orientations, crossover recombination will occur. Physical evidence was subsequently provided for DSB induced recombinational repair and for double Holliday junction intermediates(Schwacha and Kleckner, 1994; Sun et al., 1989)

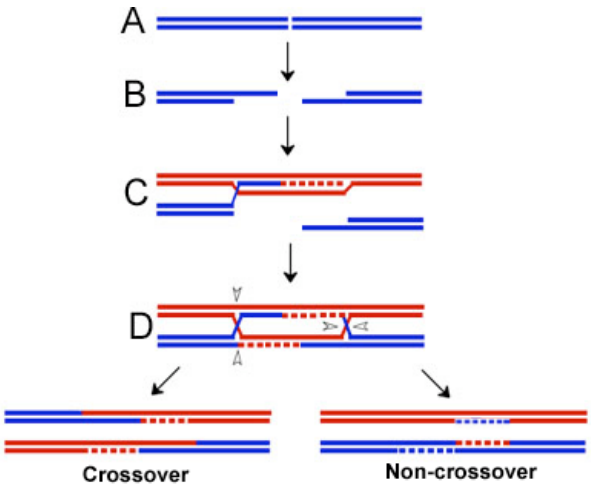

Figure 1.6 Schematic of the DNA double strand break repair model, proposed by Szostak *et al.* (1983). **A** – An unprocessed DNA double strand break. **B** – DNA ends are resected resulting in a 3` single-stranded tail either side of the break. **C** – One of the tails invades a homologous duplex creating a D-loop structure that is utilised to prime DNA synthesis. **D** – The second 3` DNA tail is captured by the D-loop and synthesis is primed on the opposing strand. At this stage, two Holliday junctions are present. These can be processed in opposite orientations to yield a crossover product or in the same orientation to yield a non-crossover product, shown bottom left and bottom right respectively.

1.2.6 Problems with the DSBR model: Ratio of crossover and non-crossover products

The resolution of Holliday junction intermediates to generate either non-crossover or crossover products would be expected to give a ratio of 1:1 for each product, assuming that the orientation of junction resolution is equivalent. While some studies demonstrated this ratio, others did not and showed a strong bias towards non-crossover products, especially in mitotic cells (Klein, 1984; Orr-Weaver and Szostak, 1983; Plessis and Dujon, 1993). Various theories were proposed in an attempt to explain the deviation from the 1:1 ratio of crossover and non-crossover products anticipated by Szostak's DSBR model.

One theory suggested that there was a preference for the orientation of Holliday junction resolution. This would result in more junctions being resolved in one particular orientation. If both recombination junction intermediates are cleaved in the same orientation the resulting

product is non-crossover, thus this preference would ultimately favour non-crossover products. Evidence for this theory came from studies demonstrating a preference of some Holliday junction resolving enzymes for a particular orientation of resolution, e.g., T4 endonuclease VII was shown to cleave the crossover strands and RuvC was shown to preferentially cleave the strands opposing the crossover strands of a Holliday junction (Bennett and West, 1995; Mueller et al., 1988). However, these enzymes are not eukaryotic and therefore do not explain the observed cleavage patterns.

Also, the DSBR model makes predictions that markers close to, and flanking a DSB should both be in regions of heteroduplex DNA, therefore it should be observed that post meiotic segregation of both flanking markers occurs frequently in non-crossover events. This is not observed, however, suggesting that non-crossover events are not symmetrically disposed either side of the double strand break (Gilbertson and Stahl, 1996).

1.2.7 Synthesis Dependent Strand Annealing

The second theory to explain the bias of non-crossover products is that Holliday junctions are not required for the generation of non-crossover products. This model of DSB repair is called Synthesis-Dependent Strand Annealing (SDSA) and assumes that once strand invasion has occurred, The 3' ends of the invading strand is extended by DNA polymerase activity while the donor DNA remains unchanged (Paques and Haber, 1999). Following synthesis, the newly synthesised strand is displaced from the template strand and returned to the broken molecule. The newly synthesised strands can then anneal to each other, and after DNA synthesis, the broken molecule is restored to a duplex state. The template duplex remains unchanged making the process a conservative, rather than semi-conservative one (Figure 1.7). Furthermore, this type of recombination is an asymmetric event since heteroduplex DNA is only generated on one side of the DSB, consistent with data of (Gilbertson and Stahl, 1996).

Evidence that Holliday junctions are not required for the formation of non-crossover products was provided by the observation that in *Saccharomyces cerevisiae*, non-crossover associated heteroduplex DNA arose before crossover associated heteroduplex DNA during meiosis (Allers and Lichten, 2001). Also, mutations such as in *ndt80* lead to defects exclusively in non-crossover recombination, therefore the two pathways are genetically separable. These findings suggested two different pathways, one involving generation of Holliday junction intermediates and leading to crossover recombination events, and the other leads to non-crossover recombination events without Holliday junctions. Thus the Szostak model of DSBR was modified to accommodate this suggestion (Figure 1.7).

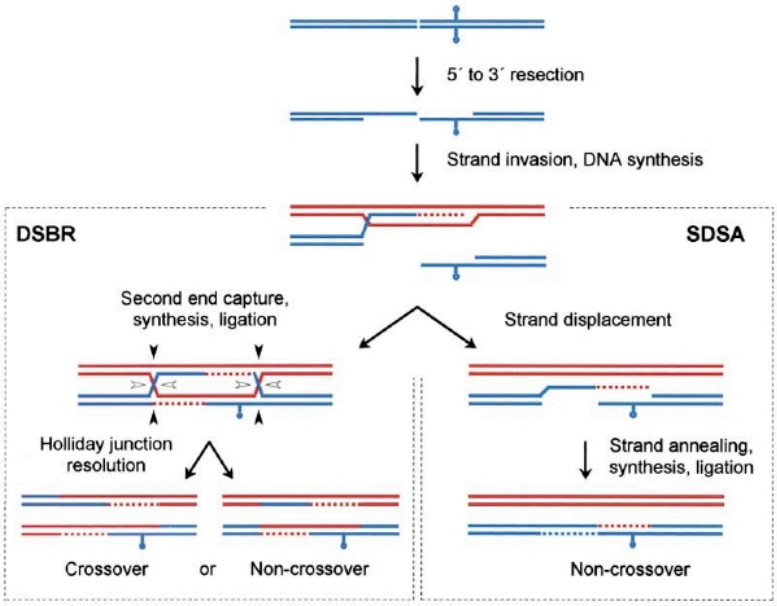

Figure 1.7 Unified model for repair of double-strand DNA breaks by either crossover recombination or non-crossover recombination, from (Allers and Lichten, 2001). As in the model of Szostak *et al*, DNA ends are resected to generate 3' ssDNA tails. One tail invades a homologous duplex and DNA synthesis is primed from the D-loop. At this point, recombination is committed to one of two pathways. **(Left)** Canonical DSBR model. The second strand is captured, DNA synthesis is primed and ligation generates a double Holliday junction intermediate. Resolution of Holliday junctions in the same or opposite orientations generates non-crossover of crossover products. **(Right)** Synthesis-dependent strand annealing. The newly synthesised tail is displaced from the D-loop and anneals to ssDNA at the opposite side of the double strand break. DNA synthesis and ligation restores the duplex.

1.2.8 Other homologous recombination pathways

The model described above shows our current understanding of the major pathways of homologous recombination. However, minor pathways also exist that will be outlined here.

Extended Synthesis-Dependent Strand Annealing

The ability of the ionising radiation-resistant bacterium *Deinococcus radiodurans* to reassemble a severely fragmented genome has been attributed to a process related to SDSA, known as extended synthesis-dependent strand annealing (ESDSA) (Zahradka et al., 2006). DNA fragments from more than one chromosomal copy undergo SDSA with each other producing dsDNA fragments with long ssDNA tails. The ssDNA tails of each fragment anneal

contiguously and gaps are filled in by DNA synthesis, followed and completed by crossovers between fragments, resulting in an intact circular chromosome.

Single Strand Annealing

Single strand annealing (SSA) is a minor repair pathway employed to repair double strand breaks (Ivanov et al., 1996; Paques and Haber, 1999). Like Non-homologous end joining (NHEJ), SSA is not a high fidelity repair pathway. For the SSA pathway of DSBR to function, repeated sequences must be present either side of the break. The dsDNA ends of the DSB are then processed in the same manner as in other forms of HR to produce 3' ssDNA tails, and if these tails extend into the repeated sequences present either side of the DSB so that the two tails can anneal at the homologous sequences. This process can generate ssDNA flaps that are then degraded by flap specific endonucleases. ssDNA gaps are filled in by a DNA polymerase to restore the double stranded DNA structure and complete the repair of the DSB. (Figure 1.8) The major disadvantage of this pathway of repair is that the sequence that is degraded between the two repeated sequences either side of the DSB is lost. If this sequence lies within a gene or other important region of DNA, the repair process itself can be highly mutagenic.

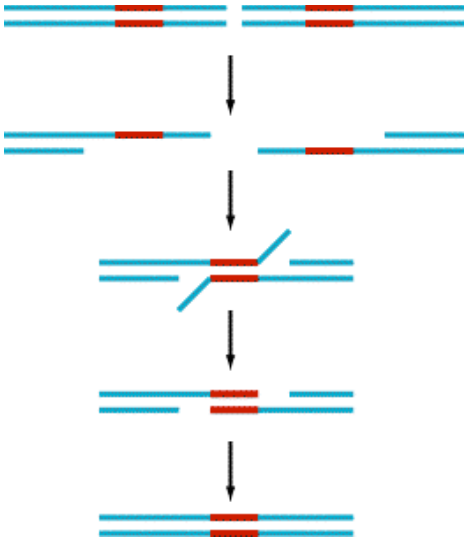

Figure 1.8 Schematic of the SSA process of DSBR. Red boxes represent repeat sequences either side of the DSB. DNA ends at the break are resected to generate 3` ssDNA tails, containing the repeat sequence. The repeat sequences present on each tail anneal and the flap of non-annealed ssDNA 3` of the repeat is degraded. ssDNA gaps are filled in by DNA polymerase activity to restore the dsDNA and repair the break. All sequence information between the homologous repeats and the initial DSB is lost.

Break Induced Replication

Break induced replication (BIR) is a further example of a HR pathway used in the repair of DSBs and is important for the restoration of collapsed replication forks. BIR requires a homologous duplex as a template for repair but, unlike some other methods of DSB repair, BIR proceeds when homology is present on the template duplex for only one side of the DSB. Alternatively, if template sequence is present for either side of the DSB but one 3` ssDNA tail invades the intact duplex faster than the other, perhaps due to a recombination hotspot, BIR

may proceed in place of either classic HR driven DSBR or SDSA. For these reasons, BIR is termed a one-ended recombination event.

As with other HR pathways, both DNA ends at the site of the DSB are resected to produce 3` ssDNA tails and one of these tails, invades the homologous duplex forming a D-loop. DNA synthesis is then primed from the D-loop but unlike other pathways of HR that require a template, replication continues until the end of the chromosome is reached (Formosa and Alberts, 1986), unless another replication fork is encountered (Kraus et al., 2001) (Figure 1.9). The result of such an extended round of DNA synthesis during BIR is a duplication of one arm of the chromosome (translocation), or in the case of organisms with a circular chromosome, rolling circle replication occurs.

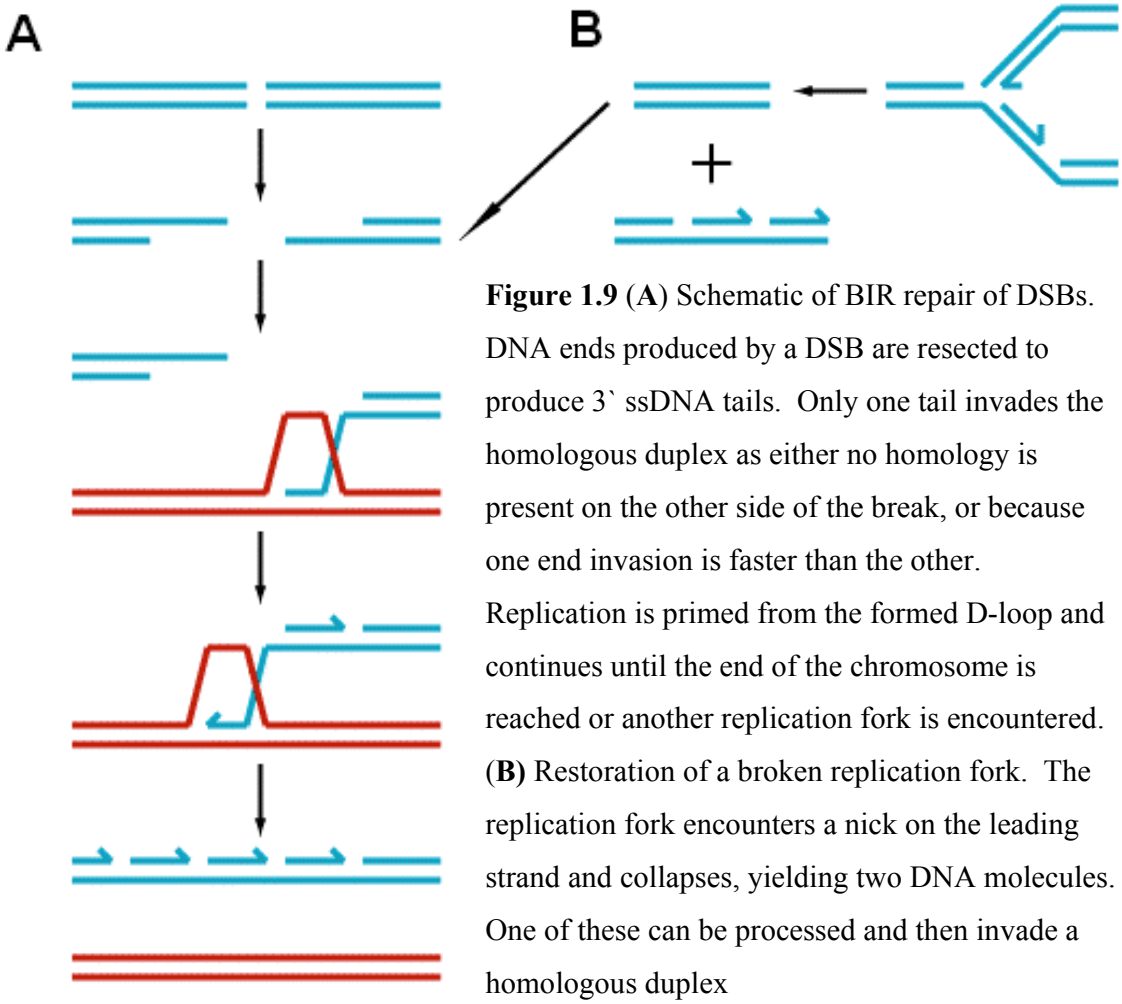

Figure 1.9 (**A**) Schematic of BIR repair of DSBs. DNA ends produced by a DSB are resected to produce 3` ssDNA tails. Only one tail invades the homologous duplex as either no homology is present on the other side of the break, or because one end invasion is faster than the other. Replication is primed from the formed D-loop and continues until the end of the chromosome is reached or another replication fork is encountered. (**B**) Restoration of a broken replication fork. The replication fork encounters a nick on the leading strand and collapses, yielding two DNA molecules. One of these can be processed and then invade a homologous duplex

1.3 Enzymology of homologous recombination

Although the mechanics and general processes involved in HR DSBR are comparable between organisms from all domains of life, the proteins that are involved can differ significantly. Some enzymatic features necessary for HR are conserved throughout all organisms with others being equivalent but not evolutionarily related to one other. The aim of this section is to summarise the main proteins involved in HR DSBR in bacteria, eukaryotes and the archaea.

1.3.1 Homologous recombination in *E.coli*

The proteins involved in homologous recombination in the bacterium *E.coli* have been studied extensively, and the process has become very well characterised. Three pathways are responsible for HR in *E.coli* and are characterised by the proteins required for the process to be performed, namely the RecBCD, RecFOR and RecE pathways.

1.3.2 RecBCD pathway

The RecBCD dependent pathway of homologous recombination is the predominant pathway in wildtype *E.coli* (Kuzminov, 1999), with the RecFOR and RecE pathways being utilised in the absence of RecBCD. In wildtype cells, DNA ends resulting from a double strand break are processed by the multi-functional RecBCD complex. RecBCD is a heterotrimeric helicase with both 5`-3` and 3`-5` activity (Dillingham et al., 2003; Taylor and Smith, 1995). It possesses an affinity for blunt or near-blunt DNA ends (Taylor and Smith, 1985) and acts to separate the double stranded DNA at a DSB. The bipolar nature of the helicase activity of RecBCD can be attributed to the two subunits, RecB and RecD, which provide the 3`-5` and 5`-3` activity respectively (Dillingham et al., 2003; Korangy and Julin, 1993; Taylor and Smith, 2003). RecB also possesses a multifunctional nuclease activity (Sun et al., 2006; Yu et al., 1998). RecC possesses no helicase activity but has a pin structure protruding from its surface that separates the strands of the duplex DNA and drives them to the other two subunits of the RecBCD complex (Singleton et al., 2004).

RecBCD unwinds the DNA duplex ends processively (Figure 1.6-B) and degrades the 3` strand through RecB nuclease activity. In addition to this, RecB occasionally nicks the 5' strand (Dixon and Kowalczykowski, 1993). This occurs as the nuclease domain of RecB is in close proximity to the point at which RecC feeds the 3' strand and this strand is therefore preferentially hydrolysed. The 5' tail is also in relatively close proximity after emerging from RecC (Singleton et al., 2004) and is therefore able to compete with the 3' tail for the nuclease site of RecB, thus resulting in occasional nicking of this strand.

This processive unwinding of the DNA duplex occurs until the RecBCD complex encounters a specific 8 bp *cis*-acting sequence known as a Chi (χ) sequence (5`-GCTGGTGG-3`) (Spies et al., 2005). χ sequences are important to the cell as they allow self recognition. Sequences not containing a χ sequence will be degraded by nuclease attack but molecules with χ present will only be degraded until a χ site is encountered. This not only protects the cell from foreign DNA but is also essential for RecBCD-dependent recombination to proceed correctly.

When a χ site is encountered, the RecBCD complex pauses and the polarity of the nuclease activity switches (Dillingham et al., 2003). The 3` DNA end is retained by RecC, effectively protecting it from the nuclease activity of RecB. The polarity of the nuclease activity switches as RecB has access to the 5` end only (Singleton et al., 2004). As the complex resects the DNA to a 3' tail, it also acts to load RecA onto it. RecA is a protein known as a recombinase and is essential for the majority of HR pathways with the exception of SSA. When it coats ssDNA as a multimer, in the form of a nucleoprotein filament, it initiates synapsis by mediating homologous pairing with the intact DNA duplex. RecA and its homologues from other species are discussed in detail later in this chapter. The nuclease domain of RecB has been implicated in the loading of RecA onto ssDNA through a specific RecA-binding pocket at the C-terminal domain (Spies et al., 2005). The positioning of RecD in the complex usually occludes this pocket but upon encountering a χ site, a conformational change occurs in the enzyme exposing the RecA binding site of RecB (Churchill and Kowalczykowski, 2000; Handa et al., 2005). When RecA has been loaded onto the single stranded tail in the form of a nucleoprotein filament and the search for homology on an intact duplex commences. When this search is completed and sufficient homology has been found, strand exchange between the two DNA molecules proceeds, which forms a D-loop on the intact duplex (Figure 1.6 C). The strand exchange reaction can proceed further in a 5` to 3` direction, on the template strand, to extend the region of heteroduplex DNA at the D-loop (reviewed in Radding, 1991). Once strand exchange has occurred, PriA binds the D-loop and primes DNA synthesis to resynthesise the lost DNA at the double strand break site (Liu et al., 1999; McGlynn et al., 1997) (Figure 1.6 C).

Following second strand capture and DNA synthesis, branch migration of the D-loop structure converts it into a Holliday junction that must then be resolved into two duplexes (Figure 1.6 D). There are two known pathways as to how this reaction proceeds: The RuvABC-dependent pathway and the RecG-dependent pathway.

1.3.3 RuvABC-dependent resolution

The RuvABC complex is required for the processing of recombination intermediates (reviewed in West, 1997). RuvA and RuvB proteins bind specifically to Holliday junctions (HJs),

promoting branch migration. The RuvAB complex is recruited to the HJ by a tetramer of RuvA and this tetramer binds the junction and recruits RuvB. Specifically, two hexameric rings of RuvB are recruited to opposite arms of the junction structure (Parsons et al., 1995). RuvB possesses a helicase activity that, in conjunction with the holding of the junction by RuvA, drives ATP dependent branch migration of the junction. This activity is ATP-dependent.

The enzyme responsible for the cleavage of the HJ structure in this pathway is RuvC and its activity is linked to the RuvAB helicase complex. The three proteins together are known as a resolvasome and as RuvAB-driven branch migration proceeds, RuvC scans for the consensus sequence 5`-$^{A}/_{T}$TT^$^{G}/_{C}$-3` and, when encountered, cleaves the opposing strands of the junction.

1.3.4 RecG-dependent resolution

The alternative HJ resolution pathway to the RuvABC-dependent pathway is the RecG-dependent pathway (reviewed in Briggs et al., 2004). Like the RuvAB complex, RecG is also structure specific for HJs and is a DNA helicase that is able to catalyse the branch migration of them and other recombination intermediates. It does not share homology with any of the RuvABC complex and instead is partially homologous to the translocase protein Mfd. RecG possesses no HJ resolution activity and does not interact with the resolvase RuvC. Instead, RecG requires a second HJ resolvase, RusA (reviewed in Sharples, 2001). In the absence of functional RecBCD, cells are hypersensitive to UV light and ionising radiation as well as deficient in transductional and conjugational recombination, stressing the importance of the protein complex for efficient recombination. However, other conditional recombination pathways are available to the organism under these circumstances.

1.3.5 RecFOR-dependent recombination

In the absence of the RecBCD pathway of recombination, DSBs can be repaired by the alternative RecFOR pathway with proteins RecF, RecO and RecR (reviewed in Cox, 2007). For this pathway of recombination to become available to the cell, other genes must first be inactivated to suppress the absence of RecBCD. RecBCD binds to DNA ends and protects them from aberrant nuclease degradation and subsequent loss of the recombination substrate. In its absence, the DNA ends produced by a DSB must be protected and allowed to persist so that processing in preparation for synapsis can occur. In order to achieve this, the gene *sbcB* must be inactivated. *sbcB* encodes Exonuclease I, a protein capable of degrading DNA ends (Kushner et al., 1972; Kushner et al., 1971). In addition, either *sbcC* or *sbcD* must be inactivated. These genes encode the heterodimeric nuclease SbcCD that is also capable of degrading DNA ends and causing the loss of the recombination substrate (Lloyd and Low, 1996). Inactivation of either gene is sufficient to inactivate the dimeric protein product (Lloyd

and Buckman, 1985). In the absence of functional Exonuclease I and SbcCD nucleases, DNA ends are able to persist *in vivo* without the need for RecBCD protection, hence the nomenclature of the genes (**S**uppressor of Rec**BC**). ssDNA ends are necessary for recombinational repair at a DSB. In the RecFOR pathway, the dsDNA ends resulting from a DSB are processed to ssDNA 3` tails by the helicase activity of RecQ in conjunction with the 5`-3` nuclease activity of RecJ (reviewed in Kowalczykowski, 2000). In the absence of RecBCD, ssDNA substrates become coated with the **s**ingle-**s**trand **b**inding protein, SSB. SSB prevents RecA binding to ssDNA, therefore in the RecFOR-dependent pathway, the combined activity of the three proteins acts to displace SSB and load the RecA recombinase (Morimatsu and Kowalczykowski, 2003). RecR interacts with either RecO or RecF, forming either a RecFR or RecOR complex (Honda et al., 2006). The RecOR complex acts to facilitate the loading of RecA onto ssDNA, ensures persistent binding to prevent the dissociation of the recombinase. The RecFR complex prevents the RecA nucleoprotein filament extending into regions of dsDNA, where the filament would be inactive (Webb et al., 1997). Once RecA loading is complete, the homologous recombination process continues as in the wildtype strain.

RecFOR dependent homologous recombination is also active in wildtype *recBCD*$^{+}$ *E.coli* (reviewed in Kowalczykowski, 2000). In the presence of RecBCD and SbcBC, RecFOR act to load RecA specifically onto gapped DNA, i.e. a region of ssDNA flanked by dsDNA. The protein complexes formed by the three proteins are the same as in the case of RecFOR dependent-recombination at a DSB, with RecOR facilitating the loading of RecA and RecFR preventing the extension of the nucleoprotein filament into regions of dsDNA. Initiation of recombination from a ssDNA gap is important in the context of spontaneous DNA damage and in the recovery of stalled replication forks.

1.3.6 RecET-dependent recombination

The RecET pathway of recombination (reviewed in Hall and Kolodner, 1994), like the RecFOR pathway of recombination at DSBs, also requires suppression to compensate for the absence of RecBCD. However, in the case of the *recET* pathway, genes must be activated instead of inactivated. The genes that must be activated for the RecET pathway are *recE* and *recT* themselves. These genes are present on the defective Rac prophage in the chromosome of some *E.coli* strains and mutations in the promoter can enable the transcription of *recE* and *recT*. The *recE* gene product is Exonuclease VIII (RecE) and is thought to substitute for the nuclease activity of RecBCD in DNA end processing. The *recT* gene product, RecT, possesses a renaturation, or strand-annealing, activity similar to that observed in Rad52 in eukaryotes (discussed later in this chapter). Additionally, it shares fundamental homology-recognition properties with RecA, acting analogously to the recombinase (Noirot et al., 2003). This activity

permits strand exchange activity in the absence of the RecBCD-mediated loading of RecA and this pathway is therefore additionally RecA independent.

1.3.7 Homologous recombination in other bacteria

The vast majority of studies of bacterial homologous recombination in bacteria have used *E.coli* as a model organism. While the basic process of HR is virtually identical in most studied bacteria to date, the proteins involved can be analogous rather than homologous. For example, while RecF pathway of recombination is highly conserved in many sequenced bacteria (e.g. *Aquifex aeolicus, Helicobacter pylori, Rickettsia prowazekii, Deinococcus radiodurans*), clear homologues of RecBCD are lacking in many species with the exception with the partially homologous AddAB system being present in at least twelve different bacteria (reviewed in Chedin and Kowalczykowski, 2002).

AddAB-dependent homologous recombination

In many bacteria, no true homologues of RecBCD proteins have been observed. It is proposed that an alternative protein complex carries out a role analogous to RecBCD in other bacteria, AddAB. *B. subtilis* and *L. lactis* are the only two organisms where substantial information exists regarding AddAB and its role in cellular metabolism. AddAB is a nuclease helicase complex, like RecBCD. Inactivation of AddAB results in reduced cell viability and sensitivity to UV irradiation (Chedin and Kowalczykowski, 2002; Halpern et al., 2004; Kooistra et al., 1988). Like RecBCD, AddAB processes DNA ends to generate 3' ssDNA tails. AddA provides the helicase activity of the complex, and both AddA and AddB possess nuclease activity (Yeeles and Dillingham, 2007). When the complex encounters a recombination hotspot sequence, analogous to chi, in *E.coli*, the nuclease activity responsible for cleavage in the 3' to 5' direction is attenuated and the 5' to 3' nuclease activity remains unaffected. This results in the production of single stranded DNA tails (Yeeles and Dillingham, 2007).

Homologous recombination in Deinococcus radiodurans

While many bacteria share the same basic pathways of recombination, *Deinococcus radiodurans* is theorised to possess a novel recombination pathway. *Deinococcus radiodurans* is an extremely ionising radiation-resistant bacterium and its ability to reassemble a severely fragmented genome has been attributed to a process related to SDSA known as extended synthesis-dependent strand annealing (ESDSA) (Zahradka et al., 2006). DNA fragments from more than one chromosomal copy undergo SDSA with each other, with both processed ssDNA ends invading homologous duplexes and being ejected following DNA synthesis. This produce dsDNA fragments with long ssDNA tails. The ssDNA tails of each fragment anneal

contiguously and gaps are filled in by DNA synthesis, followed and completed by crossovers between fragments, resulting in an intact circular chromosome.

1.3.8 Homologous recombination in eukaryotes and archaea

The processes and enzymology of homologous recombination have been studied extensively in simple eukaryotes such as yeast. Many archaeal proteins proposed to be involved in homologous recombination have been characterised biochemically. However, very little genetic information about the function of these proteins and their involvement in recombination, if any, has been elucidated. Therefore, very little is known about the true enzymology and processes of homologous recombination in archaea. Because archaea and eukaryotes share more common mechanisms of information processing than with bacteria, homologous recombination in these two domains will be discussed together.

1.3.9 Processing of DSB ends

In *E.coli,* the ends of DSBs are processed by RecBCD to generate 3' ssDNA tails. The processing of DNA ends in eukaryotes and archaea is less well understood, with the nuclease(s) involved being unknown. A complex containing Rad50 and Mre11, which are homologues of bacterial SbcD and SbcC, has been implicated in the end processing of DSBs (Symington, 2002). Both Rad50 and Mre11 are conserved in archaea. Eukaryotic Mre11 possesses a weak 3' to 5' exonuclease activity that has been demonstrated to facilitate the repair of DSBs and the human Rad50-Mre11-Nbs1 complex exhibits a weak ATP stimulated DNA unwinding activity (Paull & Gellert, 1999). However, the polarity of Mre11 nuclease activity is the opposite to that required in the generation of 3' ssDNA tails. Finally, *rad50, mre11* and *xrs2* (*nbs1*) mutants do not exhibit significant defects in mitotic recombination (Saeki et al., 1980). Additionally, Δ*mre11* and Δ*rad50* strains of the archaeal species *Haloferax volcanii* are hyper-recombinogenic (T. Allers, unpublished data). Thus the role of Rad50 and Mre11 in end-processing has yet to be confirmed.

1.3.10 Strand exchange

Homologous pairing and strand exchange reactions are catalysed by a family of conserved recombinase enzymes. The bacterial recombinase is RecA and is discussed in detail later in this chapter, along with the eukaryotic and archaeal recombinases discussed here. Two recombinases exist in eukaryotes, Rad51 and Dmc1. Both enzymes are homologous to bacterial RecA. Rad51 has a role in both mitotic and meiotic recombination and DNA repair, and catalyses strand exchange. Second strand capture of the displaced strand is proposed to be catalysed by the strand annealing activity of Rad52. This activity also requires the interaction of Rad52 with ssDNA-bound RPA (Sugiyama et al., 2006)

A second recombinase exists in eukaryotes, Dmc1. Unlike Rad51, Dmc1 functions exclusively in meiotic recombination. Dmc1 binds to both dsDNA and ssDNA, possesses a weak ATPase activity and catalyses strand exchange (Masson et al, 1999),

RadA is the archaeal functional counterpart and homologue of Rad51 and has been characterised both biochemically and genetically. Deletion of *Haloferax volcanii* RadA results in increased sensitivity to ethylmethane sulfonate and UV light, and cells are recombination deficient (Woods and Dyall-Smith, 1997). Studies of *Sulfolobus solfataricus* RadA have shown that it can catalyse strand exchange, like Rad51 and RecA (Seitz et al, 1998).

1.3.11 Holliday junction branch migration

Following the invasion of an intact duplex by ssDNA, the region of heteroduplex DNA is extended by helicase activity. In bacteria, this is achieved by RuvAB complex (Parsons et al, 1995b; Parsons et al, 1992; Shiba et al, 1991). Eukaryotic Rad54 has been implicated in several stages of the process of homologous recombination and has recently been shown to demonstrate Holliday junction branch migration (Bugreev et al., 2006). It has also been shown to be able to dissociate recombination intermediates through this branch migration activity.

To date, no known archaeal proteins capable of branch migration have been discovered. One archaeal protein, Hjm/Hel308, with homology to bacterial RecQ and eukaryotic Hel308, was proposed as a branch migration enzyme (Fujikane et al, 2005). However, it was later shown to preferentially bind to forked DNA structures (Guy and Bolt, 2005). Therefore, the branch migration protein in archaea is unclear.

1.3.12 Holliday junction cleavage

Following branch migration, Holliday junctions must be cleaved to restore a two duplex state. In bacteria, this resolution is carried out by RuvC or, in *E.coli* in the absence of RuvC, RusA can carry out this role (Mahdi et al, 1996). A eukaryotic resolvase has remained elusive. Partial purification of human cell extracts revealed two proteins with Holliday resolution activity (Constantinou et al., 2002), thus the Mus81-Mms4 heterodimer was initially proposed as a resolvase in eukaryotes (Haber and Heyer, 2001). It was shown to cleave a range of branched DNA structures (Kaliraman et al, 2001), but the preferred substrate was shown to be a duplex Y structure, suggesting that it may function in processing stalled replication forks, rather than Holliday junctions (Kaliraman et al, 2001). Furthermore, Mus81-Mms4 cleaved Holliday junctions cannot be ligated suggesting asymmetrical cleavage that is not consistent with other resolvases (Constantinou et al., 2002).

The situation in archaea is different, with three Holliday junction resolvases having been identified and characterised. The first archaeal Holliday junction resolvase was discovered in *Pyrococcus furiosus* and was named Hjc (Komori et al., 1999; Kvaratskhelia et al., 2001). Hjc was later confirmed as a resolvase as *Methanothermobacter thermautotrophicus* Hjc restores the DNA repair deficiency of *E.coli* RuvC mutants (Bolt et al., 2001). Hjc forms homodimers (Nishino et al., 2001) and introduces symmetrical nicks into Holliday junctions, as observed with bacterial RuvC (Komori et al., 1999).

The crenarchaea possess an additional resolvase called Hje, discovered in *Sulfolobus solfataricus* (Kvaratskhelia et al., 2001). Hje cleaves independently of DNA sequence, like Hjc, but only nicks continuous strands of junctions in the stacked X-form. The euryarchaea also possess a second resolvase, Hjr. Hjr was discovered in *Pyrococcus furiosus* (Kvaratskhelia et al., 2001) and introduces symmetrical nicks into Holliday junctions, as is characteristic of other resolvases. Both Hje and Hjr are thought to be viral in origin.

1.4 Recombinases

Recombinases are enzymes that are essential for homologous recombination. They are proteins that catalyse homologous base-pairing and strand exchange and without them recombination is abortive at an early stage. Therefore, recombinases are ubiquitous throughout bacteria (RecA), eukaryotes (Rad51, Dmc1), archaea (RadA) and viruses (UvsX).

1.4.1 RecA

E.coli RecA was discovered in 1965 by screening for recombination deficient mutants (Clark and Margulies, 1965; Witkin, 1969). Mutants of RecA were shown to be sensitive to UV irradiation and deficient for homologous recombination. RecA binds to ssDNA in a sequence non-specific manner and polymerises on DNA in a 5' to 3' orientation, forming right handed helical filaments (Register and Griffith, 1985). A contiguous RecA nucleoprotein filament is required for efficient strand exchange and a saturated filament requires 1 RecA molecule per 3 nucleotides of ssDNA (Chrysogelos et al., 1983). ATP increases the binding affinity of RecA to DNA and stabilises the nucleoprotein filament (Roman and Kowalczykowski, 1986). Although RecA is an ATPase with conserved Walker A and Walker B motifs for binding and hydrolysis of ATP, hydrolysis is not required for DNA binding or strand exchange (Jain et al., 1994). Instead, it is required for strand exchange to proceed in a unidirectional manner (Kim et al., 1992). Furthermore, hydrolysis of ATP is required for the disassociation of RecA from DNA, as ADP-bound RecA exhibits a lower DNA binding affinity than ATP-bound RecA (Kowalczykowski, 1991).

Once formed, RecA filaments mediate strand exchange with homologous duplexes, forming regions of triplex DNA (Rao et al., 1993; Rao et al., 1991; Rao and Radding, 1993). *In vivo*, RecA mediated strand exchange requires a minimum of 23-40 bp of homology to proceed (King and Richardson, 1986; Shen and Huang, 1986). RecA also promotes the ATP and ssDNA dependent cleavage of the LexA repressor (Little et al., 1980), inducing SOS responses.

1.4.2 Rad51

Rad51 was discovered in *Saccharomyces cerevisisiae*, based on sequence homology to *E.coli* RecA (Little et al., 1980; Shinohara et al., 1992). Since this discovery, Rad51 has been subsequently found in all sequenced eukaryotic genomes. Homology shared between RecA and Rad51 centres on the core of the protein containing the RecA fold, which includes ATP binding and hydrolysis motifs. Rad51 has the same stoichiometry as RecA, with 1 Rad51 molecule per 3 nucleotides for efficient filament formation (Ogawa et al., 1993; Sung and Robberson, 1995). Yeast and human Rad51 binds DNA in nucleoprotein filaments analogous to bacterial RecA (Benson et al., 1994; Ogawa et al., 1993).

However, several differences between the structure and function of Rad51 and RecA exist. RecA has a C-terminal extension that is important for DNA binding, which is absent in Rad51 (Aihara et al., 1997; Kurumizaka et al., 1996). Furthermore, a positive patch of residues present in the N-terminus of Rad51, which does not have a corresponding region in RecA, is important for DNA binding (Aihara et al., 1999). The Rad51 polymerisation motif differs from that of RecA, with Rad51 polymerisation mediated by the insertion of an invariant phenylalanine residue into a conserved hydrophobic socket of a second Rad51 monomer. Rad51 filament formation also proceeds in the opposite polarity to RecA filament formation, occurring in a 3' to 5' direction (Sung and Robberson, 1995). Also, it has been recently observed that Rad51 filaments are not contiguous like RecA filaments. Instead each nucleoprotein filament consists of a string of many small filament patches that are only a few tens of monomers long, and this conformation is proposed to increase flexibility of the filament, facilitating strand exchange (Heijden et al., 2007; Modesti et al., 2007).

Yeast Rad51 mutants exhibit defects in homologous pairing, decreased viability during sporulation and delayed synapsis (Rockmill et al., 1995; Shinohara et al., 1992). Additionally, these mutants are highly sensitive to DNA damaging agents, methyl methanesulfonate and ionising radiation (Game and Mortimer, 1974). Depletion of Rad51 in chicken DT40 cells results in the accumulation of spontaneous chromosomal breaks (Sonoda et al, 1998) and Rad51 knockout mice are embryonic lethal (Lim and Hasty, 1996).

1.4.3 Dmc1

Dmc1 (Disrupted meiotic cDNA protein 1) is a second eukaryotic recombinase that is specific to meiotic recombination (Bishop et al, 1992). Dmc1 foci have been observed during meiosis and colocalise with Rad51 (Bishop, 1994). Dmc1 binds both ssDNA and dsDNA, has a weak ATP activity and catalyses strand exchange (Li et al., 1997; Masson et al., 1999). Early reports suggested that Dmc1 did not form helical nucleoprotein filaments like Rad51, instead forming octameric ring structure (Masson et al., 1999; Passy et al., 1999). However, subsequent analyses demonstrated that Dmc1-ssDNA filaments do form (Chang et al., 2005; Lee et al., 2005). Dmc1 knockout mice are viable but infertile (Pittman et al., 1998a; Yoshida et al., 1998) and Dmc1 mutations cause cell cycle arrest and recombination deficiencies in *S.cerevisciae* (Bishop et al, 1992).

1.4.4 RadA

RadA is the archaeal homologue of RecA and Rad51, and was discovered in crenarchaeal and euryarchaeal genomes (Sandler et al., 1996). RadA shares greater sequence similarity to Rad51 than to RecA (~40% identity and ~20% identity, respectively. RadA from both crenarchaeota and euryarcheaota has DNA dependent ATPase activity, forms nucleoprotein filaments and catalyses homologous pairing and strand exchange (Komori et al., 2000a; Seitz et al., 1998). Polymerisation of archaeal RadA is principally the same as with eukaryotic Rad51 (Shin et al., 2003) and stoichiometry is the same as Rad51 and RecA, with one RadA monomer per 3 nucleotides (Ariza et al., 2005). Structurally, Rad51 and RadA are strikingly similar(Shin et al., 2003). Deletion of *Haloferax volcanii radA* results in increased sensitivity to ethylmethane sulfonate and UV light, and cells are recombination deficient (Woods and Dyall-Smith, 1997).

1.5 Recombination mediator proteins

Recombinases can not usually function efficiently alone, often requiring the activity of other proteins to facilitate the loading or stabilisation of the recombinase. These proteins are known as mediator proteins and will be discussed here.

1.5.1 RecA mediators

A paradoxical mediator of RecA is SSB. SSB is a single stranded binding protein that destabilises secondary structure in ssDNA, facilitating the loading of RecA (Kowalczykowski et al., 1987). However, by binding ssDNA, SSB competes with binding sites with RecA. As SSB has a higher binding affinity for DNA, than RecA, it inhibits the formation of nucleoprotein filaments (Umezu et al., 1993). For this reason, additional proteins are required to facilitate RecA loading onto SSB coated ssDNA (Morimatsu and Kowalczykowski, 2003).

RecF, RecO and RecR carry out this role at ssDNA gaps (Umezu et al., 1993). RecOR complex is proposed to destabilise DNA-bound SSB and stabilise the binding of RecA to DNA (Shan et al, 1997). Despite this mediator activity, recent studies show that SSB also inhibits the binding of RecOR to ssDNA *in vitro*, thus slowing RecOR-mediated RecA nucleation on ssDNA (Hobbs et al., 2007). A RecFR complex limits extension of RecA filaments beyond ssDNA gaps into regions of dsDNA (Webb et al., 1997). RecF also alleviates RecX inhibition of RecA function (Lusetti et al., 2004; Lusetti et al., 2006).

An additional recombination mediator protein has recently been characterised. DprA is present in most bacterial species and functions to overcome the RecA binding inhibition of SSB. Furthermore, it acts to align DNA molecules, facilitating the formation of joint molecules. DprA interacts with RecA and is proposed to interact with SSB (Mortier-Barriere et al., 2007).

1.5.2 Rad51 mediators

In an analogous role to SSB, eukaryotic RPA (Replication Protein A) prevents secondary structure formation in ssDNA therefore promoting Rad51 filament formation and recombination (Sugiyama et al, 1997). However, just as SSB prevents RecA binding to ssDNA, so does RPA prevent Rad51 binding to ssDNA. The DNA binding activity of Rad51 is enhanced by interactions with Rad52, which stimulates the displacement of RPA (New et al., 1998; Shinohara et al., 1998; Sugiyama et al., 1997; Sung, 1997a). In addition to interacting with Rad51, Rad52 also interacts directly with ssDNA bound RPA (Hays et al, 1998). To promote ssDNA binding by Rad51, the co-complex of Rad52/RPA/ssDNA is necessary, followed by recruitment of Rad51 onto the ssDNA. (Sugiyama & Kowalczykowski, 2002). Once Rad51 is bound to ssDNA, cooperative binding between the assembling filament and Rad51 protomers has been shown to be sufficient to displace RPA without the need for Rad52 (Sugiyama & Kowalczykowski, 2002).

The fungal paralogues of Rad51, Rad55 and Rad57, form a heterodimeric complex that is also capable of overcoming inhibition of Rad51-mediated strand exchange by RPA (Sung, 1997). Rad55-57 promotes and stabilizes Rad51-ssDNA complexes (Fortin and Symington, 2002). Rad55 mutants are sensitive to ionizing radiation and meiosis in mutant cells is a lethal event (Lovett and Mortimer, 1987). Also, Rad51 is slower to bind to ssDNA in *rad55* mutants (Sugawara et al., 2003).

Rad54, a SWI2/SNF2 family protein, has a mediator role throughout recombination. Rad54 acts in concert with Rad52 and with Rad55-57 complex to stabilize Rad51 nucleoprotein filaments (Wolner et al., 2003).

The tumour suppressor proteins BRCA1 and BRCA2 have been shown to co-localise with Rad51 in damage induced nuclear foci (Chen et al., 1998; Scully et al., 1997). BRCA2 has been shown to interact with Rad51, while BRCA1 co-localises with Rad51 via interactions with BRCA2 (Chen et al., 1998; Wong et al., 1997). BRCA2 interacts with Rad51 through repeat sequences called BRC motifs and has been implicated in deploying Rad51 at sites of DNA damage, and sequestering it when it is not required (Wong et al., 1997; Yang et al., 2005). Both BRCA1 and BRCA2 are required for efficient homologous recombination with deletion of either gene resulting in genomic rearrangement and chromosome breaks (Bhattacharyya et al., 2000; Moynahan et al., 1999; Moynahan et al., 2001; Patel et al., 1998; Xu et al., 1999; Yu et al., 2000). The *C.elegans* homologue of BRCA2 (CeBRC-2) has been shown to promote D-loop formation by Rad51 and stabilizes Rad51 nucleoprotein filaments (Petalcorin et al., 2007; Petalcorin et al., 2006).

1.5.3 Dmc1 mediators

Like Rad51 catalysed strand exchange, RPA is required for Dmc1 catalysed strand exchange, most probably to remove secondary structures from DNA (Sehorn et al., 2004). Also like Rad51 catalysed recombination, BRCA2 is required for normal levels of meiotic recombination, and interacts with Dmc1 (Sharan et al., 2004; Siaud et al., 2004). The heterodimeric complex, Hop2/Mnd1 has been shown to stimulate Dmc1 mediated D-loop formation and strand exchange and acts to juxtapose homologues (Chen et al., 2004; Petukhova et al., 2005). The mammalian Hop2/Mnd1 complex also stimulates Rad51 catalysed recombination (Enomoto et al., 2006). The Rad54 homologue, Tid1, plays an important role in meiotic recombination and interacts with both Rad51 and Dmc1 during meiotic recombination (Catlett and Forsburg, 2003; Dresser et al., 1997; Shinohara et al., 1997). Tid1 stimulates the formation of D-loops by Rad51 and promotes dissociation of Dmc1 from non-recombinogenic sites on meiotic chromosome (Holzen et al., 2006; Petukhova et al., 2000).

1.5.4 RadA mediators

Currently, there are no known mediators of RadA catalysed recombination, in archaea. However, homologues of the eukaryotic single strand binding protein, RPA, are present in the archaea, suggesting that mechanisms exist to overcome inhibition of RadA binding of DNA by RPA, analogous to Rad51/RPA and RecA/SSB (Haseltine and Kowalczykowski, 2002; Kelly et al., 1998; Komori and Ishino, 2001; Wadsworth and White, 2001). Furthermore RPA has been shown to interact with RadA and stimulate strand exchange *in vitro* (Komori and Ishino, 2001). It is unknown what is responsible for overcoming inhibition of RadA ssDNA binding by RPA. However, RadB, a RadA paralogue has been shown to interact with RadA *in vitro*, and has been implicated in facilitating loading of RadA onto RPA coated ssDNA (Komori et al., 2000b;

Sandler et al., 1999; Sandler et al., 1996). The genetic analysis of RadB is the subject of this thesis and a discussion of RadB is presented in Chapter 3: Characterisation of RadB, a RadA paralogue.

1.6 Recombinase paralogues

No bacterial paralogues of RecA have been observed to date. However, eukaryotic genomes encode a number of Rad51 paralogues. Biochemical and genetic analysis has implicated these proteins in homologous recombination

1.6.1 Mammalian Rad51 paralogues

Mammalian genomes encode a total of five Rad51 paralogues. The first two to be identified are XRCC2 and XRCC3 (X-ray Cross Complementation proteins 2 and 3). These proteins were identified by complementation of mitomycin C and X-ray irradiation sensitivity of irs1 and irs1SF hamster cell lines (Jones et al., 1987; Liu et al., 1998). Later, three other paralogues were identified, Rad51B, Rad51C and Rad51D. These paralogues were identified based on their sequence similarity to Rad51 (Albala et al., 1997; Dosanjh et al., 1998; Pittman et al., 1998b). Cell lines mutated for any of the five paralogues are viable, but show a reduction in DNA-damage induced Rad51 foci and increased sensitivity to DNA crosslinking agents and ionising radiation, suggesting a role for the paralogues as Rad51 accessory proteins (Deans et al., 2003; Takata et al., 2000; Takata et al., 2001). Haploinsufficiency of Rad51B causes fragmentation of the centrosome and aneuploidy in human cells (Date et al., 2006). Rad51C deficiency in male mice leads to early prophase I arrest and female mouse oocytes display precocious separation of sister chromatids at metaphase II (Kuznetsov et al., 2007). Rad51D mutant cells display elevated levels of mutagenesis (Hinz et al., 2006) and has been in telomere maintenance (Tarsounas et al., 2004).

Biochemical studies of these paralogues have shown that Rad51B, Rad51C and Rad51D exhibit a weak DNA-stimulated ATPase activity (Braybrooke et al., 2000; Lio et al., 2003) and the ATPase activity of Rad51D is required for resistance to DNA crosslinking agents (Gruver et al., 2005). Conversely, XRCC2 does not bind DNA, but possesses a weak ATP binding activity and very weak ATPase activity (Shim et al., 2004). hXRCC2 enhances Rad51 focus formation and DNA strand exchange (O'Regan et al., 2001).

Yeast two-hybrid analysis has shown that two distinct complexes are formed from these paralogues: Rad51B-Rad51C-Rad51D-XRCC2 (BCDX2) and Rad51C-XRCC3 (CX3) (Masson et al., 2001; Schild et al., 2000). The CX3 complex has been shown to be important for the processing of Holliday junctions. Depletion of Rad51C from partially purified cell

extracts resulted in a reduction in Holliday junction cleavage and branch migration, and cells lines deficient in either Rad51C or XRCC3 accumulated Holliday junction intermediates (Liu et al., 2004b; Sharan and Kuznetsov, 2007), The BCDX2 complex has been implicated in an earlier stage of recombination, facilitating loading of Rad51 onto ssDNA (O'Regan et al., 2001; Sigurdsson et al., 2001). Additionally, BCDX2 has been shown to preferentially bind to branched DNA substrates, suggesting that it may function in late recombination (Yokoyama et al., 2004).

1.6.2 Fungal paralogues

Fungal genomes do not encode the five Rad51 paralogues present encoded by mammalian cells. Instead, they contain two different Rad51 paralogues, Rad55 and Rad57. These two proteins form a stable heterodimeric complex (Rad55-57) (Sung, 1997). This complex has been shown to interact with Rad51 via Rad55 and stimulates Rad51 catalysed strand exchange (Hays et al., 1995; Johnson and Symington, 1995; Sung, 1997b). Rad55-57 has been implicated in overcoming RPA inhibition of Rad51 ssDNA binding, by promoting and stabilising Rad51 nucleoprotein filaments (Fortin and Symington, 2002). Additionally, Rad55 is a substrate for replication block and DNA damage checkpoints. It becomes phosphorylated in response to DNA damage by Mec1 and Dun1 kinases, and Rad53, and deletion of Mec1 leads to a decrease in homologous recombination following DNA damage (Bashkirov et al., 2006; Bashkirov et al., 2000; Herzberg et al., 2006).

1.6.3 *Caenorhabditis elegans* paralogue

Caenorhabditis elegans encodes only one Rad51 paralogue, RFS-1. RFS-1 is dispensable for Rad-51 recruitment to meiotic and ionizing radiation induced double strand breaks, and following the collapse of replication forks, but is essential for recruitment of Rad51 to replication fork blocks, induced by mitomycin C (Ward et al., 2007).

1.6.4 Archaeal RadA paralogues

To date, only one RadA paralogue has been reported: RadB. This paralogue was discovered based on sequence similarity to RadA (Sandler et al, 1999). As discussed, some biochemical characterisation of RadB has been carried out, yet no genetic data has been obtained. Hence, the purpose of this thesis is to attempt to elucidate the role of RadB through genetic analyses. RadB is discussed in depth in Chapter 3: Characterisation of RadB, a RadA paralogue.

1.7 *Haloferax volcanii* – A model organism for archaeal genetic

A significant problem that has hampered the study of archaea lies in the fact that, until recently, there were no model organisms for genetic studies: Some species are ideal for biochemical

studies but not ideal for genetic studies, such as *Sulfolobus solfataricus* and *Methanothermobacter thermoautotrophicum*, due to anaerobic requirements, difficulty of transformation and extreme temperatures required for cultivation. The archaeal species utilised in this study is *Haloferax volcanii*. *H. volcanii* is a member of the euryarchaeota and lives at 2.5M NaCl, and can even survive in saturated conditions. It grows at optimally at 45° C in the presence of oxygen, and has a 4.2 Mb genome with a G+C content of approximately 65%. (Hartman et al, in preparation) *H. volcanii* cells are disk shaped and show involuted forms in the presence of NaCl. In the laboratory, *H. volcanii* produces a characteristic pink pigment.

The reasons for studying this particular archaeon are numerous. *H. volcanii* is easily cultured in the laboratory and will form colonies on solid media. With a generation time of approximately 3 hours, they grow fast enough that they can be effectively studied. Secondly, an extensive array of genetic tools is available for studying this archaeon (Allers et al., 2004; Bitan-Banin et al., 2003; Dyall-Smith and Doolittle, 1994; Holmes and Dyall-Smith, 1990; Ortenberg et al., 2000).

H. volcanii cells are naturally competent and can be transformed with the use of PEG600. Antibiotics are available for use with antibiotic resistance markers, e.g. mevinolin. Better still, a variety of auxotrophic markers are available, which, in conjunction with the use of selective media, are extremely useful in the process of genetic manipulation. Shuttle vectors for episomal expression of genes and a uracil/5-FOA counterselectable marker system have been developed for *Haloferax volcanii*. The former provides a means of complementation of genes and the latter allows the manipulation and analysis of the chromosome through targeting gene deletion and gene mutation, by recombination between transformed plasmids and the chromosome (Figure 2.1 Chapter 2).

An inducible promoter has recently been developed which will be invaluable for studying the importance and dosage effects of genes (Large et al, in press). Furthermore, work has commenced on the development of an archaeal two-hybrid system that will prove vital for elucidating protein:protein interactions *in vivo*.

Chapter 2: Materials and Methods

2.1 Oligonucleotides

Oligo	Sequence	Use
BGABBF	CGAGCTCGGCACCATGGCTGAGACGT	Insertion for bgaHa-Bb allele
BGABBR	CGACGTCTCAGCCATGGTGCCGAGCT	Insertion for bgaHa-Bb allele
BGABEF	GTTACGAGGCCGCAGCTGTCGAGGCA	Insertion for bgaHa-Be allele
BGABER	GTAACTGCCTCGACAGCTGCGGCCTC	Insertion for bgaHa-Be allele
BGABHF	CGCGAGTGTGCGCTCGAGTCGAAGGT	Insertion for bgaHa-Bh allele
BGABHR	CGCGACCTTCGACTCGAGCGCACACT	Insertion for bgaHa-Bh allele
D1SEQF	CCCGTCGGGAACCGAACC	Sequencing of dp1
D1SEQR	GTCAGTAGTGAAACGGTCGCC	Sequencing of dp1
EXTF	ACCGCGAGGTCGTGTTTGCG	K36A mutation
EXTR	TCACGCGGGTCACGTTCCC	K36A mutation
H206AF2	GGTTTCGCCCGGGCTTTCTCCAGC	H206A mutation
H206AR2	GCTGGAGAAAGCCCGGGCGAAACC	H206A mutation
HEXTF	GCGCGTAATACGACTCACTATAGGG	H206A mutation
HEXTR	CGGTCGACCGCTTCCAACAGC	H206A mutation
HVRDBF	GCTCGACGACCTCCTCGA	radB probe
HVRDBR	GTTTCGCGCGGTGTTTCT	radB probe
K36AF	CGACGTTCGTGGCGCCGGCCGCGG	K36A mutation
K36AR	CCGCGGCCGGCGCCACGAACGTCG	K36A mutation
RADAF	GGGGATCCGTGGGACTAACCGCGCTCG CCCGTCGTGCCTG	cloning/sequencing of radA
RADAR	CGTCGGATCCCAGCGTTACCCCCACGT CGCCGTCG	cloning/sequencing of radA
RADARTF	GACGATACGCTTGTCGCCC	radA RT-PCR
RADARTR	GTCCGCCTCCTCTGTGTTGAC	radA RT-PCR
RADBRTF2	GCGGTCGGTTATCTTGAACG	radB RT-PCR
RADBRTR1	GTCACCCACCTGCTGTCG	radB RT-PCR
RBDN1	CGACGCGACCGGTGAGACGACCC	Deletion of radB
RBDN2	GTGCCACCGGTCGAAAAAGACCCCGG	Deletion of radB
RBDX1	CGTAATACGACTCACTATAGGGCG	Deletion of radB
RBDX2	AAGTCCGCGGCGGCCGCGACTATCACG	Deletion of radB
RPOARTF	CGGCGAGCACCTGATTGAC	rpoA RT-PCR
RPOARTR	ACGGACGAGGAAGCAGACG	rpoA RT-PCR

2.2 Plasmids

pTA	Description
pMDS41	Hf volcanii Δ*radA* (*Nco*I–*Not*I deletion of *radA*) constructed from pSJS1140, with addition of MevR fragment from pMDS28 (Woods and Dyall-Smith, 1997)
41	pBluescript II SK+ with *Hvo* 6.0 kb *Mlu*I chromosomal fragment containing *radB* (*rad51*, ORF1554), inserted at *Bss*HII sites
48	pBluescript II SK+ with *Hvo* 4.0 kb *Xma*I chromosomal fragment containing *hjc* (ORF3225), inserted at *Xma*I site
50	pBluescript II SK+ with 1647 bp *Eco*47III-*Xma*I fragment of p41 containing *radB* (*rad51*, ORF1554), inserted at *Eco*RV-*Xma*I sites
pGB70	Hf volcanii *pyr*E2 ORF under ferredoxin (fdx) promoter of *Hsa* in pUC19 (Bitan-Banin et al., 2003)
54	pTA50 with 368 bp partial deletion of *radB* (*radB*Δb/b) between *Bst*BI site and *Bst*EII site (Klenow filled)
68	pTA52 with 1.3 kb *Hind*III-*Xba*I *radB*Δb/b fragment from pTA54 inserted at *Hind*III and *Xba*I
83	pTA52 with 2.44 kb *Kpn*I-*Hind*III Δ*radA* fragment (*Hind*III Klenow filled) from pMDS41 inserted at *Kpn*I and *Eco*RI (*Eco*RI Klenow filled)
131	pBluescript II SK+ with 0.7 kb *Bam*HI/*Xba*I (both Klenow filled) p.fdx::*pyrE2* fragment from pGB70 inserted at *Psi*I site
156	pTA131 + insertion of 3.5 kb *Hind*III-*Xba*I fragment containing *bgaHa-Bb* allele
158	pTA131 + insertion of 3.5 kb *Hind*III-*Xba*I fragment containing *bgaHa-Bh* allele
159	pTA131 + insertion of 3.5 kb *Hind*III-*Xba*I fragment containing *bgaHa-Kp* allele
168	pGB70 with leuAa2 oligos containing *Bss*HII site inserted at *Aat*II site of *leuB* (*leuB-Aa2*)
188	pTA131 + insertion of 3.5 kb *Hin*DIII-*Xba*I fragment containing *bgaHa-Be* allele
191	pTA176 (puc19) + insertion of 2.85kb *Sac*I fragment of *hjc* subclone from pTA48
230	pTA131 with insertion of 3.75 kb *Nco*I-*Hind*III (both blunt-ended) fragment containing pHV2 origin from pWL-Nov, at *Pci*I site (blunt-ended)
236	pTA196 with deletion of 366 bp *Psh*AI fragment containing remainder of *hjc* ORF, to give complete *hjc* deletion
289	pTA131 with insertion of 337bp Δ*radB* PCR construct, inserted at *Not*I and *Kpn*I sites. Generated by RBDN1/RBDX1, RBDN2/RBDX2 PCR, digested with *Not*I and *Kpn*I
312	pTA131 with insertion of 337bp Δ*radB* PCR construct, inserted at *Not*I and *Kpn*I sites. Generated by RBDN1/RBDX1, RBDN2/RBDX2 PCR, digested with *Not*I and *Kpn*I (dam-)
354	Shuttle vector based on pTA131 with 948 bp *Bmg*BI-*Eco*RV fragment from pTA250 (containing *Hv* ori pHV1/4). Inserted at klenow blunted *Pci*I site.
357	Shuttle vector based on pTA131 with 948bp *Bmg*BI-*Eco*RV fragment from pTA250 (containing *Hv* ori pHV1/4). Inserted at klenow blunted *Pci*I site.

622	pTA693 with replacement of *Cla*I-*Bst*EII radB fragment with *Cla*I-*Bst*EII *radB-H206A* PCR product
627	pTA693 with replacement of *Bsp*EI-*Bst*EII *radB* fragment with *Bsp*EI-*Bst*EII *radB-K36A* PCR product
693	pTA131 with insertion of 1.1 kb *Kpn*I-*Bsp*EI (klenow filled) fragment from pTA50 containing *radB*. Inserted at *Kpn*I/*Not*I (klenow filled)
769	pTA131 + 1.7 kb *Kpn*I-*Bam*HI *radA-A196V* fragment, inserted at *Kpn*I/*Bam*HI
778	pTA131 + 1.7 kb *Kpn*I-*Bam*HI *radA-A196V* fragment, inserted at *Kpn*I/*Bam*HI

2.3 *Haloferax volcanii* strains

H	Parent	Genotype	Notes
26	H18	Δ*pyrE2*	Loss of pTA53 (Δ*pyrE2*, NovR) from *pyrE2* locus, leaving behind Δ*pyrE2*
56	H26	Δ*pyrE2, radA+[ΔradA, pyrE2+]*	Integration of pTA83 (Δ*radA*, pyrE2+) at *radA* locus
57	H26	Δ*pyrE2, radB+[radBΔb/b, pyrE2+]*	Integration of pTA68 (*radB*Δb/b, *pyrE2*+) at *radB* locus
64	H57	Δ*pyrE2, radB*Δ*b/b*	Loss of pTA68 (*radB*Δb/b, *pyrE2*+) from *radB* locus, leaving behind *radB*Δb/b
97	H56	Δ*pyrE2,* Δ*radA*	Loss of pTA83 (Δ*radA*, *pyrE2*+) from *radA* locus, leaving behind Δ*radA*
151	H64	Δ*pyrE2,* Δ*radB, radA+[*Δ*radA, pyrE2+]*	Integration of pTA83 (Δ*radA*, *pyrE2*+) at *radA* locus
160	H64	Δ*pyrE2, hjc+[*Δ*hjc, pyrE2+]*	Integration of pTA236 (Δ*hjc*, *pyrE2*+) at *hjc* locus
186	H151	Δ*pyrE2,* Δ*radB,* Δ*radA*	Loss of pTA83 (Δ*radA*, *pyrE2*+) from *radA* locus, leaving behind Δ*radA*
187	H160	Δ*pyrE2,* Δ*radB,* Δ*hjc*	Loss of pTA236 (Δ*hjc*, *pyrE2*+) from hjc locus, leaving behind Δ*hjc*
188	H160	Δ*pyrE2,* Δ*radB,* Δ*hjc*	Loss of pTA236 (Δ*hjc*, *pyrE2*+) from *hjc* locus, leaving behind Δ*hjc*
195	H181	Δ*pyrE2* Δ*trpA leuB-Ag1 bgaHa-Bb* Δ*hdrB*	Loss of pTA160 (Δ*hdrB*, *pyrE2*+) from *hdrB* locus, leaving behind Δ*hdrB*
238	H195	Δ*pyrE2* Δ*trpA leuB-Ag1 bgaHa-Bb* Δ*hdrB, hjc+[*Δ*hjc, pyrE2+]*	Integration of pTA236 (Δ*hjc*, *pyrE2*+) at *hjc* locus
257	H195	Δ*pyrE2* Δ*trpA leuB-Ag1 bgaHa-Bb* Δ*hdrB, radB+[*Δ*radB, pyrE2+]*	Integration of pTA312 (Δ*radB*, *pyrE2*+) at *radB* locus
282	H238	Δ*pyrE2* Δ*trpA leuB-Ag1 bgaHa-Bb* Δ*hdrB,* Δ*hjc*	Loss of pTA236 (Δ*hjc*, *pyrE2*+) from hjc locus, leaving Δ*hjc*

284	H257	Δ*pyrE2* Δ*trpA leuB-Ag1 bgaHa-Bb* Δ*hdrB,* Δ*radB*	Loss of pTA312 (Δ*radB*, *pyrE2*+) from *radB* locus, leaving behind Δ*radB*
319	H282	Δ*pyrE2* Δ*trpA leuB-Ag1 bgaHa-Bb* Δ*hdrB,* Δ*hjc, radB+[*Δ*radB, pyrE2+]*	Integration of pTA312 (Δ*radB*, *pyrE2*+) at *radB* locus
349	H319	Δ*pyrE2* Δ*trpA leuB-Ag1 bgaHa-Bb* Δ*hdrB,* Δ*hjc,* Δ*radB*	Loss of pTA312 (Δ*radB*, *pyrE2*+) from *radB* locus, leaving behind Δ*radB*
388	H351	Δ*pyrE2* Δ*trpA leuB-Ag1 bgaHa-Bb* Δ*hdrB,* Δ*radA:trpA+*	Loss of pTA325 (Δ*radA*::*trpA*+, *pyrE2*+) from *radA* locus, leaving behind Δ*radA*::*trpA*+
494	H195	Δ*pyrE2* Δ*trpA leuB-Ag1 bgaHa-Bb* Δ*hdrB* <*pyrE2+*>	Contains pTA357 (pTA354) *pyrE2* shuttle vector. Phenotypically Ura+
495	H284	Δ*pyrE2* Δ*trpA leuB-Ag1 bgaHa-Bb* Δ*hdrB,* Δ*radB* <*pyrE2+*>	Contains pTA357 (pTA354) pyrE2 shuttle vector. Phenotypically Ura+
496	H284	Δ*pyrE2* Δ*trpA leuB-Ag1 bgaHa-Bb* Δ*hdrB,* Δ*radB* <*radB+, pyrE2+*>	Contains pTA395 (pTA379) pyrE2 shuttle vector with radB. Phenotypically Ura+
497	H284	Δ*pyrE2* Δ*trpA leuB-Ag1 bgaHa-Bb* Δ*hdrB,* Δ*radB* <*radB-H206A, pyrE2+*>	Contains pTA623 (pTA622) *pyrE2* shuttle vector with *radB-H206A*. Phenotypically Ura+
498	H284	Δ*pyrE2* Δ*trpA leuB-Ag1 bgaHa-Bb* Δ*hdrB,* Δ*radB* <*radB-K36A, pyrE2+*>	Contains pTA627 (pTA624) *pyrE2* shuttle vector with *radB-K36A*. Phenotypically Ura+
513	H481	Δ*pyrE2* Δ*trpA leuB-Ag1 bgaHa-Bb* Δ*hdrB,* Δ*uvrA*	Loss of pTA596 (Δ*uvrA*, *pyrE2*+)from *uvrA* locus, leaving behind Δ*uvrA*
724	H718	Δ*pyrE2* Δ*trpA leuB-Ag1 bgaHa-Bb* Δ*hdrB,* Δ*radB, radA-A196V*	Loss of pTA778 (*radA-A196V*, *pyrE2*+) from *radA* locus, leaving behind *radA-A196V*
761	H595	Δ*pyrE2* Δ*trpA leuB-Ag1 bgaHa-Bb* Δ*hdrB,* Δ*uvrA,* Δ*radB*	Loss of pTA312 (Δ*radB*, *pyrE2*+) from *radB* locus, leaving behind Δ*radB*
769	H724	Δ*pyrE2* Δ*trpA leuB-Ag1 bgaHa-Bb* Δ*hdrB, radA-A196V*	Loss of pTA693 (*radB*+, *pyrE2*+) from *radB* locus, leaving behind *radB*+

2.4 *Escherichia coli* strains

Name	**Genotype**	**Source**
XL1-Blue	*endA1, gyrA96 (NalR), lac [F' proAB lacIqZ*Δ*M15 Tn10 (TetR)],* Δ*(mcrA)183,* Δ*(mcrCB-hsdSMR-mrr)173, recA1, relA1, supE44, thi-1*	Stratagene
N2338	*F–, ara-14, dam-3, dcm-6, fhuA31, galK2, galT22, hsdR3, lacY1, leu-6, thi-1, thr-1, tsx-78*	RG Lloyd

2.5 Materials

2.5.1 *Haloferax volcanii* media

Sterilised by autoclaving, unless otherwise stated.

30% SW

240 g NaCl, 30 g $MgCl_2 \cdot 6H_2O$, 35 g $MgSO_4 \cdot 7H_2O$, 7 g KCl, 20 ml 1 M Tris.HCl pH 7.5, dH_20 to 1 l (not autoclaved)

18% SW

200 ml 30% SW, 100ml dH_20, 2 ml $CaCl_2$

Trace elements

36 mg $MnCl_2.4H_2O$, 44 mg $ZnSO_4.7H_2O$, 230 mg $FeSO_4.7H_2O$, $CuSO_4.5H_2O$, dH_2O to 100ml

Hv-Min salts

30 ml 1M NH_4Cl, 36 ml 0.5 M $CaCl_2$, 6 ml trace elements

Hv-Min carbon source

41.7 ml 60% dl-lactic acid Na_2 salt (Sigma), 37.5 g succinic acid Na_2 salt.$6H_2O$ (Sigma), 3.15 ml 80% glycerol, dH_2O to 250ml, pH 6.5

10x YPC

50 g **Y**east extract (Difco), 10 g **P**eptone (Oxoid), 10 g **C**asamino acids, 17.6 ml 1M KOH, dH_2O to 1litre (Not autoclaved. Used immediately)

10x Ca

50 g **C**asamino acids, 23.5 ml 1M KOH, dH_20 to 1 litre (Not autoclaved. Used immediately)

Hv-YPC agar (Contains uracil, tryptophan and leucine)

5 g Agar (Bacto), 100 ml dH_2O, 200ml 30% SW, 33 ml 10x YPC, 2 ml 0.5 M $CaCl_2$. Microwaved without 10x YPC to dissolve agar. 10x YPC added, then autoclaved. $CaCl_2$ added prior to pouring.

Hv-Ca agar (Contains leucine)

5 g Agar (Bacto), 100 ml dH_20, 200 ml 30% SW, 33 ml 10x Ca, 2 ml 0.5 M $CaCl_2$, 36 µg biotin (Sigma), 288 µg thiamine (Sigma). Microwaved without 10x Ca to dissolve agar. 10x Ca added, then autoclaved. $CaCl_2$, thiamine and biotin added prior to pouring.

Hv-Min agar

5 g Agar (Bacto), 110 ml dH_20, 200 ml 30% SW, 10 ml 1 M Tris.HCl pH 7.5, 8.5 ml Hv-Min carbon source, 4 ml Hv-Min Salts, 650 µl 0.5 M KPO_4 buffer (pH 7.5), 36 µg biotin (Sigma), 288 µg thiamine (Sigma). Microwaved to dissolve agar. 1 M Tris.HCl pH 7.5 added, then autoclaved.

Hv-YPC broth (Contains uracil, tryptophan and leucine)

100 ml dH_20, 200 ml 30% SW, 33 ml 10x YPC, 2 ml 0.5 M $CaCl_2$. Autoclaved and $CaCl_2$ added when cool.

Hv-Ca+ broth (Contains leucine)

150 ml 30% SW, 7.5 ml 1 M Tris.HCl pH 7.5, 6.5 ml Hv-Min carbon source, 3 ml Hv-Min Salts, 500 µl 0.5 M KPO_4 buffer (pH 7.5), 250 µl 36 µg biotin (Sigma), 288 µg thiamine (Sigma), 25 ml 10x Ca. 30% SW autoclaved. Everything else added when cooled.

2.5.2 *Escherichia coli* media

Sterilised by autoclaving, unless otherwise stated.

LB (agar)

10 g tryptone (Bacto), 5 g yeast extract (Difco), 10 g NaCl, 10 g agar (Bacto) when required, dH_20 to 1litre

SOC

20 g tryptone (Bacto), 5 g yeast extract (Difco), 0.58 g NaCl, 0.186 g KCl, 2.03 g $MgCl_2$, 2.46 g $MgS0_4$, dH_20 to 1 litre

2.5.3 *Haloferax volcanii* media supplements

All media supplements were supplied by Sigma. Solutions were sterilised by filtration through a 0.2 µm filter.

Supplement	Abbreviation	Final concentration	Stock conc.
Leucine	+ Leu	50 µg/ml	10 mg/ml
Uracil	+Ura	50 µg/ml	50 mg/ml
Thymidine	+Thy	50 µg/ml (+50 µg/ml hypoxanthine in Hv-Ca and Hv-Min)	4 mg/l
Tryptophan	+Trp	50 µg/ml	10 mg/ml
5-FOA	+5FOA	50 µg/ml (+10 µg/ml uracil)	50 mg/ml

2.5.4 *Escherichia coli* media supplements

Supplement	Abbreviation	Final concentration
Ampicillin	+ Amp	50 µg/ml
Tetracycline	+Tet	3.5 µg/ml

2.5.5 *Haloferax volcanii* buffers and solutions

Sterilised by filtration through a 0.2 µm filter.

Buffered Spheroplasting Solution:

1 M NaCl, 27 mM KCl, 50 mM Tris.HCl pH 8.5, 15% sucrose

Unbuffered Spheroplasting Solution:

1 M NaCl, 27 mM KCl, 15% sucrose, pH 7.5

Spheroplast Dilution Solution:

23% SW, 15% sucrose, 37.5 mM $CaCl_2$

Regeneration Solution

18% SW, 1xYPC, 15% sucrose, 30 mM $CaCl_2$

Transformation Dilution Solution

18% SW, 15% sucrose, 30 mM $CaCl_2$

ST Buffer

1 M NaCl, 20 mM Tris.HCl pH 7.5

Lysis Solution

100 mM EDTA pH 8, 0.2% SDS

2.5.6 Other buffers and solutions

20x SSPE

525.9g NaCl, 82.8g NaH_2PO_4, 28.2g EDTA in 3 litres dH_20, pH 7.4

TE

10 mM Tris.HCl pH 8.0, 1 mM EDTA

TBE

89 mM Tris, 89 mM boric acid, 2 mM EDTA

TAE

40 mM Tris.HCl, 20mM acetic acid, 1 mM EDTA

Denaturing Solution

1.5 M NaCl, 0.5 N NaOH

100 x Denhardt's Solution

2% Ficoll 400, 2% PVP (poly vinyl pyrrolidone) 360, 2% BSA (bovine serum albumin)(Fraction V)

Prehybridisation Solution

24 ml dH_20, 12 ml 20x SSPE, 2 ml 20% SDS, 2 ml 100 x Denhardt's solution

Hybridisation Solution

1.5 g dextran sulphate, 9 ml 20x SSPE, 1.5 ml 20% SDS, 18 ml dH_20

Low Stringency Wash Solution

2x SSPE, 0.5% SDS

High Stringency Wash Solution

0.2xSSPE, 0.5% SDS

Neutralising Buffer

1.5 M NaCl, 0.5 M Tris.HCl, 1 mM EDTA

Gel Loading Dye (5x)

50 mM Tris.HCl, 100 mM EDTA, 15% Ficoll (w/v), 0.25% Bromophenol Blue (w/v), 0.25% Xylene Cyanol FF (w/v)

2.6 Methods

2.6.1 Derivation of *Haloferax volcanii* strain H195

H195 is a multiple auxotroph (Δ*pyrE2* Δ*trpA* Δ*hdrB leuB-Ag1 bgaHa-Bb*) (Guy et al, 2006). These markers allow a variety of genetic assays to be utilised. The derivation of H195 is summarised in Table 2.1.

Strain	Genotype	Integrated Plasmid
H26	Δ*pyrE2*	
H50	Δ*pyrE2 bgaHv*+[*bgaHa pyrE2*+]	pTA104 *bgaHa-Bb*
H54	Δ*pyrE2 bgaHa*	
H69	Δ*pyrE2 trpA*+ *leuB*+[*leuB-Ag1 pyrE2*+]	pTA123 *leuB-Ag1*
H85	Δ*pyrE2 trpA*+ *leuB-Ag1 bgaHa*+	
H132	Δ*pyrE2 trpA*+[Δ*trpA pyrE2*+] *leuB-Ag1*	pTA98 Δ*trpA*
H142	Δ*pyrE2* Δ*trpA leuB-Ag1*	
H148	Δ*pyrE2* Δ*trpA leuB-Ag1 bgaHa*+[*bgaHa-Bb pyrE2*+]	pTA156 *bgaHa*
H164	Δ*pyrE2* Δ*trpA leuB-Ag1 bgaHa-Bb*	
H181	Δ*pyrE2* Δ*trpA leuB-Ag1 bgaHa-Bb hdrB*+[Δ*hdrB pyrE2*+]	pTA160 Δ*hdrB*
H195	Δ*pyrE2* Δ*trpA leuB-Ag1 bgaHa-Bb* Δ*hdrB*	

Table 2.1 Derivation of strain H195

2.6.2 Derivation of *bgaHa* construct

The β-galactosidase gene *bgaHv* of *H. volcanii* does not appear to be functional. However, the *bgaH* gene from the related species *Haloferax alicantei* is active in *H. volcanii*, and yields colonies that stain blue when sprayed with Xgal (Holmes and Dyall-Smith, 2000). To replace *bgaHv* with a functional β-galactosidase gene, a 3439 bp *Hind*III–*Sau*3AI *H. alicantei* genomic DNA fragment from pMLH32 (Holmes and Dyall-Smith, 2000) was cloned in the *pyrE2*-marked plasmid pGB70 (Bitan-Banin et al., 2003) to generate pTA102. The Δ*pyrE2* strain H26 (Allers et al., 2004) was transformed with pTA102, and the gene knockout/replacement system described previously (Allers et al., 2004; Bitan-Banin et al., 2003) was used to isolate clones that stained blue when sprayed with Xgal. One blue-staining clone was designated H54, and used to generate a genomic library from which the recombinant β-galactosidase gene *bgaHa* was isolated as a 3310 bp *Hind*III–*Age*I fragment. The *bgaHa* fragment was cloned in pBluescript to generate pTA128 and its sequence was compared to the *H. volcanii bgaHv* and *H. alicantei bgaH* genes.

2.6.3 Computer Analyses

All primer design, sequence analysis and protein sequence analysis was carried out using MacVector 9.5.2 (Macvector Inc.). Predicted hydrophobicity plots were generated using Sweet/Eisenberg method with a window size of 3. Sequence alignments were performed using Clustal W (Thompson et al., 1994) (Gonnet Series with an open gap penalty of 15.0, extended gap penalty of 0.2 and a Delay Divergent value of 40%). Protein structures were obtained from Protein Data Bank (www.rcsb.org/pdb/) and analysed with MacPyMol (DeLano Scientific).

2.6.4 Manipulation and analysis of nucleic acids

Restriction enzymes, T4 DNA ligase, Antarctic phosphatase and Klenow (DNA polymerase I, large fragment) were supplied by New England Biolabs (NEB) unless otherwise stated.

2.6.5 PCR amplification

Amplification of DNA was performed using either Phusion or DyNAzyme, (Finnzymes). Phusion was used for amplifications where higher fidelity was required. Dynazyme was used for diagnostic amplifications. For DyNAzyme, 200 µM of each dNTP, 0.5 µM of each primer, 10-50 ng of template DNA, 1 x Optimised DyNAzyme Buffer, 5% DMSO and 1 U of Dynazyme in 50 µl volume was used for each reaction. For Phusion, 200 µM of each dNTP, 0.5 µM of each primer, 10 ng of template DNA, 1 x Phusion GC buffer (supplied), 5% DMSO and 1 U of Phusion in 50 µl volume. Reaction conditions are shown in Table 2.2. Annealing temperatures (Tm°C) were calculated using the equation.

$$81.5+(16.6*\mathrm{Log}_{10}(([Na^{+}]/1000)/(1+(0.7*[Na^{+}]/1000))))+(0.41*\%GC)-(1*(100-Homology\%))-(600/Length(bp))$$

GC refers to the percentage of guanine and cytosine present in the primer. Homology refers to the percentage homology shared between primer and template and Length refers to the length of the primer in bp. All reactions were carried out using a Techne TC-512 thermocycler.

Step	DyNAzyme	Phusion
Initial Denaturation	94°C, 120 sec	98°C, 30 sec
Denaturation	94°C, 15 sec	98°C, 10 sec
Annealing	Tm°C, 20 sec	Tm°C, 15 sec
Extension	72°C, 50 sec/kb	72°C, 20 sec/kb
Cycles	30	30
Final Extension	10 min	10 min

Table 2.2 Reaction conditions for PCR amplifications using DyNAzyme and Phusion DNA polymerases.

Amplification of templates with <100% homology to primer (Touchdown PCR)

When primers were not completely homologous to the template DNA, e.g. for introducing restriction sites or mutations into PCR products, two annealing temperatures were calculated, one based on the original percentage of homology (Tm_s) and one based on 100% homology (Tm_e). Annealing temperatures of reactions started with Tm_s and were raised by 1°C per cycle until Tm_e was reached. Subsequent cycles used Tm_e as the annealing temperature until a total of 30 cycles were complete.

2.6.6 Plasmid DNA extraction

QIAGEN QIAprep Spin Miniprep Kit or Plasmid Midi Kit was used to obtain circular plasmid DNA from *E.coli* strains by standard alkaline lysis, according to the manufacturer's guidelines. Plasmid purifications were carried out by miniprep when large yields of plasmid DNA were not required, e.g. for verification plasmids by restriction analysis and gel electrophoresis. The Plasmid Midi Kit was used when large, ultra-pure DNA yields were required, i.e. for frozen stocks of DNA and transformations of *H. volcanii*.

2.6.7 PCR purification / nucleotide removal / purification of DNA from agarose

PCR and Klenow-end filled DNA products were purified using QIAquick PCR Purification kit (QIAgen). Ligation, restriction digest and dephosphorylated DNA products were purified using QIAquick Nucleotide Removal kit (QIAgen). DNA was extracted from agarose gels using QIAquick Gel Extraction kit (QIAgen). Kits function to purify DNA by salt and pH dependent adsorption of DNA to a silica-gel membrane to separate from nucleotides and proteins, followed by elution in 30 µl volume of 10 mM Tris.HCl pH 7.5

2.6.8 Ethanol precipitation of DNA

0.1 volumes of 3 M sodium acetate pH 5.3 and 2 volumes of 100% ethanol were added to DNA samples and placed at -20°C for 2 hrs. Samples were centrifuged at 14,000 g for 30 mins at 4°C. The supernatant was removed and pellets were washed in 500 µl 70% ethanol followed by centrifugation at 14,000 g for 15 mins. The supernatant was removed and pellets were air-dried before resuspension in sterile H_20.

2.6.9 Restriction digests

All restriction enzymes were supplied by New England Biolabs (NEB). Digests were carried out as by the manufacturers instructions (NEB), except that all digests were supplemented with 200 ng/µl BSA, provided by NEB. Each 1 µg of DNA was digested with 5 units of enzyme for at least 1 hr.

2.6.10 Dephosphorylation of vector DNA

To prevent self-ligation of vector DNA, 5' phosphate groups were removed following restriction digest, using Antarctic phosphatase (NEB). Samples were incubated with 5 units Antarctic phosphatase/µg of DNA and 1 x Antarctic phosphatase buffer for 30 mins at 37°C. Phosphatase was inactivated by heating to 65°C for 15 mins, and DNA was purified using QIAquick Nucleotide Removal kit as described earlier.

2.6.11 Klenow end filling

When DNA ends were incompatible for ligation, Klenow (DNA polymerase I large fragment - NEB) was used to generate blunt ends. 1 µg DNA samples were incubated with 16 µM dNTPs, 1 x NEBuffer 2 (NEB) and 0.5 U Klenow for 30 mins at room temperature, followed by heat inactivation at 75°C for 15 mins. DNA was purified using QIAquick Nucleotide Removal kit, as described earlier.

2.6.22 Ligation of DNA

Ligations were performed using T4 DNA ligase (NEB). Reactions contained 5 U ligase, 1x T4 ligase buffer per 1 µg DNA. Ligations between substrates with either 5' or 3' overhangs were carried out at 15˚C for 16 hrs. Ligations between blunt ended DNA substrates were carried out at 4˚C for 36 hrs. Reactions were heat inactivated at 65°C for 15 mins. For vector:insert ligations, reactions contained a molar ratio of ~3:1 insert to vector DNA.

2.6.23 Agarose gel electrophoresis

Agarose gels were cast using either RESponse Research PCR agarose or AGTC Bioproducts Ltd hi-res standard agarose powder and Tris-borate EDTA (TBE) buffer (89 mM Tris base, 89 mM boric acid, 2 mM EDTA pH 8.0). PCR agarose was used for separation of small DNA fragments (i.e. 100 – 600 bp) and the standard agarose was used to resolve DNA fragments of 600 bp or more. Gels were supplemented with ethidium bromide at a final concentration of 0.5 µg/ml unless otherwise stated. DNA samples were mixed with a $^1/_5$ by final volume of 5x gel loading dye. Gels were run at 5 V/cm voltage gradient for 1 hr unless otherwise stated.

2.6.24 Agarose gel extraction and purification of DNA

DNA was visualised by UV light using a UV transilluminator (UVP inc.) and excised in the smallest gel slice possible. DNA was purified using the QIAquick gel extraction kit (QIAgen), as described earlier.

2.6.25 DNA sequencing and oligonucleotide synthesis

All sequencing reactions and analysis, and synthesis of oligonucleotides was carried out by the Biopolymer Synthesis and Analysis Unit. Sequencing was carried out using the dideoxy chain termination method (Sanger et al., 1977).

2.6.26 Generation of radiolabelled DNA probes by random priming

3 µl of template DNA (10 - 25 µg/ml), 2 µl of appropriate DNA ladder if required (1 µg/ml), and 10 µl of water were boiled for 5 minutes and then chilled on ice. 0.37 Mbq α–^{32}P dCTP (GE Healthcare, Amersham Redivue) was added along with 4 µl Hi Prime random priming mix (Roche). The mixture was incubated at 37˚C for 30 minutes and purified using a BioRad P30 column. The resulting probe was mixed with 450 µl of fish sperm DNA (10 mg/ml), boiled for 5 minutes then chilled on ice, ready for use.

2.6.27 Southern Blots

Agarose gels were stained in 1litre of 0.5µg/ml ethidium bromide solution for 30 minutes with gentle rocking. The gel was then visualised on a Geldoc (BioRad) to ensure that complete digestion of DNA had occurred. The gel was transferred to 1 litre of 0.25 M HCl for 20 minutes to depurinate DNA. The gel was then washed in 1 litre of water for 10 mins and then denatured for 40 minutes in denaturing solution. A 15 x 25 cm Zeta-Probe GT positively charged membrane (BioRad) was soaked in water for 5 minutes then transferred to sufficient denaturing buffer to cover the membrane. The membrane and gel were positioned on a Vacugene XL gel blotter (Pharmacia Biotech). Sufficient denaturing solution was poured on the gel to cover it and the DNA was transferred to the membrane for 1 hour at 40 mBar vacuum, provided by a Vacugene Pump (Pharmacia Biotech). Immediately following transfer, the membrane was washed briefly in 2x SSPE and allowed to dry on Whatman 3MM blotting paper.

DNA was crosslinked to the membrane with 150 mJ/cm^2 UV light and placed in a hybridisation tube (Techne) with 40 ml of prehybridisation solution. 800 µl of fish sperm DNA (10 mg/ml) (Roche) was boiled for 5 minutes then chilled on ice and added to the hybridisation tube. The membrane was incubated at 65˚C for 4 hours with rotation to allow prehybridisation. After 4 hours, the prehybridisation solution was replaced with 30ml hybridisation solution. A prepared radiolabelled DNA probe and fish sperm DNA were added and the membrane was hybridised overnight at 65˚C with rotation.

The following day, the hybridisation solution was replaced by 50 ml of low stringency wash solution and incubated for 5 minutes at 65˚C. The wash solution was then replaced by a further

50 ml and incubated at 65˚C. After 30 minutes, the wash solution was poured away and 50ml of high stringency wash solution was added. The membrane was incubated as before for 30 minutes before the wash solution was replaced by a further 50ml and incubated for a further 30 minutes. After the final wash, the membrane was allowed to dry briefly on 3MM Whatman blotting paper and wrapped in Saran wrap. The membrane was then allowed to expose using a phosphorimager screen (Fujifilm BAS Cassette2 2325) for at least 12 hours. The screen was then scanned using a Molecular Dynamics STORM 840 scanner and the resulting graphical file was refined using L-Process and analysed using Image Quant (Fujifilm).

2.6.28 Colony lift and colony hybridisation

An 82mm filter (Biorad) was rolled onto the surface of agar plates patched with colonies and left at room temperature for 1 min. The filter was then removed carefully and placed colony side up on blotting paper soaked with 10% SDS and left for 2 minutes to allow cell lysis. The filter was then placed colony side up on blotting paper soaked in denaturing solution for 5 minutes, to denature the DNA. Following this, the filter was then transferred, colony side up, to blotting paper soaked in neutralising buffer and left for 3 minutes. A second neutralising step was carried out as before. The filter was then washed in 2x SSPE for 5 minutes then allowed to dry briefly on fresh blotting paper.

DNA was then UV crosslinked to the filter, prehybridised, hybridised, washed, exposed and visualised in the same manner as described in the Southern Blotting methods, with the exclusion of marker ladder DNA from the probe template mixture. The DNA probe used was dependent on the procedure. If the aim was to hybridise potential clones, the probe would be a PCR amplification of a portion of the gene (> 100 bp in size). If detecting a gene deletion the probe would be a digest or amplification of a portion of the gene, not present in the deletion construct.

2.7 General *Escherichia coli* microbiology

2.7.1 Growth of *Escherichia coli* and storage

Cultures on solid media were grown at 37°C in a static incubator (LEEC). Liquid cultures were grown in the same incubator with 8 rpm rotation. For short term storage, plates and cultures were stored at 4°C. For long term storage, 25% (v/v) glycerol was added to cultures, mixed and flash frozen on dry ice. Frozen cultures were then stored at -80°C.

2.7.2 Preparation of electrocompetent *Escherichia coli* cells

An overnight culture of either strain XL-1 Blue or N2338 strain (*dam+ and dam-* strains, respectively) was grown. Antibiotic selection was dependant on the strain: XL-1 Blue

overnight cultures were supplemented with 50 µg/ml ampicillin and 3.5 µg/ml tetracycline, and N2338 overnight cultures were supplemented with 50 µg/ml ampicillin alone. Cells were diluted 1/100 in L broth, supplemented with appropriate antibiotics as described, and grown at 37˚C to A_{650} = 0.5-0.8. Cells were pelleted at 6000 g for 12 minutes at 4˚C and the supernatant was removed and the pellet resuspended in an equal volume of ice-cold sterile 1 mM HEPES (pH 7.5). This process was repeated using 0.5 volumes 1 mM HEPES, 0.25 volumes 1 mM HEPES + 10% glycerol, 0.1 volumes 1mM HEPES + 10% glycerol, and finally 0.001 volumes 1mM HEPES + 10% glycerol. Cells were flash frozen on dry ice and stored in 50 µl aliquots at -80°C.

2.7.3 Transformation of *Escherichia coli* by electroporation

1 µg of DNA in 4 µl sterile dH_20 was added to 50 µl of electrocompetent cells, on ice. The mixed sample was added to a pre-chilled electroporation cuvette (1 mm electrode gap, GENEFLOW). The cuvette was placed in an *E.coli* gene pulser (BioRad) and subjected to a 1.8 kV pulse. 1 ml of SOC was added immediately and samples were incubated at 37°C with 8 rpm rotation for 1 hr. Cells were plated onto LB+Amp plates and incubated at 37°C overnight.

2.7.4 Mini/Midi scale purifications of *Escherichia coli* plasmid DNA.

Purification of plasmid DNA was performed using the QIAquick Mini / Midi prep columns, as per the manufacturer's instructions. This method utilises alkaline lysis of cells followed by binding of plasmid DNA to an anion-exchange resin in high salt. DNA was then eluted in 50 µl buffer EB (QIAgen) for Mini-preps and 100 µl TE for Midi-preps. DNA samples were frozen at -20°C.

2.7.5 Generation of unmethylated (*dam*-) plasmid DNA

dam- (DNA adenine methylase) DNA was required for the transformation of *Haloferax volcanii* as this organism possesses a restriction endonuclease that cleaves DNA at 5'-$GA^{(CH3)}$TC-3' sequences. Therefore, unmethylated plasmid DNA was necessary to prevent degradation. This was achieved by transforming *dam- E.coli* strain N2338 with 1 µg of plasmid DNA extracted from XL1 Blue, followed by plating on LB+Amp and overnight incubation at 37°C. DNA was then extracted as usual, ready for transformation of *H.volcanii*.

2.8 General *Haloferax volcanii* microbiology

2.8.1 Growth of *Haloferax volcanii* and storage

Cultures on solid media were grown at 45°C in a static incubator (LEEC) in a plastic bag to prevent desiccation. Liquid cultures were grown in the same incubator with 8 rpm rotation. For short term storage, plates and cultures were stored at room temperature. For long term

storage, 20% glycerol (v/v) was added to cultures, mixed and flash frozen on dry ice. Frozen cultures were then stored at -80°C.

2.8.2 Extraction of genomic DNA from *Haloferax volcanii*

1 ml of culture at OD_{650} = 0.8 was transferred to a 2 ml round bottom tube. Cells were pelleted at 3300 g for 8 mins. The supernatant was removed and cells were resuspended in 200 µl of ST buffer. 200 µl of lysis buffer was then added and mixed by inversion. The cell lysate was overlaid with 1 ml of 100% ethanol to precipitate DNA at the interface. DNA was then spooled onto a capillary gel loading tip by brisk stirring at the interface and allowed to dry briefly at room temperature. The pipette tip was then transferred to 500 µl of TE and the DNA resuspended. DNA was further purified by ethanol precipitation and resuspended in 100 µl of TE buffer by agitation using an Eppendorf Thermomixer Comfort shaking hot-block (45˚C, 600 rpm) for 1 hr . Complete resuspension of DNA was achieved by incubation at 4˚C overnight.

2.8.3 Extraction of plasmid DNA from *Haloferax volcanii*

Plasmid DNA was extracted from *Haloferax volcanii* using QIAquick mini prep kit (QIAgen). The procedure was the same as for *Escherichia coli* except cells were initially resuspended in ST buffer instead of P1 buffer (NEB).

2.8.4 Generation of Plasmid-borne *Haloferax volcanii* Genomic DNA Libraries

5 µg of genomic DNA was partially digested with *Aci*I by using buffer NEB 1 instead of NEB 3 to reduce the activity of the enzyme to 25%. Additionally, instead of using 5 units of enzyme per 1 µg DNA, 0.2 units were used instead.

Digested samples were electrophoresed and a gel slice was extracted between 2.5 kb and 5 kb. Following purification, the digested genomic DNA was ligated with 3 µg of *Cla*I cut and dephosphorylated pTA230 [*pyrE2*+, pHV2 ori]. The resulting plasmid library was used to transform *E.coli* strain N2338 that was subsequently plated on LB+Amp. Colonies were swept off transformation plates after overnight incubation at 37˚C with the aid of a plate spreader and 1 ml of LB media per plate. Library DNA was extracted immediately by use of QIAgen maxiprep kit, and used to transform *Haloferax volcanii* and plated on media containing no uracil.

2.9 Genetic manipulation of *Haloferax volcanii*

The deletion of a chromosomal copy of a gene requires the identification of the gene in the genome, cloning of the gene onto a plasmid and the generation of a plasmid-borne deletion construct. The plasmid (usually pTA131) also requires *pyrE2*. The deletion construct is used

to transform the desired strain, where the plasmid integrates at the desired gene locus (Figure 2.1). Following this integration, the plasmid must recombine out of the chromosome along with the original chromosomal gene to leave behind the gene deletion construct. This is achieved by relieving selection for uracil and plating on media supplemented with 5-FOA to select against any remaining plasmid integrant cells (Figure2.1). Colonies are then hybridised with a probe derived from an internal sequence of the gene to be deleted. Colonies that do not hybridise the probe are deleted for the gene. This is then confirmed by Southern blot analysis.

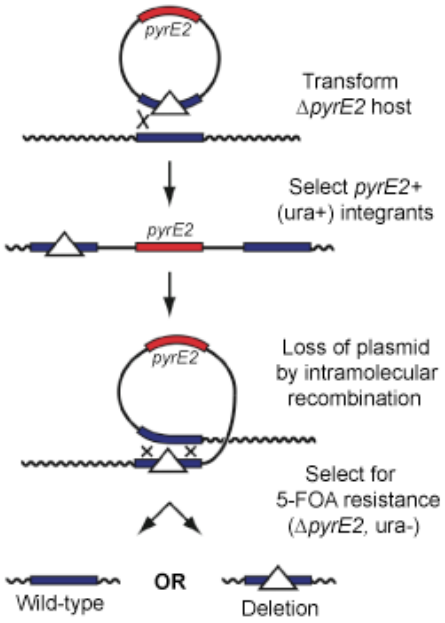

Figure 2.1 Chromosomal gene deletion by selection and counter-selection of an integrative plasmid. A Δ*pyrE2* host is transformed with a *dam*- plasmid containing *pyrE2* and a deletion construct of the desired gene. The plasmid integrates at regions of homology to the locus of the gene to be deleted, conferring uracil prototrophy (ura+). Once the integratant strain has been confirmed by Southern blot analysis, selection for uracil is relieved by serial growth in Hv-YPC (+ Thy if required). The plasmid recombines from the chromosome and ura- (Δ*pyrE2*) derivatives are selected for by plating on 5-FOA plates. Depending on the orientation of the second recombination event relative to the first, the resulting strain will be either deleted for the desired gene or remain as wild-type. These can be differentiated by colony blotting

2.9.1 Obtaining genomic clone of a gene

Predicted genes were identified using translated BLAST search (tBLASTx) (NCBI) on the *H. volcanii* genome (TIGR) using an appropriate query sequence, i.e. the desired gene from a related organism. The candidate gene in *Haloferax volcanii* was mapped and restriction sites at least 500 bp upstream and downstream (but not present in between) were located. The sites were also present in the multiple cloning site of pBluescript II SK+. Genomic DNA was isolated from strain H26, as described in 'Isolation of *Haloferax volcanii* genomic DNA' section, and digested with appropriate enzymes overnight to ensure complete digestion. Digested genomic DNA was then electrophoresed and a gel slice was extracted of the predicted fragment size. DNA was purified from agarose and ligated with cut and dephosphorylated pBluescript II SK+. Plasmid library DNA was used to transform XL-1 Blue *E.coli* and plated at appropriate dilutions on LB+Amp. Plates were incubated overnight at 37˚C and colonies were patched onto LB+Amp and allowed a further overnight incubation at 37°C. PCR primers were designed complementary to a region of the desired gene to generate a product of 150 - 500 bp. Colony lifts and blots were made of the patch plates. The PCR amplification product was used as a template for the radiolabelled probe. Colonies that hybridised with the probe contained the desired gene and were picked off the original plate and streaked on LB+Amp, and used to inoculate an LB+Amp overnight culture. Plasmid DNA was extracted from these cultures and sequenced using primers external to the gene, to confirm the desired clone.

2.9.2 Deletion constructs

Deletion constructs for the purpose of cloning into a *pyrE2* marked plasmid, pTA131, and subsequent transformation of *Haloferax volcanii* were generated by two methods.

2.9.3 Generation of deletion constructs by restriction digest

If appropriate restriction sites could be found immediately flanking or internal to the gene in question, the plasmid containing the gene was digested with the enzymes, and if necessary, the resulting DNA ends were filled in using Klenow and ligated together as described above. This method could only be carried out if the restriction sites present immediately flanking the gene to be deleted were not present elsewhere in the plasmid, excluding the gene itself.

If the deletion construct was not present on a plasmid containing a selectable marker (usually *pyrE2*, e.g. pTA131) it was excised using restriction enzymes present in the polylinker of both donor and recipient plasmid and ligated into a plasmid containing the selectable marker (e.g. pTA131). This process is summarised in Figure 2.2.

2.9.4 Generation of deletion constructs by PCR

Two pairs of primers were designed, one pair to amplify a region >150 bp upstream of the promoter of the gene to be deleted and the other pair to amplify >150 bp downstream of the termination codon of the gene to be deleted. Novel restriction sites were introduced into the primers. For the two internal primers, the same restriction site was introduced so that both PCR products could be ligated. The external primers >150 bp up and downstream of the gene included restriction sites that are present in the polylinker region of pTA131, unless otherwise stated. A maximum of 3 bp were changed to introduce these novel restriction sites, and when this was not possible, restriction sites that yield blunt ended DNA were chosen instead. Any site that was introduced was unique and was not present anywhere else in the PCR products.

Phusion DNA polymerase was used to ensure maximum fidelity. Touchdown PCR

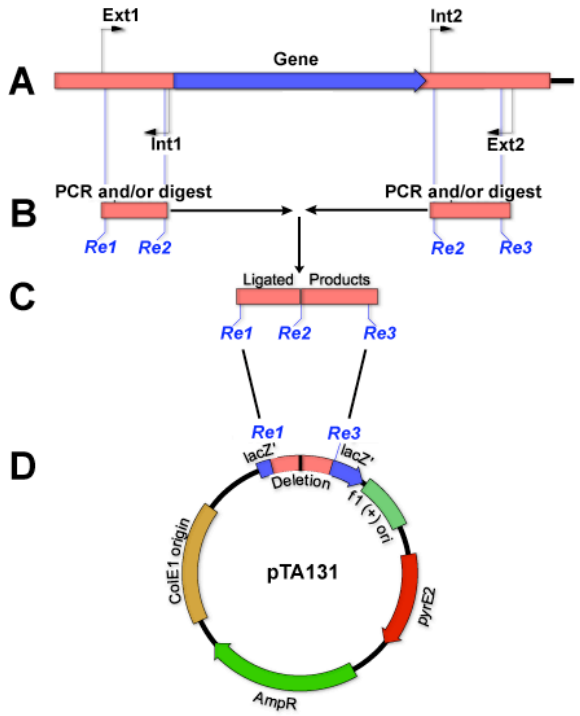

Figure 2.2 Schematic of the generation of gene deletion constructs by PCR and/or restriction digest. **Restriction Digest** – **(A)** Restriction sites flanking the gene are digested from plasmid-borne gene clone (**B**). **(C)** Products are ligated and then ligated into pTA131 polylinker (**D**) unless stated otherwise. **PCR and Digest** – (**A**) Pairs of primers are designed to amplify flanking sequence of gene (Int1 and Ext1, and Int2 and Ext2) and to contain novel restriction sites (*Re1, Re2* and *Re3*). (**B**) Amplification products are digested with *Re2* and ligated. (**C**) Ligated product is digested with *Re1* and *Re3*, and ligated into polylinker of pTA131 (**D**) unless otherwise stated.

amplifications using both sets of primers were carried out as described earlier. Products were electrophoresed and extracted from the agarose gel and digested with the restriction enzyme corresponding to the introduced sites immediately 5' and 3' of the gene to be deleted. DNA was purified using a PCR purification column (QIAgen) in accordance to the manufacturers instructions, to remove the short end fragments released following digestion. Products were then ligated together as described above, then digested with the enzymes corresponding to the introduced restriction sites distal to the gene in question, passed through a PCR purification column and ligated with pTA131 (cut with the same enzymes) (Figure 2.2).

2.9.5 Generation of mutant allele constructs

To generate alleles containing a point mutation , two pairs of PCR primers were designed: One pair to bind the sense DNA strand at the region where the mutation was to be introduced (Int1) and one at least 100 bp downstream on the antisense strand (Ext1). The other pair consisted of an antisense binding primer entirely complementary, or staggered by a few bases, to the sense primer of pair one (Int2), and a sense strand binding primer at least 100 bp upstream (Ext2). Primers Int1 and Int2 contained base substitutions that would generate the desired mutation in the two resulting PCR amplification products. Additionally, wherever possible substitutions were made to either generate or remove a restriction site to identify the mutation by restriction analysis. No more than three base substitutions were made for each primer. Ext1 and Ext2 contained unique restriction sites. Alternatively, pre-existing sites internal to the flanking primers (Ext1/Ext2) were used to subclone the final mutated allele/fragment back into the original construct (Figure 2.3)

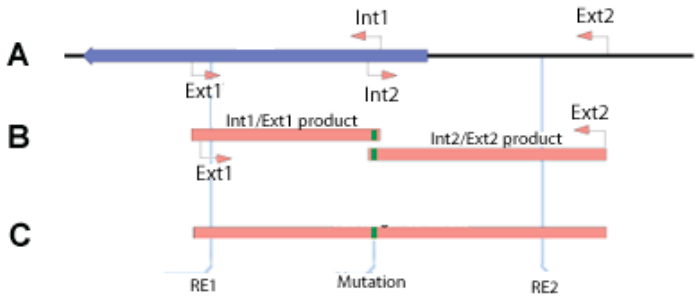

Figure 2.3 Generation of mutant alleles by PCR. **A** Primers are designed to amplify two halves of the mutant construct, with both internal primers (Int1/Int2) annealing to the point where the mutation will be introduced. Int1 and Int2 contain substitutions to generate the mutation, and a novel restriction site. **B** Amplified constructs are used as a template for second PCR, using external primers (Ext1 and Ext2). **C** – Full length product is cut with enzymes corresponding to novel restriction sites (e.g., RE1 introduced by Ext1) or sites internal to flanking primers (e.g. RE2). The mutant fragment can be used to replace a wildtype fragment on a plasmid

PCR conditions were as described previously and the amplification products were electrophoresed and extracted. 0.5 µg of each product was used as a template for one further PCR amplification using primers Ext1 and Ext2 to generate a full-length mutation product. This product was electrophoresed, gel extracted and then digested with enzymes compatible with unique restriction sites upstream and downstream of the substitutions. The original plasmid used as a template was similarly digested and ligated with the PCR product to generate a plasmid-borne full-length mutated allele. This process is summarised in Figure 2.3 .

2.9.6 Transformation of *Haloferax volcanii*

10 ml cultures were grown to OD_{650} = 0.8 and cells were pelleted by centrifugation in a 10 ml round-bottom tube at 3300 g for 10 mins. The supernatant was removed and cells were resuspended in 2ml of buffered spheroplasting solution and transferred to a 2 ml round-bottom tube (Eppendorf). Cells were pelleted again and the supernatant removed as before. Cells were resuspended gently in 600 µl buffered spheroplasting solution. 200 µl of this was used per transformation and transferred to a fresh 2 ml tube. 20 µl 0.5 M EDTA (pH 8.0) was added, mixed by gentle inversion and incubated at room temperature for 10 minutes to allow removal of the *Haloferax volcanii* S-layer (spheroplasting). A 30 µl DNA sample was prepared (15 µl unbuffered spheroplasting solution, 5 µl 0.5M EDTA (pH 0.8), 1µg plasmid DNA (containing an auxotrophic marker and gene of choice) prepared from *dam- E.coli* host, and water to final volume of 30 µl), and added to the spheroplast cells and mixed as before.

After five minutes, 250 µl of 60% polyethylene glycol 600 (PEG 600) (150 µl PEG 600 and 100 µl unbuffered spheroplasting solution) was added and mixed by gentle rocking 10 times. The mixture was incubated at room temperature for 30 minutes, then diluted with 1.5ml of spheroplast dilution solution and mixed by inversion. After 2 minutes the cells were pelleted at 3300 g for 8 mins and the cell pellet was transferred to a sterile tube containing 1 ml of regeneration solution, supplemented with 60 µg/ml thymidine if required (Δ*hdrB* strains). To allow recovery of cells, the tube was incubated for 90 minutes at 45˚C. The pellet was then resuspended by gently tapping the tube and incubated at 45°C with 8 rpm rotation for 3 hrs.

Cells were transferred to a fresh 2ml round-bottom tube and centrifuged at 3300 g for 8 mins. The cell pellet was resuspended gently in 1ml of transformation dilution solution. Appropriate dilutions were made and 100 µl of each dilution was plated on appropriate media lacking either uracil, leucine, tryptophan or thymidine, depending on the selectable marker present on the transformed plasmid (*pyrE2, leuB, trpA or hdrB*, respectively), and supplemented with appropriate additives where necessary. Plates were incubated for at least 5 days at 45˚C to allow colony growth.

2.9.7 Confirmation of transformed *Haloferax volcanii* genotypes.

If a strain was transformed with an integrating plasmid, integration of the plasmid onto the chromosome was verified by appropriate restriction digest of genomic DNA, electrophoresis of DNA on a 200 ml TAE 1% agarose gel and Southern blotting using an appropriate probe. If a strain was transformed with a replicative plasmid, the presence of the plasmid and its sequence was confirmed by extracting the plasmid DNA followed by diagnostic restriction digest and/or DNA sequencing.

2.9.8 Loss of pyrE2 marked plasmids from an integrant *Haloferax volcanii* strain

After verifying the genotype of a plasmid integrant strain, a second recombination event that would remove an integrated *pyrE2*-encoding plasmid from the chromosome was encouraged by relieving uracil selection. 5 ml of Hv-YPC broth was inoculated and incubated at 45°C with 8 rpm rotation. OD_{650} = 0.6 cultures were diluted 500-fold in fresh culture and grown again. This was repeated two more times, to encourage the integrated plasmid to recombine out of the chromosome of cells, thus becoming ura-.

1 ml of culture at OD_{650} = 0.6 was pelleted at 3300 g for 8 mins, and the cell pellet resuspended in 18% SW. Appropriate dilutions were made (10^0, 10^{-1} and 10^{-2} unless otherwise specified) and plated on Hv-Ca + 5FOA, in addition to other required additives. 5-FOA was necessary to counterselect against any remaining *pyrE2*+ (plasmid integrant) cells, therefore only Δ*pyrE2* colonies with either the original chromosomal sequence or the gene deletion/mutant allele construct would form colonies. Plates were incubated at 45˚C for at least five days to allow colony formation, and colonies patched onto YPC plates (+Thy if Δ*hdrB*) (40 patches per plate).

2.9.9 Loss of pyrE2 marked replicative plasmids from *Haloferax volcanii*

Selection for uracil was relieved as with 'Loss of *pyrE2* marked plasmids from an integrant *H. volcanii* strain', by serial propagation of cultures in media supplemented with uracil. This encourages the loss of the replicative plasmid. Cultures were plated on Hv-Ca + 5FOA agar to select against cells that still contain the replicative *pyrE2* marked plasmid.

2.9.10 Identification of desired derivative strains

Depending on the nature of the desired chromosomal replacement, different procedures were carried out to identify the correct strain. The two different methods are described: One for identifying deletion strains and the other for identifying the replacement of chromosomal genes with a different allele.

2.9.11 Gene deletion: Colony hybridisation

If the desired strain contained a deletion of a gene, 5-FOA resistant colonies were patched on YPC (+Thy if required) and grown at 45°C for 5 days. Colony lifts and hybridisations were carried out using a probe homologous to the deleted fragment. Strains deleted for the gene could be identified as they will not bind the probe.

2.9.12 Allelic replacement: colony PCR and restriction digest

If the desired strain contains a different allele to the original chromosomal allele, colony hybridisation could not be utilised as the probe would bind all colonies. Instead, cultures were grown from 5-FOA resistant colonies and genomic DNA extracted. PCRs were carried out to amplify the region of the gene containing the mutation. As described earlier, mutant alleles generally had novel restriction sites introduced or an existing one removed at the mutation site. 1 µg of the PCR product was digested with the appropriate enzyme corresponding to the restriction site introduced/lost and electrophoresed. By analysing the size of the resulting restriction fragments, the genotype of the strain could be deduced. Additionally, primers external to the gene in question were used to sequence the gene to confirm that no other undesirable mutations were present.

2.10 *Haloferax volcanii* assays

2.10.1 UV survival tests

Irradiation of cells on solid media

Strains were grown to OD_{650} = 0.8. 1 ml of culture was pelleted by centrifugation and resuspended in 1 ml of 18% SW. Serial dilutions were made from 10^0 to 10^{-6} and duplicate 20 µl drops of culture were pipetted onto Hv-YPC agar (+Thy if required). Applied culture was allowed to dry at room temperature and plates were either exposed to ultraviolet light at a rate of 1 J/m^2/second (254 nm peak) or not exposed to UV light, as a control. Plates were shielded from visible light by use of a black plastic bag to prevent photo-reactivation of DNA, and incubated at 45°C until colonies were visible.

Irradiation of cells suspended in liquid

Strains were grown until OD_{650} = 0.8. 2 ml of culture was pelleted by centrifugation and resuspended in 1 ml of 18% salt water. Samples were pipetted onto the centre of a Petri dish and a sterile, small magnetic stir bar was carefully placed into the culture spot. The plate was placed on a Stuart CB162 magnetic stirrer that was set to stir the culture rapidly without splashing. Cells were then UV irradiated as above, and following irradiation, cells were

pelleted and resuspended in the dark, in an equal volume of Hv-YPC broth. Appropriate dilutions were then made as above and 20 µl spots were pipetted onto complex media. Plates were wrapped in a black plastic bag to prevent photo-reactivation of DNA and incubated at 45°C until colonies were visible.

2.10.2 Mitomycin C sensitivity assays

Hv-YPC and Hv-YPC + Thy plates were poured as usual but were supplemented with 0.01%, 0.02% and 0.04% mitomycin C (w/v). 20 µl aliquots of OD_{650} = 0.8 culture were pipette onto plates at dilution ranging from 10^0 to 10^6 and allowed to dry. Cells were also pipetted onto YPC or YPC + Thy plates containing no mitomycin C as a control. Plates were incubated at 45°C for 5-10 days until colonies formed.

2.10.3 Growth rate assays

Colonies were used to inoculate 10 ml of Hv-YPC broth (+ Thy if required) and incubated at 45˚C until OD_{650} = 0.4. At this stage, 100 µl of the culture was plated at a dilution of 10^{-6} on complex media to determine the initial cell density. The remaining culture was diluted to 10^{-4} fold, 100 µl of each plated directly on Hv-YPC agar (+Thy if required) and 10 ml was returned to incubate at 45˚C. At regular intervals, 20 µl aliquots of culture were plated on complex media at appropriate dilutions ranging from 10^0 to 10^{-6} until $A_{650} \approx 0.8$ was reached.

2.10.4 Recombination assays

The following section describes several *Haloferax volcanii* transformation assays designed to test the proficiency of recombination. Some aspects are common to all procedures and these will be outlined first.

Initial cell density

All cultures used for transformation were grown until OD_{650} = 0.8 so that cells were in early stationary phase. Liquid media used was Hv-YPC broth (+Thy if required), unless otherwise stated.

Transforming plasmids

1 µg of plasmid DNA was used to transform strains unless otherwise stated.

Plating of transformants

Transformants were plated on media to select for the appropriate marker(s) on the transforming plasmid, either containing no uracil and/or no leucine, as outlined in each protocol. Additional media supplements were added where necessary, e.g. if the strain being transformed was also

trpA- but selection of tryptophan was not relevant to the assay, media was supplemented with tryptophan. Transformants were plated at dilutions ranging from 10^0 to 10^{-3}.

Viable cell count

It was essential to determine the total surviving cell count for all transformation assays. This was obtained by plating dilutions of the transformations on non-selective media (Hv-YPC, + Thy if required) at dilutions ranging from 10^{-4} to 10^{-6}.

Recovery phase and subsequent growth

All transformations were allowed to recover for 4.5 hrs at 45˚C, 1.5 hrs as a pellet with no agitation followed by 3 hrs resuspended and with rotation. Following plating, transformants were incubated for 8 - 10 days at 45˚C

Plasmid by chromosome crossover recombination frequency assay

Cells were transformed with pTA159 [*pyrE2+, bgaHa-Kp*]. The number of *pyrE2+* colonies was scored to measure the proportion of cells carrying out crossover recombination by integration of the plasmid at the *bgaHa* locus.

Non-crossover vs crossover recombination assay

Cells were transformed with pTA168 [*pyrE2+, leuB-Aa2*]. Transformants were plated on Hv-Min +Trp+Thy+Ura to select for cells that had undergone a recombination event between plasmid-borne *leuB-Aa2* allele and chromosomal *leuB-Ag1* allele (generating a wildtype *leu+* allele), whether crossover or non-crossover. Colonies were patched on Hv-Min +Trp+Thy , to select for crossover recombination events in cells that had integrated the plasmid and become *pyrE2+ leu+*, and on Hv-Min +Trp+Thy+Ura as a control to ensure that all colonies patched were *leu+*. From these data, a percentage of crossover events (*leuB+ pyrE2+*) vs total recombination events (*leuB+*) could be derived, therefore the remaining recombination events (*leuB+, pyrE2*$^{--}$) were non-crossover recombination events.

Transformation was also carried out using water instead of DNA, to control for reversion of the mutant chromosomal *leu*B-*Ag1* allele to wildtype. The rate of reversion of the chromosomal *leu*B-*Ag2* allele was calculated by dividing the number of colonies present on water control plates by the viable count. This value was then used as a weighting index and multiplied by the viable count for the pTA168 transformation. The resulting value was the expected number of colonies present that were l*euB+* through reversion and not by recombination with pTA168. However, no reversions were observed in any of the trials.

Efficiency of crossover recombination with varying lengths of homology

Cells were transformed with pTA156 [*pyrE2+, bgaHa-Bb*], pTA158 [*pyrE2+, bgaHa-Bh*], pTA159 [*pyrE2+, bgaHa-Kp*] and pTA188 [*pyrE2+, bgaHa-Be*]. Following growth, plates were sprayed with Bluetech X-β-gal solution using an atomiser. Plates were then incubated overnight at 45˚C. The following day, blue colonies and pink colonies was scored.

2.10.5 Induction of transcription after DNA damage

Preparation of Samples

Cultures for each strain were grown to OD_{650} = 0.6 and 1 ml was pelleted at 3300 g, followed by resuspension in 18% SW. The sample was separated into two equal 0.5 ml aliquots. One aliquot was UV irradiated (as described in 'UV Irradiation of Liquid Culture') at 20 J/m^2 and the other mock treated (treated the same as the other sample, except without UV irradiation. Both samples were pelleted at 3300 g and resuspended in 0.5 ml Hv-YPC+Thy broth, in the dark and incubated at 45°C with 8 rpm rotation for 30 mins.

Cells from both samples were pelleted and lysed, and RNA protected from degradation, by addition of RNA lysis solution (containing guanidine thiocyanate and β-mercaptoethanol) (Promega).

Isolation of total Haloferax volcanii *cell RNA*

Once samples were lysed, RNA extraction proceeded using a Promega SV Total RNA Isolation kit, where RNA is bound to a silica membrane, DNase treated and eluted. The manufacturer's protocol was followed with two exceptions. Following pelleting, cells were not resuspended in the provided resuspension buffer as this would cause cell lysis through osmotic shock. Instead, the cell pellet was lysed directly with the provided lysis buffer. Secondly, following DNase treatment of the obtained RNA samples, an additional thorough DNase treatment was carried out using Ambion Turbo-DNA free kit, as described in the protocol. The concentration and 260:280 nm ratio of each RNA sample was measured using a Beckman Coulter DU530 spectrophotometer. Samples were separated into small aliquots and stored at -80˚C until required to minimise degradation.

Analysis of Transcripts

Primers were designed that would bind internal to the gene in question, to generate a PCR amplification product of 200 - 300 bp. 100 ng of RNA from each sample was used as a template for reverse transcription PCRs (RT-PCR) using a QIAgen One-Step RT-PCR kit.

Reactions comprised of 1x QIAGEN One-Step RT-PCR Buffer, 400 µM of each dNTP, 0.6 µM of each primer, 3 U SUPERase-in (RNase inhibitor -Ambion), 10 ng RNA, 1 µl QIAGEN One-Step RT-PCR Enzyme Mix, in 25 µl total volume. Reaction conditions were titrated and optimal amplification was obtained with the following conditions.

Step	Time	Temperature
Reverse Transcription	30 min	50°C
DNA polymerase activation	15 min	95°C
Denaturation	0.5 min	94°C
Annealing	1 min	52.2°C
Extension	1 min	72°C
Cycles	26	
Final Extension	10 min	72°C

The resulting DNA amplification products were analysed by electrophoresis, ethidium bromide staining and comparison of band intensity using ImageGauge V4.22 (Fujifilm).

Chapter 3: Characterisation of RadB, a RadA paralogue

3.1 Introduction

In addition to RadA, the archaea possess a second Rad51 homologue, RadB. This protein was discovered on the basis of sequence similarity to Rad51 (Sandler et al., 1999). The primary structure of the RadB monomer shares considerable similarity to the core domains of Rad51 and RadA (Komori et al., 2000b) (Figure 3.1). Early studies of *Pyrococcus kodakaraensis* RadB (Pk-REC) suggested that it is a recombinase, like RadA, as it was reported to complement the UV irradiation sensitivity of *E.coli* RecA mutants (Rashid et al., 1996). It was also suggested that RadB possessed double and single stranded nuclease activity (Rashid et al., 1999; Rashid et al., 1997). However, these observations have since been disproved (Inwood et al., 2001) and the function of RadB remains elusive.

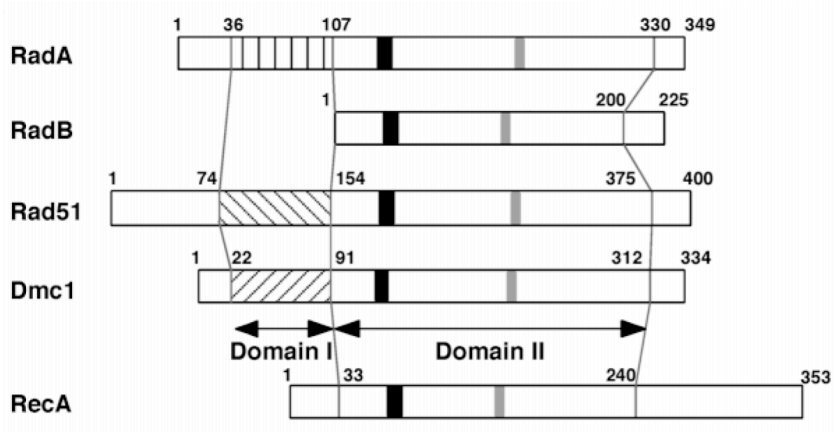

Figure 3.1 Structure comparison of Rad51/RecA family proteins. RadA and RadB have 54 and 29% similarity to Rad51, respectively. The sequence similarity between RadA and RadB is 33%. RadB lacks the conserved N-terminal domain (Domain I) conserved in Rad51 and RadA and consists solely of the conserved core domain (Domain II). This domain contains both Walker A and Walker B motifs for ATP binding and hydrolysis (represented in black and grey, respectively). Figure from (Komori et al., 2000b)

Pyrococcus furiosus (*Pfu*) RadB binds both single and double stranded DNA, with a higher affinity than RadA. RadB also binds ATP but only has an extremely weak ATPase activity, in contrast to RadA (Komori et al., 2000b). Like Rad51 paralogues, RadB does not catalyse

strand exchange and is therefore not a recombinase. Instead, RadB has been implicated as an accessory protein, analogous to eukaryotic Rad55-57 complex (Komori et al., 2000b; Sandler et al., 1999). This hypothesis is reinforced by the demonstration of interactions between RadA and RadB *in vitro* (Komori et al., 2000b). Furthermore, RadB may possess additional roles in recombination. Yeast two-hybrid and immunoprecipitation analysis showed that RadB interacts with Hjc, an archaeal Holliday junction resolvase, and DP1, the small proof reading subunit of archaeal DNA polymerase, PolD (Hayashi et al., 1999; Jokela et al., 2004).

The crystal structure of *Thermococcus kodakaraensis* (*Tko*) RadB has been published (Akiba et al., 2005). *Tko* RadB was shown to crystallise as a dimer, with two orientations depending on salt concentration. In the Type I crystal (Figure 3.2), RadB monomers interact via basic and acidic patches, back to back, and have been proposed to form helical filaments. Although *Pfu* and *Tko* RadB filaments can form filaments in the absence of DNA the number of observed filaments decreases in the presence of DNA (Akiba et al., 2005; Komori et al., 2000b). Furthermore, the low intracellular concentration of RadB is unlikely to correlate with the formation of long helical structures *in vivo* (Reich et al., 2001). Interacting monomers of the Type 2 crystals face opposite directions, therefore making it unlikely that a complex larger than

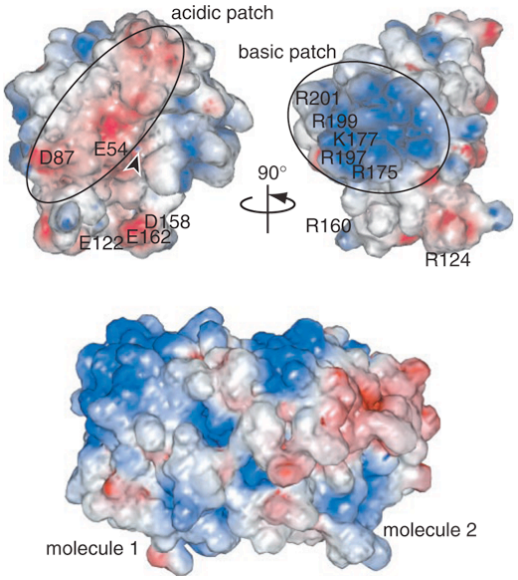

Figure 3.2 Taken from (Akiba et al., 2005).Surface electrostatic potentials of *Tko*-RadB in the type 1 crystal. Acidic regions are coloured red and basic regions are coloured blue. Two RadB monomers are shown at the top, with residues involved in the intermolecular interface shown labelled with the one latter amino acid code and residue number. ATP binding site is represented with an arrowhead. A dimer of RadB is shown at the bottom of the figure.

a dimer could form (Akiba et al., 2005). The *in vivo* form, if not both, of RadB oligomerisation is currently unknown.

While significant progress has been made in characterising RadB *in vitro*, no *in vivo* genetic data exists prior to this thesis. In this chapter, *radB* is deleted from the *H.volcanii* genome, along with *radA* and *hjc*, and analysis of growth rates, DNA damage sensitivity, and analysis of *radB* and *radA* transcript levels following DNA damage has been carried out. Additionally, two point mutant alleles of *radB* were generated in an attempt to elucidate the importance of ATP and DNA binding by RadB.

3.2 Results

3.2.1 Cloning of *radB* and partial deletions

Cloning of *Haloferax volcanii radB* gene and the generation of strains containing partial deletions of the gene was carried out prior to the commencement of this PhD study by Thorsten Allers and Greg Ngo. As this information has not been described elsewhere and because of the importance of this work to subsequent studies of *Hvo* RadB, it will be described in detail in this section.

3.2.2 Identification and cloning of *radB*

The sequence of the *Haloferax volcanii radB* ORF, as annotated by the University of Scranton was obtained. *radB* was annotated as ORF RVO01554 on contig 06302 at position 1286 – 2482 bp. Restriction analysis of contig 06302 was carried out to determine the best approach for cloning *radB* into a plasmid construct. *Mlu*I restriction sites were present 5035 bp upstream and 226 bp downstream of ORF1554 that would generate a fragment of 5950 bp upon digestion. Genomic DNA from wildtype *Haloferax volcanii* was digested with *Mlu*I, electrophoresed and a fragment of approximately 6kb was extracted and purified. Total fragment DNA was then ligated to the *Mlu*I compatible *Bss*HII sites of pBluescript II SK+ and used to transform XL1-Blue strain *E.coli*. Transformants were plated on LB + Amp and following overnight incubation at 37°C, colonies were patched on fresh LB + Amp and allowed to grow overnight at 37˚C.

Colony lifts were made of the patched plate and it was blotted with a radiolabelled *radB* probe, the template of which was generated by PCR amplification of *Hvo* genomic DNA using primers HVRDBF and HVRDBR. Following blotting, washing and exposure of the colony lift membrane, a colony patch that bound the radioactive probe was streaked on LB + Amp (pTA41) (Figure 3.3)

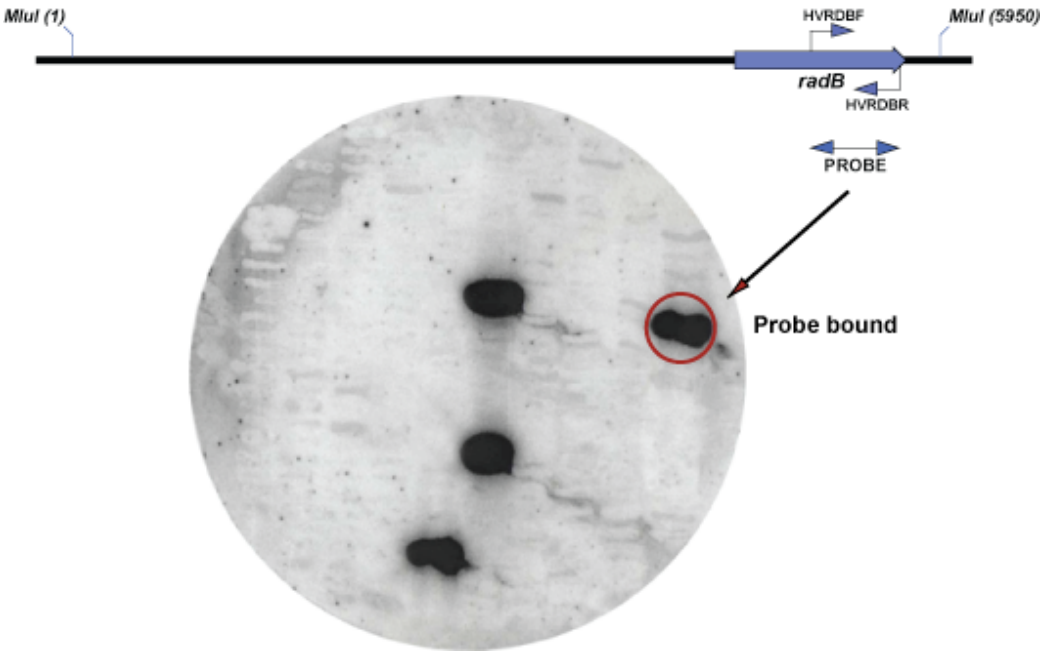

Figure 3.3 Colony hybridisation of *E.coli* patches containing *H.volcanii ~6* kb *Mlu*I digested DNA, plasmid-borne fragments, potentially containing *radB*. The probe template was generated by amplification of a fragment of chromosomal *radB*. Colonies that bound the probe contained pBluescript II SK+ with the *Mlu*I fragment containing *radB*. (pTA41, see Figure 3.5)

3.2.3 Confirmation of *radB* gene

To confirm that the putative *radB* gene present on pTA41 was correctly annotated, the ORF, RVO01554 was used as a translated BLAST query (tblastx) against the genome of all sequenced archaeal on the National Centre for Biotechnology Information (NCBI) website (http://www.ncbi.nlm.nih.gov/). The results showed that RVO01554 sequence did contain *radB*. However, the *Haloferax volcanii radB* ORF as annotated by Scranton University was 1196 bp in length, significantly longer than other archaeal *radB* ORFs, which were all approximately 700 bp in length. The extra ~500 bp sequence present in the annotated *H. volcanii radB* gene was present upstream of the start codon of other *radB* genes.

This suggested that the annotation of *H. volcanii radB* was incorrect. Thus, the genuine start codon of the gene was searched for ~500 bp into the misannotated ORF, to match *radB* lengths from other archaeal species. The likely start codon was found (GTG) and *radB* was reannotated in pTA41 (Figure 3.5 (top)).

3.2.4 Subcloning of *radB*

Hvo radB was subcloned by digesting pTA41 with *Eco47*III *and Xma*I and ligating the resulting 1647 bp *radB* containing fragment with pBluescript II SK+, digested with *Eco*RV and *Xma*I (pTA50) (Figure 3.5). All mutants, deletion constructs and sublcones of *radB* described in this thesis are derived from pTA50 rather than pTA41, due to the shorter length of the insert and the vector having an intact polylinker region.

3.2.5 Generation of *radB* partial deletion

A deletion construct of *radB* was generated based on the chromosomal sequences present in pTA50; *radB* Δ*b/b*. The *radB* Δ*b/b* construct was generated by deleting a 374 bp fragment of the *radB* ORF between the *Bst*EII and *Bst*BI restriction sites, in pTA50 to generate pTA54 (Figure 3.5). pTA54-borne *radB*Δ*b/b* was digested with *Hind*III and *Xba*I and the 1.3 kb fragment containing the deletion allele was inserted at the *Hind*III and *Xba*I sites of pGB70 (Bitan-Banin et al., 2003). [*pyrE2*+ on pUC19]. pGB70 contains the *pyrE2* gene that confers uracil auxotrophy (ura+). The pTA54 insert derivative plasmid was designated pTA68. (Figure 3.5)

The *pyrE2* selectable marker is used for selection and counter selection during the transformation of *H. volcanii,* especially in gene deletion. Upon transformation of *H. volcanii* with plasmids containing *pyrE2* and homology to the chromosome (in this case, a partial deletion of *radB* with homology to the *radB* locus), cells that integrate the plasmid by HR become ura+, and are selected by plating on media lacking uracil. Selection of *pyrE2* is then relieved by growing cultures of the integrant strain in complex Hv-YPC broth (contains uracil). This allows the plasmid to recombine out of the chromosome, with equal chances of leaving the chromosomal gene (i.e. *radB*) and leaving the mutant allele on the chromosome (i.e. *radB*Δ*b/b*). (Figure 3.4) Cells that have lost the plasmid from the chromosome are selected by plating on media containing 5FOA and a small amount of uracil. 5FOA is toxic to *pyrE2*+ strains, therefore only cells that have lost the plasmid will form colonies, surviving on the small amount of uracil present in the media. Full details of this procedure are in Materials and Methods section.

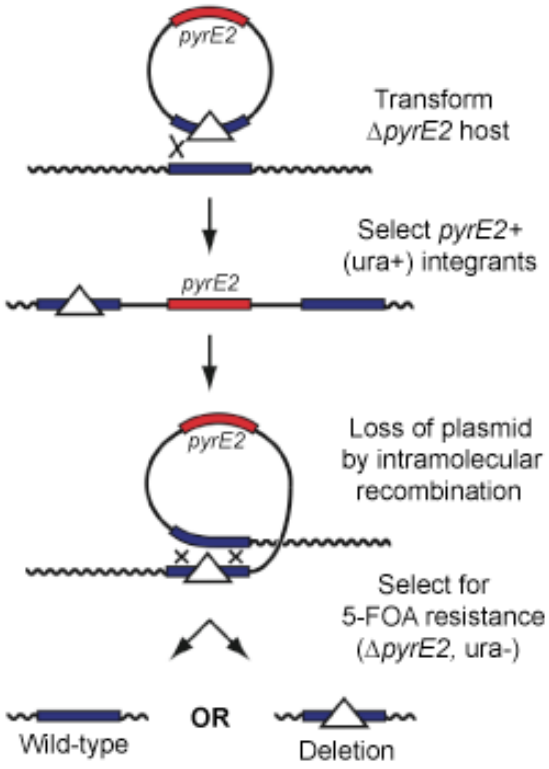

Figure 3.4 Chromosomal gene deletion by selection and counter-selection of an integrative plasmid. A Δ*pyrE2* host is transformed with a *dam*- plasmid containing *pyrE2* and a deletion construct of the desired gene. The plasmid integrates at regions of homology to the locus of the gene to be deleted, conferring uracil prototrophy (ura+). Once the integratant strain has been confirmed by Southern blot analysis, selection for uracil is relieved by serial growth in Hv-YPC (+ Thy if required). The plasmid recombines from the chromosome and ura- (Δ*pyrE2*) derivatives are selected for by plating on 5-FOA plates. Depending on the orientation of the second recombination event relative to the first, the resulting strain will be either deleted for the desired gene or remain as wild-type. These can be differentiated between by colony blotting using a probe internal to the coding sequence of the gene.

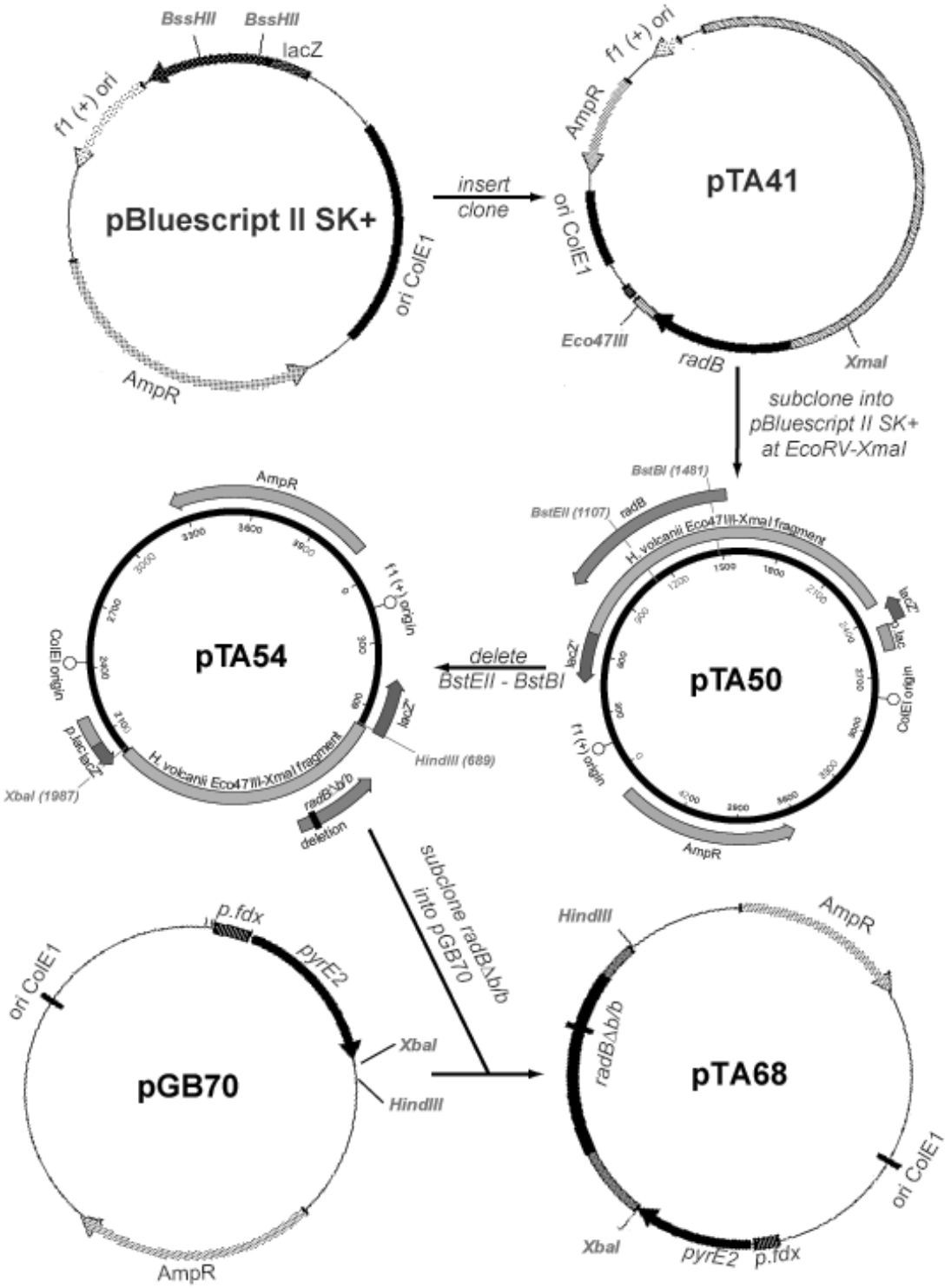

Figure 3.5 Generation of pTA41, containing the original ~6 kb *Mlu*I *radB* genomic fragment, pTA50, a subclone of pTA41, pTA54, a partial deletion of *radB* (*radB*Δ*b/b*) on pBluescript II SK+, and pTA68, *radB*Δ*b/b* in pGB70, containing *pyrE2.*

Generation of a radBΔb/b strain of Haloferax volcanii

pTA68 was used to transform the *dam- E.coli* strain, N2338, and plasmid DNA isolated from this strain was used to transform *Haloferax volcanii* strain H26 Δ*pyrE2*. Transformants that had integrated the plasmid at the *radB* locus were selected by plating on Hv-Ca. As pTA68 is marked with *pyrE2*, following integration at the *radB* locus, integrants will be ura+ and therefore able to grow on media lacking uracil (Hv-Ca). The integration was confirmed by restriction digest with *Eco*47III/*Hpa*I and Southern blot analysis using a radiolabelled pTA50 *Bsp*EI-*Hind*III radB fragment as a probe. The integrant strain for *radBΔb/b* (pTA68) was designated H57.

Loss of the integrated plasmids was encouraged by serial growth and dilution of H57 in Hv-YPC broth. Hv-YPC was used as it contains uracil, thus relieving selection for the integrated plasmid, pTA68, allowing a second recombination event to occur, excising the plasmid from the chromosome. Cultures were grown to A_{650} = ~0.6 at 45°C and diluted in 500 fold in fresh Hv-YPC broth. This was repeated twice, to allow time for this second recombination event, followed by plating on Hv-Ca + 5FOA media. The presence of 5FOA in the media is toxic to ura+ cells, i.e. those that still have pTA68 integrated. Therefore, only cells that have lost pTA68 from the chromosome will form colonies.

Colonies that contained the mutant allele but no wildtype *radB* sequence were detected by colony hybridisation using a 372 bp *Bst*BI/*Bst*EII fragment as a probe for *radBΔb/b*. Colonies that did not hybridise the probe contained the deletion construct at the *radB* locus, rather than *radB*+. To ensure that all copies of the chromosome contained this deletion and that it was at the correct locus, Southern blot analysis was used as before. The strain derived from H57 was designated H64 (*radBΔb/b*) (Figure 3.6)

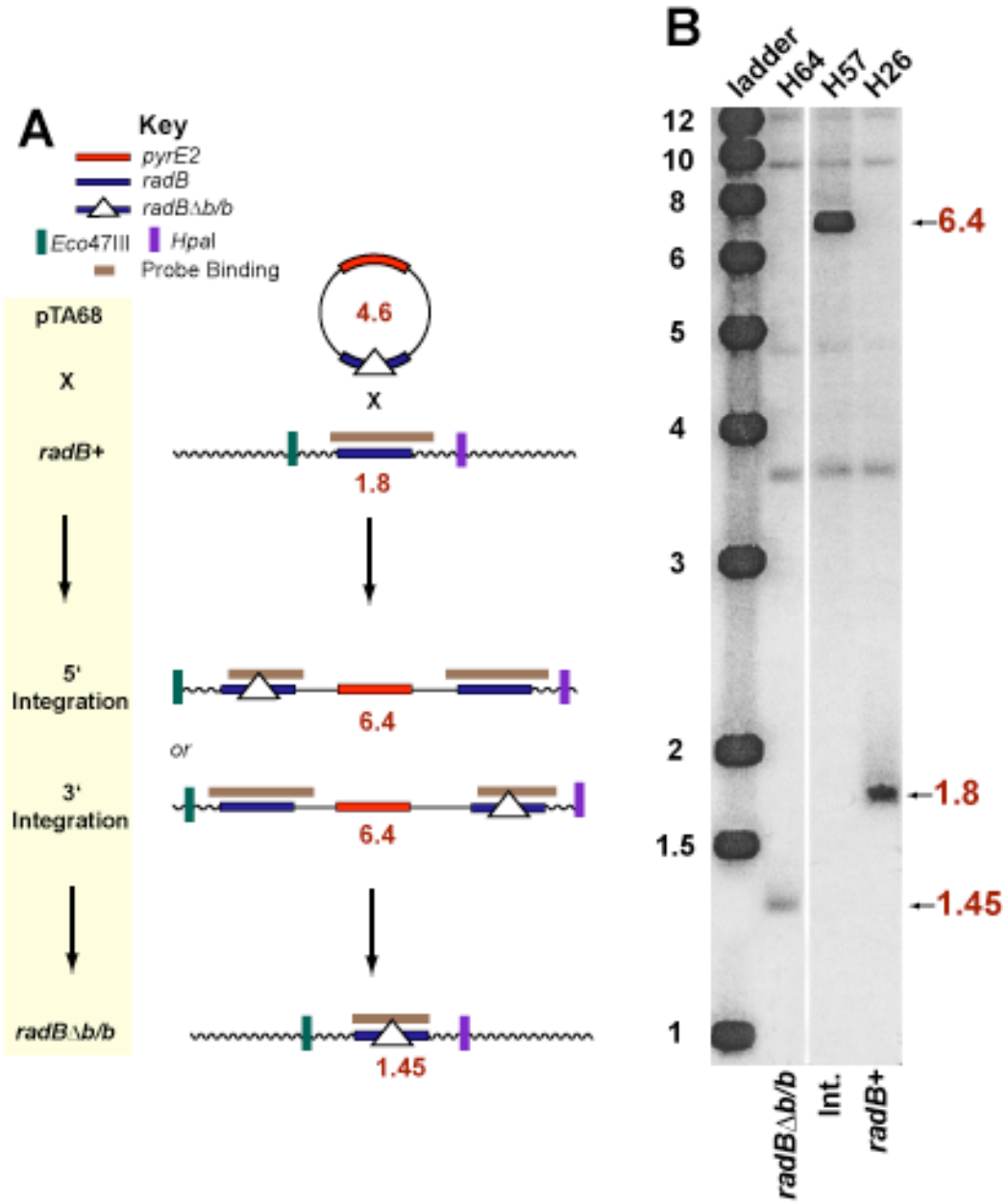

Figure 3.6 A - Schematic of the integration of the pTA68-borne *radBΔb/b* construct at the chromosomal *radB*+ locus of H26, indicating both possible integration events, 5' and 3' (H57 - see Figure 3.6 B) and the resulting chromosomal deletion (H64 - see Figure 3.6 B). The restriction enzymes used to digest chromosomal DNA are displayed and resulting fragment sizes (kb). **B** - Southern blot showing restriction digests of H64, H57 and H26 DNA following digestion with *Eco47*III and *Hpa*I, and hybridisation with the radiolabelled pTA50 *BspE*I-*Hind*III *radB* fragment. The ladder used was 1kb ladder (NEB). Fragment sizes are indicated on the right of the blot, measured in kilobases.

3.2.6 Phenotypic analysis of *radB* partial deletion strains

Growth rates

An initial observation was that H64 (*radB*Δ*b/b*) was slower growing compared to H26 (*radB*+), demonstrating that RadB might be important for normal growth. To quantify the slow growth phenotype exhibited by H64 (*radB*Δ*b/b*), enumeration of cell count by plating of culture onto solid media was deemed necessary to distinguish between growth of normal dividing cells and those undergoing filamentous growth. This assay involved growing cultures in Hv-YPC broth until A_{650}=0.4, then diluting the cultures 1/10000 in the same volume. Cultures were then incubated at 45˚C until early stationary phase was reached (A_{650} = 0.8). Aliquots were plated on Hv-YPC plates at regular intervals. Plates were incubated at 45˚C for 5 days and the number of colonies counted. (Figure 3.7)

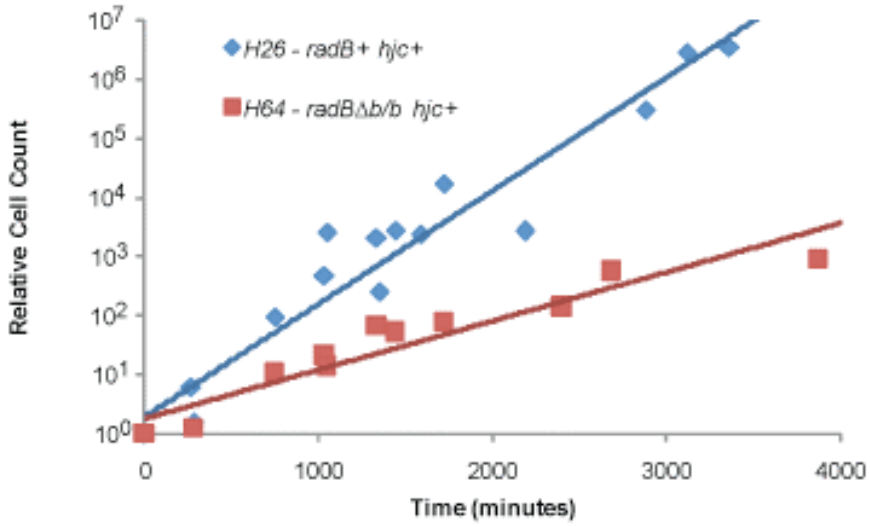

Figure 3.7 Growth analysis of H26 (*radB*+) and its derivative strain H64 (*radB*Δ*b/b*). Relative cell count is calculated as a proportion of the cells present at time = 0 minutes. All data points are the consolidation of data obtained from three trials.

From the equations derived from the trendlines shown in Figure 3.7, the generation time (g) of each strain could be calculated using the equation:

$$g = (\log_{10} N_L - \log_{10} N_E) / \log_{10} 2$$

$$\text{Generation time} = g / (L\text{-}E)$$

The number of generations in a particular time frame (g) is calculated by taking two points on the trendline, in exponential growth phase and deducting the $\log_{10}$ of the number of cells present at the earlier time point (N_E) from the $\log_{10}$ of the number of cells present at the latter time point (N_L). This value is then divided by the constant of $\log_{10}2$ to give the number of generations in the given time frame. By dividing the number of hours between the two points (L and E) on the trendline and dividing this value by g, the resulting value is the generation time of the particular strain. This calculation was carried out for the strains tested in this experiment and are displayed in Table 3.1 below.

Strain	**H26**	**H64**
	radB+	***radBΔb/b***
Generation Time (mins)	156	363

Table 3.1 Calculated generation times for tested strains H26 (*radB+*) and H64 (*radBΔb/b*)

Figure 3.7 and Table 3.1 demonstrate that H64 (*radBΔb/b*) grows significantly slower than H26 (*radB+*). This indicates that RadB is required for normal growth of *Haloferax volcanii*. Whether the partial deletion of *radB* is equivalent to a full-length deletion of the gene is unknown at this point, and will be addressed later in this chapter.

UV sensitivity

Ultraviolet light exposure not only damages nucleotides, generating 6-4 photoproducts and cyclobutane pyrimidine dimers, but it can indirectly generate DNA double strand breaks that must be repaired by either non-homologous end joining or homologous recombination. This can occur as UV light can cause single stranded breaks in DNA and if a replication fork encounters such a lesion, a double strand break will occur (Figure 3.8). The replication fork can be rescued and restarted by homologous recombination; therefore UV irradiation of strains can provide an indication of whether defects exist in homologous recombination.

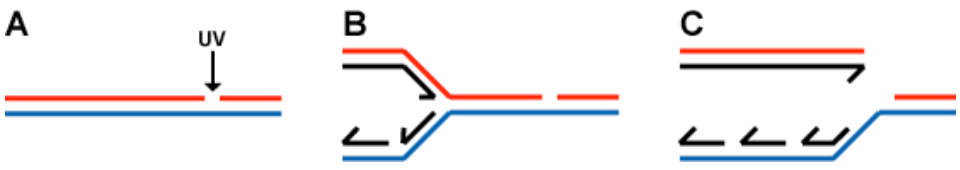

Figure 3.8 Replication fork collapse induced by UV irradiation. **A** - UV light causes a single stranded DNA break. **B** - Replication proceeds towards unrepaired lesion. **C** - Replication fork encounters lesion and collapses, generating a double stranded break

H26 (*radB*+) and H64 (*radB*Δ*b/b*) cells were exposed to varying doses of UV light on Hv-YPC plates and incubated at 45°C, for 5 days in the dark to prevent photoreactivation of DNA (Figure 3.9).

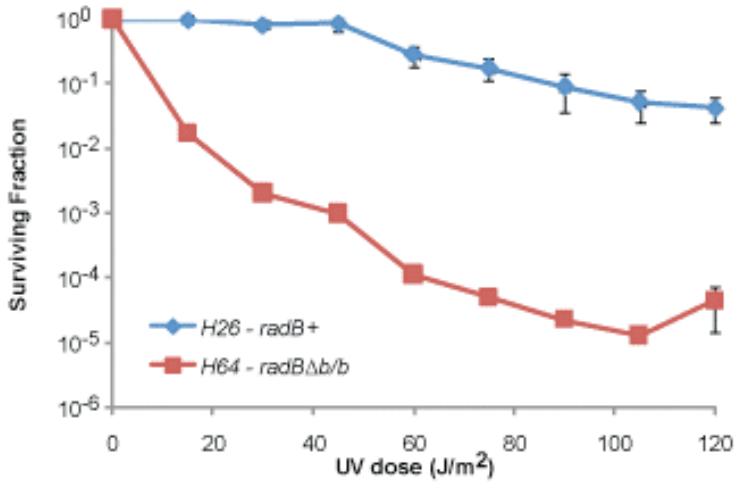

Figure 3.9 Comparison of surviving fractions of *radB*+ (H26) and *radB*Δ*b/b* (H64) strains, following UV irradiation. All data points are calculated as the mean value of three trials. Error bars are bases on standard error. Only relevant genotypes are shown.

Figure 3.9 shows that H64 (*radB*Δ*b/b*) is significantly more sensitive to UV irradiation than H26 (*radB*+). This demonstrates that *radB* is important for the repair of UV induced lesions, as well as for normal growth. At this stage it is not known whether the severe UV sensitivity phenotype of H64 is due to a defect in recombination, as it could be equally likely due to a nucleotide excision repair (NER) defect. This issue is addressed later in this chapter.

The work described from this point onwards was carried out as part of the research project by myself, except where otherwise stated.

3.2.7 Upstream element and promoter analysis of *radB*

The studies carried out in this laboratory on *Haloferax volcanii radB* prior to this project provided valuable insight into the proposed chromosomal location of the gene and some preliminary information on the Δ*radB* strain phenotype. However, the University of Scranton had annotated *radB* incorrectly. Though this was resolved before this project commenced, it was decided that analyses of *radB* promoter sequences should be carried out to ensure that the annotation of *radB* was correct and that subsequent studies were therefore reliable. To confirm the start codon of *radB*, sequences upstream of this region were analysed to identify the location of the *radB* promoter. Archaeal promoters have a TATA-box and basal-regulation element (BRE) positioned 25-30 bp upstream of the translational initiation site (Reeve, 2003),

with the BRE being located upstream of the TATA-box. The TATA-box of promoters is the site of DNA melting prior to transcriptional initiation and is bound by a TATA binding protein (TBP). Melting of DNA is facilitated by the high A+T% of the TATA box, as base pairing between adenine and thymine is weaker than between cytosine and guanine. The BRE is the site of binding for transcription factor B (TFB), a protein that stabilises the binding of TBPs to the TATA box (Reeve, 2003). Mutagenesis of these elements has shown that their sequences contribute directly to the strength of the promoter (Soppa, 2001). Different consensus sequences have been established for the TATA-box in different archaeal species, with halophilic TATA-boxes having a consensus sequence of NTTTWWWN (W = A or T; N = any nucleotide), whereas the BRE is generally defined as being purine rich (Soppa, 2001). (Figure 3.10)

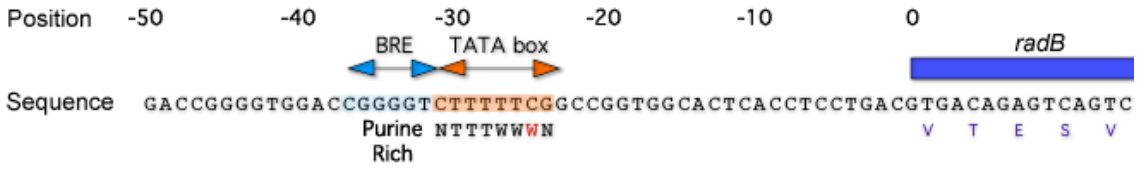

Figure 3.10 Schematic of the proposed *radB* promoter. The BRE and TATA-box are highlighted in blue and orange, respectively. The consensus sequence for haloarchaeal TATA-boxes is displayed under the TATA-box: Nucleotides in black conform to the haloarchaeal TATA-box consensus sequence, whereas those in red do not.

Figure 3.10 shows the position of the proposed promoter elements of *radB*. A TATA box was identified that corresponds almost perfectly with the haloarchaeal TATA-box consensus. The BRE was not as well conserved as the TATA-box and therefore more difficult to identify. It appears to consist of a tract of four guanine residues immediately upstream of the TATA-box. As discussed above, archaeal promoters are typically 25 - 30 bp upstream of the start codon: The predicted *radB* promoter shown in Figure 3.10 lies 24 bp upstream of the proposed GTG start codon of *radB*, as expected.

Summary

Prior to the start of this PhD, the position of the *radB* start codon was identified by comparing translated sequences of the *H.volcanii* ORF proposed to contain *radB* with other archaeal RadB sequences, highlighting a misannotation of the Scranton annotated *radB*. During this PhD, the *radB* promoter sequence has been identified. The first codon of *radB* is GTG (GUG) and

therefore encodes a valine residue instead of a methionine residue: A feature common to 18% of all identified *Haloferax volcanii* genes (Chuck Daniels, personal communication)

The start codon of *radB* is positioned at 1539-1541 bp of pTA50 (Figure 3.11) and the TAG (UAG) stop codon is located at positions 852-854 bp. The coding sequence of *Haloferax volcanii radB* is therefore 690 bp in length, encoding a protein consisting of 230 residues. This is similar to RadB proteins from other archaeal species, which can range from 225 - 245 residues in length. The BRE and TATA-box of *radB* are located at positions 1573-1578 and 1565-1572 of pTA50, respectively. (Figure 3.11)

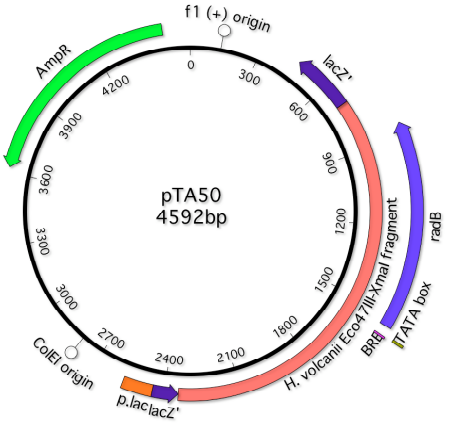

Figure 3.11 Plasmid map of pTA50, annotated with the promoter elements and coding sequence of *Haloferax volcanii radB*

3.2.8 Analysis of the *radB* chromosomal locus

The *Haloferax volcanii radB* chromosomal locus was analysed to determine if other genes were upstream or downstream of *radB*. The reasons for this analysis were two-fold. The first reason was to determine whether *radB* is contained within an operon. Operons are DNA sequences that contain several genes in tandem which are transcribed together into polycistronic mRNA, and are found in archaea as well as bacteria. Proteins encoded by genes contained within an operon are often related in function. In the thermophilic euryarchaeon, *Pyrococcus furiosus, radB* is contained within an operon with four other genes, encoding DP1, the small subunit of the archaeal DNA polymerase PolD, DP2, the large subunit of PolD, Orc1, a replication origin recognition complex, and a protein of unknown function (Hayashi et al., 1999). It was later demonstrated through yeast two-hybrid analysis that RadB interacts with both DP1 and itself, and DP1 interacts with RadB, Orc1 and DP2 (Hayashi et al., 1999).

If *Hvo-radB* were present in an operon, deleting the gene would pose some technical difficulties such as sharing of its promoter with other genes in the operon. It would, however, suggest that the function of RadB is strongly linked with the functions of other genes in the operon, providing insight into its function. A related reason for analysing the chromosomal locus of *radB* and the surrounding regions was that before a full-length deletion of *radB* could be constructed and used to replace the full-length gene on the chromosome, it was necessary to ensure that such a deletion would have no polar effects on neighbouring genes, if not in an operon. For example, a deletion construct might also delete part of any neighbouring genes or their promoters, therefore any Δ*radB* phenotype might actually be due to the disruption of a neighbouring gene. To analyse the *Haloferax volcanii radB* chromosomal locus, DNA sequence data ranging from 5 kb upstream to 5 kb downstream of *radB* was translated in all frames and compared with existing proteins, through a tblastx search of all sequenced genomes (as of 10/02/04). The results of the search are displayed in Figure 3.12

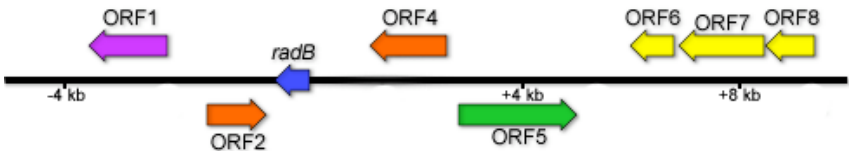

ORF	Protein	Organism	Expected	Location (bp)
1	Type II secretion system protein	*Hma*	6.9e-124	+1976→+3445
2	Hypothetical protein rrnAC1525	*Hma*	3.2e-145	+1256→+114
3	RadB	*Hvo*	0	NA
4	Hypothetical protein rrnAC1529	*Hma*	2.2e-138	-3839→-2394
5	Cdc48	*Hma*	0	-4033→-6264
6	PstB2	*Hsa*	3.8e-106	-8074→-7229
7	PstA2	*Hsa*	2.3e-135	-9754→-8129
8	PstC2	*Hsa*	1.1e-129	-10078→-9759

Figure 3.12 ORFs located near the *radB* chromosomal locus. All predicted ORFs within 10 kb either side of *radB* are annotated. Table shows proteins encoded by the respective ORFs, based on translated matches from a BLASTX search. ORFs of the same colour either encode or hypothetically encode proteins that are functionally related. The organisms from which the proteins originate are displayed along with the expected values for each match. *Hma* = *Haloarcula marismortui* ATCC 43049, *Hsa* = Halobacterium sp. NRC-1. The final column shows distance relative to *radB*. Distances of upstream/downstream genes are measured from start/stop codon, respectively

Unlike *Pyrococcus furiosus radB*, *Haloferax volcanii radB* is not located within an operon with potentially related genes. The closest gene to *radB* is located 114 bp downstream, and transcribed in the opposite direction to *radB*, and the closest gene upstream is located 2.4 kb away. Based on this information, a strategy to generate a full-length deletion of the RadB coding sequence that would not exhibit polar effects on nearby genes was devised, and is presented later in this chapter.

While there are several other genes located in the vicinity of *Haloferax volcanii radB*, none of which are predicted to be involved in DNA recombination or repair. Two conserved genes coding for hypothetical proteins rrnAC1525 and rrnAC1529 are present and the former of which could be a membrane spanning transporter protein. A gene coding for a type II secretion system protein containing an ATPase domain is located 2 kb downstream of *radB* and ~7-10 kb upstream of *radB* lie three related genes, homologous to the bacterial PstABCS system that functions in phosphate uptake. The only gene located near *radB* that might code for a protein involved in DNA metabolism is *cdc48* that encodes a cell division control protein. Cdc48 is a chaperone-like ATPase and proposed to be involved in translation.

3.2.9 Full-length deletion of *Haloferax volcanii* chromosomal *radB*

Although an internal partial deletion of *radB* had been generated and characterised, to ensure that the data obtained was correct and not the result of expression of a truncated RadB protein, a full-length deletion of the *radB* coding sequence was generated.

Two pairs of PCR primers were designed to amplify the upstream and downstream sequences flanking *radB*, as described in "Generation of deletion constructs by PCR" in Materials and Methods. Primers, in pairs, were designated RBDN1/RBDX1, and RBDN2/RBDX2. RBDN1 and RBDN2 were designed to bind 10 bp downstream and 13 bp upstream of *radB*, respectively, and both contained a novel *Age*I site used for digesting and ligating the two products together following amplification. RBDX1 and RBDX2 were designed to bind 228 bp and 197 bp upstream and downstream of *radB,* respectively (Figure 3.13). A novel *Not*I restriction site was introduced into RBDX2 and a unique *Kpn*I site was already present in RBDX1, for the purposes of digestion and ligation of the full-length product into the multiple cloning site of the *pyrE2* marked plasmid pTA131.

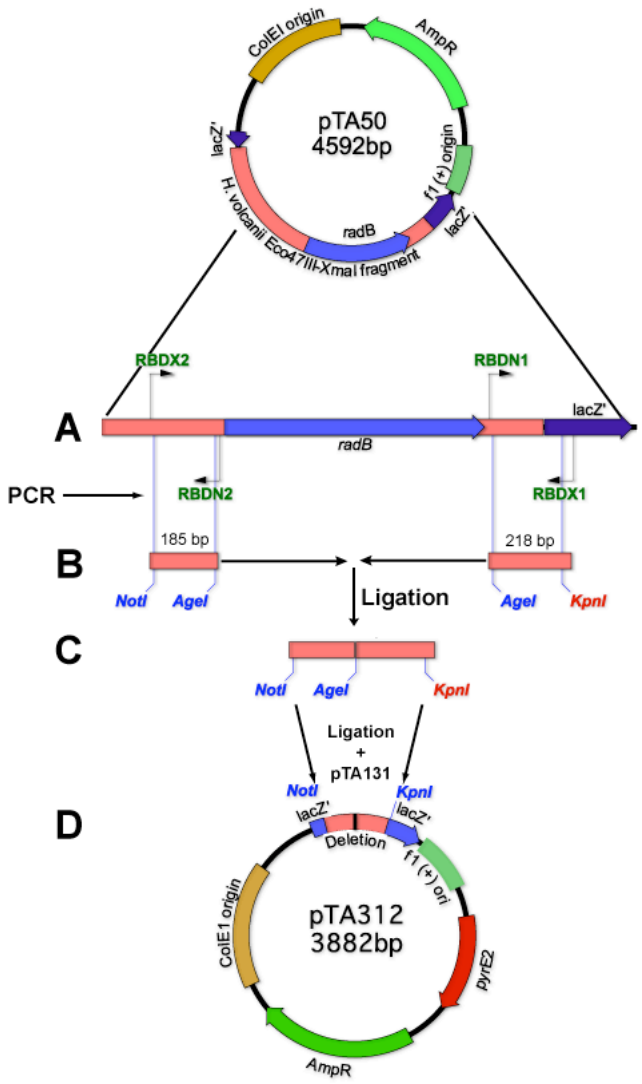

Figure 3.13 Construction of Δ*radB* construct and pTA312. **A** - Amplification of flanking regions of *radB* with primers RBDN/X1 and RBDN/X2. *Kpn*I site is coloured red to indicate that the restriction site was pre-existing and not introduced to the amplification product, as was the case for *Not*I and *Age*I sites. **B** - Digestion of products with *Age*I. **C** - Ligation of products at compatible *Age*I sites generating the Δ*radB* construct, followed by digestion with *Kpn*I and *Not*I. **D** - Ligation of Δ*radB* construct with *Not*I/*Kpn*I-digested pTA131 to generate pTA289. The *dam*- version of this plasmid used for *Haloferax volcanii* transformations is pTA312, and is displayed above.

PCR amplifications using RBDN1/RBDX1 and RBDN2/RBDX2 were carried out and the resulting amplification products of 218bp and 185 bp, respectively, were electrophoresed, extracted from the gel and purified. Both products were digested with *Age*I and ligated to generate the Δ*radB* construct. The ligated product was digested with *Not*I and *Kpn*I to generate a 337 bp fragment that was ligated into the *Not*I and *Kpn*I sites present in the multiple cloning site of pTA131. The plasmid was designated pTA289. Following extraction from *E.coli* XL-1 Blue, the pTA289 was used to transform *dam- E.coli* strain, N2338. *dam-* plasmid DNA was extracted and designated as pTA312.

1 µg of pTA312 was used to transform strain H195 (Δ*pyrE2* Δ*trpA* Δ*hdrB leuB-Ag1 bgaHa-Bb*) rather than H26 (Δ*pyrE2*) as the additional selectable markers present in H195 are necessary for experiments described later in this thesis. Transformants were plated on Hv-Ca + Trp + Thy (tryptophan and thymidine were required due to the additional auxotrophy of H195, compared to H26), to select for ura+ pTA312 integrants. Resulting colonies were grown overnight in Hv-YPC + Thy broth and genomic DNA was isolated. Each sample was digested with *Nru*I and *Mlu*I overnight, to ensure complete digestion, along with a sample of H195 genomic DNA as a control. Digested DNA was electrophoresed and Southern blot analysis was carried out using the 337 bp *Kpn*I-*Not*I Δ*radB* construct fragment of pTA289 as a template for the radioactive probe. A correct 3' integrant strain was identified and designated as H257 (Figure 3.14).

H257 was serially propagated and diluted in Hv-YPC + Thy broth to relieve selection for the integrated plasmid, followed by plating on Hv-Ca + Trp + Thy + 5FOA to select against remaining pTA312 integrants. A colony lift and hybridisation was carried out using a 373bp *Bst*EII-*Bst*BI fragment of pTA50 consisting of *radB* coding sequence as a probe template. Genomic DNA was prepared from colony patches that did not bind the probe (Figure 3.15). This DNA was then digested with *Nru*I and *Mlu*I and Southern blot analysis was carried out as before to determine whether *radB* had been deleted (Figure 3.14). Once confirmed, the strain was designated H284.

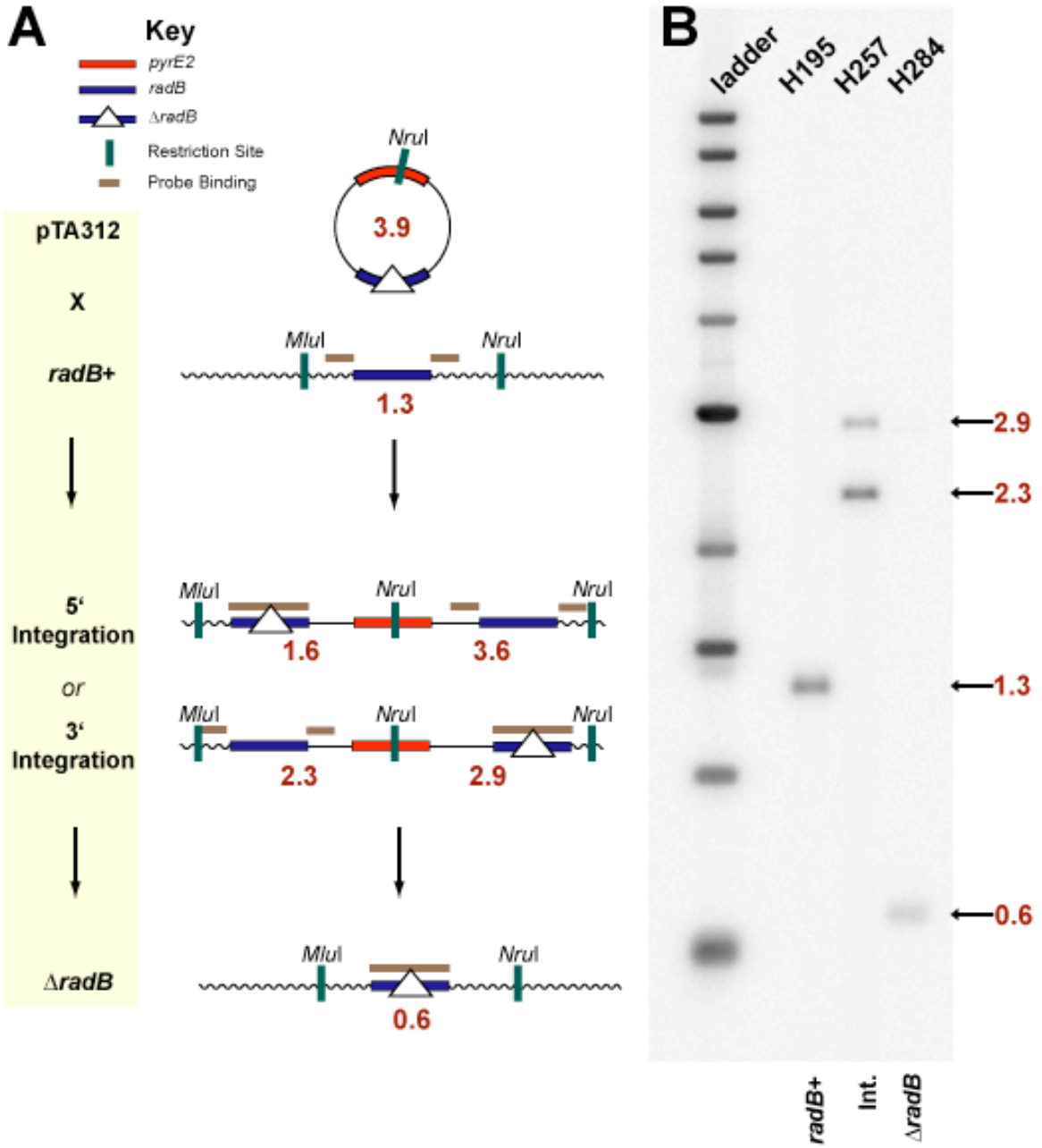

Figure 3.14 A - Schematic of the integration of the pTA312-borne Δ*radB* construct at the chromosomal *radB*+ locus of H195, with both possible integration events, 5' and 3' (H257 - see Figure 3.14 B) and the resulting chromosomal deletion (H284 - see Figure 3.14 B). The restriction enzymes used to digest chromosomal DNA are displayed, as are resulting fragment sizes (kb). **B** - Southern blot showing restriction digests of H195, H257 and H284 DNA following digestion with *Mlu*I and *Nru*I, and hybridisation with the radiolabelled pTA312 *Kpn*I-*Not*I Δ*radB* fragment. The ladder used was 1kb ladder (NEB). Fragment sizes are indicated on the right of the blot, measured in kilobases.

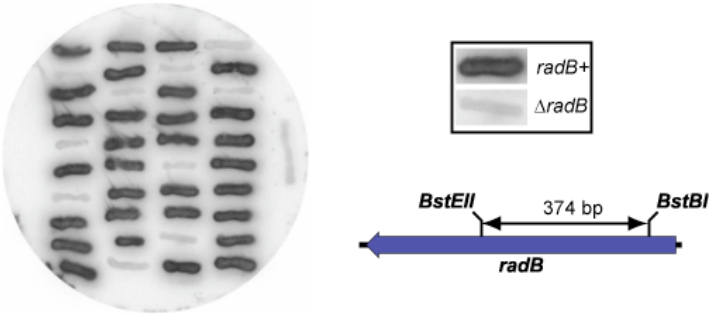

Figure 3.15 Colony hybridisation of patched colonies following 5-FOA counterselection of integrated pTA312. Colony patches that hybridise the 374 bp *Bst*EII-*Bst*BI radiolabelled *radB* fragment are *radB*+ and appear darker than those that are Δ*radB*.

3.2.10 Phenotypic analysis of Δ*radB* strain, H284

Once it had been confirmed that *radB* had been deleted from strain H195 to generate strain H284, analyses were carried out to measure growth of the strain, and survival following UV irradiation and exposure to the crosslinking agent mitomycin C.

Growth Rate

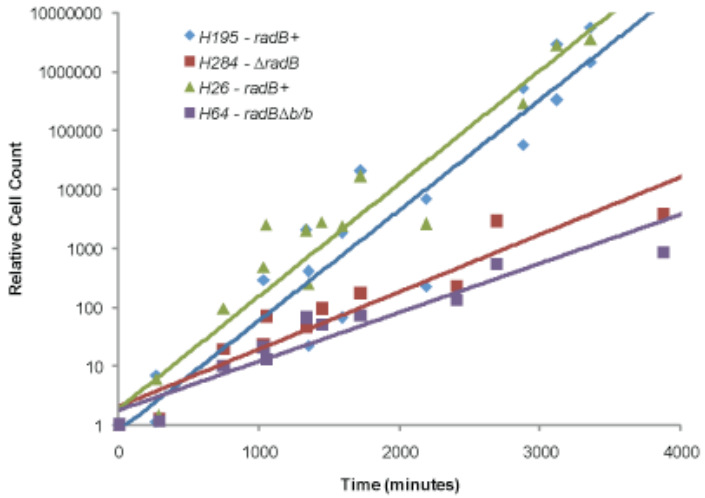

Figure 3.16 Growth analysis of H195 (*radB*+) and its derivative strain H284 (Δ*radB*), and H26 (*radB*+) and its derivative strain H64 (*radB*Δ*b/b*). Relative cell count is calculated as a proportion of the cells present at time = 0 minutes. All data points are the consolidation of data from three trials.

To quantify the slow growth phenotype associated with H284 (Δ*radB*), enumeration of cell count by plating of culture onto solid media was deemed necessary to distinguish The growth rate assay was carried out as before. (Figure 3.16)

Strain	**H195**	**H284**	**H26**	**H64**
Generation Time (mins)	160	331	156	363

Table 3.2 Calculated generation times for tested strains H195 (*radB*+), H284 (Δ*radB*), H26 (*radB*+) and H64 (*radB*Δ*b/b*)

Figure 3.16 and Table 3.2 demonstrate that in the absence of RadB, strains grow significantly slower than when RadB is present. This indicates that RadB is required for normal growth of *Haloferax volcanii*. Additionally, the growth rates of H195 and H26 (*radB*+), and H284 (Δ*radB*) and H64 (*radB*Δ*b/b*) are comparable. This suggests that the different auxotrophic backgrounds of H26 (Δ*pyrE2*) and H195 (Δ*pyrE2* Δ*trpA* Δ*hdrB leuB-Ag1 bgaHa-Bb*) do not affect growth rates significantly. Furthermore, these data show that growth rates are equivalent in strains with the partial deletion of *radB* (H64, *radB*Δ*b/b*), and strains with the complete deletion, (H284 Δ*radB*).

Survival following UV irradiation

A 374 bp deletion of *radB* (*radB*Δ*b/b)* results in the strain (H64) being sensitive to UV irradiation. To determine whether the same phenotype is observed with a deletion of the entire coding sequence of *radB*, strains H195 (*radB*+) and H284 (Δ*radB*), UV survival assays were carried out as before. (Figure 3.17).

Figure 3.17 below shows that *radB*Δ*b/b* deletion strain (H64) and Δ*radB* strain (H284) are significantly more sensitive to UV irradiation when compared to their respective *radB*+ parent strains (H26 and H195 respectively). Additionally, it appears that the strain background has no significant effect on UV sensitivity, i.e. H26 is Δ*pyrE2 trpA*+ *hdrB*+ *leuB*+ whereas H195 is (Δ*pyrE2* Δ*trpA* Δ*hdrB leuB-Ag1* and is therefore incapable of synthesising tryptophan and thymidine and leucine. Both strains are incapable of uracil biosynthesis (Δ*pyrE2*). Although there is a small difference between the UV sensitivity of their respective daughter strains, H64 (*radB*Δ*b/b*) and H284 (Δ*radB*), with H64 being more sensitive that H284, this appears to be due to stochastic variation. Thus, regardless of whether the deletion of *radB* is complete or partial (*radB*Δ*b/b*), sensitivity to UV light appears the same. This suggests that the *radB*Δ*b/b* strain is a phenocopy of the Δ*radB* mutant.

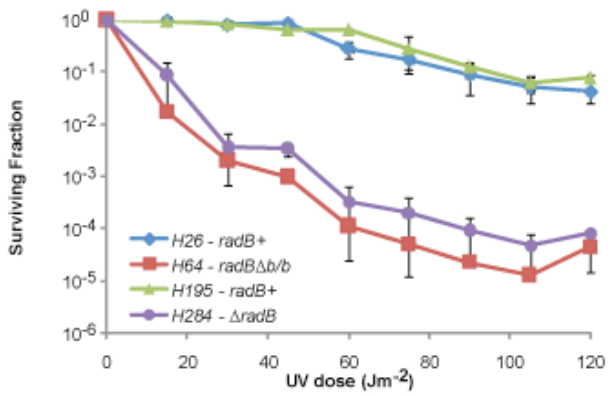

Figure 3.17 Comparison of surviving fractions of H195 (*radB*+) and H284 (Δ*radB*) with H26 (*radB*+) and H64 (*radB*Δ*b/b*) following UV irradiation. H195 and H284 have different auxotrophic markers to H26 and H64 (see text). All data points are calculated as the mean value of three trials. Error bars are bases on standard error.

Summary

The UV survival data indicates that RadB is a DNA repair protein, since deletion strains have a lower survival frequency after DNA damage. At this stage it is unknown whether RadB functions in homologous recombination (HR) or nucleotide excision repair (NER), as both pathways can be utilised to repair lesions generated by UV light, depending on the stage at which they are repaired, i.e. pre-replication or post-replication. It is more likely that RadB is a HR protein because it is homologous to other recombinase proteins and furthermore, *Haloferax volcanii* possesses genes homologous to both the bacterial nucleotide excision repair pathway genes (e.g. *uvrA, uvrD*) and the eukaryotic nucleotide excision repair pathway genes (e.g. *xpf, fen1* (Roberts et al, 2003)). Δ*uvrA* strains are extremely sensitive to UV irradiation suggesting that *Hvo*-UvrA is a functional homologue of bacterial UvrA (Z. Duan, unpublished data).

Detection of epistatic relationship between uvrA *and* radB

To provide evidence that RadB is a recombination protein rather than a nucleotide excision repair protein, epistatic analyses of *radB* on *uvrA* was carried out. An existing Δ*uvrA* strain (H513) (Z. Duan, unpublished data) was deleted for *radB* in the same manner as described previously in this chapter to generate a Δ*uvrA radB* strain (H761). UV irradiation survival assays were carried out in conjunction with H513 (Δ*uvrA* in H195 background) and H284 (Δ*radB*) to determine if a Δ*uvrA radB* strain was equally sensitive to UV irradiation as either of the single deletion strains alone. If this was the case, it would be a strong indication that both RadB and UvrA function in the same pathway, i.e. nucleotide excision repair. The deletion of

one gene abrogates this process, and any additional deletion of genes in the pathway would not worsen the phenotype. If however, the Δ*radB* Δ*uvrA* double deletion strain showed a more severe reduction in survival following UV irradiation, it would imply that the two protein products function in different pathways, i.e. nucleotide excision repair and homologous recombination. (Figure 3.18)

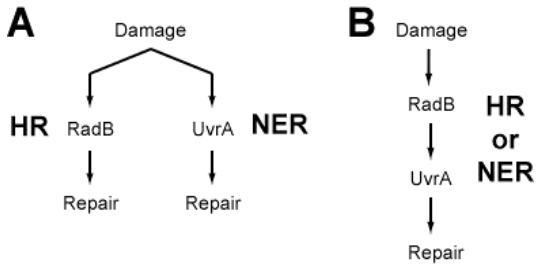

Figure 3.18 Schematic of possible relationships between UvrA and RadB in terms of DNA repair. **A** - RadB and UvrA are synergistic., i.e. homologous recombination (HR) and nucleotide excision repair (NER). Deletion of either *radB* or *uvrA* will result in one repair pathway being defective, but leaving the other pathway still available for repair. Deletion of both *radB* and *uvrA* will result in both pathways being defective; therefore the strain would exhibit a more severe repair defect phenotype than either single deletion alone. **B** - RadB and UvrA act in the same pathway, NER (or HR). Deletion of either *uvrA* or *radB* prevents the repair pathway being utilised therefore deletion of both genes would result in no additional repair defect compared to either single deletion alone.

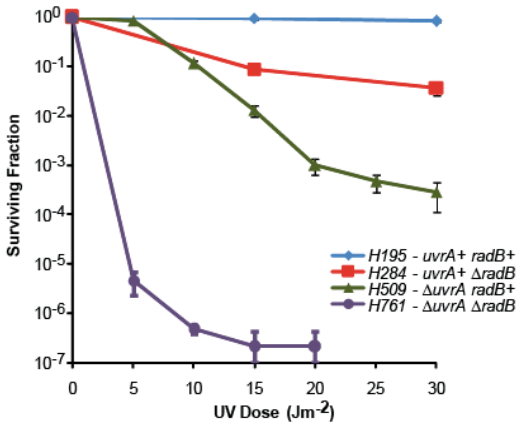

Figure 3.19 Comparison of surviving fractions of H195 (*radB*+ *uvrA*+), H284 (Δ*radB* *uvrA*+), H509 (*radB*+ Δ*uvrA*) and H761 (Δ*uvrA* Δ*radB*) following UV irradiation. All data points are calculated as the mean value of three trials. Error bars are bases on standard error. Only relevant genotypes are shown.

Figure 3.19 shows that the single deletion strains, H284 (Δ*radB uvrA*+) and H509 (Δ*uvrA radB*+) are more sensitive to UV irradiation than H195 (*radB*+ *uvrA*+) and that the double deletion strain, H761 (Δ*uvrA* Δ*radB*) is extremely sensitive to UV irradiation, more so than either single deletion strain. This is a good indication that RadB and UvrA function in different pathways, both capable of repairing UV induced DNA damage. As UvrA is most likely to function in NER, this suggests that RadB might function in HR. More direct studies of the effect of Δ*radB* on homologous recombination are shown in Chapter 4: 'Genetic Analysis of Homologous Recombination in RadB, RadA and Hjc Mutants'

Sensitivity to mitomycin C

As a means of further testing the DNA damage sensitivity phenotype of Δ*radB* strains H64 and H284, their *radB*+ parent strains H26 and H195, respectively, were plated on Hv-YPC or Hv-YPC + Thy media supplemented with the DNA crosslinking agent, mitomycin C. Inter- and intra- strand DNA crosslinks are potent lesions that can block the progression of DNA and RNA polymerases by covalently linking DNA strands together. Reports have shown that recombination defective organisms are hypersensitive to mitomycin C, e.g. *mRAD54*$^{-/-}$ embryonic stem (ES) cells show reduced levels of recombination and are extremely sensitive to mitomycin C (Essers et al., 1997; Essers et al., 2000), and *Brca1*-deficient ES cells that are defective in homology-directed repair are 100-fold more sensitive to mitomycin C (Moynahan et al., 2001). Generally bulky lesions, such as those generated by mitomycin-C are repaired in bacteria by nucleotide excision repair and recombinational repair pathways, rather than base excision repair (Hornback and Roop, 2006); this situation may be mirrored in the archaea. It has recently been shown that mutants of *rfs-1*, the single *C.elegans* Rad51 paralogue, are sensitive to mitomycin C and RFS-1 is proposed to promote homologous recombination at replication fork barriers (Ward et al., 2007).

Figure 3.20 shows that, while *radB*+ strains (H195 and H26) are highly resistant to the doses of mitomycin C used in this assay, strains containing *radB* deletions are exquisitely sensitive, i.e. H284 (Δ*radB*) and H64 (*radB*Δ*b/b*). This demonstrates that RadB is highly important for the repair of crosslinked DNA. Furthermore, these data demonstrate that the type of *radB* deletion does not affect the phenotype, with both H64 (*radB*Δ*b/b*) and H284 (Δ*radB*) being equally sensitive. Finally, the strain background differences between H26 and H195 derived strains do not affect the sensitivity to mitomycin C.

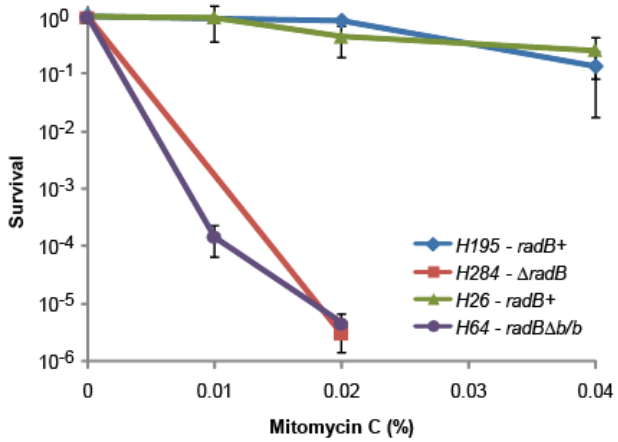

Figure 3.20 Survival of strains H195 (*radB*+), H284 (Δ*radB*), H26 (*radB*+) and H64 (*radB*Δ*b/b*) when grown on media supplemented with mitomcyin C. All data points are calculated as the mean value of three trials. Error bars are calculated as standard error.

Summary

It has been demonstrated that both the partial deletion of *radB* (*radB*Δ*b/b*) and the complete deletion of *radB* in *H. volcanii* lead to equally defective phenotypes. Strains are slower growing and more sensitive to UV irradiation and mitomycin C than *radB*+ strains. Furthermore, it has been demonstrated that the strain background of H195 (Δ*pyrE2* Δ*trpA* Δ*hdrB leuB-Ag1 bgaHa-Bb*) and H26 (Δ*pyrE2*) do not alter the growth or UV sensitivity phenotypes. It has been demonstrated that RadB is unlikely to function in NER, as no epistatic relationship between UvrA and RadB has been detected. This finding might suggest that RadB functions in the HR pathway. HR is required for the restart of broken replication forks and can be used for the repair of UV induced lesions that lead to double strand breaks when encountered by a replication fork. Additionally, mitomycin C generated DNA crosslinks tend to be repaired by NER or HR in bacteria (Hornback and Roop, 2006). If RadB does function in HR, as might be expected of a RadA paralogue, Δ*radB* strains would be defective in HR and therefore defective in the reestablishment of replication forks, manifesting as a slow growth phenotype, and more sensitive to UV irradiation and mitomycin C.

Finally, the extreme sensitivity to mitomycin C compared to the relatively less extreme sensitivity to UV induced lesions could be due to the nature of the assay. In the UV survival assays, cells are transiently exposed to UV light then allowed to recover. In the mitomycin C assay, cells are constantly exposed to the toxin as it is included into the plates, therefore a lower frequency of survival might be expected.

3.2.11 Characterisation of Hjc, PolD and RadA

RadB from *Pyrococcus furiosus* has been shown to interact *in vitro* with several other proteins involved in DNA repair (Hayashi et al., 1999). These proteins are Hjc, a Holliday junction resolvase (Bolt et al., 2001; Dorazi et al., 2006; Komori et al., 1999), Dp1, the proofreading subunit of the archaeal DNA polymerase PolD (Tang et al., 2004), and RadA, the archaeal Rad51/RecA homologue (Sandler et al., 1999; Sandler et al., 1996; Woods and Dyall-Smith, 1997). These interactions, especially the interaction of RadB with Hjc and RadA, suggest a function in recombination. Thus, to elucidate any epistatic effect between these genes, attempts were made to delete them from *H. volcanii* in H195 (*radB*+) and H284 (Δ*radB*).

3.2.12 Chromosomal deletion of *radA*

Strains deleted for *radA* were generated by T. Allers, prior to this work. These strains are H97 (Δ*radA*) and H186 (Δ*radA radB*Δ*b/b*), in a H26 strain background. Strains H26 (*radB*+) and H64 (*radB*Δ*b/b*) were each transformed with 1 µg pTA83 (Δ*radA*:*pyrE2*) (Figure 3.21), which was generated prior to this thesis by T. Allers. Ura+ integrants of the Δ*radA* construct at the chromosomal *radA* locus were selected by plating transformants on Hv-Ca. Integrant strains were verified by *Mlu*I digest of genomic DNA, gel electrophoresis and Southern blot, using a *Sph*I-*Eco*RI fragment of pMDS41 (Woods and Dyall-Smith, 1997) as a template for the probe (Figure 3.22). Integrant derivatives of H26 and H64 were designated H56 and H151, respectively. Loss of the integrated plasmid was encouraged by serial growth of H56 and H151 in Hv-YPC broth, followed by plating on Hv-Ca + 5FOA. 5FOA resistant colonies (ura-) were patched onto Hv-YPC and incubated for 5 days at 45°C. Colony lift and hybridisation with a *Nco*I-*Not*I fragment of pSJS1140 (Sandler et al., 1996; Woods and Dyall-Smith, 1997), consisting of the *radA* coding sequence. Colonies that did not hybridise the probe were

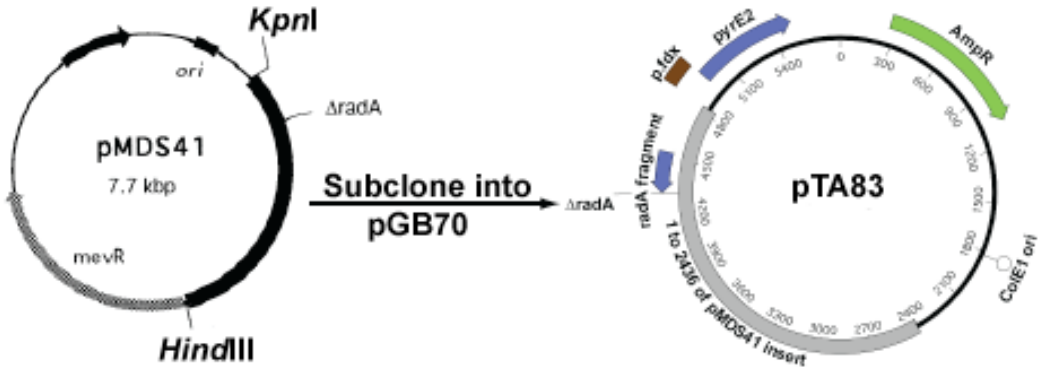

Figure 3.21 Subcloning of Δ*radA* construct from pMDS41 (Woods and Dyall-Smith, 1997) into *pyrE2* plasmid, pGB70 (Bitan-Banin et al., 2003) at *Hind*III site (filled in by Klenow), to generate pTA83. pMDS41 was obtained from Mike Dyall-Smith (University of Melbourne)

subjected to Southern blot analysis as before (*Mlu*I digest, *Sph*I-*Eco*RI fragment of pMDS41 as a probe template) (Figure 3.22). Δ*radA* derivative strains of H56 and H151 were designated H97 (*radB*+ Δ*radA*) and H186 (*radB*Δ*b/b* Δ*radA*), respectively.

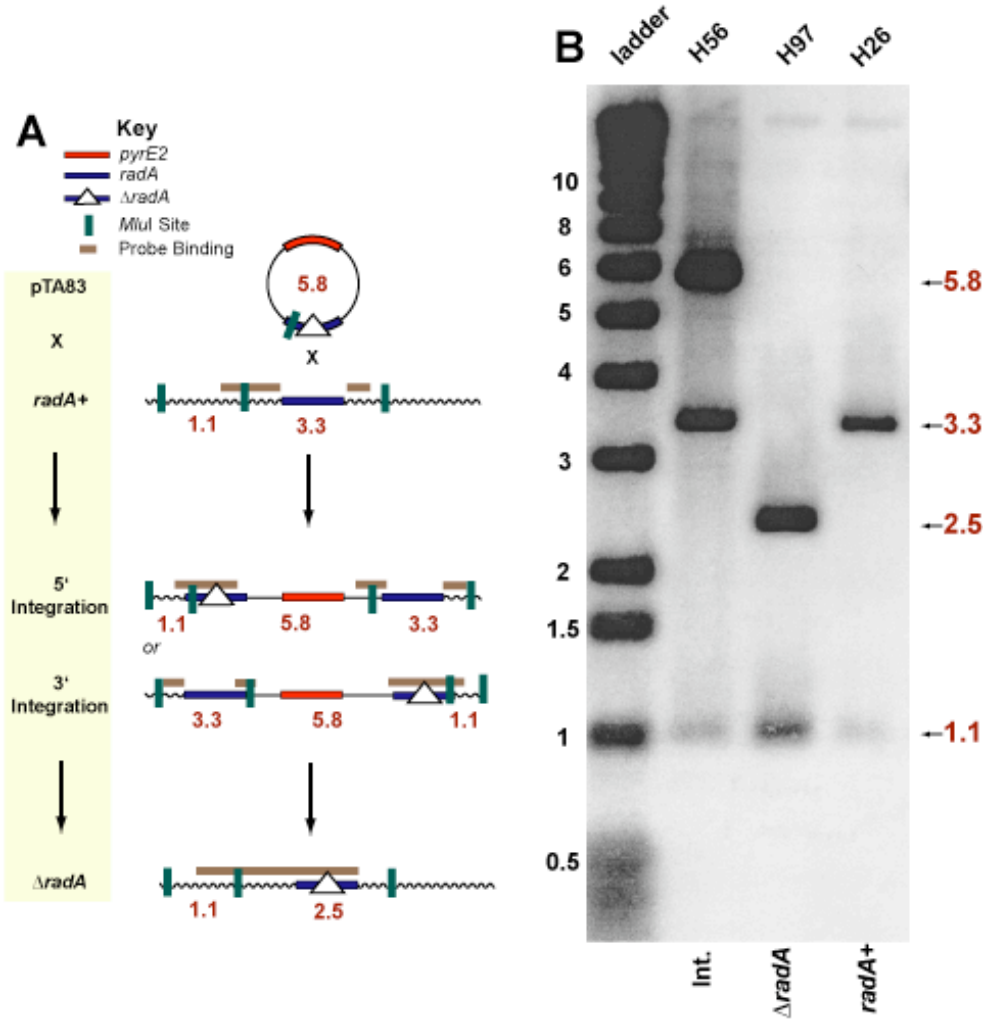

Figure 3.22 Schematic of the integration of the pTA83-borne Δ*radA* construct at the chromosomal *radA*+ locus of H26 (*radB*+) and H64 (*radB*Δ*b/b*), with possible integration events, 5' and 3' (H56 - see Figure 3.22 B) and the resulting chromosomal deletion (H97 - see Figure 3.22 B). The restriction enzymes used to digest chromosomal DNA are displayed with resulting fragment sizes (kb). **B** - Southern blot showing restriction digests of H26, H56 and H97 DNA following digestion with *Mlu*I, and hybridisation with the radiolabelled pMDS41 *Sph*I-*Eco*RI Δ*radA* fragment. The ladder used was 1kb ladder (NEB). Fragment sizes are indicated on the right of the blot, measured in kilobases. Southern blots of H64 (*radB*Δ*b/b*), integrant (H151) and Δ*radA* deletion strain (H186) had the same restriction fragments as the H26 derived strains, and are not shown.

3.2.13 Chromosomal deletion of *hjc*

Strains H195 (*radB*+) and H284 (Δ*radB*) were each transformed with 1 µg pTA236 (Δ*hjc*:*pyrE2*) (Figure 3.23), which was generated prior to this thesis by T. Allers. Ura+ integrants of the Δ*hjc* construct at the chromosomal *hjc* locus were selected by plating transformants on Hv-Ca + Trp + Thy. Integrant strains were verified by *Bsa*AI digest of genomic DNA, gel electrophoresis and Southern blot, using a 453 bp *Age*I-*Mlu*I Δ*hjc* fragment of pTA236 as a template for the probe (Figure 3.24). 5' integrants of H195 and H284 were designated H238 and H319, respectively. Loss of the integrated plasmid was encouraged by growth of H238 and H319 in Hv-YPC + Thy broth, followed by plating on Hv-Ca + Trp + Thy + 5FOA. 5FOA resistant colonies (ura-) were patched onto Hv-YPC + Thy and incubated for 5 days at 45°C. Colony lift and colony hybridisation with a 143 bp *Bsa*AI-*Stu*I fragment of pTA191, consisting of a central region of *hjc* was carried out. Colonies that did not hybridise

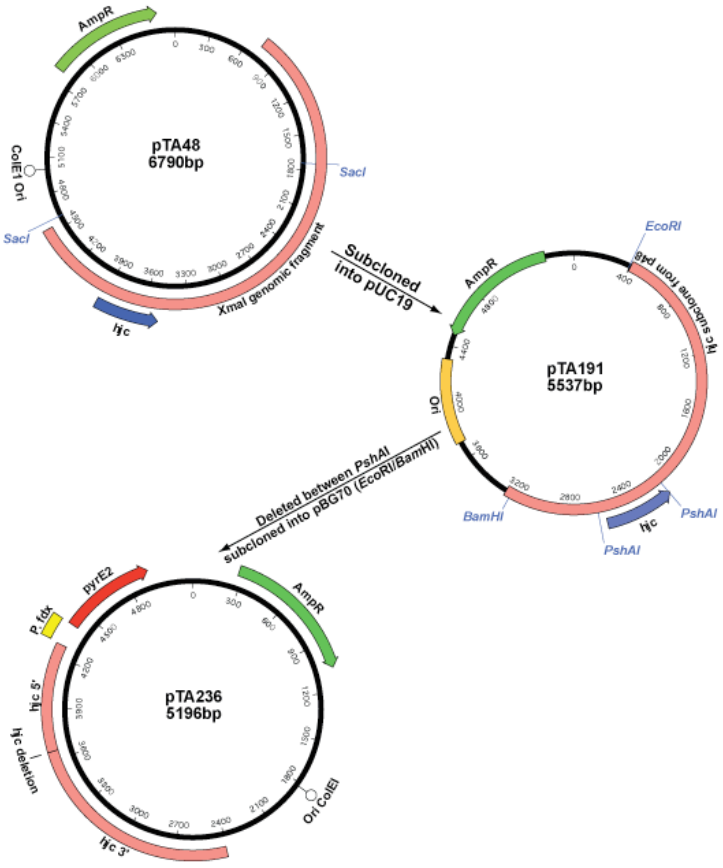

Figure 3.23 Construction of pTA236. A 4 kb *Xba*I fragment containing *H.volcanii hjc* was cloned into pBluescript II SK+ (pTA48). From pTA48, a *Sac*I fragment containing *hjc* was subcloned into pUC19 (pTA191). *hjc* was deleted from pTA191 by *Psh*AI digest and re-ligation, followed by subcloning a *Bam*HI-*Eco*RI fragment containing the deletion construct onto pGB70 at *Bam*HI/*Xmn*I sites, generating pTA236.

the probe were subjected to Southern blot analysis as before (*Bsa*AI digest, *Age*I-*Mlu*I fragment of pTA236 as a probe template) (Figure 3.25). Δ*hjc* derivative strains of H238 and H319 were designated H282 (*radB*+ Δ*hjc*) and H349 (Δ*radB* Δ*hjc*) (Figure 3.24)

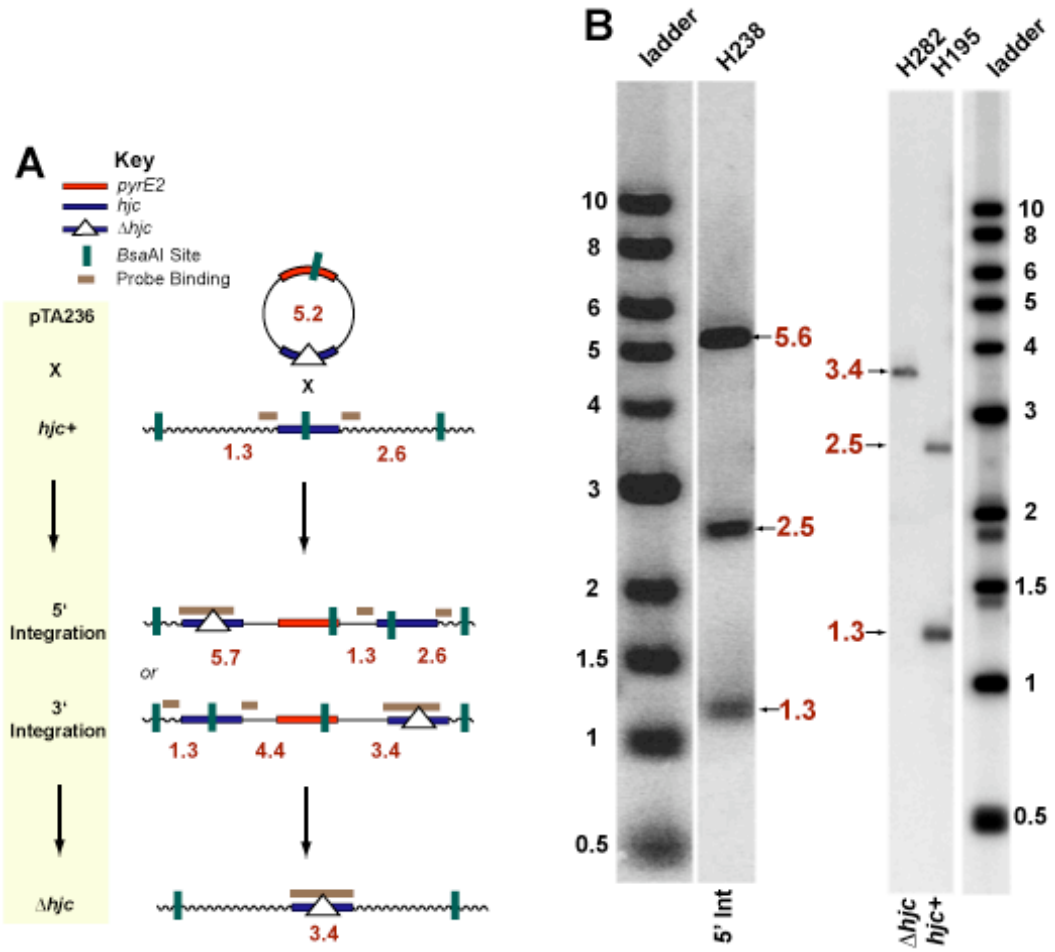

Figure 3.24 A - Schematic of the integration of the pTA236-borne Δ*hjc* construct at the chromosomal *hjc*+ locus of H195, with both possible integration events, 5' and 3' (H238 - see Figure 3.24 B) and the resulting chromosomal deletion (H282 - see Figure 3.24 B). The restriction enzyme used to digest chromosomal DNA is displayed and resulting fragment sizes are displayed in kilobases. **B** - Southern blot showing restriction digests of H195, H238 and H282 DNA following digestion with *Bsa*AI, and hybridisation with the radiolabelled 453 bp pTA236 *Age*I-*Mlu*I Δ*hjc* fragment. The ladder used was 1kb ladder (NEB). Fragment sizes are indicated on the right of the blot, measured in kilobases. Southern blots of H284 (Δ*radB*) integrant (H319) and Δ*hjc* deletion strain (H349) had the same restriction fragments as the H195 derived strains, and are not shown.

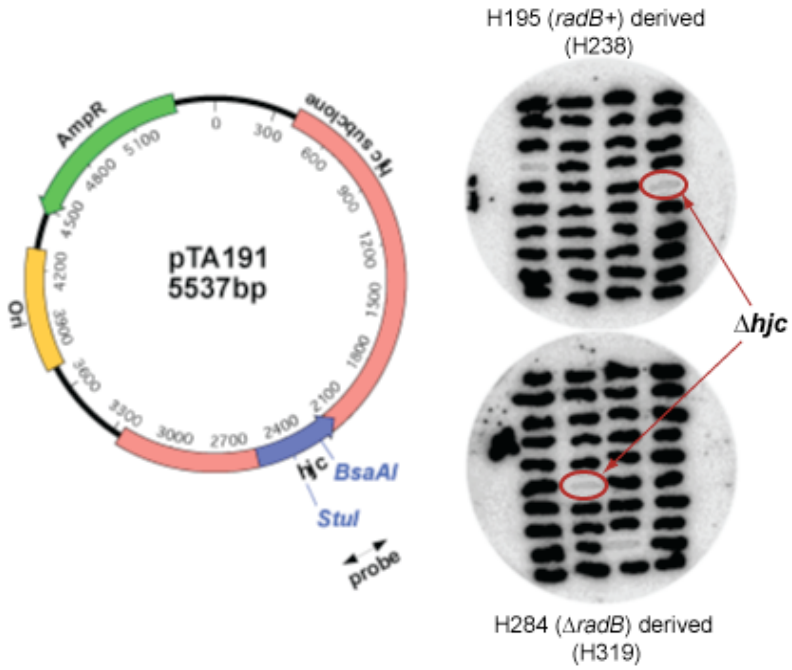

Figure 3.25 Colony hybridisations of H195 (*radB*+) and H284 (ΔradB) derived strains. The probe used to hybridise was a *Bsa*AI-*Stu*I fragment of pTA191, containing sequence internal to *hjc*. Numbers in parentheses represent the integrant strains prior to relieving uracil selection and plating on Hv-Ca + Trp + Thy + 5FOA, to select for ura- derivatives.

3.2.14 Chromosomal deletion of *dp1*

dp1 codes for the proofreading subunit of the archaeal DNA polymerase, PolD. Attempts were made to delete *dp1* from the *H.volcanii* genome, but no deletion strains were obtained following screening of > 500 colonies, following plating on Hv-Ca+5FOA plates (the stage at which either a deletion or wildtype allele will be observed), suggesting that the deletion of *dp1* might not be possible through this method of gene deletion. Furthermore, the experiment was repeated with the plasmid-borne deletion of *dp1* being marked with *trpA*. Despite selection for tryptophan being maintained throughout the deletion process, no deletion colonies were observed.

3.2.15 Phenotypic analysis of Δ*hjc* and Δ*radA*

Assays that were used to characterise Δ*radB* strains were also used to characterise strains deleted for *hjc* and *radA*. Strains were tested for growth rates, UV survival and sensitivity to the DNA crosslinking agent, mitomycin C. Strains used in these assays are shown in Table 3.3

Strain	Genotype	Background
H26	*radA*+ *radB*+ *hjc*+	H26
H64	*radA*+ ***radB*Δ*b/b*** *hjc*+	H26
H97	Δ***radA*** *radB*+ *hjc*+	H26
H186	Δ***radA radB*Δ*b/b*** *hjc*+	H26
H195	*radA*+ *radB*+ *hjc*+	H195
H282	*radA*+ *radB*+ Δ***hjc***	H195
H284	*radA*+ Δ***radB*** *hjc*+	H195
H349	*radA*+ Δ***radB*** Δ***hjc***	H195

Table 3.3 Strains used in growth rate, UV sensitivity and mitomycin C sensitivity assays

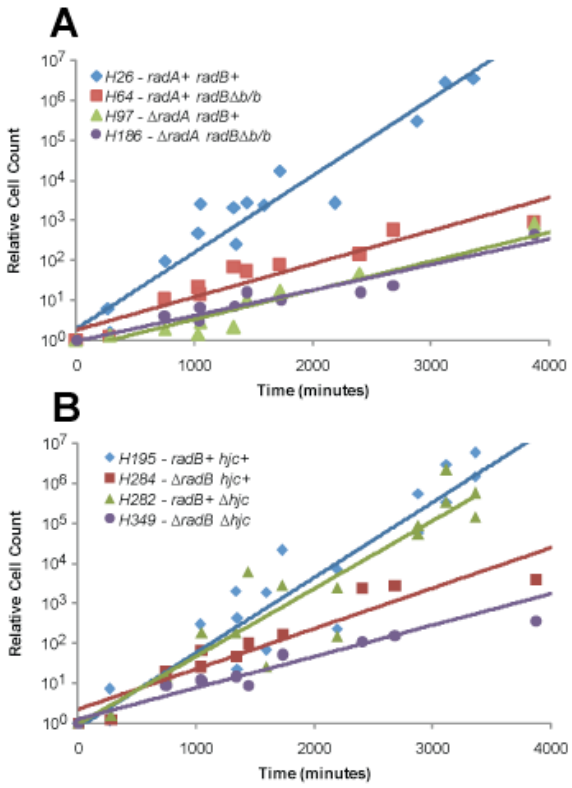

Figure 3.26 Growth rates in strains deleted for genes that encode proteins shown to interact with RadB *in vitro*. **A** Growth rates of H26 (*radA*+ *radB*+), H64 (*radA*+ *radB*Δ*b/b*), H97 (Δ*radA radB*+) and H186 (Δ*radA radB*Δ*b/b*) to determine the effect of Δ*radA*. **B** Growth rates of H195 (*hjc*+ *radB*+), H284 (*hjc*+ Δ*radB*), H282 (Δ*hjc radB*+) and H349 (Δ*hjc* Δ*radB*), to determine the effect of Δ*hjc*. Relative cell count is calculated as a proportion of the cells present at time = 0 minutes. Data points are consolidated from three trials.

Growth rates

Growth rates for strains were determined as before. Cultures were grown to A_{650} = 0.4 and diluted 1 in 10000. Cultures were then incubated at 45°C and aliquots were plated on Hv-YPC (+ Thy for H195 derivatives) at appropriate dilutions, at regular intervals (Figure 3.26)

A

Strain	**H26**	**H64**	**H97**	**H186**
Relevant genotype	*radA*+ *radB*+	*radA*+ *radB*Δ*b/b*	Δ*radA* *radB*+	Δ*radA* *radB*Δ*b/b*
Generation Time (mins)	156	363	415	475

B

Strain	**H195**	**H284**	**H282**	**H349**
Relevant genotype	*hjc*+ *radB*+	*hjc*+ Δ*radB*	Δ*hjc* *radB*+	Δ*hjc* Δ*radB*
Generation Time (mins)	160	331	177	385

Table 3.4 Calculated generation times for tested strains, in minutes **A** H26 (*radA*+ *radB*+), H64 (*radA*+ *radB*Δ*b/b*), H97 (Δ*radA radB*+) and H187 (Δ*radA radB*Δ*b/b*) **B** H195 (*hjc*+ *radB*+), H284 (*hjc*+ Δ*radB*), H282 (Δ*hjc radB*+) and H349 (Δ*hjc* Δ*radB*). Only relevant genotypes are shown

Effect of ΔradA *on growth rates*

Figure 3.26-A and Table 3.4-A show that H97 (Δ*radA radB*+) is significantly slower growing than the H26 (*radA*+ *radB*+) indicating that RadA is important for normal growth (Woods and Dyall-Smith, 1997). H97 growth rates are only slightly slower than H64 (*radA*+ *radB*Δ*b/b*) suggesting that RadA and RadB have near equal importance in normal growth. The double deletion strain, H186 (Δ*radA radB*Δ*b/b*) exhibits the same growth rate as H97 (Δ*radA radB*Δ*b/b*). This strongly suggests that RadA and RadB function in the same pathway, and that *radA* is epistatic to *radB*.

Effect of Δhjc *on growth rates*

Figure 3.26-B and Table 3.4-B show that H282 (Δ*hjc radB*+) displays comparable growth rates to H195 (*hjc*+ *radB*+), suggesting that Hjc is not required for normal growth. However, H349 (Δ*hjc* Δ*radB*) exhibits slower growth rates than H284 (*hjc*+ Δ*radB*), suggesting that Hjc is important for normal growth, in the absence of RadB.

Survival following UV irradiation

To determine the sensitivity to UV irradiation, strains were plated on Hv-YPC (+ Thy for H195 derivative strains) and exposed to varying doses of UV light. Plates were then incubated at 45°C for 5 days, in the dark. (Figure 3.27)

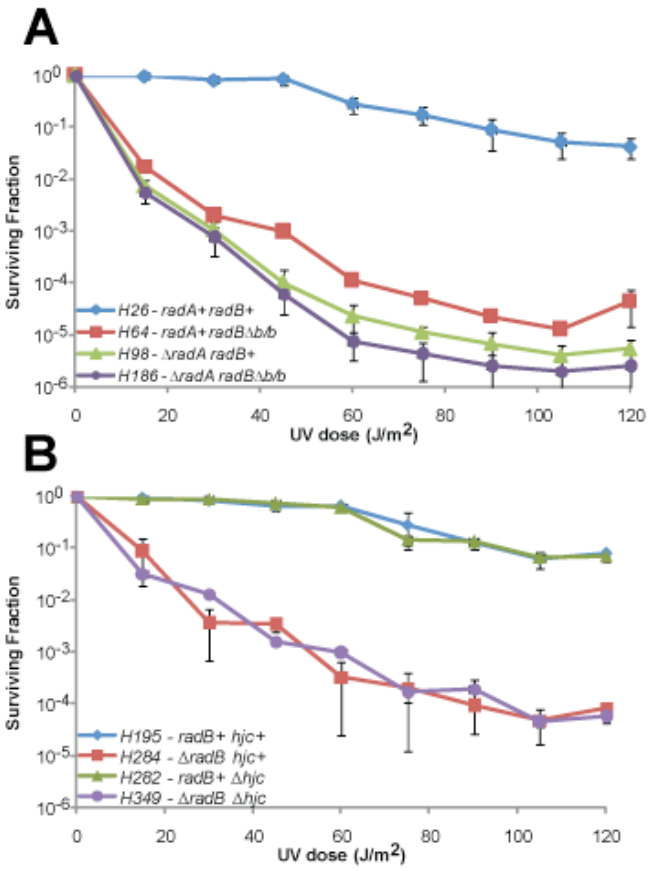

Figure 3.27 UV sensitivity in strains deleted for genes that encode proteins shown to interact with RadB *in vitro*. **A** Sensitivity of H26 (*radA*+ *radB*+), H64 (*radA*+ *radB*Δ*b/b*), H97 (Δ*radA radB*+) and H186 (Δ*radA radB*Δ*b/b*), to determine the effect of Δ*radA*. **B** Sensitivity of H195 (*hjc*+ *radB*+), H284 (*hjc*+ Δ*radB*), H282 (Δ*hjc radB*+) and H349 (Δ*hjc* Δ*radB*), to determine the effect of Δ*hjc* All data points are calculated as the mean value of 3 trials. Error bars are calculated as standard error. Only relevant genotypes are shown.

Effect of ΔradA *on UV sensitivity*

Figure 3.27-A shows that H97 (Δ*radA radB*+) is more sensitive to UV irradiation than H26 (*radA*+ *radB*+) indicating that RadA is important in the repair of UV induced DNA damage (Woods and Dyall-Smith, 1997). H97 survival frequencies are also only slightly lower than H64 (*radA*+ *radB*Δ*b/b*) suggesting that RadA and RadB have near equal importance in UV damage repair. The double deletion strain, H186 (Δ*radA radB*Δ*b/b*) exhibits the same sensitivity as H97 (Δ*radA radB*Δ*b/b*). This, coupled with the growth rate comparisons of these strains, strongly suggests that RadA and RadB function in the same pathway, and that *radA* is epistatic to *radB*.

Effect of Δhjc *on UV sensitivity*

Figure 3.27-B shows that H282 (Δ*hjc radB*+) displays identical UV survival frequencies to H195 (*hjc*+ *radB*+), suggesting that Hjc is not required for the repair of UV induced DNA damage. Additionally, H349 (Δ*hjc* Δ*radB*) exhibits comparable UV sensitivity to H284 (*hjc*+ Δ*radB*), suggesting that Hjc is not important for the repair of UV induced DNA damage in the absence of RadB, contrasting with its role in growth in the absence of RadB.

Sensitivity to mitomycin C

Mitomycin C generates DNA crosslinks. These lesions can be repaired by homologous recombination. To determine whether RadA or Hjc are important in the repair of mitomycin C induced lesions, strains were plated on Hv-YPC (+ Thy for H195 derivative strains) containing mitomycin C. (Figure 3.28)

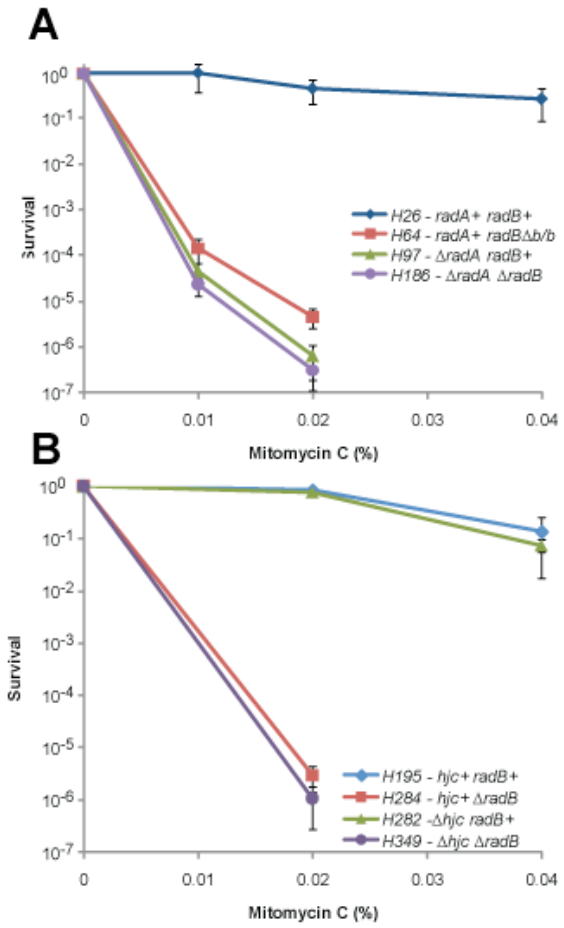

Figure 3.28 Mitomycin C sensitivity in strains deleted for genes that encode proteins shown to interact with RadB *in vitro*. **A** Sensitivity of H26 (*radA*+ *radB*+), H64 (*radA*+ *radB*Δ*b/b*), H97 (Δ*radA radB*+) and H186 (Δ*radA radB*Δ*b/b*), to determine the effect of Δ*radA*. **B** Sensitivity of H195 (*hjc*+ *radB*+), H284 (*hjc*+ Δ*radB*), H282 (Δ*hjc radB*+) and H349 (Δ*hjc* Δ*radB*), to determine the effect of Δ*hjc* All data points are calculated as the mean value of 3 trials. Error bars are calculated as standard error. Only relevant genotypes are shown.

Effect of ΔradA *on mitomycin C sensitivity*

Figure 3.28-A shows that H97 (Δ*radA radB*+) is more sensitive to mitomycin C exposure than H26 (*radA*+ *radB*+), indicating that RadA is important in the repair of crosslinked DNA. H97 survival frequencies are also only slightly lower than H64 (*radA*+ *radB*Δ*b/b*) suggesting that RadA and RadB have near equal importance in this repair. The double deletion strain, H186 (Δ*radA radB*Δ*b/b*) exhibits the same sensitivity as H97 (Δ*radA radB*Δ*b/b*).

Effect of Δhjc *on mitomycin C sensitivity*

Figure 3.28-B shows that H282 (Δ*hjc radB*+) displays identical mitomycin C survival frequencies to H195 (*hjc*+ *radB*+), suggesting that Hjc is not required for the repair of crosslinked DNA. Additionally, H349 (Δ*hjc* Δ*radB*) exhibits comparable mitomycin C sensitivity to H284 (*hjc*+ Δ*radB*), suggesting that Hjc is not important for the repair of crosslinked DNA in the absence of RadB, contrasting with its role in growth in the absence of RadB.

Summary

Phenotypic analysis of ΔradA

In this section it has been demonstrated that the deletion of *radA* is highly detrimental to *H.volcanii*. H97 (Δ*radA radB*+) exhibits significantly slower growth rates than the *radA*+ strain, H26, with an average generation time 2.5 fold longer than observed in H26 (Table 3.4-A). This indicates that, like RadB, RadA is required during normal growth. As RadA is the archaeal recombinase, it is likely that this requirement during growth is concerned with DNA replication restart. If a replication fork encounters nicked DNA, the fork can collapse (Figure 3.8) and generate a double strand DNA end. Replication forks can be re-established through strand invasion by a strand of the broken duplex into the second (intact) duplex. This D-loop structure can then be utilised to prime DNA synthesis, a process known as break induced replication (reviewed in Kraus et al., 2001). Alternatively, if a polymerase-blocking lesion is encountered, the replication complex can dissociate and the replication fork can regress to form a chicken foot junction (effectively a Holliday junction), which can then be resolved to generate two duplexes. From this, strand invasion can occur as described above to ultimately restart replication. Both of these means of resetting a replication fork require homologous recombination, therefore any defects in recombination might be expected to hinder DNA synthesis and result in slow growth rates.

H186 (Δ*radA radB*Δ*b/b*) displays similar growth rate defects to H97 (Δ*radA radB*+) and is only slightly slower growing than H64 (*radA*+ *radB*Δ*b/b*) (Figure 3.26 and Table 3.4-A). If RadA and RadB functioned in different pathways, it would be expected that the growth defects associated with each protein would be additive. As this is not the case, this is a clear indication that RadA and RadB function in the same pathway, most likely homologous recombination, with both proteins having near equal importance for normal growth. This epistatic relationship is also observed with the UV sensitivities of the strains assayed. H97 (Δ*radA radB*+) is only marginally more sensitive to UV irradiation than H64 (*radA*+ *radB*Δ*b/b*) with H186 (Δ*radA*

*radB*Δ*b/b*) exhibiting equal sensitivity to H97 (Figure 3.27-A). This demonstrates that *radA* is epistatic to *radB* for the repair of UV induced lesions. These lesions are likely to be single stranded DNA nicks that result in double stranded DNA breaks when encountered by replication forks (Figure 3.8).

Similarly, both H64 (*radA*+ *radB*Δ*b/b*) and H97 (Δ*radA radB*Δ*b/b*) display similar extreme sensitivity to mitomycin C, with H97 being marginally more sensitive (Figure 3.28-A). This demonstrates that RadA and RadB are both required for the efficient repair of cross-linked DNA lesions, which, in bacteria, are predominantly repaired by NER or homologous recombination in bacteria (Hornback and Roop, 2006). As with growth defects and UV sensitivity, H186 (Δ*radA radB*Δ*b/b*) and H97 (Δ*radA radB*+) are equally sensitive to mitomycin C, demonstrating that *radB* is epistatic to *radA* for this type of DNA damage.

These data, coupled with the synergistic relationship of *radB* and *uvrA* (Figure 3.19) strongly suggest that RadB functions in homologous recombination. Additionally, RadB is nearly as important as RadA for efficient growth and repair of some DNA lesions.

Phenotypic analysis of Δhjc

It has been demonstrated in this section that Hjc does not appear to be required under normal growth conditions or for the repair of UV or mitomycin C induced DNA lesions. Growth rates of H282 (Δ*hjc radB*+) are virtually identical to those exhibited by H195 (*hjc*+ *radB*+) (Figure 3.26-B), demonstrating either that the cleavage of Holliday junctions is not required under normal growth conditions or, more likely, that Hjc is not the primary Holliday junction resolvase in *H. volcanii.* As RadA is required during normal growth, it would be expected that homologous recombination is required. Unless all recombination during normal growth is non-crossover recombination (synthesis dependent strand annealing (Allers and Lichten, 2001)) which does not require a Holliday junction intermediate), it would be expected that Holliday junction resolvase is required. Thus, Hjc is not likely to be the primary resolvase, in *H.volcanii*. However H349 (Δ*hjc* Δ*radB*) growth rates are moderately slower than those observed in H284 (*hjc*+ Δ*radB*) (Figure 3.26-B). This could suggest a minor role for Hjc, only when RadB is absent. Alternatively, RadB might be able to compensate for the absence of Hjc therefore the phenotypic effects of Δ*hjc* would only be observed in the absence of RadB.

H282 (Δ*hjc radB*+) is no more sensitive to UV irradiation or mitomycin C than H195 (*hjc*+ *radB*+) indicating that Hjc is not required for the repair of DNA lesions induced by these sources, again suggesting that Hjc might not be the primary resolvase in *H. volcanii*. Since RadA is required for the repair of these forms of damage, this will involve homologous

recombination. Unless all recombinational repair of these lesions is by synthesis dependent strand annealing (where no Holliday junctions are required), it would be expected that a resolvase would be required. Furthermore, the mitomycin C and UV sensitivity of a Δ*radB* strain (H284, *hjc*+ Δ*radB*) is not worsened in the absence of Hjc (H349, Δ*hjc* Δ*radB*) (Figure 3.27 and Figure 3.28).

3.2.16 Mutational analysis of RadB

It has been demonstrated that deletion of *radB* leads to slow growth and hypersensitivity to UV irradiation and mitomycin C, most likely due to its role in homologous recombination. *In vitro* studies of RadB in *Pyrococcus furiosus* have shown that RadB binds both double and single stranded DNA, binds ATP and has a very weak ATPase activity (Komori et al., 2000b).To further dissect the role of RadB, two point mutations were introduced into *radB* in an attempt to disrupt the DNA and ATP binding activities of the protein.

3.2.17 Identification of the RadB ATP binding motif

Proteins that possess ATP binding and hydrolysis activity have characteristic domains known as Walker A and Walker B motifs. Walker A motifs have a consensus $^{G}/_{A}XXXGK^{T}/_{S}$ and all contain an invariant lysine that is necessary for ATP binding. The Walker A motif of *Pyrococcus furiosus* RadB was identified by Komori *et al* (2000b). To find the equivalent motif and conserved lysine in *H. volcanii* RadB, a multiple alignment of RadB proteins from various archaeal species was carried out. RadB sequences analysed (with accession numbers) were from *Pyrococcus furiosus* (P81415)*, Pyrococcus abyssi* (Q9V2F6)*, Halobacterium salinarum* (Q9HPF2)*, Thermoplasma volcanium* (Q97B99)*, Thermoplasma acidophilum* (Q9HJD3) and *Methanothermobacter thermautotrophicus* (O27728). The alignment was carried out using ClustalW in MacVector 9.5.2. Figure 3.29 shows the Walker A motif of *H. volcanii* RadB and the invariant lysine, necessary for ATP binding, at residue 36 (K36).

Figure 3.29 Alignment of RadB sequences to determine the position of the *H. volcanii* Walker A motif with motif $^{G}/_{A}XXXGK^{T}/_{S}$. This motif is highlighted in yellow. The invariant lysine residue of the Walker A box is highlighted in red.

3.2.18 Identification of the RadB DNA binding motif

Although RadB lacks the helix-hairpin-helix DNA binding motif found in RadA/Rad51(Komori et al., 2000b; Shin et al., 2003), it has been shown to bind both single and double stranded DNA, suggesting an alternate means of DNA binding. It was shown that a highly conserved motif at the C-terminus of RadB contributes to DNA binding (Guy et al., 2006; Shin et al., 2003). This motif is a basic patch of residues with consensus $^{R}/_{K}$HR (Figure 3.30). Mutation of histidine-206 to an alanine residue in *Hvo*-RadB reduces DNA binding of RadB, approximately 10-fold, and it is proposed that this mutation disrupts interactions between H206 and DNA backbone oxygen. Thus, the *in vivo* effect of this mutation (*radB-H206A*) was studied.

Figure 3.30 Conserved basic patch at the C-terminus of all RadB proteins, implicated in DNA binding. Figure taken from (Guy et al., 2006)

3.2.19 Generation of ATP and DNA binding mutations in Hvo-RadB (Guy et al., 2006)

Replicative plasmids containing either *radB-K36A,* a putative ATP binding mutant, or *radB-H206A*, a putative DNA binding mutant, were generated. Primer pairs EXTF/K36AR and K36AF/EXTR were designed that would bind to pTA50 (encoding *radB*). K36AF and K36AR bind to *radB* at the region that encodes K36, and contained base pair substitutions that, when the mutant gene is expressed, would generate a lysine to alanine mutation at residue 36 (K36A). This nucleotide substitution also generates a novel *Hae*II site at the mutation site. Amplifications of each half of the mutant construct were electrophoresed and purified. 250 ng of each product was used as a template for a further amplification, using external primers EXTF and EXTR. The final amplification product was purified, digested with *Bsp*EI and *Bst*EII and used to replace the wildtype *Bsp*EI-*Bst*EII fragment of pTA50. The full-length *radB-K36A* gene was ligated into the shuttle vector, pTA354, at the *Kpn*I and *Not*I sites (pTA627) (Figure 3.31).

The same procedure was carried out to generate *radB*-H206A. Primer pairs H206AF2/HEXTR and H206AR2/HEXTF were used for the amplifications, with HEXTF and HEXTR containing substitutions to generate the H206A mutation, and a novel *Xma*I site. The final amplification product was digested with *Cla*I and *BstE*II and used to replace the wildtype fragment of *radB* in

pTA50. The full-length *radB-H206A* gene was ligated into the shuttle vector, pTA354, at the *Kpn*I and *Not*I sites (pTA622). A schematic of the generation of mutation alleles in this manner is shown in Chapter 2 and Figure 3.31.

Both plasmids were confirmed by diagnostic digest (*Hae*II for pTA627 and *Xma*I for pTA622) and sequencing.

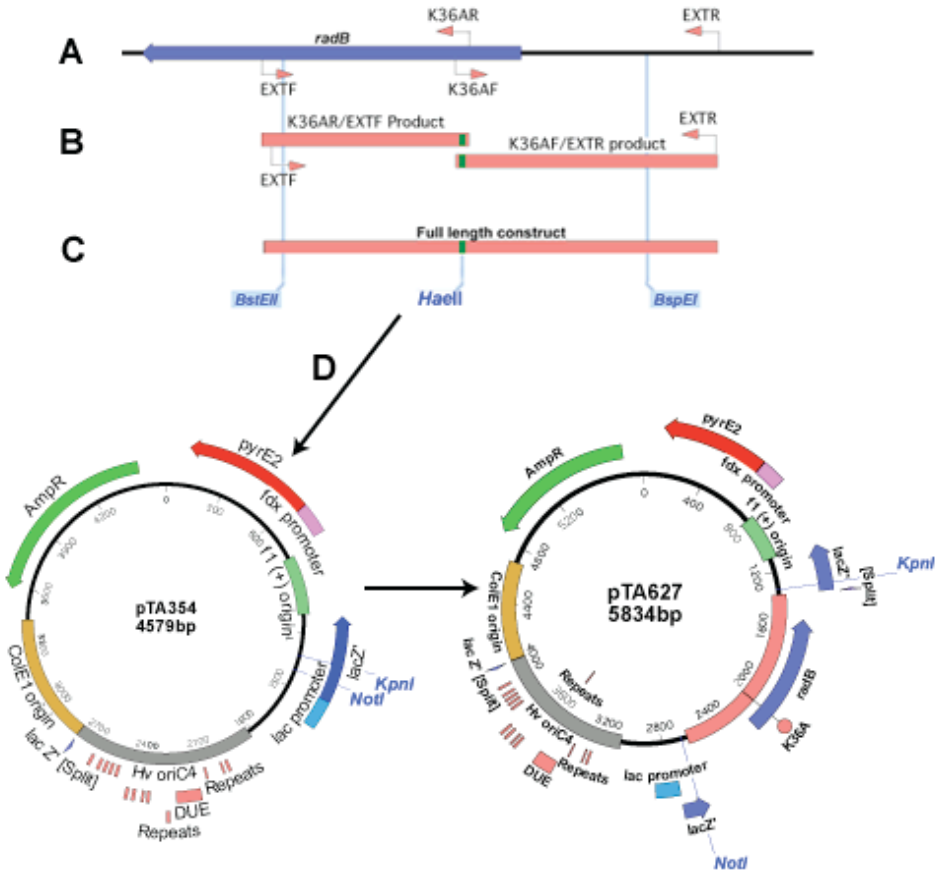

Figure 3.31 Generation of *radB-K36A* by PCR. **A** – Primer pairs amplify two halves of the construct. Internal primers for each pair (K36AF and K36AR) contain nucleotide substitutions that generate the mutation, and a novel *Hae*II site. **B** – A second amplification with EXTF and EXTR, using the previous products as template DNA. **C** – Full construct is digested with *Bst*EII and *Bsp*EI. **D** – Mutant fragment is used to replace same fragment of *radB* in pTA50, then a *Kpn*I-*Not*I fragment containing the construct is ligated into the same sites of pTA354 (pTA627). *radB-H206A* was generated by principally the same method.

Both pTA622 (*radB-H206A, pyrE2*+) and pTA627 (*radB-K36A, pyrE2*+) were used to transform H284 (Δ*radB* Δ*pyrE2*), generating H497 and H498 respectively. Three additional strains were generated, by transformation of H195 (*radB*+) with pTA354 (empty shuttle vector, *pyrE2*+) (H495), and transformation of H284 (Δ*radB,* Δ*pyrE2*) with pTA379 (*radB*+*, pyrE2*+) (H496) and pTA357 (empty shuttle vector, *pyrE2*+) (H494). All strains were confirmed by extracting plasmid DNA followed by diagnostic digests and sequencing.

UV survival

Strains H494, H495, H496, H497 and H498 were exposed to varying doses of UV irradiation on Hv-Ca + Trp + Thy plates and incubated in the dark at 45°C for 5 days (Figure 3.32).

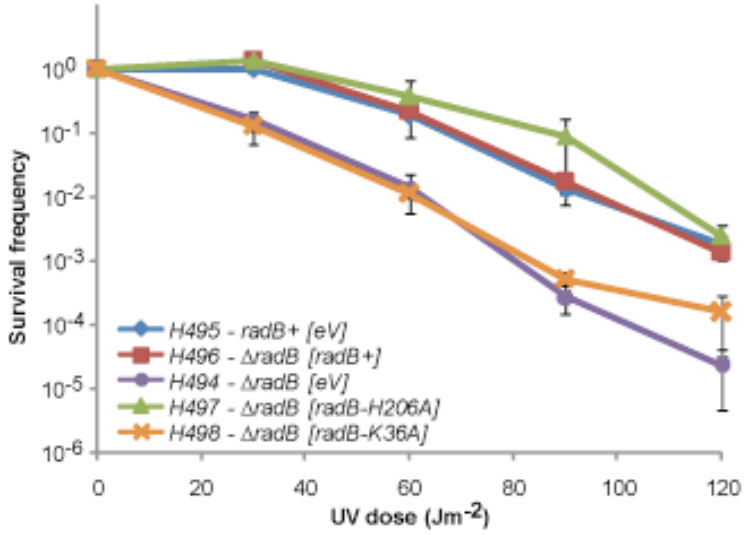

Figure 3.32 Survival of strains following UV irradiation. eV denotes empty vector (pTA357, *dam*- pTA354). Plasmids present in each strain are described in text. H495 (*radB*+ [eV]) and H496 (Δ*radB* [*radB*+]) were used as controls to ensure that survival frequencies were equivalent when *radB* is expressed episomally or chromosomally. All data points are calculated as the mean of 3 trials. Error bars are calculated as standard error.

Figure 3.32 shows that strains expressing *radB* episomally (H496) are as resistant to UV irradiation as strains expressing *radB* chromosomally (H495). This control demonstrates that the episomal expression of the mutant genes, *radB-K36A* and *radB-H206A*, is likely to be equivalent to the chromosomal expression of these genes, and that no dosage effects are likely to adversely affect results.

ATP binding is required for RadB function

Figure 3.32 shows that strains expressing *radB-K36A* (H498) are as hypersensitive to UV irradiation as Δ*radB* strains (H494). This suggests that the ATP binding activity of RadB is essential for RadB functionality.

DNA binding by the KHR basic patch of RadB is not essential for RadB function

Figure 3.32 shows that strains expressing *radB-H206A* (H497) are as resistant to UV irradiation as *radB*+ strains (H495 and H496). This suggests that a reduction in the DNA binding activity of RadB due to H206A does not negatively affect its function *in vivo*.

3.2.20 Analysis of radA and radB transcript levels following DNA damage

Analyses of transcriptional regulation have been carried out in archaeal species, including a study on transcriptional regulation of *radA* in the hyperthermophilic archaeon *Sulfolobus solfataricus* and the mesophilic archaeon *Methanococcus jannaschii* (Reich et al., 2001). Following exposure to methylmethane sulfonate or UV light, *radA* transcript levels increased in both species with a more marked increase in levels in *Sulfolobus solfataricaus*. Further transcriptional regulation studies were carried out by DiRuggiero *et al* (Williams et al., 2007) using microarray analyses of the euryarchaeal hyperthermophile *Pyrococcus furiosus.* DiRuggiero's results showed a moderate upregulation in *radA* transcript levels but no significant increase in transcript levels of *radB*.

To determine whether transcription of *radA* and *radB* is upregulated following DNA damage in *H.volcanii*, RNA was extracted from cells that had been exposed to 20 Jm^{-2} UV irradiation and allowed to recover at 45°C for 30 minutes, alongside cells that had not been exposed to UV irradiation. 20 Jm^{-2} UV irradiation was used to minimise cell death while still stimulating a DNA damage response from the cell. Following RNA extraction, RT-PCR was used to measure transcript levels of *radA* (RADARTF/RADARTR primers) and *radB* (RADBRTF2/RADBRTR1). RT-PCR denotes reverse transcriptional PCR, where RNA is used as a template for an RNA dependent DNA polymerase. Following an initial amplification, this polymerase is inactivated and a second DNA dependent DNA polymerase amplifies from the newly synthesised DNA, as with normal PCRs. As a control, *rpoA* transcripts were also amplified (RPOARTF/RPOARTR). *rpoA* encodes an RNA polymerase subunit and was chosen as it has been demonstrated that transcript levels of this gene do not change depending on the growth phase of the cell (Tom Batstone, University of Nottingham, personal communication). (Figure 3.33).

Figure 3.33 shows that transcript levels of *rpoA* do not change following DNA damage, as predicted. This is also true for *radB* transcript levels, showing that expression of *radB* is not induced in response to DNA damage. Conversely, *radA* transcription was upregulated 2.5 fold following 20 Jm^{-2} UV irradiation. This demonstrates that *radA*, but not *radB* transcription is induced by DNA damage.

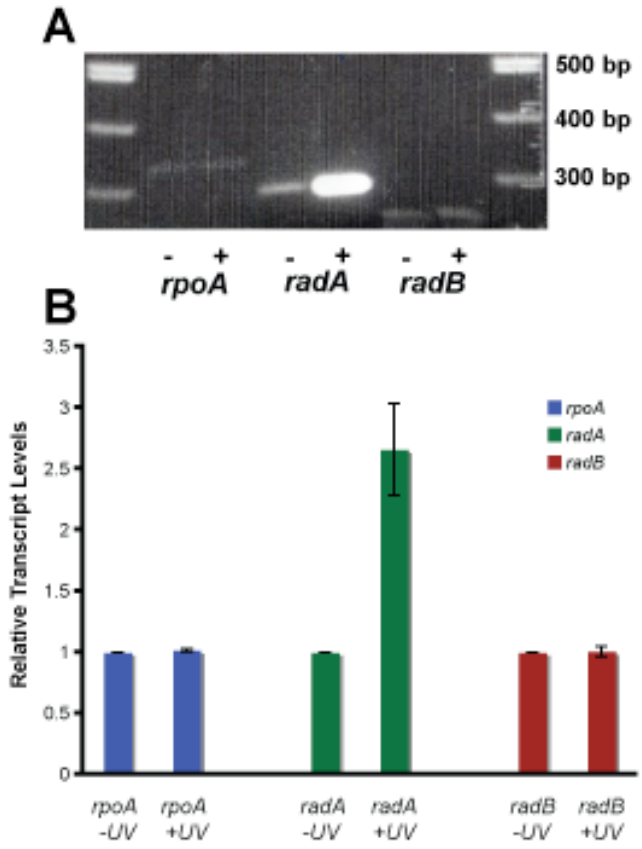

Figure 3.33 A - Relative RNA transcript levels of *rpoA, radA* and *radB* when cells are not exposed to UV irradiation (-) or 20 Jm^{-2} UV irradiation (+). **B** – Graphical representation of relative transcript levels. Levels were measured by analysing relative intensity of DNA bands using ImageQuant (Fujifilm) All results shown are calculated as the average of 3 trials. Error bars are calculated as standard error.

3.3 Discussion

The results presented in this chapter show that RadB is a DNA repair protein. This is suggested by Δ*radB* strains being hypersensitive to DNA damage, induced by UV irradiation and mitomycin C. As RadB is paralagous to RadA and not involved in NER as evidenced by a synergistic relationship between *uvrA* and *radB* in terms of UV survival. It is therefore likely that RadB functions in recombination. This hypothesis is strongly reinforced by the observation that Δ*radA* Δ*radB* strains exhibit equal sensitivity to UV irradiation as Δ*radA* single mutants, indicating that *radB* is epistatic to *radA*. Furthermore, recombination is required as a pathway of replication fork repair, a process required under normal growth, and Δ*radB* and Δ*radA* strains are slow growing. Double deletion strains are as slow growing as Δ*radA* strains, suggesting that the growth defects are due to defects in recombination, and that RadB is required in conjunction with RadA. In fact, wherever Δ*radA* strains show a defective phenotype, Δ*radB* strains exhibit a similar, marginally less severe phenotype.

It has been shown here that this binding of ATP by RadB is essential for its activity, as demonstrated by *radB-K36A* strains being phenotypically identical to Δ*radB* strains in terms of UV sensitivity. Although RadB has been shown to bind ATP *in vitro*, its rate of hydrolysis is extremely low (Komori et al., 2000b). Later, it was demonstrated that ATP binding of RadB induces a conformational change in the protein (Guy et al., 2006). It is possible that native RadB exists in an inactive form until required and that the conformationally altered RadB represents the active form of the protein. Thus, abolishment of RadB ATP binding could prevent activation of RadB.

Transcription of *radA*, but not *radB,* is induced by DNA damage (Figure 3.33). Thus, RadB might not be required in large quantities like RadA, which is required in the assembly of extensive nucleoprotein filaments. RadB is proposed to function as a homodimer (Akiba et al., 2005; Guy et al., 2006) and therefore less RadB would be required by the cell, in comparison with RadA. Induction of *radA* might be necessary as it would be energetically inefficient to have excess RadA in the cell when it is not required. Furthermore, the presence of constitutively high intracellular RadA levels might interfere with other information processing mechanisms such as transcription and translation. A reason why *radB* transcription is not upregulated following DNA damage might be that RadB is required equally during normal growth and under stress conditions. A further possibility is that RadB might exist in an inactive form and that instead of a transcriptional response to DNA damage, RadB itself is modified following DNA damage. This hypothesis is reinforced by the observed conformational change of RadB when bound to ATP (Guy et al., 2006), and that abolishment of ATP binding leads to a Δ*radB* phenocopy. Additional possible mechanisms of post translational modification in RadB

could exist to activate the protein. For example, Rad55/57 complex, a fungal paralogue of Rad51, is phosphorylated in response to DNA damage (Bashkirov et al., 2006; Bashkirov et al., 2000; Herzberg et al., 2006) and mutation of these phosphorylation sites leads to repair defects.

In contrast to ATP binding by RadB, DNA binding by the KHR basic patch of RadB does not appear to be as important for its function. By mutating the proposed KHR DNA binding motif (Guy et al., 2006), a strain expressing *radB-H206A* was generated. This strain showed no sensitivity to UV irradiation beyond that observed in *radB*+ strains, demonstrating that DNA binding by this region is not important for the repair of DNA damage, at least in terms of UV irradiation. The DNA binding affinity of RadB-H206A is approximately 10-fold lower than wild-type RadB (Guy et al., 2006), which might be sufficient for RadB to function.

Finally, genetic analysis of the archaeal Holliday junction resolvase Hjc reveals that it is not required for normal growth or the repair of UV and mitomycin C induced DNA lesions. As RadA is necessary for the efficient repair of these lesions, suggesting that homologous recombination is required, it is likely either that Hjc does not function during recombination, or that a second undiscovered resolvase exists that is redundant to Hjc. It has been demonstrated that Hjc can compensate for mutations in *ruvC* in *E.coli* (Bolt et al., 2001), and that Hjc readily cleaves Holliday junctions *in vitro* (Dorazi et al., 2006). Thus, it is likely that *H.volcanii* Hjc is a true Holliday junction resolvase, but that a second resolvase exists that can compensate for Δ*hjc*.

Hjc does not appear to be required in the absence of RadB, either, with the exception that Δ*radB* Δ*hjc* strains are slower growing that Δ*radB hjc*+ strains. This could suggest a role for Hjc in a minor RadB-independent pathway of recombination, but no role in RadB-dependent recombination. This is reinforced by the observed inhibition of Hjc in the presence of RadB and ATP (Komori et al., 2000b).

Chapter 4: Genetic Analysis of Homologous Recombination in RadB, RadA and Hjc Mutants

4.1 Introduction

4.1.1 Recombination

Homologous recombination (HR) is a ubiquitous process. HR is necessary for ensuring genetic diversity through crossover and gene conversion events as well as representing a major pathway for the repair of DNA double strand breaks (DSBs), along with non-homologous end joining (NHEJ). The basic process of HR involves the resection of the DNA ends present at a DSB to 3' ssDNA tails, by exonuclease activity (e.g. RecBCD in *E.coli*). Following resection, RecA/Rad51/RadA (in bacteria, eukaryotes and archaea, respectively), is loaded onto the single stranded DNA and monomers of this protein cooperatively bind to form long helical nucleoprotein filaments along the DNA. This active filament then undergoes a search for homologous sequences on other DNA molecules, e.g. a homologous chromosome or intra-chromosomal repeated sequences. Once homology has been found, strand exchange occurs whereby the invading strand base pairs with the second DNA molecule, forming a D-loop structure. DNA synthesis is then primed from the invading strand. At this stage, two outcomes are possible. The invading strand and newly synthesised DNA can be ejected by helicase activity (e.g. BLM helicase in *Drosophila melanogaster* (Weinert and Rio, 2007) followed by binding to ssDNA at the opposite side of the break. DNA synthesis is primed to fill in the gapped DNA followed by ligation to restore the DNA duplex. This process is synthesis dependent strand annealing (SDSA) and generates a non-crossover product with the template duplex containing no heteroduplex DNA and the repaired duplex only containing heteroduplex DNA at the region of newly synthesised DNA.

Alternatively, instead of the invading strand being ejected from the D-loop, the second ssDNA tail from the opposite side of the DNA break can base pair with the other strand of the template DNA molecule at the D-loop followed by priming of DNA synthesis. DNA ends are ligated together and two Holliday junction (HJ) structures are formed. The HJs can migrate powered by helicase activity (e.g. RuvAB in bacteria) to generate larger regions of heteroduplex DNA. The HJs are then cleaved by Holliday junction resolvases (e.g. RuvC in bacteria) and depending on the orientation of cleavage, the resulting duplexes will be crossover or non-crossover products: If both junctions are cleaved in opposite orientations, the products will be crossover products and if the junctions are cleaved in the same orientation, the product will be non-crossover. However, it is widely accepted that the generation of non-crossover products

predominantly occurs through the SDSA pathway (Allers and Lichten, 2001). These pathways are summarised in Figure 1.7, Chapter 1.

4.1.2 Recombinase paralogues

The requirement for the recombinase proteins (RecA/Rad51/RadA) is paramount for the process of HR to occur. In the absence of a recombinase, no homology search or strand invasion can occur, with the exception of minor RecA/Rad51-independent recombination pathways such as RecET-dependent, Rad52-dependent recombination (Noirot et al., 2003; Tsukamoto et al., 2003) and a *Saccharomyces cerevisiae* Rad51-independent pathway of break induced replication (Lydeard et al., 2007). While the recombinase proteins have diverged, especially RecA in relation to Rad51 and RadA, they all maintain core features. They are DNA-dependent ATPases (reviewed in Shin et al., 2004) that form long active nucleoprotein filaments on ssDNA, and catalyse the ensuing homology search and strand exchange. Furthermore, RecA and Rad51 are unable to self-load onto DNA due to SSB (single strand binding protein, in bacteria) and RPA (replication protein A, in eukaryotes) competitively binding the ssDNA substrate. Recombination mediator proteins are needed to load RecA/Rad51. In bacteria, this is achieved by RecBCD (in *E.coli*) or RecFOR. Additionally, it has recently been reported that DprA, a widely conserved bacterial protein, lower SSBs inhibition on RecA DNA binding (Mortier-Barriere et al., 2007). In eukaryotes, Rad52 and Rad55/57 fulfil this role. While RecBCD and RecFOR share no homology with RecA, and Rad52 shares no homology with Rad51, Rad55/57 is a Rad51 paralogue and several eukaryotic Rad51 paralogues exist that are implicated in the process of HR, e.g. Rad51B, Rad51C, Rad51D, XRCC2 and XRCC3 are all mammalian paralogues of Rad5 and are all implicated in HR.

It is currently unknown whether similar mediator proteins are required for the loading of RadA onto ssDNA or if such loading is required at all. However, homologues of RPA exist in the archaeal domain suggesting that the same competitive binding of ssDNA by recombinase and single strand binding protein occurs in the archaea.

Taking into account that all Rad51 paralogues are implicated in the process of HR, that RadA is closely related to Rad51 and that RadB is the sole euryarchaeal paralogue of RadA, studies of the effect of RadB on *in vivo* recombination were carried out. By studying the frequency of plasmid by chromosome recombination in *radB*+ or Δ*radB Haloferax volcanii* strains, insight into the role of RadB could be gained and also determine whether it is important for efficient recombination. In addition, Δ*radA* and Δ*hjc* strains were studied. Previous studies have shown that RadA is required for recombination and that Δ*radA* strains of *Haloferax volcanii* are

completely defective for recombination (Woods and Dyall-Smith, 1997). However, while it has been shown that the *hjc* encoded protein Hjc, from *Methanothermobacter thermautotrophicus,* cleaves Holliday junctions (Bolt et al., 2001), that PCNA stimulates the cleavage activity of *Sulfolobus solfataricus* Hjc (Dorazi et al., 2006) and that an interaction between *Pyrococcus furiosus* RadB and Hjc has been detected by immunoprecipitation assays (Komori et al., 2000b; Komori et al., 1999), no *in vivo* data exists on the importance of Hjc or its suggested interaction with RadB.

4.1.3 Aims

The experiments described in this chapter aim to elucidate the role of the three proteins, RadA, RadB and Hjc, in recombination. Assays were carried out to determine both the frequencies of crossover and non-crossover recombination. Additionally, the effect of altering the length of homology available as a substrate for recombination on these deletion strains is described.

4.2 Results

4.2.1 Transformation efficiency and its effect on apparent recombination frequencies

Before the recombination assays described in this chapter were carried out, an important control experiment was necessary. While it is likely that the deletion of genes proposed to be involved in homologous recombination would result in altered recombination frequencies, it is essential to distinguish between actual recombinogenic events and other factors that could skew the observed results. Specifically, the process of transforming a strain with plasmid DNA could affect the observed recombination frequencies.

The transformation of *Haloferax volcanii* with plasmid DNA is a multi-step process. The process of transformation itself could significantly affect cell survival. As a necessary step to the process, the S-layer, the surface protein layer encapsulating the cell has to be removed from the cells by chelation of Mg^{2+}, which is required for the S-layer, with EDTA thus spheroplasting the cells. As spheroplasts, cells are more susceptible to lysis either spontaneously or through forces applied from centrifugation or pipetting. Some strains could be more sensitive to lysis than others so this factor is taken into account by measuring the viable cell count following the transformation procedure so that any recombination events can be measured relative to the cell viability. Secondly, the plasmid DNA must then enter the cell. It can not simply be assumed that the frequency of DNA uptake is equal in all strains and

measuring the viable cell count following transformation will not provide any information on the efficiency of DNA uptake. Due to the nature of the experiments described in this chapter, any reduction in the efficiency of DNA uptake and transformation efficiency could be misinterpreted as a reduction in the frequency of recombination, whereas the truth could be that the strains in question carry out homologous recombination at equal frequencies and efficiency, assuming that the plasmid DNA is present in the first place. Finally, if the plasmid is an integrative one, it is only at this stage that the recombinogenic ability of the strain is tested by integration of the plasmid onto the chromosome at regions of homology. Thus, to measure the recombination efficiency of a strain, it is necessary to first determine the efficiency of DNA uptake for each strain assayed.

An assay to determine the transformation efficiency (specifically the efficiency of DNA entry into the cell) of each strain used in this chapter was carried out, independent of homologous recombination frequencies. This was achieved by transforming each strain with 1 μg of the replicative plasmid, pTA357. pTA357, like all the plasmids utilised in this chapter, contains the *pyrE2* gene that when expressed confers uracil prototrophy (ura+) to Δ*pyrE2* (ura-) strains. This selectable marker was used to measure the transformation efficiency of each strain by comparing the number of colonies present on selective media (Hv-Ca + Trp + Thy. Tryptophan and thymidine were supplemented as strains used in this chapter are Δ*trpA* and Δ*hdrB*), i.e. those that have uptaken pTA357 and are expressing *pyrE2*, with the number of colonies present on complex, non-selective media (Hv-YPC + Thy), i.e. the total viable count. In addition to the *pyrE2* gene, pTA357 contains ori-pHV1/4, a *H. volcanii* origin of replication present on the mini-chromosomes pHV1 and pHV4 (Norais 2007). The presence of this origin is important for two reasons. Firstly, it permits the replication of pTA357 thus ensuring transformed cells and daughter cells are ura+, without the need for recombination to integrate the plasmid onto the chromosome at regions of homology. Secondly, the presence of this origin actually prevents the integration of pTA357 onto the chromosome at regions of homology as this origin is not tolerated on the same chromosome by *Haloferax volcanii* (T. Allers, unpublished data). This prevention of integration effectively ensures that all factors associated with recombination are eliminated from this assay and any ura+ colonies observed following growth on selective media will be due solely to the transformation of the plasmid DNA.

The resulting frequency derived for the transformation efficiency of each strain can then be used to correct any results obtained from the recombination assays in this chapter, thus providing a true value of the frequency of recombination. I.e.

$$\frac{\text{Observed recombination frequency}}{\text{Transformation frequency}} = \text{True recombination frequency}$$

Results

The results of the transformation frequency of pTA357 into H195 (*radA+, radB+ hjc+*), H282 (*radA+, radB+,* Δ*hjc*), H284 (*radA+,* Δ*radB, hjc+*), H349 (*radA+,* Δ*radB,* Δ*hjc*) and H388 (Δ*radA, radB+, hjc+*) as measured by the number of ura+ colonies relative to the number of viable cells are displayed in Figure 4.1.

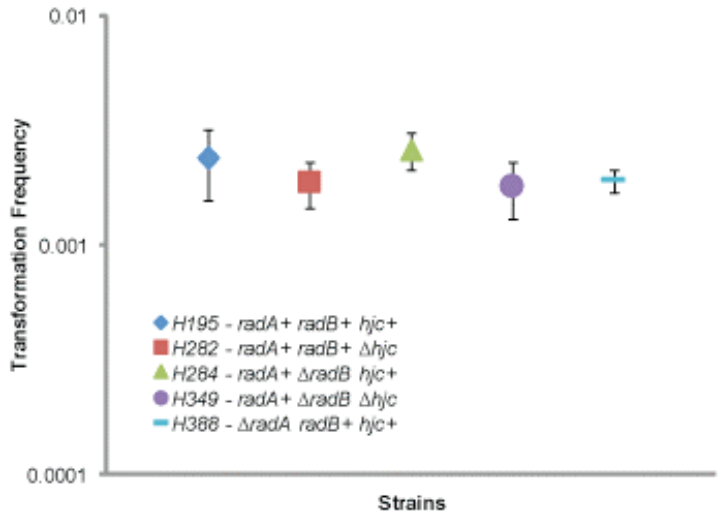

Figure 4.1 Transformation frequencies of pTA357 into H195 (*radA+, radB+ hjc+*), H282 (*radA+, radB+,* Δ*hjc*), H284 (*radA+,* Δ*radB, hjc+*), H349 (*radA+,* Δ*radB,* Δ*hjc*) and H388 (Δ*radA, radB+, hjc+*) as measured by the number of ura+ colonies relative to the number of viable cells. All data points are calculated as the mean value of three trials. Error bars are calculated as standard error. Only relevant genotypes are indicated. 1 µg of DNA was used per transformation.

Transformation efficiencies are independent of RadA, RadB and Hjc

Figure 4.1 shows that the tested strains have similar transformation efficiencies and therefore, the transformation efficiency of *H. volcanii* is independent of the presence or absence of RadA, RadB and Hjc. Therefore, the analyses of the recombination data and the differences between strains reported in this chapter are valid and for this reason, no correction factor was applied to the observed frequencies. The term 'recombination frequency' refers to the compounded transformation frequency and recombination frequency of each strain tested.

4.2.2 Analysis of crossover recombination rates

Haloferax volcanii strains deleted for *pyrE2,* H195 (*radA+, radB+ hjc+*), H282 (*radA+, radB+,* Δ*hjc*), H284 (*radA+,* Δ*radB, hjc+*), H349 (*radA+,* Δ*radB,* Δ*hjc*) and H388 (Δ*radA, radB+, hjc+*) were transformed with the non-replicative plasmid pTA159. pTA159 contains 3.5kb of near perfect sequence homology to the *bgaHa* locus, present on the *Haloferax volcanii* chromosome. Homology is not perfect as the *bgaHa* sequences on the plasmid and chromosome differ due to two different oligonucleotide insertions. The plasmid-borne sequence is a *bgaHa-Kp* allele and the chromosomal copy is a *bgaHa-Bb* allele. These heteroalleles are not important to this assay but become important in later assays described in this chapter. pTA159 also contains a *Haloferax volcanii* selectable marker, *pyrE2,* under the control of the constitutive ferodoxin promoter, p.fdx. Other sequences present on the plasmid, i.e. *bla* (beta lactamase- AmpR) for ampicillin resistance and ColE1 origin of replication are for the purposes of cloning in *E.coli*. Following transformation with 1 µg of pTA159, cells that integrate the plasmid onto their chromosome at the *bgaHa* locus through crossover recombination will also integrate the plasmid-borne *pyrE2* gene, thus conferring uracil prototrophy (Figure 4.2). Cells can only recombine at the *bgaHa* locus as this is the only homology to the Haloferax chromosome present on the plasmid. Cells can not become prototrophic for uracil except for a crossover event that integrates the plasmid, due to it being a non-replicative plasmid. The frequencies of crossover recombination were measured by dividing the number of ura+ colonies that were selected by plating of transformants on media lacking uracil (Hv-Ca + Trp + Thy) by the total viable cell count, determined by spotting transformants on non-selective, complex media (Hv-YPC + Thy) (Figure 4.3).

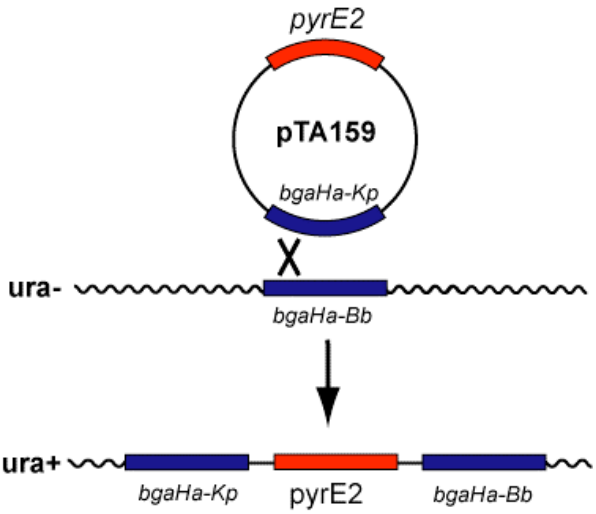

Figure 4.2 Schematic of crossover recombination assay. When a plasmid (pTA159) containing *pyrE2* and genomic homology (*bgaHa)* recombines into the chromosome, the strain becomes prototrophic for uracil and can be selected for by plating on media lacking uracil. The frequency of recombination can then be calculated by dividing the number of colonies present on selective media lacking uracil (Hv-Ca + Trp + Thy), by the number of colonies present on complex media containing uracil (Hv-YPC + Thy)

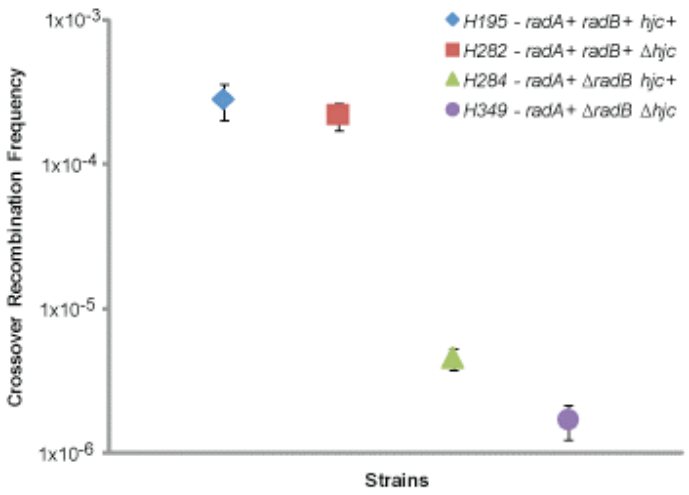

Figure 4.3 Rates of crossover recombination between pTA159 and chromosome at the *bgaHa* locus in strains H195 (*radA+, radB+ hjc+*), H282 (*radA+, radB+,* Δ*hjc*), H284 (*radA+,* Δ*radB, hjc+*) and H349 (*radA+,* Δ*radB,* Δ*hjc*). No crossover recombinants were detected with H388 (Δ*radA, radB+, hjc+*) (data not shown). Mean values and standard error are calculated based on 7 trials. Only relevant genotypes are displayed. 1 µg of DNA was used per transformation.

Results

RadA is essential for crossover recombination

In all trials of the pTA159 plasmid by chromosome crossover recombination assay, no ura+ transformants were observed in H388 (Δ*radA radB+ hjc+*). This reinforces the previous findings of Woods and Dyall-Smith (Woods and Dyall-Smith, 1997) that RadA is essential for crossover recombination. In its absence, no homology search or strand exchange can occur and therefore the recombination pathway is effectively blocked.

RadB is required for efficient crossover recombination

Figure 4.3 shows that levels of crossover recombination in Δ*radB*

strains are significantly lower than those observed in *radB+* strains. For H195, the number of recombinant Ura+ cells per viable cell was calculated at 2.8×10^{-4}, or 1 recombinant for every 3,570 cells. In sharp contrast, H284 provides a value of 4.54×10^{-6}, or 1 recombinant per 220,000 cells. Therefore, strains deleted for *radB* carry out crossover recombination at ~1.6% efficiency compared to *radB+* strains. This assay provides clear evidence that RadB is

involved in crossover recombination and in its absence, this form of recombination proceeds less efficiently.

The role of Hjc in crossover recombination is minor

Figure 4.3 also demonstrates that the presence or absence of *hjc* appears to have little bearing on the rates of recombination. The recombination frequency of H282 is 2.19×10^{-4} compared to 2.8×10^{-4} observed in the parental *hjc*+ strain, H195. This equates to a 22% reduction in the frequency of successful crossover recombination if *hjc* is absent. Due to the similarity between the two frequencies, an unpaired unequal variance T-test was carried out on the data to determine whether or not the means are significantly different. Unequal variance was assumed based on the results of a Fisher's exact test.

T-Test result (unequal variance): $p = 0.481$

As the result above is greater than 0.05, the T-Test shows that there is no significant difference between the mean frequencies of recombination between H195 and H282, thus the crossover recombination frequencies observed in these strains is assumed to be the same. While the assumption was made that the variance of both samples was unequal, the same test carried out with the assumption that means are in fact equal yielded a similar result ($p = 0.481$)

Unlike the comparison between H195 and H282, the difference between the mean frequencies of recombination for H284 (Δ*radB*) and H349 (Δ*radB* Δ*hjc*) are more pronounced (4.54×10^{-6} and 1.69×10^{-6} respectively), representing a 63% reduction in successful crossover recombination events. A one tailed T-Test (calculation here) assuming unequal variance to determine whether H349 showed significantly lower frequencies of crossover recombination when compared to H284 provides a p value of 0.0277. This result suggests that, with 95% confidence ($p<0.05$), the two means are different and that H349 does successfully carry out crossover recombination at a lower rate than its parental *hjc*+ strain, H284.

These data suggest that Hjc does not contribute significantly to crossover recombination events except when RadB is also absent, and even in this situation its contribution is minor with its absence only reducing crossover recombination rates by less than two-fold. One possible explanation for this observation is that when RadB is present and utilised during crossover recombination, as is the case in H195 and H282, Hjc might not be required in that specific pathway of recombination. However, in the absence of RadB, a second minor RadB-independent crossover recombination pathway that depends on Holliday junction resolution by Hjc could become the dominant pathway. This pathway would be a minor pathway as evidenced by the greatly reduced frequencies of crossover recombination in Δ*radB* strains. In

such a case, an absence of Hjc would reduce the crossover recombination frequencies further still, as seen in H349 compared with H284.

The fact that the effect of deleting *hjc* on crossover recombination frequencies is slight suggests strongly that a second Holliday junction resolvase is encoded in *Haloferax volcanii*. Holliday junctions are essential intermediates during crossover recombination and therefore if this type of recombination is to proceed, Holliday junction resolution must occur. As crossover recombination frequencies are not reduced severely or abolished entirely in the absence of Hjc, this suggests that a second resolvase exists that has yet to be identified.

4.2.3 Analysis of non-crossover recombination rates

While Δ*radB* strains undergo crossover recombination at a much lower frequency than *radB*+ strains, it is not yet known whether the rates of non-crossover recombination are affected in a similar manner. RadB may act in both crossover and non-crossover pathways of recombination or solely in crossover recombination. A further assay was performed utilising plasmid by chromosome recombination (Figure 4.4).

The plasmid utilised in this experiment is pTA168, containing *pyrE2* and a mutant allele of the leucine biosynthesis gene, *leuB* (Allers et al., 2004). This particular allele (*leuB-Aa2*) contains an oligonucleotide insertion towards the 5' of the gene. Strain H195 and its derivative strains, including H282, H284 and H349 contain a different *leuB* allele (*leuB-Ag1*) in place of the wildtype copy. This mutant allele has a similar oligonucleotide insertion towards the 3' end of the gene.

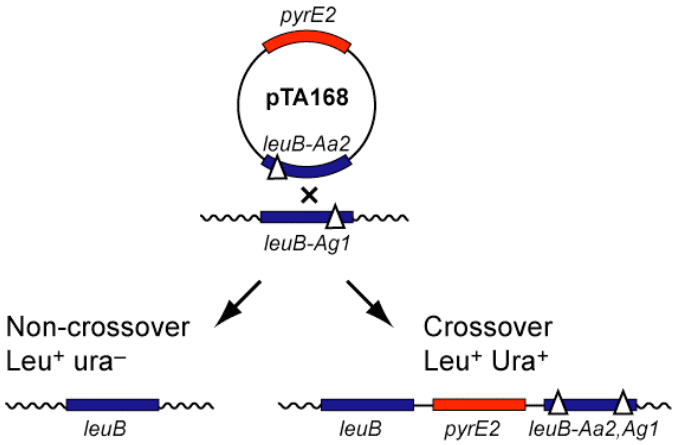

Figure 4.4 Schematic of non-crossover recombination assay. An integrative plasmid containing *pyrE2* and a mutant *leuB* allele (pTA168) is used to transform ura- leu- (i.e. *leuB-Ag1*) strains. Following selection for leu+ colonies by plating on media lacking leucine (Hv-Min + Trp + Thy + Ura), colonies have either undergone gene conversion of the chromosomal mutant *leuB* allele and become leu+ ura- (non-crossover recombination) or have integrated the plasmid onto the chromosome at the *leuB* locus, becoming both leu+ and ura+ (crossover recombination). These two events can be distinguished by patching of leu+ colonies on media lacking uracil (Hv-Min + Trp + Thy). Cells that grow on this media are crossover recombinants and those that do not have undergone gene conversion.

Once the strain has been transformed with 1 µg pTA168, one or more of several events can occur. **(1)** The plasmid and chromosomal *leuB* alleles could undergo crossover recombination between the two oligonucleotide insertions, resulting in two chromosomal *leuB* alleles: *leuB-Aa2-Ag*1 and wildtype *leuB*. The integrant strain would be both ura+ and prototrophic for leucine (leu+) (Figure 4.4). **(2)** The plasmid-borne *leuB-Aa2* sequence is used to gene convert the chromosomal *leuB-Ag1* allele to wildtype *leuB*. While the strain would now be leu+, it would not have integrated the plasmid and therefore be ura- (Figure 4.4).

All transformants are plated on media lacking leucine (Hv-Min + Trp + Thy + Ura), therefore selecting for both outcomes described above: Non-crossover recombinants (leu+ ura-) and crossover recombinants (leu+ ura+) would both be selected for. When leu+ colonies are visible after 5 days growth at 45°C, they are patched onto media that lacks uracil (Hv-Min + Trp + Thy). By patching on this media, only crossover recombinants (leu+ ura+) will grow, with non-crossover recombinants being unable to grow (leu+ ura-). The percentage of crossover and non-crossover recombination events can then be calculated. The total frequency of recombination can be calculated by counting the number of colonies present on the initial

transformation plates, lacking leucine and dividing this figure by the viable cell count, obtained by spotting transformants on non-selective, complex media (Hv-YPC + Thy) at appropriate dilutions. The frequency of crossover and non-crossover recombination can then be calculated by multiplying the total frequency of recombination by the fraction of colonies that grew and did not grow following patching of colonies on plates described above, respectively, i.e.,

Non-crossover frequency = Total recombination frequency (leu+) × % (leu+ ura-)

Crossover frequency = Total recombination frequency (leu+) x % (leu+ ura+)

Two further possible outcomes exist that are not selected for in this assay due to the transformed strains being leu- therefore being unable to grow on media lacking leucine (Hv-Min + Trp + Thy + Ura). **(3)** Like (1), crossover recombination occurs between the plasmid-borne and chromosomal *leuB* alleles but instead of strand exchange occurring between the two oligonucleotide insertions, it instead occurs outside of them i.e. either upstream of the *leuB-Aa2* oligonucleotide insertion or downstream of the *leuB-Ag1* oligonucleotide insertion. This would result in the integration of the plasmid onto the chromosome, becoming ura+. However, the resulting integrant strain will be leu- as it would contain two mutant copies of *leuB,* one being *leuB-Aa2* and the other being *leuB-Ag1*. **(4)** Instead of the integration of the plasmid, the chromosomal *leuB-Ag1* allele could undergo gene conversion but unlike the case of (2) where the chromosomal *leuB-Ag1* allele is converted to wildtype, the plasmid-borne *leuB-Aa2* instead converts it to either a *leuB-Aa2* or *leuB-Aa2-Ag1* allele. This strain would be ura- as the *pyrE2* gene would not have integrated onto the chromosome. Also the strain would be leu- as it would contain a mutant *leuB* allele. These outcomes are displayed in Figure 4.5. Plating transformants on media lacking leucine can select against all of these possibilities.

The results of these experiments can be seen in Table 4.1 and Figure 4.6.

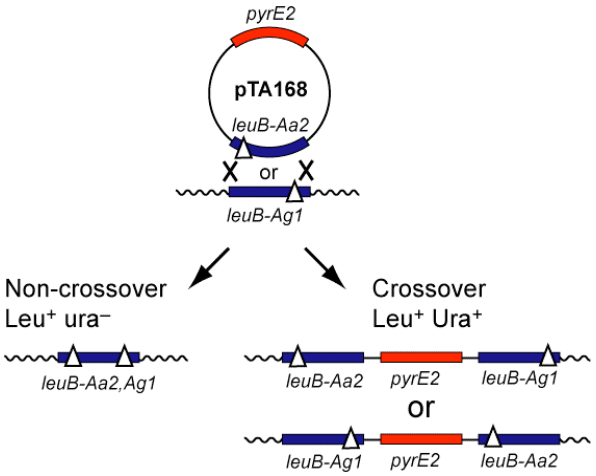

Figure 4.5 Events selected against in the pTA168 recombination assay. Colonies have either undergone gene conversion of the chromosomal mutant *leuB* allele and become leu- ura- (non-crossover recombination) or have integrated the plasmid onto the chromosome at the *leuB* locus, becoming leu- and ura+ (crossover recombination).

Results

Frequency of Recombination	**H195**	**H282** Δ***hjc***	**H284** Δ***radB***	**H349** Δ***radB hjc***	**H388** Δ***radA***
Total	$1.4x10^{-5}$	$1.1x10^{-5}$ (84.0%)	$2.3x10^{-6}$ (16.7%)	$1.6x10^{-6}$ (12.2%)	0
Crossover	$3.1x10^{-6}$	$2.6x10^{-6}$ (82.3%)	$2.0x10^{-7}$ (6.5%)	$1.2x10^{-7}$ (4.0%)	0
Non-Crossover	$1.0x10^{-5}$	$8.8x10^{-6}$ (84.5%)	$2.1x10^{-6}$ (19.8%)	$1.5x10^{-6}$ (14.6%)	0
Crossover/Total	**22.7%**	**22.3%**	**8.8%**	**7.4%**	**N/A**

Table 4.1 Crossover, non-crossover and total recombination frequencies between pTA168 and the chromosomal *leuB* locus. Percentages in parentheses represent the frequency of the type of recombination compared to H195.

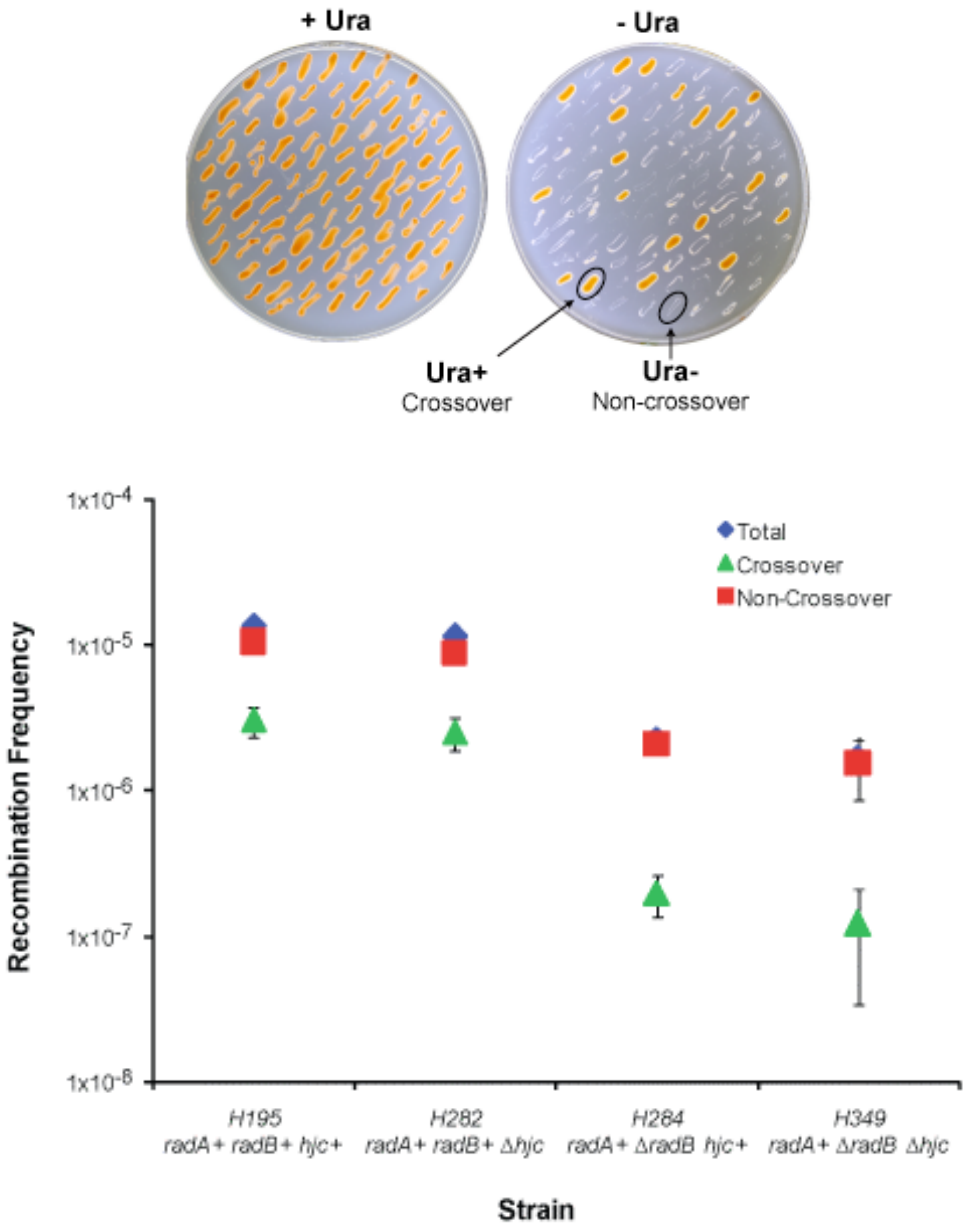

Figure 4.6 (Top) pTA168 transformants patched on Hv-Min + Trp + Thy plates, either with or without uracil. Cells that have gene converted the chromosomal *leuB-Ag1* allele without integrating pTA168 at the *leuB* locus will not grow on plates lacking uracil. Only pTA168 integrants (crossover recombinants) grow on this media. **(Bottom)** Total, crossover and non-crossover (gene conversion) recombination frequencies for strains H195 (*radA+, radB+ hjc+*), H282 (*radA+, radB+, Δhjc*), H284 (*radA+, ΔradB, hjc+*), and H349 (*radA+, ΔradB, Δhjc*). H388 (*ΔradA, radB+, hjc+*) are not shown as no recombination was detected. All data points are calculated as the mean value of at least three trials. Error bars are calculated as standard error. Only relevant genotypes are displayed. All strains were transformed with 1 µg DNA.

RadA is essential for both crossover and non-crossover recombination

Not only is RadA essential for crossover recombination, but it is also necessary for non-crossover recombination. In its absence, neither type of recombination was detectable in this plasmid by chromosome recombination assay. This does not eliminate the possibility of a RadA-independent pathway of homologous recombination. In eukaryotes, Rad51-independent recombination exists that instead depends on Rad59 and the strand annealing properties of Rad52 (Cortes-Ledesma et al., 2004). Similarly, in bacteria, although recombination frequencies are greatly reduced in the absence of RecA, a minor pathway of RecA-independent homologous recombination exists, the RecET pathway (Noirot et al., 2003). However, the observations that crossover and non-crossover recombination are undetectable in Δ*radA* strains of *Haloferax volcanii* highlights the importance of RadA for at least the majority of recombination events.

The role of RadB is more important in crossover recombination than non-crossover

Figure 4.6 shows that both crossover and non-crossover recombination occur at a lower frequency in the absence of RadB (H284 and H349) when compared with a *radB*+ strain (H195 and H282), therefore RadB is involved in both pathways. However, the comparison of recombination frequencies to H195 frequencies in Table 4.1 show that crossover recombination is affected more severely than non-crossover recombination, in both H284 and H349. In both H284 and H349, crossover recombination frequencies are approximately 20-fold lower (~5%) than H195 whereas non-crossover frequencies are only 5-6-fold lower (~15-20%). This implies that while RadB is important for both crossover and non-crossover pathways of recombination, it plays a more critical role in crossover recombination.

Δ*hjc does not affect crossover and non-crossover recombination frequencies*

Figure 4.6 and Table 4.1 show that non-crossover recombination frequencies are not significantly affected by the presence or absence of Hjc. The frequencies observed in H282 (*radA*+ *radB*+ Δhjc) are comparable to those observed in H195 (*radA*+ *radB*+ *hjc*+). Similarly, crossover recombination frequencies between pTA168 and the chromosomal *leuB-Ag1* allele are comparable between H282 and H195. This result is in agreement with the results obtained from the crossover recombination assay whereby the integration frequency of pTA159 (*pyrE2*+ with 3.5kb homology to chromosome at *bgaHa* locus) into the chromosome is measured (Figure 4.3). Although Table 4.1 displays a ~15% reduction in crossover and non-crossover recombination frequencies in the absence of Hjc (H282 compared to H195), these appear to be within experimental error and unlikely to be significant. T-test analyses (5

samples in each data array, unpaired, equal variance) confirm that the observed differences in crossover, non-crossover and total recombination frequencies are not significant with 95% confidence (p=0.29, p=0.22, p=0.23, respectively, i.e. p>0.05 in each case). However, more trials of this experiment might highlight a small but significant difference in these frequencies.

Furthermore, crossover and non-crossover recombination frequencies do not appear to be dependent on Hjc in the absence of RadB, as illustrated by the comparable frequencies observed between H284 (*radA*+ Δ*radB hjc*+) and H349 (*radA*+ Δ*radB* Δ*hjc*). T-test analyses (5 samples in each data array, unpaired, equal variance) confirm that the small observed differences in recombination frequencies between these two strains are insignificant with 95% confidence, i.e. p>0.05 (Crossover: p=0.25, non-crossover: p=0.24, total: p=0.22). However, when crossover recombination frequencies were analysed in H284 (*radA*+ Δ*radB hjc*+) and H349 (*radA*+ Δ*radB* Δ*hjc*) using pTA159, as described above, the difference in frequencies was found to be significant. Possible reasons for this observed difference are discussed later in this chapter.

Crossover recombination frequencies might be locus-dependent

It is notable that, with the *leuB* alleles (pTA168), crossover recombination frequencies in all strains tested are significantly lower than those observed when using *BgaHa* sequences present on pTA159. The most likely explanation for this result is that there is less homology on pTA168 available for recombination to occur, compared with homology present on pTA159. Alternatively, it is possible that not all regions of the genome will have equal recombination frequencies. This is especially true in eukaryotic genomes where some genomic loci exhibit higher levels of recombination than others (Lichten and Goldman, 1995). It could be the case that the *bgaHa* locus present in these strains of *H. volcanii* represent a recombination hotspot or that a lower than average frequency of recombination is observed at the *leuB* locus. It is worth noting that *bgaHa* is present on the chromosome in all DS70 derivative strains (encompassing all the strains utilised in this work), and not on pHV4, as it is in the wildtype and DS2 background *Haloferax volcanii* genome sequences (M. Hawkins, unpublished data). The reason for this translocation of *bgaHa* is unknown but it could be the case that the *bgaHa* locus itself represents a recombination hotspot, therefore the repositioning of the gene would be more likely.

Regardless of the reason for more recombination occurring at the *bgaHa* locus, compared to the *leuB* locus, what is also noticeable is the difference observed in crossover recombination frequencies at these loci when comparing Δ*radB* and *radB*+ strains. Table 4.2 below illustrates this point.

	H195	**H282**	**H284**	**H349**
bgaHa	$2.8x10^{-4}$	$2.2x10^{-4}$	$4.5x10^{-6}$	$1.7x10^{-6}$
leuB	$3.1x10^{-6}$	$2.6x10^{-6}$	$2.0x10^{-7}$	$1.2x10^{-7}$
leuB*:*bgaHa	1:91	1:83	1:23	1:14

Table 4.2 A comparison of crossover recombination rates at the *leuB* and *bgaHa* loci between chromosome and plasmid. The bottom line of the table represents the ratio of crossover recombination frequencies at the *leuB* locus to the frequency at the *bgaHa* locus.

Table 4.2 above demonstrates the differences in relative frequency of crossover recombination at the *leuB* and *bgaHa* loci, between Δ*radB* (H284 and H349) and *radB*+ (H195 and H282) strains. Strains that are *radB*+ appear to be more sensitive either to sequence homology available for recombination or to locus specific features that alter the frequency of recombination, when compared to Δ*radB* strains. Both H195 and H282 experience a 91-fold and 83-fold reduction in crossover recombination relative frequencies at the *leuB* locus (pTA168) compared with at the *bgaHa* (pTA159). The Δ*radB* strains H284 and H349, on the other hand, experience a smaller decrease in relative frequencies, i.e. a 23-fold and 14-fold reduction in crossover recombination relative frequencies at the *leuB* locus compared with *bgaHa* locus respectively. At this point it should be noted that although the reduction in crossover recombination frequencies for H284 and H349 is less severe than in H195 and H282, the two Δ*radB* strains still carry out crossover recombination at a lower absolute frequency than their respective *radB*+ parent strains. For this reason, increases and decreases in recombination frequencies are described as relative increases/decreases.

As discussed, the most likely explanation for the observed differences in crossover recombination frequencies at the *leuB* and *bgaHa* loci is due to the difference in available homology length, with approximately seven times the homology length available in the latter. However, this does not explain the observed differences in relative frequencies between *radB*+ and Δ*radB* strains at these two loci. One possible explanation is that *radB*+ strains are more sensitive to the length of homology available for crossover recombination than Δ*radB* strains, i.e. *radB*+ strains experience a greater relative reduction in recombination frequencies per base pair reduction in homology length, than Δ*radB* strains. Conversely, *radB*+ strains would also

exhibit greater relative increases in crossover recombination frequency per base pair increase of homology length, whereas Δ*radB* strains would exhibit a lesser relative increase.

To test whether the observed changes in relative recombination frequencies between *radB*+ and Δ*radB* strains at the *bgaHa* and *leuB* loci is in fact due to a difference in sensitivity to homology length between these strains, rather than one of the two loci being a recombination hotspot, a more complete study on the effects of homology length and its effect on crossover recombination rates was carried out.

4.2.4 Effect of homology length on crossover recombination in *radB*+ and Δ*radB* strains

Δ*radB* strains of *Haloferax volcanii* recombine at lower frequencies than *radB*+ strains with regards to both crossover and non-crossover recombination. In addition, although crossover recombination frequencies are lower in Δ*radB* strains, they appear to be less dependent on the length of substrate homology available when compared to *radB*+ strains. This was suggested by the larger relative decrease in *radB*+ strain crossover recombination frequencies observed in assays using pTA168 (containing 0.5kb of homology from the *leuB* locus) compared with assays using pTA159 (containing 3.5kb of homology from the *bgaHa* locus).

Δ*radB* strains demonstrated a less pronounced decrease in relative frequencies, suggesting that the absence of *radB* reduces the effect of limiting sequence length on crossover recombination. It might be the case that a RadB-dependent recombination pathway is highly efficient when substrate homology is longer, and that a second, less efficient RadB independent pathway is utilised when only limited substrate length is available for recombination. Alternatively, the two pathways might simply be the same but in the absence of RadB, longer lengths of substrate cannot be utilised efficiently.

However, the length of available homology for crossover recombination is not the only factor that could affect the observed differences in frequencies. Due to the two different recombination substrates described (from pTA159 and pTA168) containing different sequences, frequencies of crossover recombination derived from these two sequences cannot be accurately compared, as there may be loci specific effects such as one of either *bgaHa* or *leuB* being a recombination hotspot. For this reason, experiments were carried out whereby the available substrate length for crossover recombination was altered and frequencies were measured.

Plasmid-borne *bgaHa* sequences of varying length were utilised to measure the frequency of crossover recombination between plasmid and chromosome and the effect of changing substrate length. By utilising the same loci for all assays and only varying the substrate length,

locus specific effects are eliminated. Therefore the experiments described here should directly represent the effect of altering substrate length independent of other factors.

To determine quantitatively and accurately the effect of available sequence homology length on the frequency of recombination in *radB*+ and Δ*radB* strains, an assay utilising pTA159 and 3 similar plasmids, pTA156, pTA158 and pTA188, containing *bgaHa* was carried out. The three additional plasmids used in this assay are identical to pTA159 except the oligonucleotide insertions are at different positions on the *bgaHa* coding sequence. Figure 4.7 shows the positions of the insertions in these *bgaHa* alleles relative to the *bgaHa-Bb* chromosomal allele in H195, H282, H284 and H349. Table 4.3 shows the oligonucleotides used for insertion into *bgaHa*.

Allele	Plasmid	Oligonucletide insertions	Inserted at:
bgaHa-Bb	pTA156	BGABBF/BGABBR	*Bst*BI
bgaHa-Bh	pTA158	BGABHF/BGABHR	*Bss*HII
bgaHa-Kp	pTA159	BGAKPF/BGAKPR	*Kpn*I
bgaHa-Be	pTA188	BGABEF/BGABER	*Bst*EII

Table 4.3 *bgaHa* alleles, generated by insertion of oligonucleotides at restriction sites in *bgaHa* sequence. The allele, plasmid that the allele is present on, oligonucleotides inserted, and restriction sites at which insertions were made, are shown.

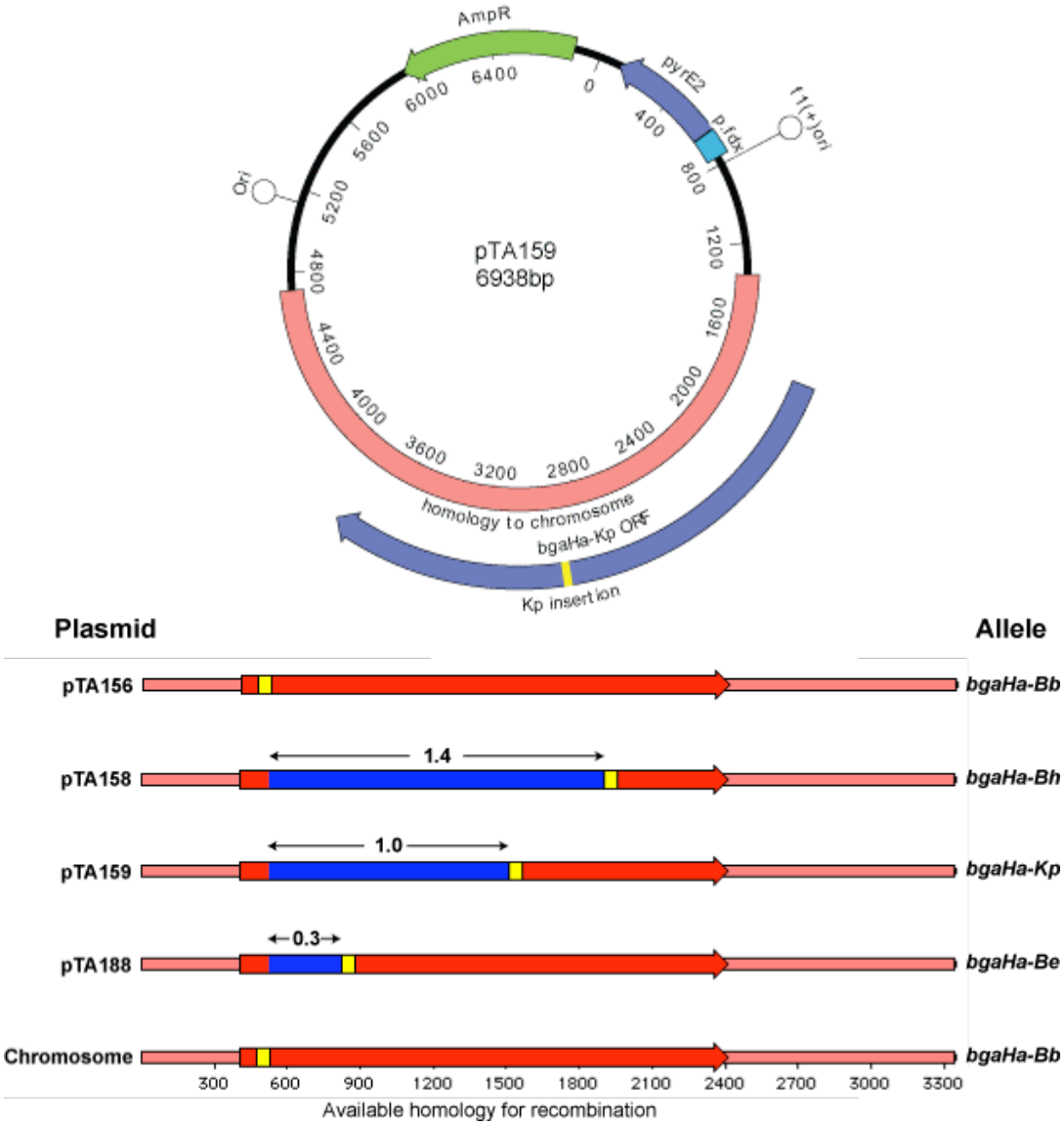

Figure 4.7 (Top) Schematic of pTA159 as an example of the plasmids used in this assay. pTA156, pTA158 and pTA188 are identical to pTA159 except for the positioning of the oligonucleotide insertions in *bgaHa*. **(Bottom)** Different plasmid-borne alleles of *bgaHa* used in this crossover recombination assay. The bottom sequence represents the *bgaHa-Bb* allele present on the chromosome of H195, H282, H284 and H349. Yellow boxes represent the oligonucleotide insertions at unique restriction sites which generate a +2 frameshift mutation. Blue regions and accompanying values represent the homology available (in kilobases) for generation, by recombination, of a blue colony phenotype. Recombination occuring at any other region will generate a red colony phenotype.

Four alleles of *bgaHa* were generated by insertion of oligonucleotide sequences at points along the coding sequence of the gene (Figure 4.7). These mutant alleles were named after the restriction site that the oligonucleotide sequence was inserted, i.e. *bgaHa-Bb* for an insertion at the *Bst*BI site, *bgaHa-Be* for *Bst*EII, *bgaHa-Kp* for *Kpn*I and *bgaHa-Bh* for an insertion at *Bss*HII site. H195, H282, H284 and H349 all contain the *bgaHa-Bb* allele, as shown in Figure 4.7.

As in the non-crossover recombination assay using different *leuB* alleles, the position at which strand exchange occurs along the *bgaHa* coding sequence to integrate the plasmid determines whether the resulting gene will be functional. In this assay *bgaHa*+ was detected by spraying with X-gal. Colonies that are *bgaHa*+ develop a blue colouration rather than remaining red/pink. The positions of the insertions in the *bgaHa* coding sequence determine the length of sequence available for recombination to generate a wildtype copy of *bgaHa* and therefore a blue colony upon plating, incubation and spraying with Xgal. The frequency of recombination that yields a blue colony will be scored for each strain and plasmid combination and plotted for comparison.

In this assay it was assumed that RadA catalysed strand exchange and any branch migration of Holliday junctions is impeded by heterologous sequences. If this is not the case, strand exchange could potentially occur outside of the region between the two insertion mutations on plasmid and chromosome, and migrate inwards to generate symmetrical heteroduplex DNA. This, followed by gene conversion restoring the mutant allele to *bgaHa*+ would result in a blue colony phenotype, even though the initial steps of recombination occurred outside the region proposed to generate a blue colony phenotype. While the assumption that branch migration will not proceed through the heterologous sequences generated by the oligonucleotide insertions may not be accurate, insight can be gained by comparing the observed frequencies with the expected frequencies of a blue colony phenotype. The expected frequencies of *bgaHa*+ were calculated by the equation:

$$\textbf{Total crossover recombination frequency (i.e. ura+/viable count)} \times \frac{\textbf{`Blue' Homology} \text{ (bp)}}{\textbf{Total Homology} \text{ (bp)}}$$

If the observed frequencies differ significantly from the expected frequencies, this could suggest that it is not only recombination inside the region between the two insertion mutations on plasmid and chromosome that is able to generate a blue colony phenotype and that such branch migration through heterology may be occurring. This aspect will be discussed further later.

Controls

Reversion Mutation Rates of the Chromosomal bgaHa-Bb *Allele*

Transformations with pTA156, containing the *bgaHa-Bb* allele, were carried out as a control to determine the frequency of reversion of the chromosomal *bgaHa-Bb* allele. As both the plasmid-borne and chromosomal mutant *bgaHa* alleles are identical, it was predicted that no transformants would display a blue colony (*bgaHa*+) phenotype except as the result of a reversion of *bgaHa-Bb*, possibly through template slippage during DNA replication. It was important to determine the rates of reversion of *bgaHa-Bb* to *bgaHa* for all the strains tested as such mutations would alter the data generated by the assay by generating false positive results for the frequencies of recombination.

In all trials carried out, no blue colony phenotype was observed for H195, H282, H284 and H349 when transformed with pTA156, indicating that the reversion rate of the *bgaHa-Bb* allele was sufficiently low to not skew the observed rates of crossover recombination. As at least 1000 colonies were scored for each strain, this provides an estimate of the maximum likelihood of reversion of the *bgaHa-Bb* allele to *bgaHa*+. i.e., p(rate of reversion) < 0.001 per integration event.

Absolute Frequencies of Crossover Recombination

To validate this assay, it was determined whether the frequency of total crossover recombination (i.e. ura+ transformants) between chromosome and plasmid is the same for all plasmids tested. The only difference between each plasmid used is the position of the oligonucleotide insertion present in the *bgaHa* coding sequence. Also, each plasmid has insertions of the same length. For these reasons it is expected that total crossover recombination frequencies when transforming with each plasmid would be comparable. If however, the frequencies of recombination vary depending on the plasmid used to transform each strain it would demonstrate that the frequency of crossover recombination is affected by the position of small regions of heterologous DNA sequences.

Frequencies of recombination were determined for each strain/plasmid combination as before by dividing the number of *ura*+ transformants (both red and blue) by the viable cell count (Figure 4.8). All strains were transformed with 1 μg of plasmid DNA.

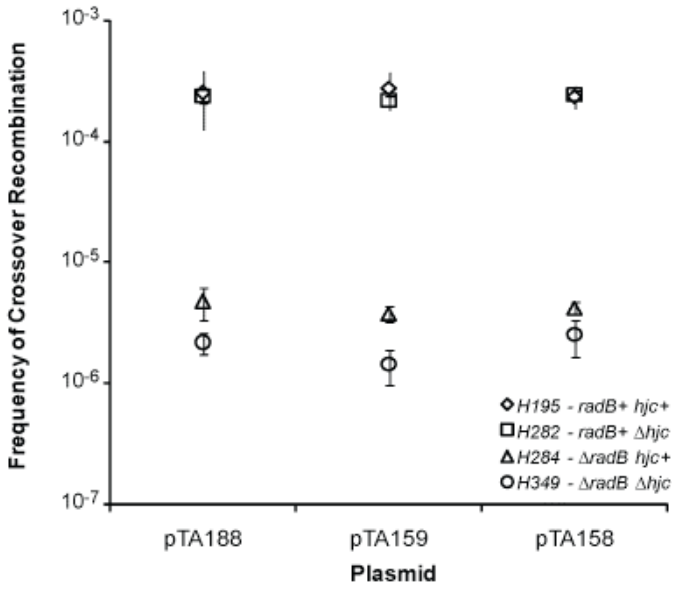

Figure 4.8 Frequencies of crossover recombination between chromosomal and plasmid-borne *bgaHa* alleles, *bgaHa-Be* (pTA188), *bgaHa-Kp* (pTA159) and *bgaHa-Bh* (pTA158). Frequencies were calculated by dividing *ura*+ transformants by total viable cell count. All data points are calculated as the mean of at least five trials. Error bars are based on standard error. Only relevant genotypes are displayed. All strains were transformed with 1 μg DNA.

Figure 4.8 shows that there is no significant difference between the frequencies of crossover recombination observed between the three plasmids. This indicates that homologous crossover recombination can occur equally efficiently regardless of the position of short patches of heterology.

Experiments were then carried out to score the number of red and blue colony phenotype transformants upon plating on selective media and subsequent growth (Figure 4.9).

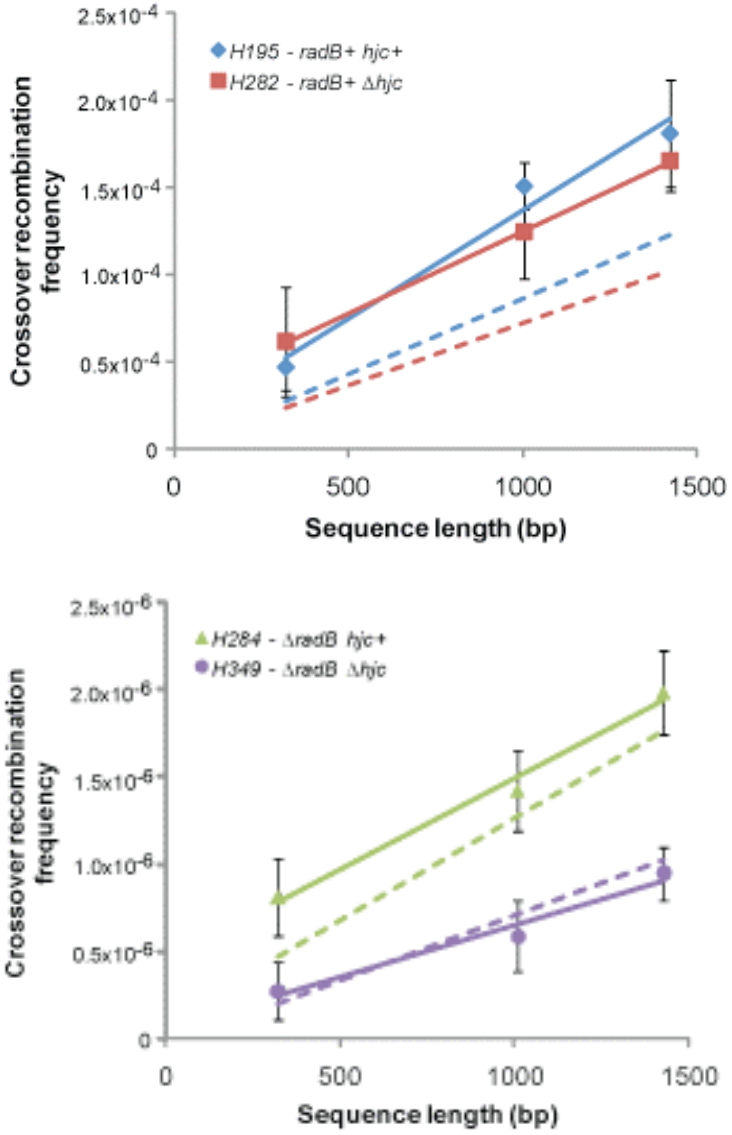

Figure 4.9 Effect of changing length of substrate homology on the frequency of crossover recombination. X axis values represent the length of homology available to generate a blue colony phenotype (*bgaHa*+ transformant). Y axis values represent the frequency of crossover recombination events that generate a blue colony phenotype. Dashed lines represent the expected frequencies for each strain based directly on the percentage of total homology available to generate a blue colony phenotype multiplied by the total frequency of crossover recombination (ura+). All data points represent the mean of at least 5 trials. Error bars are based on standard error. All R^2 values for trend lines are >0.95. Only relevant genotypes are displayed. All strains were transformed with 1 µg DNA.

Strain	Observed (Δfrequency/bp)	Expected (Δfrequency/bp)
H195 – *radB*+ *hjc*+	1.24×10^{-7}	8.69×10^{-8}
H282 – *radB*+ Δ*hjc*	9.39×10^{-8}	7.13×10^{-8}
H284 - Δ*radB hjc*+	1.05×10^{-9}	1.17×10^{-9}
H349 - Δ*radB* Δ*hjc*	5.71×10^{-10}	7.24×10^{-10}

Table 4.4 Changes in frequency of crossover recombination per increase/decrease of substrate length by 1 bp. E.g. for H195, an increase of 1 bp in substrate length will result in an increase in the frequency of crossover recombination by 1.24×10^{-7}. Values are calculated as the formula for each trend line (Figure 4.9).

Figure 4.9 and Table 4.4 show that **(a)** crossover recombination frequencies increase in all strains as substrate length increases, **(b)** the relationship between substrate length and crossover recombination frequencies is linear, **(c)** the X-axis intersect is higher than 0 bp suggesting recombination can occur with no homology, for all strains, **(d)** the observed frequencies of crossover recombination are significantly higher than expected in H195 (*radB*+ *hjc*+) and H282 (*radB*+ Δ*hjc*), **(e)** *radB*+ strains are more sensitive to changes in substrate length than Δ*radB* strains and **(f)** crossover recombination frequencies are significantly higher at longer substrate lengths for H284 (Δ*radB hjc*+) compared to H349 (Δ*radB* Δ*hjc*) frequencies. These points will be discussed here.

The frequency of crossover recombination increases with substrate length

Figure 4.9 shows that the frequency of blue colony phenotype transformants (*bgaHa*+ events) increases as the length of substrate increases. This is true for all strains tested regardless of whether RadB and/or Hjc are present or not. Thus, the frequency of crossover recombination increases with DNA substrate length. The increase/decrease in crossover recombination frequency per base pair increase/decrease in substrate length, for each strain tested, is shown in Table 4.4.

The relationship between recombination frequency and substrate length is linear

Figure 4.9 shows the expected frequencies of crossover recombination with changing substrate length for each strain tested. Expected frequencies were calculated by:

Total crossover recombination frequency X '<u>Blue' Homology</u> (bp)
(i.e. ura+/viable count) **Total Homology** (bp)

Figure 4.9 and Table 4.4 both show that the gradients of the expected lines (i.e., the expected change in recombination frequency per change in substrate length) correlate well with the observed changes in frequencies. Trend lines are linear with high R^2 values (>0.95). This shows that the relationship between the frequency of crossover recombination and substrate length is linear and predictable for substrate lengths between 323 bp and 1425 bp.

The relationship between recombination frequency and substrate length is different between 0 bp and 323 bp length

The available data cannot be extrapolated to shorter substrate lengths accurately, i.e. substrate lengths less than 323 bp. For example, if trend lines (Figure 4.9) for H195 and H282 were extrapolated back to x=0 (i.e. 0 bp of sequence available for homologous recombination), the expected frequencies of crossover recombination would be ~$1x10^{-5}$ and ~$3x10^{-5}$ respectively. This can not be true as evidenced by the control transformation with pTA156 that contains 0 bp substrate length available to generate a blue colony phenotype (*bgaHa*+) generating no blue colonies. It has been shown that there is a minimum unit of homology length at which recombination can occur efficiently and below this length the frequency of recombination drops off sharply. This fragment is known as a MEPS (minimum efficiency processing segment) (Shen and Huang, 1986). With the available data, it is not possible to tell at what length of homology the frequency of recombination drops sharply in *Haloferax volcanii*. Experiments using shorter substrates would be required to elucidate this. Thus, it must be assumed that between 0 bp and 323 bp of available substrate, a sharper decrease in crossover recombination frequency would occur in H195 and H282 per decrease in substrate length, i.e. a change in linearity to that observed between 323 bp and 1425 bp substrate length.

While the same observation is true for H284 (Δ*radB hjc*+) and H349 (Δ*radB* Δ*hjc*), if the 'observed' trend line is extrapolated to 0 bp of sequence substrate, the predicted crossover recombination is closer to zero (~$4x10^{-7}$ and ~$2x10^{-8}$, respectively) than in H195 and H282 (~$1x10^{-5}$ and ~$3x10^{-5}$, respectively). It is possible that below 323 bp of substrate, the linearity of the relationship between recombination frequency and substrate length does not change as sharply in Δ*radB* strains as it does in *radB*+ strains. i.e., *radB*+ strains are more sensitive than

Δ*radB* strains to changes in substrate length, below 323 bp. However, it should be noted that at all substrate lengths tested, the crossover recombination frequency of Δ*radB* strains was significantly lower than that observed in *radB*+ strains. Thus, extrapolating the trend lines of Δ*radB* strains back to a substrate length of zero would naturally result in a recombination frequency closer to zero, than in a *radB*+ strain.

The frequency of bgaHa+ *is significantly higher than expected in H195 and H282*

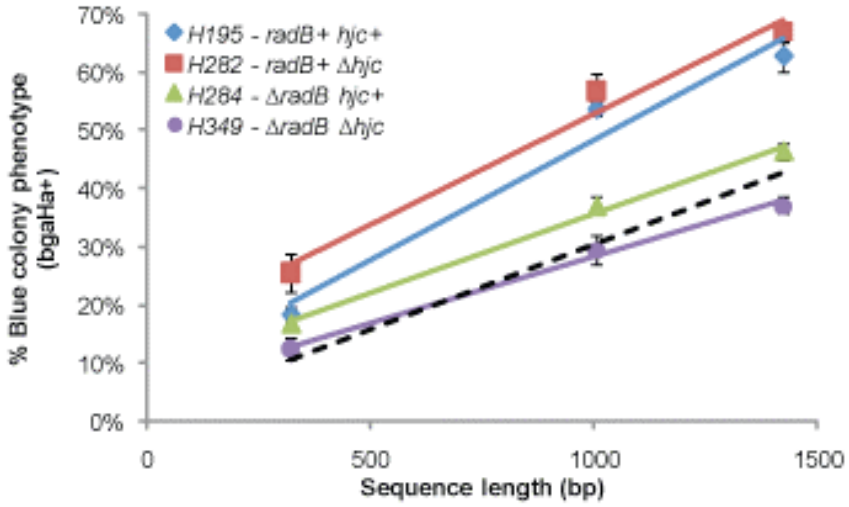

Figure 4.10 Crossover recombination frequencies presented as the proportion of crossover recombination that generates a blue colony phenotype (*bgaHa*+) at different substrate lengths. The black dashed line represents the expected percentage of *bgaHa*+ recombinants, as calculated by dividing the substrate length available to generate a blue colony phenotype by the total substrate length available to generate either a blue or red colony phenotype. All data points are calculated as the mean value of at least 5 trials. Error bars are calculated as standard error. All trend lines have an R^2 value of >0.95

Figure 4.10 shows the previously observed crossover recombination frequencies that are *bgaHa*+ represented as proportions of blue colonies (*bgaHa*+) of total colonies. The reason for this was to clearly illustrate the observed frequencies of *bgaHa*+ of H195 (*radB*+ *hjc*+) and H282 (*radB*+ Δ*hjc*) and that they are significantly higher than the expected frequencies. The figure shows that the change in crossover recombination frequencies, i.e. the frequency of a blue colony phenotype (*bgaHa*+) changes with substrate length linearly as predicted. However, the relative frequencies of *bgaHa*+ in H195 and H282 are significantly higher than expected. For example, with pTA159, there is ~1 kb of 'blue' substrate and ~2.4 kb of 'red' substrate, therefore it would be expected that ~30% of all crossover recombinants (ura+) would be blue (1

kb/3.4 kb=~0.3). However, for H195 (*radB*+ *hjc*+), H282 (*radB*+ Δhjc) the observed percentages of blue colonies (*bgaHa*+) are 54% and 57%, respectively (Figure 4.10). H349 (Δ*radB* Δhjc) and H284 (Δ*radB hjc*+) data follow the expected proportions of blue and red colony phenotypes with H284 (Δ*radB hjc*+) proportions being very slightly above the expected values.

This could imply that the central region of the *bgaHa* locus that in this assay is utilised to generate a *bgaHa*+ recombinant might represent a recombination hotspot. Furthermore, this hotspot would be RadB dependent. Thus, the frequency of *bgaHa*+ would be expected to be higher than expected in *radB*+ strains (H195 and H282) but as expected in Δ*radB* strains (H284 and H349)

radB+ *strains are more sensitive to changes in substrate length than* ΔradB *strains*

Figure 4.9 and Table 4.4 show that the increase in recombination frequencies of H195 and H282 per base pair increase in homology is greater than that observed in both H284 and H349. Figure 4.10 and Table 4.5 shows the necessary increase/decrease in substrate length to achieve an increase/decrease in the percentage of blue colonies by 1%.

Strain	ΔSubstrate length for 1% change in proportion of blue colonies
H195 – *radB*+ *hjc*+	24 bp
H282 – *radB*+ Δ*hjc*	27 bp
H284 - Δ*radB hjc*+	37 bp
H349 - Δ*radB* Δ*hjc*	44 bp

Table 4.5 Increase/decrease in substrate length that will generate a 1% increase/decrease in the observed percentage of blue colonies, based on trendlines shown in Figure 4.10. For example, a 24 bp and 37 bp increase in substrate length will generate 1% more blue colonies in H195 and H284, respectively, but the actual change in the frequency of crossover recombination to generate a blue colony will be different. For frequencies of recombination, see Table 4.4. Figures in this table are only accurate for substrate lengths between 323 and 1245 bp.

ΔradB *relative crossover recombination frequencies are not elevated compared to* radB+ *frequencies at shorter substrate lengths*

It has been previously shown in this chapter that at the *bgaHa* locus, with ~3.5kb of substrate, Δ*radB* strain (H284) crossover recombination frequencies were less than 2% of a *radB*+ strain (H195) (Figure 4.3). At the *leuB* locus with ~0.5 kb of substrate, however, Δ*radB* strain crossover recombination frequencies were reduced to a lesser extent compared to the *radB*+ strain (~6.5%) (Figure 4.6 and Table 4.1). This raises the question of whether RadB is not as important at lower substrate lengths compared to longer substrates lengths, or whether the observed differences in frequency were due to locus specific effects.

In this assay, substrates of varying length from the same locus, *bgaHa,* were utilised to accurately determine the effect of substrate length on relative crossover recombination frequencies between H195 and H284. The results show that at each substrate length, the relative crossover recombination frequency between H195 and H284 does not differ significantly, when comparing relative frequencies between pTA158, pTA159 and pTA158 (Figure 4.11, blue diamonds). Thus, the observed differences between crossover recombination frequencies between H195 and H284 at the *bgaHa* and *leuB* loci (Figure 4.11, red squares) are not likely to be due to the difference in substrate length. Instead, it is likely that locus specific effects are responsible.

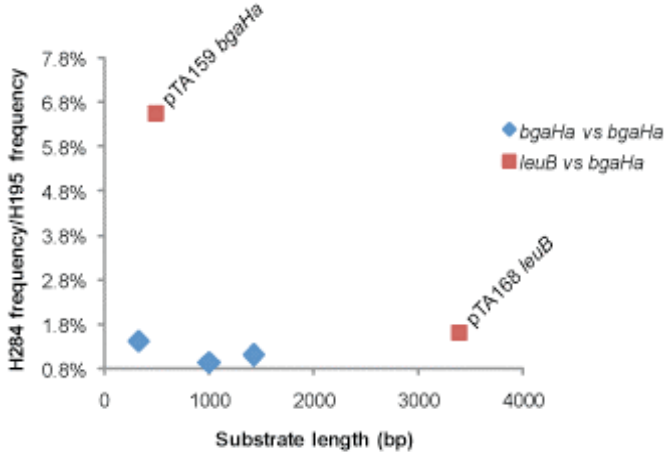

Figure 4.11 Comparison of H195 (*radB*+ *hjc*+) and H284 (Δ*radB hjc*+) crossover recombination frequencies at different substrate lengths, presented as H284 frequencies as a percentage of H195 frequencies. Red squares represent the relative frequencies of pTA168 frequencies of ura+ (*leuB,* ~0.5kb substrate) and pTA159 frequencies of ura+ (*bgaHa,* ~3.4kb). Blue diamonds represent the relative frequencies of pTA188, pTA159 and pTA158 frequencies of ura+, *bgaHa*+ (blue colony phenotype) (*bgaHa,* 0.3kb, 1.0kb and 1.4kb, respectively).

4.3 Discussion

Recombination Substrates

All plasmids used to assay recombination in these studies were intact circular molecules. While it is highly probable that many of the plasmid molecules used to transform strains of *Haloferax volcanii* will be damaged with nicks and possibly with double stranded DNA breaks, cells transformed with cut (linear) plasmid DNA exhibit much lower frequencies of recombination between plasmid and chromosome (T Allers, unpublished results). These observations are in contrast to yeast recombination, where recombination frequencies between plasmid and chromosome are highly elevated if the plasmid DNA is first linearised. Thus, it is possible that double strand breaks are not the primary substrate for homologous recombination in *Haloferax volcanii*. Alternatively, artificially generated double strand breaks are not good substrates for homologous recombination, and instead breaks might be introduced endogenously, similar to the yeast I-SceI system.

RadA

RadA is essential for both non-crossover and crossover recombination

RadA is the functional homologue of eukaryotic Rad51 and bacterial RecA. It is required for homologous recombination in archaea (Seitz et al., 1998; Woods and Dyall-Smith, 1997). RadA, like other recombinases, forms extensive nucleoprotein filaments on ssDNA (Wu et al., 2004), catalyses a homology search in other duplexes and once complete, catalyses strand exchange. Recombinases act at an early stage during homologous recombination and are essential for efficient recombination to proceed.

Following the deletion of the *Haloferax volcanii radA* gene, cells were unable to carry out homologous recombination, both crossover and non-crossover, confirming previous observations (Woods and Dyall-Smith, 1997). Without RadA, no homology search and/or strand invasion can occur, effectively blocking the downstream processes in the recombination pathway.

Examples of Rad51/RecA-independent homologous recombination exist. In bacteria, the strand annealing activity of RecT allows limited recombination through the RecET pathway (Noirot et al., 2003). Similarly, in eukaryotes, the recombination mediator protein required for Rad51-dependent recombination, Rad52 also possesses strand annealing activity and Rad51-independent recombination can occur through this feature of Rad52 (Tsukamoto et al., 2003). As no crossover or non-crossover recombination was observed in the studies presented here,

this might suggest that no such pathways exist in the archaea. However, the assays utilised to study recombination in this work probably do not cover all possible mechanisms and pathways of recombination. For example, further studies assaying recombination initiated by ssDNA gaps or following replication fork collapse in a Δ*radA* background might elucidate RadA-independent pathways of recombination. Furthermore, it is possible that prophage encoded recombinases exist in archaeal genomes that might act to suppress Δ*radA* if activated.

RadB

RadB is a RadA paralogue. While it possesses different structural and biochemical properties to its recombinase paralogue, such as being unable to catalyse strand exchange, possessing extremely low rates of ATP hydrolysis and different monomer:monomer interaction domains (Akiba et al., 2005; Komori et al., 1999; Shin et al., 2003), data presented in this chapter demonstrate its importance in efficient homologous recombination.

RadB is required for efficient crossover recombination

By studying the effects of deleting *radB* on plasmid by chromosome crossover recombination frequencies, the results show that RadB is essential for efficient homologous recombination to proceed. In its absence, crossover recombination frequencies at the *bgaHa* locus are reduced to less than 2% of those observed in *radB*+ strains. This finding was confirmed not to be locus specific for *bgaHa* by assaying crossover recombination at the *leuB* locus, where crossover recombination frequencies were ~6% of those observed in *radB*+ strains.

RadB's role is equally important at all recombination substrate lengths

Interestingly, the difference in frequency of crossover recombination between *radB*+ and Δ*radB* strains was greater at the *bgaHa* locus, where ~3.4 kb of substrate was available for crossover recombination, when compared to the *leuB* locus where only ~0.5 kb of substrate was available for crossover recombination. At the *bgaHa* locus, Δ*radB* strains recombined at ~2% compared to *radB*+ strains whereas at the *leuB* locus, Δ*radB* strains recombined at ~6% of *radB*+ levels. While only a relatively minor difference in crossover recombination frequencies at these two loci, it was reproducible. This suggested that the function of RadB may be less important during crossover recombination events with shorter substrate lengths. However, when comparing frequencies of *radB*+ and Δ*radB* strains using different substrate lengths of *bgaHa*, it was found that Δ*radB* frequencies were approximately 1% of *radB*+ frequencies at all substrate lengths. This demonstrates that RadB is required for efficient crossover recombination and that the requirement is equal at all substrate lengths.

The explanation for the differences in crossover recombination relative frequencies between *radB*+ (H195) and Δ*radB* (H284) at the *bgaHa* locus and *leuB* locus, could be that *bgaHa* is a recombination hotspot, more specifically, perhaps a RadB-dependent recombination hotspot. In the strains used in this laboratory, *bgaHa* is located on the main chromosome and not on the mini-chromosome, pHV4, as it is in the wildtype strain. This translocation of the *bgaHa* gene could have occurred due to the new locus being highly recombinogenic. If true, it is possible that when RadB is present, higher frequencies of recombination are observed at this region compared with other regions of the genome, and that RadB is necessary to utilise this recombination hotspot efficiently. In its absence, the recombination hotspot might not be utilisable and therefore frequencies could be comparable genome-wide. To test this theory, plasmid-borne chromosomal sequences from regions of the *Haloferax volcanii* genome other than the *bgaHa* locus could be used in recombination assays similar to the ones described here, to determine if locus specific fluctuations in crossover recombination are only exhibited by *radB*+ strains.

RadB is required for efficient non-crossover recombination

Not only is RadB necessary for efficient crossover recombination and equally important at all recombination substrate lengths, it is also important for efficient non-crossover recombination (gene conversion). This was elucidated by determining the frequency of gene conversion of the chromosomal *leuB-Ag1* allele to *leuB*+ through non-crossover recombination with pTA168, the Δ*radB* strain, H284, exhibited non-crossover recombination frequencies of 15% of those observed in *radB*+ strain, H195. Thus, RadB is likely to be required for efficient homologous recombination of all types.

RadB is likely to function early during homologous recombination

The canonical model for homologous recombination separates into two pathways that can result in crossover (DSBR) or non-crossover recombination (SDSA) (Figure 4.12). The finding that deleting *radB* results in reduced frequencies for both crossover and non-crossover recombination suggests that RadB might act prior to this divide in the recombination pathways, and therefore acts at an early stage of recombination, like RadA (Figure 4.12).

Recombination is proposed to commence with a double strand break. The DNA ends are resected to generate 3' ssDNA tails. In archaea, RadA assembles on the ssDNA as a nucleoprotein filament that is then proficient for homology searching in other DNA sequences. Once homology is found, strand invasion of the RadA coated ssDNA into the homologous duplex can proceed. The recombination pathway then splits into two, either generating a crossover or non-crossover product (Figure 4.12). Without RadA, recombination can not proceed as no homology search or strand invasion can occur, blocking the downstream processes of recombination. Thus, in the absence of RadA, neither crossover nor non-crossover recombination can occur. The Δ*radB* recombination phenotype is less severe than the Δ*radA* recombination phenotype but results in a global reduction in recombination frequencies, therefore it is likely that RadB acts at an early stage of recombination affecting both crossover and non-crossover pathways.

If RadB is acting at an early stage of recombination, this narrows down its potential role. Studies have shown that RadB possesses no nuclease activity (C. Guy, personal communication) therefore it does not process DNA ends to 3' ssDNA tails. However, it could be involved in this resection step through interaction with a nuclease, though no such interaction has yet been reported. Alternatively, RadB might act with RadA in nucleoprotein filament formation and/or strand exchange. This possibility is reinforced by the previously observed interaction between RadA and RadB (Komori et al., 2000b). Furthermore, it has been shown in this study that *radA* transcript levels are significantly higher than *radB* transcripts with transcription of *radA* being induced following DNA damage, while *radB* transcription remains constant. In *Pyrococcus furiosus*, RadA protein levels are 200-fold higher than RadB levels (Komori et al., 2000b; Reich et al., 2001). If RadB is a recombination mediator protein that interacts with RadA, it is possible that much lower intracellular concentrations are required and that no induction of *radB* transcription would be required following DNA damage due to sufficient RadB protein being present already.

Finally, RadB could function during DNA synthesis following strand invasion, a process required by both SDSA and DSBR recombination. While RadB is not a DNA polymerase, it has been demonstrated to interact with DP1, the small exonuclease subunit of DNA polymerase PolD (Hayashi et al., 1999). If this interaction occurs *in vivo*, RadB might be necessary for efficient DNA synthesis.

RadB might possess a further, later role specific to crossover recombination

Δ*radB* strains exhibit a greater decrease in crossover recombination frequencies than non-crossover recombination frequencies (~6.5% and ~20% of *radB*+ strain frequencies at the *leuB*

locus, respectively). This observation implies an additional, later role for RadB in homologous recombination specific to the DSBR pathway that is necessary to generate crossover products.

It is possible that RadB is involved in second strand capture following DNA synthesis from the first invading strand. This involvement could either be at the stage of forming RadA nucleoprotein filaments on ssDNA, the ensuing homology search or the strand invasion event itself (Figure 4.12). In the SDSA pathway of non-crossover recombination, only one RadA nucleoprotein filament and one strand invasion event is required whereas in the DSBR pathway of (predominantly) crossover recombination, two such events must occur. As the frequency of non-crossover recombination in Δ*radB* strains is reduced to 20% of *radB*+ frequency, it might follow that with an extra strand invasion event, the expected frequency would be 20% x 20% = 4% of *radB*+ frequencies. This value is close to the observed relative frequency of crossover recombination in Δ*radB* strains compared to *radB*+ strains (~6.5%). This reinforces the idea that RadB might function with RadA in either the formation of RadA nucleoprotein filaments or in strand exchange (Figure 4.12).

An alternative explanation could be due to the length of substrate homology available for recombination in each assay. It has been shown that efficient crossover recombination generally requires a greater length of substrate than non-crossover recombination (Jinks-Robertson et al., 1993), and substrate length could be limited in this assay. In the crossover recombination assays using pTA159 described earlier in this chapter, the homology between plasmid and chromosome at the *bgaHa* locus equates to ~3.4kb. With pTA168, less substrate is available for recombination to take place at the *leuB* locus: ~2kb of substrate is present on the plasmid, but only recombination occurring at the ~500bp sequences between the *leuB-Aa2* and *leuB-Ag1* mutations will generate a leu+ recombinant. It is possible that 500bp of substrate is sufficient for non-crossover recombination to proceed efficiently in *Haloferax volcanii*, but is not sufficient for crossover recombination to take place equally well. However, the minimum amount of substrate required for recombination in *E.coli* is ~30 to 40 bp (Shen and Huang, 1986). This substrate requirement is far smaller than the available substrate on either pTA159 or pTA168, suggesting that limiting substrate is not an issue. Additionally, in this chapter, crossover recombination has been shown to proceed efficiently at 323 bp of substrate (pTA188, *bgaHa* locus), therefore it would be expected that non-crossover recombination would be able to proceed efficiently also.

RadB has also been shown to interact with Hjc, a Holliday junction resolvase, *in vitro*. A further explanation for the greater reduction in crossover recombination frequencies than non-crossover frequencies could be due to this interaction. While RadB is likely to be acting at an early stage of recombination (Figure 4.12), it may have an additional role in a late stage of recombination in conjunction with Hjc. If RadB is absent Hjc might not be able to function as effectively. As Hjc would only be required when Holliday junctions are a recombination intermediate, i.e. in the crossover pathway of recombination, the effects of Δ*radB* on crossover recombination frequencies would be more profound than the effects on non-crossover recombination frequencies, as no Holliday junction intermediates exist in the SDSA pathway. However, a major problem with this theory is that Δ*hjc* strains (H282) are as proficient for crossover recombination as *hjc*+ (H195) strains suggesting that Hjc is not required for Holliday junction resolution during crossover recombination in the assays used here.

The previously suggested idea that RadB might be involved in the DNA synthesis steps of recombination is undermined by the fact that crossover recombination frequencies are reduced more than non-crossover frequencies in Δ*radB* strains. If RadB was required for efficient DNA synthesis during recombination, it would be expected that both crossover and non-crossover pathways would be affected equally due to both requiring two DNA synthesis events to restore a two duplex state.

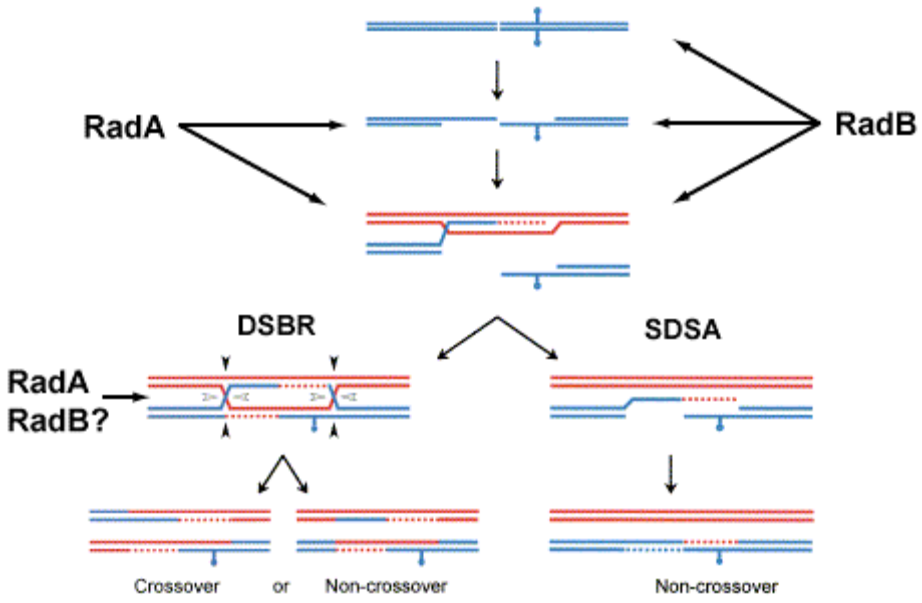

Figure 4.12 Schematic of the processes involved to generate crossover and non-crossover recombinants. The double strand break repair (DSBR) pathway can theoretically generate both crossover and non-crossover products but the predominant pathway for the generation of non-crossover recombinants is synthesis-dependent strand annealing (SDSA). As both crossover and non-crossover recombination frequencies are reduced in Δ*radB* strains, this implies an early role for RadB. As crossover recombination frequencies are affected more severely than non-crossover frequencies, RadB, like RadA might also be involved in second strand capture in the DSBR pathway. Thus, in its absence, crossover recombination frequencies will be severely reduced than non-crossover recombination frequencies. Diagram adapted from (Allers and Lichten, 2001).

Homologous recombination defects lead to increased sensitivity to DNA damage

Since both RadA and RadB are necessary for efficient homologous recombination, it can be concluded that recombination defects in Δ*radA,* Δ*radB and* Δ*radA radB* strains (H97, H64 and H186) cause the previously observed sensitivity to UV light and mitomycin C in these strains. UV induced lesions generated in experiments from this work can not be repaired through photoreactivation as plates are incubated in the dark, therefore the majority of UV lesions such as 6'-4' photoproducts and thymine dimers are repaired predominantly by nucleotide excision repair. However, UV light can nick DNA and if two nicks are close to each other, the DNA duplex can break, generating a double-stranded DNA break. This lesion is the primary substrate for repair by homologous recombination. Additionally, thymine dimers, 6-4 - photoproducts and crosslinked DNA, generated by mitomycin C, can all be repaired via homologous recombination. When a replication fork encounters such a lesion it can be regressed to form a four-way 'chicken-foot' junction (essentially a Holliday junction), allowing the lesion downstream of the fork to be repaired. Following the repair of the lesion, the fork can be restored by progressing the fork to its original state. Alternatively, the four-way chicken foot junction can be cleaved to generate two duplexes. Through homologous recombination, one of these DNA molecules can invade the other and replication is primed. This process is called break induced replication (BIR) and relies on homologous recombination.

Homologous recombination defects lead to a slow growth phenotype

Both *radA* and *radB* strains are slower growing than *radA*+ and *radB*+ strains, as demonstrated in chapter 3. Since both RadA and RadB are required for efficient homologous recombination, it can be concluded that such defects in recombination are responsible for the slow growth phenotype of these deletion strains. The reason for this is likely to be due to defective restart of DNA replication. Replication forks can collapse during DNA synthesis and as mentioned above, they can be restored through homologous recombination by BIR. In the absence of RadA or/and RadB, this process would be defective and therefore DNA synthesis would be slowed significantly. Consequently, cells would require more time to replicate their genome and therefore have a longer generation time.

Hjc

Hjc is an archaeal Holliday junction resolvase. Its activity has been demonstrated through heterologous genetics, whereby *Mth*-Hjc was expressed in a *ruvC* mutant *E.coli* strain (Bolt et al., 2001) and shown to be activated by PCNA (Dorazi et al., 2006). Hjc was able to

compensate for the absence of the bacterial Holliday junction resolvase, RuvC, demonstrating its ability to resolve Holliday junctions.

Hjc is conserved in both the euryarchaeota and crenarchaeota and is one of two Holliday junction resolvases identified in the archaea to date. The other resolvase, Hje (Holliday junction endonuclease) is only present in the crenarchaeal species *Sulfolobus sofataricus* (Kvaratskhelia and White, 2000) and is very similar to Hjc. The genetic studies of homologous recombination and the effect of Hjc, presented here have yielded some surprising results.

Hjc is probably not the primary Holliday junction resolvase in Haloferax volcanii

Data presented in this chapter show that Hjc is not required for efficient crossover recombination. If Hjc were the primary Holliday junction resolvase in all archaea, it would be expected that crossover recombination frequencies would be severely reduced in its absence, due to Holliday junctions being an intermediate of crossover recombination. In fact, in the Δ*hjc* strain, H282, crossover recombination frequencies were not significantly different to those observed in the parental *hjc*+ strain, H195. There are two possible explanations for this observation. Hjc might not be the primary Holliday junction resolvase in archaea and an as yet undiscovered resolvase is required for crossover recombination. Alternatively, a second resolvase exists and shares the role of Holliday junction resolution with Hjc. If either protein encoding gene is deleted, the presence of the other resolvase is sufficient to compensate, i.e. the two resolvases are redundant. In *E.coli*, both RuvC and RusA are potent Holliday junction resolvases. RuvC is the primary resolvase but in *ruvC* mutant strains, RusA compensates for the absence of RuvC (Sharples, 2001). This situation could be mirrored in the archaea.

A minor requirement for Hjc exists in the absence of RadB

Unlike the situation described above, where crossover recombination frequencies are not significantly different between *radB*+ *hjc*+ strains (H195) and *radB*+ Δ*hjc* strains (H282), there is a small (2-fold) but significant reduction in crossover recombination frequencies in the Δ*radB hjc* strain, H349, and the Δ*radB hjc*+ strain, H284. This suggests that while Hjc is not required for crossover recombination when RadB is present, there is a minor requirement for Hjc when RadB is absent. A possible explanation for this observation could be due to the existence of two recombination pathways existing, an efficient RadB-dependent pathway and an inefficient RadB-independent pathway. RadB interacts with Hjc, as observed *in vitro* (Komori et al., 2000b). It has been demonstrated that in *Pyrococcus furiosus,* the Holliday junction cleavage activity of Hjc is inhibited in the presence of RadB and ATP (Komori et al., 2000b). This could imply that RadB acts to prevent Hjc activity and to recruit a second

resolvase to cleave recombination intermediates of RadB-dependent recombination. Hjc would only be utilised under certain circumstances, i.e. in the inefficient, RadB-independent pathway. This could explain why no reduction in crossover recombination frequencies is observed in H282 (*radB*+ Δ*hjc*), as a second resolvase would be available to cleave Holliday junctions efficiently. In H284 (Δ*radB hjc*+), efficient RadB-dependent recombination can not proceed due to the absence of RadB. At the same time, inhibition of Hjc would be relieved allowing the resolvase to cleave Holliday junction intermediates. In the absence of both Hjc and RadB (H349, Δ*radB hjc*), RadB-dependent recombination could not proceed, nor would Hjc be available to cleave Holliday junctions in the minor RadB-independent pathway, with the cell instead relying on the second resolvase for cleavage activity.

The Hjc requirement in the absence of RadB could be substrate length dependent

Crossover recombination frequencies are reduced ~2 fold in the absence of both Hjc and RadB (H349) in comparison to when RadB is absent but Hjc is present (H284). This was observed using crossover recombination assays with pTA159 (*bgaHa* locus, ~3.4 kb of substrate). In contrast, no such difference in frequencies of crossover recombination was observed between H284 and H349 when assays using pTA168 (*leuB* locus, ~0.5 kb of sequence substrate). There are two possible reasons for this. Firstly, fewer trials were carried out using pTA168 (n=5) were carried out using pTA159 (n=12). If more trials were carried out using pTA168, the differences in recombination frequencies between H284 and H349 might become statistically significant.

The second explanation for the difference in crossover recombination rates between H284 and H349 being insignificant when using pTA168, but being significant when using pTA159, could be due to the differences in the plasmids used in each experiment. pTA159 contains ~3.5kb of homology (*bgaHa* locus) to the chromosome whereas pTA168 contains only ~0.5kb of homology to generate a *leu*+ colony (*leuB* locus). It is possible that in the absence of RadB, Hjc is required for recombination in a RadB-independent pathway at regions of longer homology (pTA159), but not required for crossover recombination at regions of shorter homology lengths (pTA168). This is reinforced by the observations described here show that a significant difference in crossover recombination frequencies is only observed in the absence of RadB.

If this is true, the effect of Hjc on crossover recombination frequencies is only minor at best, as discussed previously, and it is highly likely that a second, as yet undiscovered, Holliday junction resolvase exists in *Haloferax volcanii*.

Hjc is not required for non-crossover recombination

Unsurprisingly, non-crossover recombination frequencies of the Δhjc strain H282 were not significantly different to those observed in the radB+ strain H195. As no Holliday junctions are formed in the SDSA pathway of recombination, which generates exclusively non-crossover products, it is unlikely that any Holliday junction resolving enzyme would be required.

Proportions of bgaHa+ *colonies at different substrate lengths may differ from the expected proportions, in* radB+ *strains*

Assays to determine the dependence of crossover recombination frequencies on available substrate length demonstrate that frequencies of crossover recombination increased linearly with increases in substrate length. Crossover recombination frequencies were determined by the frequency of recombination in between oligonucleotide insertions in *bgaHa* alleles present on the chromosome and transformed plasmid. The distance between insertions was altered and the frequency of crossover recombination was based on the frequency of *ura*+ *bgaHa*+ (i.e. a blue colony phenotype). However, it was noticed that the proportions of blue and red colonies differed significantly from the expected proportions, as determined by multiplying the frequency of *ura*+ recombinants by the percentage of substrate available to become *bgaHa*+ (Figure 4.9 and 4.10). Both H195 (*radB*+ *hjc*+) and H282 (*radB*+ Δ*hjc*) displayed significantly higher proportions of blue colonies, i.e. *bgaHa*+. There are two possible explanations for this observation. Firstly, it could be due to the nature of the assay. Figure 4.7 shows that there is a central region of substrate that will generate a blue colony phenotype if recombination occurs between the two oligonucleotide insertions. Flanking this region are regions of substrate that will generate a red colony phenotype. It is possible that this configuration alters the expected proportion of blue and red colonies due to the regions of 'red' homology not being contiguous. Observed proportions might correlate better with expected proportions if two contiguous regions of substrate that generate either a blue or red colony phenotype were present on the plasmid, instead (Figure 4.13). This could reduce factors such as the minimum sequence requirement for efficient homologous recombination. Alternatively, the actual length of substrate on the transformed plasmid could be altered directly. However, this can not explain why observed proportions do not match expected proportions in *radB*+ strains but do match in Δ*radB* strains.

A second possible explanation for the observed proportions of blue and red colony phenotypes arising through crossover recombination differing from the expected proportions could be due to branch migration of Holliday junctions occurring through the oligonucleotide insertions in the *bgaHa* alleles (Figure 4.14).

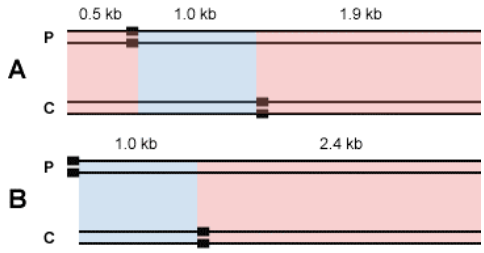

Figure 4.13 Altering the configuration of substrates available to generate blue or red colonies might change the observed proportions of each phenotype. **A** – substrate present on pTA159 (P) and substrate present on the chromosome (C). 'Red' substrate homology is interrupted by 'blue' substrate homology and therefore the total 2.4 kb of red homology in this configuration might not be as recombinogenic as if it was in one segment **(B).**

It should be noted that although Figure 4.14 shows how branch migration could change a potential red colony phenotype to a blue colony phenotype, the reverse situation could also occur. At face value, it might be expected that the two events would effectively cancel each other out and that proportions would, on average, be the same as the expected proportions. However, as the region of substrate required to generate a blue colony phenotype is central, it is possible that Holliday junctions are more likely to be cleaved in this region thus generating a blue colony phenotype. Alternatively, while Hjc has no sequence specificity for cleavage, a second resolvase may cleave junctions at specific sequences. These sequences might be overrepresented in the region of 'blue' substrate or underrepresented in the regions of 'red' homology.

Additionally, the schematic shown in Figure 4.14 relies on non-stochastic correction of mismatches through mismatch repair. Instead, a directed repair would be required to ensure that correction was uni-directional.

If such branch migration is occurring, the fact that disproportionate red/blue colony phenotypes are only observed in *radB*+ strains (H195 and H282) and not in Δ*radB* strains, could imply a role for RadB in branch migration of Holliday junctions. While it is almost certain that RadB itself can not directly migrate junctions, due to it not possessing helicase activity, it is possible that it might recruit a branch migration protein to Holliday junctions. Thus, in the absence of RadB, no such migration occurs and therefore frequencies of blue/red colonies match the expected values.

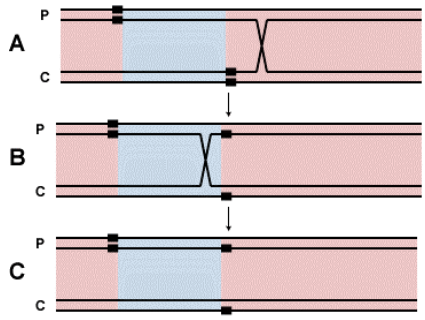

Figure 4.14 Schematic of how branch migration of Holliday junctions through heterologous sequences could generate unexpected proportions of blue and red colony phenotypes. 'P' and 'C' signify plasmid and chromosomal alleles of *bgaHa,* respectively. Regions coloured red and blue represent the regions where recombination must occur to generate a red or blue colony phenotype, assuming no branch migration. **A -** Strand invasion and consequently, Holliday junction formation occurs outside of the region required to generate a blue colony, therefore a red colony phenotype would be expected. **B** – Branch migration drives the Holliday junction past the oligonucleotide insertion, present on the chromosomal *bgaHa-Bb* allele, and into the region required to generate a blue colony phenotype. **C –** Holliday junction resolution proceeds leaving heteroduplex DNA on the chromosomal and integrated plasmid *bgaHa* alleles. If the chromosomal allele is repaired to *bgaHa*+, a blue colony phenotype would be observed.

Chapter 5: Isolation and characterization of a suppressor of Δ*radB*

5.1 Introduction

5.1.1 Bacterial suppressors

Suppressors are mutations that arise in one gene that suppress the phenotypic expression of another gene, usually of a mutant gene or gene deletion. Previously characterised suppressors manifest themselves in a variety of ways. One extensively studied example relevant to homologous recombination is the suppression of *recB, recC and recBC* strains of *E.coli* by mutations in *sbcB* and *sbcCD* (Lloyd and Buckman, 1985). RecB is generally necessary for efficient homologous recombination in *E.coli*. RecB and RecC form part of the heterotrimeric complex, RecBCD. RecB is a potent DNA exonuclease (Sun et al., 2006; Yu et al., 1998), and RecC and RecD are helicases (Dillingham et al., 2003; Korangy and Julin, 1993; Taylor and Smith, 2003). RecBCD degrades dsDNA ends in a 3' to 5' orientation with occasional nicking of the opposing strand. Upon encountering a specific sequence known as χ (5'-GCTGGTGG-3'), the polarity of RecBCD nuclease activity changes to 5' to 3' and a 3' single stranded DNA tail is generated. RecBC is then able to load RecA onto this single stranded tail and strand exchange can then occur. In the absence of *recBC*, recombination efficiency is reduced to approximately 1% of wildtype levels. The cause of this reduction in recombination efficiency is due to the DNA ends at a double strand break becoming degraded. RecBCD protects these DNA ends from aberrant degradation by other nucleases and when the enzyme is absent this protection is lost, DNA ends are degraded and the potential for recombination to occur diminishes. Therefore, DNA ends must persist for efficient recombination to occur. The *recBC*$^-$ phenotype can be suppressed by the inactivation of three genes, *sbcB* and *sbcCD*. *sbcB* encodes Exonuclease I in *E.coli*, a protein capable of degrading DNA ends. *sbcC* and *sbcD* encode the heterodimeric nuclease SbcCD, a bacterial homologue of Mre11-Rad50, which is also capable of degrading DNA ends and causing the loss of the recombination substrate. Inactivation of either gene is sufficient to inactivate the dimeric protein product. In the absence of functional Exonuclease I and SbcCD nucleases, DNA ends are able to persist *in vivo* without the need for RecBCD protection. The alternate, RecFOR-dependent pathway of recombination can then proceed whereby DNA ends are unwound by RecQ helicase activity, 3' ssDNA tails are generated by RecJ 5'-3' activity (Kowalczykowski, 2000) and RecA is loaded onto SSB coated ssDNA by RecFOR (Morimatsu and Kowalczykowski, 2003)

5.1.2 Eukaryotic suppressors

Examples of suppression exist in eukaryotic DNA repair systems. One example relevant to this work is suppression of *rad55* and *rad57* mutants. Fortin and Symington (Fortin and Symington, 2002) isolated alleles of Rad51 that are capable of suppressing the γ-ray sensitivity of *rad55* and *rad57* mutants in *Saccharomyces cerevisiae*. *RAD55* and *RAD57* encode the two Rad51 paralogs that constitute the stable heterodimeric Rad55-57 complex. Rad55-57 overcomes the inhibition of Rad51-promoted strand exchange imposed by RPA, a ssDNA binding protein that competes with Rad51 for substrate binding (Sung, 1997). In the absence of the Rad55-Rad57 complex, Rad51 foci fail to assemble during meiotic recombination (Gasior et al., 2001) and mitotic cells exhibit sensitivity to γ-radiation. Six mutant alleles of Rad51 consisting of single amino acid substitutions were found to be capable of suppressing this sensitivity. Five of these mutations are implicated in DNA binding. Rad51-L119P is present in the N-terminus of Rad51 in a domain implicated in protein-protein interactions and DNA binding. Rad51-I345T showed increased DNA binding to both ss- and dsDNA and is able to displace RPA from ssDNA, alleviating the need for Rad55/57.

Prior to the isolation of Rad51 mutations capable of suppressing the *rad55/rad57* phenotype, Smith and Rothstein (Smith and Rothstein, 1999) isolated an allele of *RFA1* that encodes the large subunit of RPA in *Saccharomyces cerevisiae,* which suppresses *RAD52*-dependent DSBR. Rad52, like Rad55-Rad57, is implicated in promoting and stabilizing Rad51-ssDNA and is indispensable for meiotic recombination in *Saccharomyces cerevisiae* (Lovett and Mortimer, 1987). In the absence of Rad52, ssDNA-bound RPA is likely to inhibit strand-annealing events. However, in *RAD52* strains encoding Rfa1-D228Y, this inhibition is overcome allowing a limited form of DSBR to occur in the form of strand annealing. For example, a HO site flanked by direct repeats can act as a substrate for single strand annealing, following processing by nucleases.

Suppressors are not always manifested as mutations. For example, *RAD51* expressed on a high copy number plasmid partially suppresses the radiation sensitivity associated with *rad55* and/or *rad57* mutants (Hays et al., 1995; Johnson and Symington, 1995). To date, no suppressors have been documented in the field of archaeal HR and DSBR. This chapter outlines a novel suppressor of the recombination defects and DNA damage sensitivity associated with Δ*radB* strains of *Haloferax volcanii*.

5.2 Results

5.2.1 Isolation of a suppressor of Δ*radB*

Prior to the commencement of this study, the archaeal Holliday junction resolvase gene, *hjc*, was deleted from a *radB*Δ*b/b* strain (H64) as described in the '*Gene Deletion*' section in Materials and Methods, by Greg Ngo. The intermediate integrant strain (H160) was serially propagated, plated on Hv-Ca + 5FOA and incubated at 45˚C for 8 days. After this time, colonies were visible on the plates. However, in addition to the small colonies expected of a *radB*Δ*b/b* or Δ*radB* strain, a number of significantly larger colonies were also present. Both small and large colonies were picked and streaked on Hv-YPC media. Southern analysis showed that *hjc* had been deleted from both colonies of small and large size. These *radB*Δ*b/b* Δ*hjc* strains were designated H187 and H188, respectively. Differential colony size is not unusual in *Haloferax volcanii* following plating on selective media. However, upon restreaking on complex media, H187 appeared phenotypically identical to other *radB*Δ*b/b* strains in terms of growth rate whereas H188 colonies were visible sooner, growing faster than anticipated, more similar to wildtype growth rates than those expected of a *radB*Δ*b/b* or Δ*radB* strain. This suggested that strain H188, but not H187, contained a suppressor mutation capable of at least suppressing the slow growth phenotype characteristic of *radB*Δ*b/b* / Δ*radB* strains. This suppressor of RadB was named *srbA*.

5.2.2 Determining the extent of suppression of Δ*radB* by *srbA*

Methods

To determine whether *srbA* also suppresses aspects of the Δ*radB* phenotype other than slow growth rate, recombination and UV irradiation survival assays were carried out on H187 (*radB*Δ*b/b*, Δ*hjc*) and H188 (*radB*Δ*b/b*, Δ*hjc, srbA*).

The growth rate of both H187 (*radB*Δ*b/b* Δ*hjc*) and H188 (*radB*Δ*b/b* Δ*hjc srbA*) was quantified and compared to those of the parental strain, H64 (*radB*Δ*b/b)*, and to the original strain of the same background, H26 (*radB*+). Enumeration of viable cells by plating of culture onto solid media was deemed necessary to distinguish between growth of normal dividing cells and those undergoing filamentous growth, as opposed to measuring the optical density of cultures. This assay involved growing cultures in Hv-YPC broth until OD =0.4, then diluting the cultures 1/10000 in the same volume. Cultures were then incubated at 45˚C, rotating at 8 rpm until early stationary phase was reached (A_{650} = 0.8). Aliquots were plated periodically on Hv-YPC plates at appropriate dilutions. Plates were incubated at 45˚C for 5 days and the number of colonies counted.

Crossover recombination rates for H187 and H188 were determined by transforming each strain with 1 µg of an integrating plasmid (pTA159) containing *pyrE2,* and sequences homologous to chromosomal sequences, i.e. *bgaHa*. Transformants were then plated on Hv-Ca media at appropriate dilutions and incubated at 45˚C for 8 days. As no uracil is present in this media, the only way a cell can form a colony is by acquiring the *pyrE2* gene. As the plasmid contains no archaeal origin of replication, the cell must integrate the plasmid, containing the *pyrE2* gene, onto the chromosome at the *bgaHa* locus, by a single, or odd number of crossover HR event. Therefore, each colony represented a successful crossover recombination event. A viable cell count was obtained by plating aliquots of the transformants on Hv-YPC media at appropriate dilutions followed by incubation at 45˚C for 5 days. The number of colonies present on selective media was compared to the viable count, providing a value representative of the frequency of crossover recombination in each strain.

UV irradiation survival assays were carried out by growing each strain in Hv-YPC broth until A_{650} = 0.8. Appropriate dilutions were made of each culture and spotted onto Hv-YPC media in 20 µl spots. Once the spots of culture had dried into the plates, cells were exposed to varying doses of UV light, sealed in a black plastic bag to prevent photoreactivation and incubated at 45˚C for 5 days. Following growth, colonies were counted to give an indication of the survival rate for each strain, following irradiation.

Results

Growth Rates

Assays to determine the growth rate of the tested strains in liquid culture show that strain H188 (*radB*Δ*b/b* Δ*hjc srbA*) appears to grow at a rate approaching H26 (*radB*+) levels and H187 (*radB*Δ*b/b* Δ*hjc*) grows significantly slower, typical of a Δ*radB* phenotype (such as is observed in the case of H64 (*radB*Δ*b/b*)). Spotting of liquid culture onto solid media showed that cell samples from wildtype (H26) and from the suppressor strain (H188) were capable of forming colonies at apparently equal efficiency, eliminating the possibility that the increased growth rate observed in liquid culture was due to filamentous growth. Growth rates between H26 and H188 were also comparable. These data are displayed in Figure 5.1.

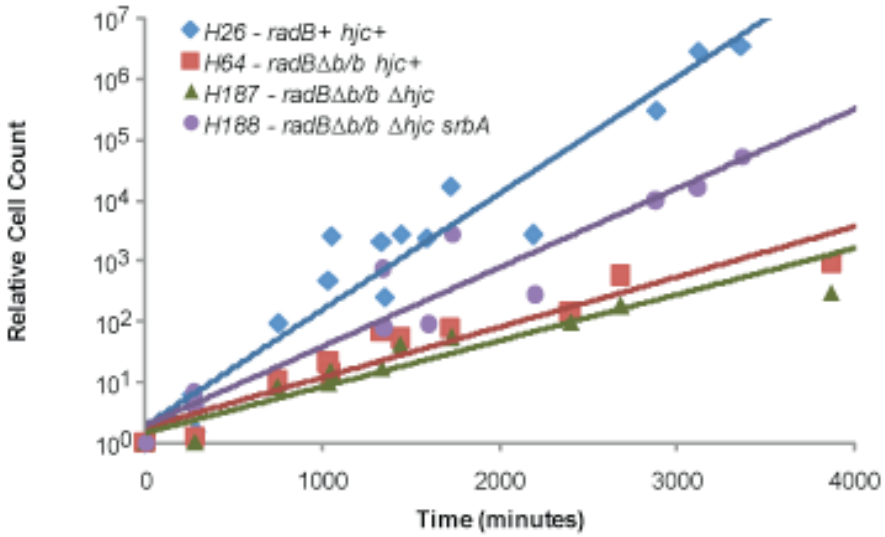

Figure 5.1 Growth rates of H26 (*radB+ hjc+*), H64 (*radBΔb/b hjc+*), H187 (*radBΔb/b Δhjc*) and H188 (*radBΔb/b Δhjc srbA*). Cultures were grown continuously at 45°C with rotation (8 rpm) and spotted onto complex media (Hv-YPC) at several time intervals. Relative cell count is calculated as the relative number of cells compared to time = 0 minutes. All data points are a consolidation of data obtained from three trials.

Figure 5.1 shows that H188 (*radBΔb/b Δhjc srbA*) grows significantly faster than H187 *radBΔb/b Δhjc*) and H64 *radBΔb/b hjc+*), indicating that *srbA* partially suppresses the slow growth phenotype associated with Δ*radB*. However, suppression is not complete as evidenced by H188 having a slower growth rate than H26 (*radB+ hjc+*).

From the equations derived from the trendlines shown in Figure 5.1, the generation time (g) of each strain could be calculated using the equation:

$$g = (\log_{10} N_L - \log_{10} N_E) / \log_{10} 2$$

$$\text{Generation time} = g / (L-E)$$

The number of generations in a particular time frame (g) is calculated by taking two points on the trendline, in exponential growth phase and deducting the $\log_{10}$ of the number of cells present at the earlier time point (N_E) from the $\log_{10}$ of the number of cells present at the latter time point (N_L). This value is then divided by the constant of $\log_{10}2$ to give the number of generations in the given time frame. By dividing the number of hours between the two points (L = end time, E = start time) the trendline and dividing this value by g, the resulting value is the generation time of the particular strain. This calculation was carried out for the strains tested in this experiment and are displayed in Table 5.1 below.

Strain	H26	H64	H187	H188
Generation Time (mins)	156	363	396	230

Table 5.1 Calculated generation times for tested strains H26 (*radB*+ *hjc*+), H64 (*radB*Δ*b/b hjc*+), H187 (*radB*Δ*b/b* Δ*hjc*) and H188 (*radB*Δ*b/b* Δ*hjc srbA*).

Crossover recombination frequencies

The results obtained from the recombination assay (Figure 5.2) show that H187 (*radB*Δ*b/b* Δ*hjc*) exhibits the expected levels of crossover recombination associated with *radB*Δ*b/b* / (Δ*radB hjc* strains), i.e., approximately 2-5% of wildtype level. Strain H188 exhibits higher than expected levels of recombination approaching those observed in a wildtype strain. This is a clear indication that the suppressor mutation not only suppresses the slow growth phenotype of a *radB* deletion but can also compensate for the diminished levels of recombination.

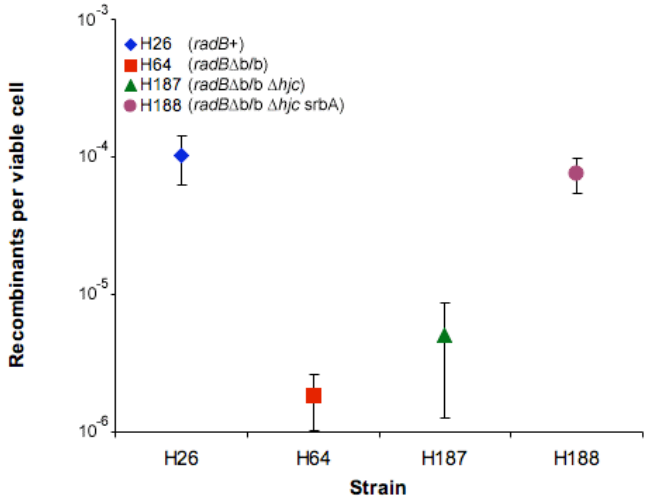

Figure 5.2 Comparison of the recombination efficiencies observed in *radB*+ (H26) and *radB*Δ*b/b* (H64) strains with those observed in *radB*Δ*b/b* Δ*hjc* (H187) and *radB*Δ*b/b* Δ*hjc srbA* (H188). All data points are calculated as the mean value of at least three trials. Error bars are calculated using standard error based on at least three trials.

UV Survival Rates

Figure 5.3 shows the observed survival of the strains following UV irradiation. As with the recombination defect associated with Δ*radB* (Figure 5.2), *srbA* appears to suppress the UV sensitivity phenotype of Δ*radB* with H188 exhibiting UV resistant equal to a *radB*+ strain (H26). The survival rate of H187 was the same as observed in other *radB*Δ*b/b* and Δ*radB* strains. These data demonstrate that the *srbA* mutation suppresses the DNA repair defects associated with Δ*radB*.

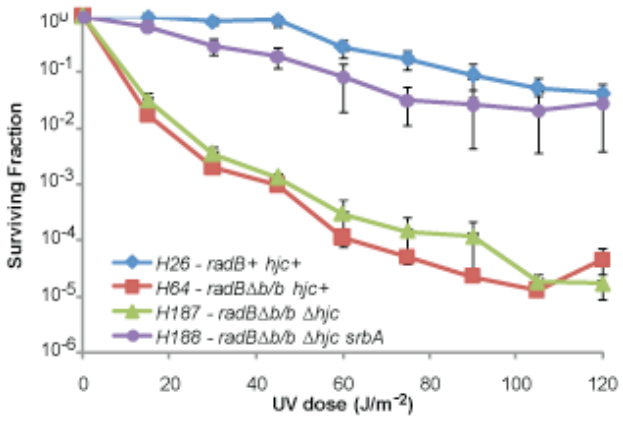

Figure 5.3. Survival of *radB*+ (H26), *radB*Δ*b/b* (H64), *radB*Δ*b/b* Δ*hjc* (H187) and *radB*Δ*b/b* Δ*hjc srbA* (H188) strains following UV irradiation. All data points are calculated as the mean value of at least three trials. Error bars are calculated using standard error based on at least three trials.

Summary

The assays described above revealed that the *srbA* mutation in H188 is not only capable of suppressing the slow growth phenotype associated with Δ*radB* strains, but is also able to suppress the other characteristic features of this genotype: The *srbA* mutation suppresses the UV sensitivity and crossover recombination defects associated with a Δ*radB* and *radB*Δ*b/b* genotype, as demonstrated by the identical survival frequency of H188 and H26 following UV irradiation, and the similar crossover recombination frequencies of the two strains. Furthermore, the growth rate defect associated with Δ*radB* was partially suppressed in H188.

5.2.3 Identification of the *srbA* suppressor mutation

Two methods were employed to identify the locus of the suppressor mutation.

Genomic library of H188

The first method employed to identify the Δ*radB* suppressor mutation was to generate a plasmid library containing genomic DNA from the *srbA* strain, H188. As the genome of H188 contains *srbA* and H187 does not, DNA from the former was used to transform the latter in an attempt to confer suppression on H187. UV irradiation was used to screen for transformed H187 cells that had acquired *srbA*, as they would survive at a much higher frequency than H187 cells without *srbA*. ~1% of Δ*radB / radB*Δ*b/b* cells survive whereas over 10% of *radB*+ cells survive following 60 J/m^2 UV irradiation, when irradiated on Hv-Ca media (see Figure 3.32 in Chapter 3). Plasmid DNA could then be extracted from candidate survivors and the library fragment contained in the multiple cloning site could be sequenced to identify *srbA*. This strategy relies on the *srbA* being a dominant mutation.

The restriction enzyme *Aci*I (5'-C^CGC-3') was used to partially digest the genomic DNA. This enzyme has a high frequency of restriction sites in the *Haloferax* genome. The base composition of the genome is approximately 65% guanine and cytosine. Based on this, it is calculated that there are an estimated ~43,000 *Aci*I sites (=0.325^4 * 4,200,000 bp), i.e. an expected site once every 90bp (=1/(0.325^4)). This high frequency of restriction ensures near random cleavage through partial digestion and provides a near complete and even coverage of the genome. Additionally, *Aci*I was a good candidate for generating the library, as the resulting fragments would contain compatible DNA ends with *Cla*I (5'-AT^CGAT-3'). A *Cla*I site is present in the multiple cloning site of pTA354 (Norais et al., 2007), a *pyrE2* marked shuttle vector containing origin of replication, pHV1/4, the recipient plasmid for the library.

Reaction conditions that favoured digestion of genomic DNA to generate 2.5-5 kb fragments were determined by titrating the concentration of enzyme used per reaction ranging from 0.1 - 1 unit/µg of DNA. Additionally, all reactions were carried out using a non-optimal restriction buffer, i.e. NEBuffer 1 (25% activity) instead of NEBuffer 3 (100% activity), and reactions were quenched after exactly 30 minutes to ensure digestion was not complete. Titration analysis showed that 0.2 units of *Aci*I provided the highest concentration of digested fragments within the desired size range of 2.5-5 kb.

Genomic DNA fragments were inserted into the polylinker region of pTA354 (Norais et al., 2007) at the *ClaI* site. pTA354 was used for this purpose as it is a replicating plasmid and therefore does not require integration onto the chromosome to be heritable. Secondly, the

presence of *ori-phV1/4* prevents any integration onto the main chromosome, as integration of this origin sequence on the main chromosome is not tolerated (T. Allers, unpublished results). This was advantageous as it allowed easy extraction and analysis of any plasmid DNA that might contain *srbA*.

H187 was transformed with the library DNA and plated on Hv-Ca media and irradiated with 60 J/m^2 UV light to select for transformants that had gained resistance to this level of DNA damage. To enhance the UV resistance selection further, colonies that grew were replica plated onto selective media and UV irradiated with the same dose again.

Results

27 UV resistant colonies were confirmed following selection. Eight of these were grown and plasmid DNA was extracted and sequenced. These strains all contained plasmid DNA with the same insert. Sequence data showed that the insert present on these plasmids was the coding sequence for the *Haloferax volcanii* beta galactosidase gene. Mutations in this gene are unlikely to confer resistance to DNA damage, and this possibility was eliminated by two methods: The first test was to extract the plasmid from these strains and re-transform H187 with the DNA to see if suppression was conferred. This was not observed, and transformants were as sensitive to UV irradiation as typical Δ*radB* / *radB*Δ*b/b* strains.

Secondly, when the plasmid DNA was cured from these strains (by relieving selection for the pTA354-borne *pyrE2* gene with overnight growth in complex media, followed by plating of cells on Hv-Ca + 5FOA), cells that could form colonies were still resistant to UV irradiation, comparable to H26 (*radB*+) cells. This might have been due to a mutation in the plasmid-borne *bgaHv* gene converting the chromosomal allele, therefore conferring suppression. However, this does not eliminate the possibility that a pre-existing chromosomal mutation existed in these strains (not necessarily in the *bgaHv* gene) that conferred suppression.

Together these observations strongly suggest that the *bgaHv* gene was not responsible for suppressing the Δ*radB* phenotype and that suppression was instead a result of a pre-existing mutation present in the transformed cells. This is likely if the *srbA* mutation arises early and easily during normal growth. Since cells containing this mutation would out-compete those without due to the growth and DNA repair advantage and therefore it would appear that the suppressor has been successfully isolated on pTA354 several times.

Analysis of genes that encode RadB associated proteins

As a more directed approach to determining the nature of *srbA*, genes encoding proteins that have been demonstrated to interact with RadB (Hayashi et al., 1999) *in vitro* were examined to determine whether any mutations were present in the coding sequences of these genes in H187 (*radB*Δ*b/b* Δ*hjc*) and H188 (*radB*Δ*b/b* Δ*hjc srbA*). Sequences were also analysed from H26 (*radB*+) for comparative purposes, as H26 is a parent strain of both other strains. RadB from *Pyrococcus furiosus* has been shown to interact with Hjc (a Holliday junction resolvase), DP1 (the small exonuclease subunit of the DNA polymerase PolD), RadA (the archaeal Rad51/RecA recombinase homologue) and with itself (RadB can form dimers or filaments (Akiba et al., 2005; Hayashi et al., 1999)). RadB and Hjc were disregarded, as both *radB* and *hjc* were not present in H188. Therefore, *radA* and *dp1* were considered as candidates for the observed suppression of the Δ*radB* phenotype.

Suppressor mutations in *dp1* or *radA* might be present in the coding region. Such suppression has been observed previously. For example, mutations in the coding sequence of Rad51 can alleviate the need for Rad55/57 during recombination (Fortin and Symington, 2002). Alternatively, any differences observed in the promoter sequences of these genes could result in an up or down-regulation of transcription. Other studies have shown that such changes in expression of a gene can confer suppression of the phenotypes associated with related gene products, e.g. *RAD51* expressed on a high copy number plasmid partially suppresses the radiation sensitivity associated with *rad55* and/or *rad57* mutants (Hays et al., 1995; Johnson and Symington, 1995).

PCR primers were designed to amplify the chromosomal copy of *dp1* (D1SEQF/DP1SEQR) and *radA* (RADAF/RADAR) and 150 bp upstream of the start codon to include their respective upstream BRE (TFB recognition element) sequences and TATA boxes. Both *dp1* and *radA* were amplified from H188, H187 and H26 genomic DNA, and sequenced using the same forward and reverse primers used for amplification. (See Materials and Methods for primers).

Results

A single nucleotide substitution is present in H188 radA *coding sequence*

Sequence data showed no difference between any of the three strains in the coding sequence of *dp1*, or in its promoter sequence, suggesting that the Δ*radB* suppressor, *srbA*, is not directly caused by a mutation in DP1. However, sequence of *radA* of H188 (*radB*Δ*b/b* Δ*hjc srbA*) differed to that of H187 (*radB*Δ*b/b* Δ*hjc*) and H26 (*radB*+) at a single nucleotide (Figure 5.4).

The mutation present in the coding sequence of H188 *radA* is a cytosine to thymine transition at nucleotide 588 that, when translated, generates an alanine to valine substitution at residue 196 of RadA. Additionally, this mutation eliminates an *Nru*I restriction site at this position (5'-TCGCGA-3' mutated to 5'-TCGTCA-3'), which is useful for identification of this mutation by restriction digest.

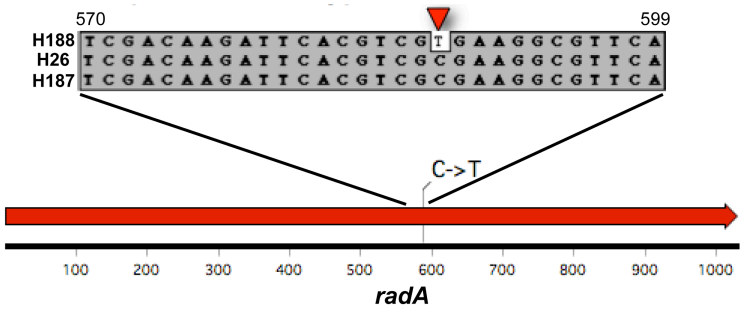

Figure 5.4 Location of cytosine to thymine mutation in *radA* of H188 (*radB*Δ*b/b* Δ*hjc srbA*), in comparison to H26 (*radB*+ *hjc*+) and H187 (*radB*Δ*b/b* Δ*hjc*) *radA* sequences.

5.2.4 Generation of *radA-A196V* Δ*radB* strain

To determine whether RadA-A196V is the cause of the suppression of the Δ*radB* phenotype (i.e. *srbA*) the *radA-A196V* coding sequence was used to replace the wildtype *radA* sequence present in H284 (Δ*radB*). The aims of this experiment were to determine whether RadA-A196V is a suppressor of the Δ*radB* phenotype, and whether RadA-A196V alone is the sole suppresser the Δ*radB* phenotype. H284 is from a different strain background to H188 and it is therefore unlikely that any pre-existing suppressor mutations that are present in H188 and H187 would also be present in H284. Furthermore, the *radB* deletion present in H284 is a complete deletion of the coding sequence whereas the deletion present in H188 is only a partial deletion of *radB*. Although the phenotypes resulting from these two genotypes have been shown to be identical so far, as described in chapter 3, suppression might only be conferred in a *radB*Δ*b/b* strain and not in a Δ*radB* strain. Finally, H188 is deleted for *hjc*, whereas H284 is not. This experiment could help determine whether the absence of Hjc is a requirement for suppression.

The *radA-A196V* coding sequence was obtained by amplification of *radA-A196V* from the genomic DNA of the original *srbA* strain, H188. Primers used for this amplification were as before (RADAF and RADAR), and the mutation was confirmed by restriction digest of the PCR product with *Nru*I as the presence of the point mutation eliminates an *Nru*I restriction site present in the wildtype sequence.

The amplification product was digested with *Eco*RV and *Not*I resulting in a 1.3kb fragment containing *radA-A196V*. This was ligated into the multiple cloning site of the *pyrE2* marked suicide plasmid, pTA131, and designated pTA769. *dam*- DNA of this plasmid (pTA778) was used to transform the Δ*radB* strain, H284. The gene knockout technique described in Materials and Methods was used to replace *radA* with *radA-A196V*. Integrants were analysed by digestion and Southern blot of genomic DNA with *Nru*I, and probing with a DNA fragment containing *radA* coding sequence. Replacement of the wildtype gene with the mutant copy was determined by selecting for ura- colonies from counter-selection plates (Hv-Ca + Trp + Thy + 5FOA) and amplifying the *radA* locus using *radA* specific primers, RADAR and RADAF. The resulting amplification product was digested with *Nru*I to determine the presence or absence of the restriction site at the site of the *radA* mutation. A clone lacking the *Nru*I site contained the mutant *radA* coding sequence and was sequenced using primers RADAF/RADAF to confirm no additional mutations were present. The resulting strain was designated H724.

5.2.5 Phenotypic analysis of H724 (*radA-A196V*, Δ*radB*)

H724 was subjected to the same analyses carried out on previous strains, i.e., sensitivity to UV irradiation and to the chemical toxin mitomycin C. Other phenotypic features were analysed by determination of growth and cell division rate, crossover and non-crossover recombination frequencies and frequencies of recombination relative to the length of available homologous sequences. These analyses were performed alongside three control strains. H195 (*radB*+ *radA*+) and H284 (Δ*radB radA*+) and H188 (*radB*Δ*b/b* Δ*hjc srbA*) wherever possible. H188 was utilised to determine whether the absence of Hjc or the partial deletion of *radB,* rather than the complete deletion in H724, affect suppression of the Δ*radB* phenotype.

Growth rate

H188, (*radB*Δ*b/b* Δ*hjc srbA*) was characterised as a suppressor strain by partially suppressing slow growth, therefore the growth rate of H724 (*radA-A196V*, Δ*radB*) was determined to discover whether RadA-A196V can suppress the slow growth phenotype (Figure 5.5).

Strain	H195	H284	H724	H188
Generation Time (mins)	160	310	207	230

Table 5.2 Calculated generation times for tested strains H195 (*radA*+ *radB*+), H284 (*radA*+ Δ*radB*), H724 (*radA-A196V* Δ*radB*) and H188 (*radB*Δ*b/b* Δ*hjc srbA*).

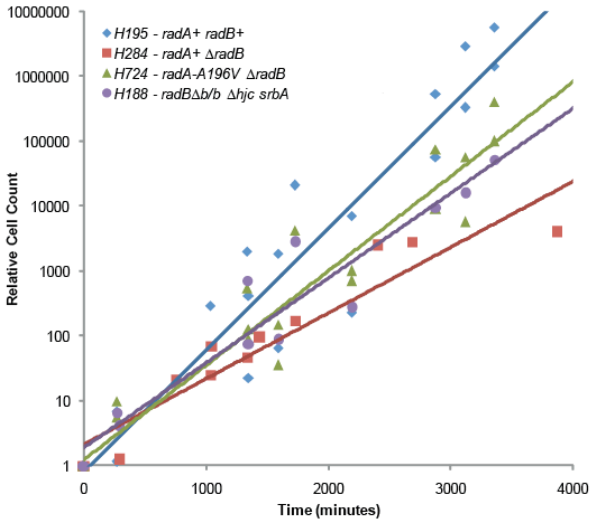

Figure 5.5 Growth rates of H195 (*radB+ hjc+*), H284(Δ*radB hjc+*), H724 (*radA-A196V* Δ*radB*) and H188 (*radB*Δ*b/b* Δ*hjc srbA*). Cultures were grown continuously at 45°C with rotation (8 rpm) and spotted onto complex media (Hv-YPC) at several time intervals. Relative cell count is calculated as the relative number of cells compared to time = 0 minutes. All data points are a consolidation of data obtained from three trials.

RadA-A196V partially suppresses the ΔradB *slow growth phenotype*

Figure 5.5 and Table 5.2 show that H724 (*radA-A196V* Δ*radB*) has a significantly faster growth rate than H284 (*radA+* Δ*radB*), demonstrating that RadA-A196V suppresses the slow growth phenotype associated with Δ*radB*. Like H188 (*radB*Δ*b/b* Δ*hjc srbA*), H724 growth rates are slower than H26 and H195, the parental *radA+ radB+* strains and are comparable to each other. This strongly indicates that the sole suppressor of the Δ*radB* growth defect phenotype is RadA-A196V, with no secondary suppressors being responsible for the observed suppressed growth phenotype in H188.

Hjc and partial deletion of radB *do not affect suppression*

The growth rates for H724 (*radA-A196V* Δ*radB*) and H188 (*radB*Δ*b/b* Δ*hjc srbA*) are virtually identical. Thus, it is unlikely that suppression of the slow growth phenotype associated with Δ*radB* is dependent on the absence of Hjc, or the partial deletion of *radB* rather than the complete deletion.

UV sensitivity

H724 was irradiated with varying doses of UV light ranging from 0 Jm^{-2} to 120 Jm^{-2}.

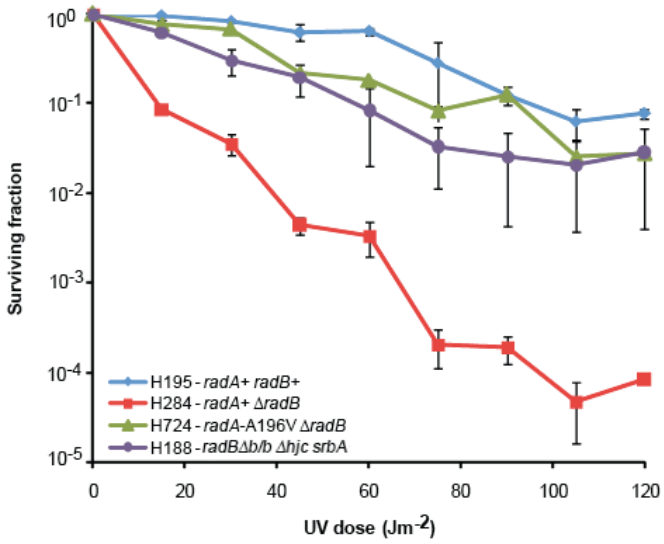

Figure 5.6 Comparison of UV sensitivity of H195 (*radA*+ *radB*+), H284 (*radA*+ Δ*radB*), H724 (*radA-A196V* Δ*radB*) and H188 (*radB*Δ*b/b* Δ*hjc srbA*). All data points are calculated as the mean of at least three trials. Error bars are calculated as standard error.

RadA-A196V completely suppresses the ΔradB *UV sensitivity phenotype*

Figure 5.6 shows that H724 (*radA-A196V* Δ*radB*) is as UV resistant as H195 (*radA*+ *radB*+). Both of these strains have a greater survival frequency compared to H284 (*radA*+ Δ*radB*). Additionally, the UV resistance phenotype of H724 is comparable to that of H188 (*radB*Δ*b/b* Δ*hjc srbA*) indicating that suppression of the UV sensitivity phenotype observed in H188 and H724 is due to RadA-A196V.

H724 might repair UV induced lesions more slowly than H195

Although the survival frequency of H724 (*radA-A196V* Δ*radB*) and H195 (*radA*+ *radB*+) are identical, H724 colonies that had grown after UV irradiation and incubation at 45°C for 5 days were significantly smaller than those of H195. H724 colonies appeared to be the same size as H284 colonies (*radA*+ Δ*radB*) (Figure 5.7). This could be due to the slower growth rate of H724. Alternatively, while H724 is able to repair UV induced lesions more efficiently due to RadA-A196V, the repair of these lesions may be slower than in H195 (*radA*+ *radB*+). Thus, replication and cell growth could be impeded until the less efficient repair process is completed and the lesions removed.

Figure 5.7 Comparison of colony sizes from different strains, following UV irradiation and then incubation at 45°C for 5 days.

Hjc and partial deletion of radB *do not affect suppression*

As with the observed growth rates, the UV resistance of H724 (*radA-A196V* Δ*radB*) and H188 (*radB*Δ*b/b* Δ*hjc srbA*) are virtually identical. Thus, it is unlikely that suppression of the UV sensitivity phenotype associated with Δ*radB* is dependent on the absence of Hjc or the partial, rather than the complete deletion of *radB*.

Crossover recombination proficiency

Crossover recombination assays using pTA159, identical to those described in Chapter 4, were carried out. Cells that integrate pTA159 at the *bgaHa* locus become ura+. By dividing this figure by the viable cell count, as determined by plating on Hv-YPC+Thy media, the frequency of crossover recombination can be calculated.

RadA-A196V completely suppresses the ΔradB *crossover recombination defect*

The results shown in Figure 5.8 show that H724 (*radA-A196V* Δ*radB*) is capable of efficient crossover recombination, equivalent to that observed in H195 (*radA+ radB+*). H195 has a crossover recombination frequency of 2.8×10^{-4} and H724 has a moderately higher frequency of 3.75×10^{-4}, suggesting that strains deleted for RadB but with RadA-A196V can carry out crossover recombination ~34% more frequently than strains with RadA and RadB present. However, an unpaired T-test returns a p value of 0.63 and the difference between results is therefore not significant (i.e. $p>0.05$). Thus, the suppression of the inefficient recombination phenotype of a typical Δ*radB* appears to be complete in the presence of RadA-A196V, but RadA-A196V does not elevate crossover recombination frequencies above H195 frequencies.

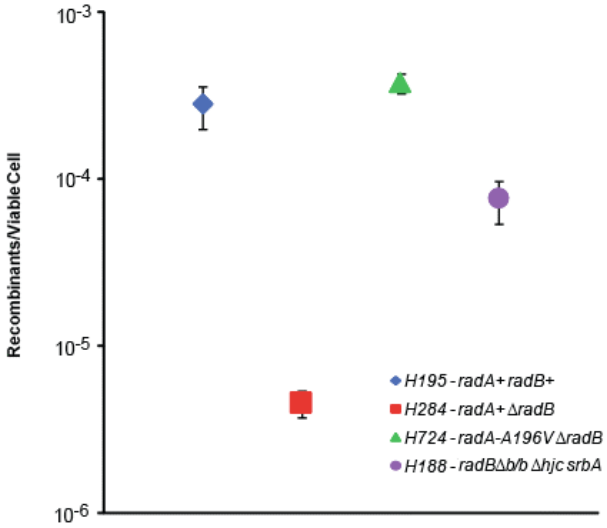

Figure 5.8 Comparison of the crossover recombination frequencies observed in H195 (*radA*+ *radB*+), H284 (*radA*+ Δ*radB*), H724 (*radA-A196V* Δ*radB*) and H188 (*radB*Δ*b/b* Δ*hjc srbA*) as calculated by the frequency of pTA159 transformed ura+ integrants as a proportion of total viable cells (ura+ and ura-). All data points are calculated as the mean of at least three trials. Error bars are calculated as standard error.

Hjc and partial deletion of radB *is unlikely to affect suppression*

It is notable that the levels of crossover recombination observed in H188 are approximately five-fold lower than those in H195 and H724. However, it should also be noted that the *radA*+ *radB*+ strain that H188 is derived from, H26, has a crossover recombination frequency approximately three-fold lower than that of H195. (1.03×10^{-4} vs 2.81×10^{-4}, respectively, from Chapter 4)). As a consequence of this, the recombination frequencies observed in H188 are comparable to those observed in H26 (see Figure 5.2). Thus, it is unlikely that suppression of the UV sensitivity phenotype associated with Δ*radB* is dependent on the absence of Hjc or the partial deletion of *radB*, rather than the complete deletion.

Non-crossover Recombination Efficiency

In Δ*radB* strains, non-crossover recombination frequencies are significantly lower than those observed in *radB*+ strains, approximately ~20% of *radB*+ levels. Until now, it has not been possible to determine whether H188 (*radB*Δ*b/b* Δ*hjc srbA*) is suppressed for this non-crossover recombination defect. This is because the assay requires a strain to be transformed with the

integrative plasmid, pTA168, containing *pyr*E2 and the *leuB-Aa2* allele. If recombination occurs between the *leuB-Aa2* allele and a chromosomal *leuB-Ag1* allele, recombinants can be leu+. If they are also ura+, the plasmid, and *pyr*E2 has integrated and therefore the event is a crossover one. If, however, the strain is ura-, gene conversion without crossover has occurred at the *leuB* locus. This assay is not utilisable with H188 as it is *leuB*+, rather than *leuB-Ag1*.

The non-crossover recombination assay was carried out on H724 (*radA-A196V* Δ*radB*) to determine whether RadA-A196V is able to suppress the non-crossover recombination deficiency associated with Δ*radB*.

Frequency of Recombination	**H195** ***radA+*** ***radB+***	**H284** ***radA+*** **Δ*radB***	**H724** ***radA-A196V*** **Δ*radB***
Total	$1.4x10^{-5}$	$2.3x10^{-6}$ (16.7%)	$6.9x10^{-6}$ (50.9%)
Crossover	$3.1x10^{-6}$	$2.0x10^{-7}$ (6.5%)	$1.4x10^{-6}$ (46.6%)
Non-Crossover	$1.0x10^{-5}$	$2.1x10^{-6}$ (19.8%)	$5.5x10^{-6}$ (52.1%)
Crossover/Total	**22.7%**	**8.8%**	**21.3%**

Table 5.3 Crossover, non-crossover and total recombination frequencies between pTA168 and the chromosomal leuB locus. Percentages in parentheses represent the frequency of the type of recombination compared to the H195 frequency

RadA-A196V partially suppresses the non-crossover recombination phenotype of ΔradB

Figure 5.9 and Table 5.3 show that the non-crossover recombination defect associated with Δ*radB* is partially suppressed by RadA-A196V, restoring frequencies from 19.8% (H284) to 52.1% (H724) of H195 frequencies. This suggests that suppression is not complete, unlike with crossover recombination as assayed by transforming strains with pTA159 (*bgaHa* allele) and scoring ura+ colonies, where suppression was complete. While this difference in non-crossover recombination frequencies between H195 and H724 could be due to stochastic effects and a difference in the number of trials performed on each strain (5 for H195, 3 for H724), non-pairwise, one tailed T-test analysis shows that the difference is significant at the 95% confidence level ($p=0.004$, i.e. $p<0.05$). Thus, these data suggest that RadA-A196V is able to partially suppress the non-crossover recombination defects associated with Δ*radB*.

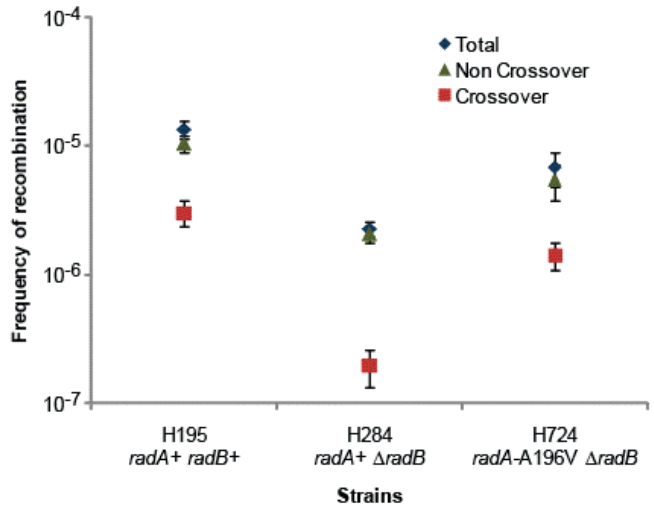

Figure 5.9 Total, crossover and non-crossover (gene conversion) recombination frequencies for strains H195 (*radA+, radB+ hjc+*), H284 (*radA+, ΔradB, hjc+*), and H724 (*radA-A196V, ΔradB*), as assayed by counting leu+ (total), leu+ ura- (non-crossover) and leu+ ura+ (crossover) colonies following transformation with pTA168. All data points are calculated as the mean value of at least three trials. Error bars are calculated as standard error.

The relative frequency of crossover recombination events as a function of total recombination events for H724 is comparable to that of H195 (22.7% and 21.3% crossover recombination, respectively). Thus, RadA-A196V restores the relative frequencies of crossover recombination to *radA+ radB+* levels.

RadA-A196V suppression of recombination defects may be locus/substrate-dependent

It should be noted that not only is the frequency of non-crossover recombination lower in H724 than in H195, but that crossover recombination frequencies are also 47% of H195 frequencies (Table 5.3). A non-pairwise, one tailed T-test showed that this modest difference in frequencies is significant at the 95% confidence level ($p=0.035$, i.e. $p<0.05$). This is surprising since the previous assay of crossover recombination, using pTA159, demonstrated that crossover recombination frequencies exhibited by H724 were the same as those exhibited by H195 (Figure 5.8).

There are two possible reasons for the difference in crossover recombination frequencies between H195 (*radA+ radB+*) and H724 (*radA-A196V ΔradB*), in each assay. Firstly, pTA159 contains ~3.4 kb of substrate for recombination with the chromosome, whereas pTA168 only has ~0.5 kb. It is possible that RadA-A196V suppresses recombination defects completely

when longer substrate lengths are available for recombination (i.e. in pTA159). Conversely, at lower substrate lengths (i.e. in pTA168), RadA-A196V can only partially suppress the Δ*radB* phenotype. RadB itself might be required for H195 frequencies of recombination at this substrate length. An alternative reason is that pTA159 and pTA168 recombine with the chromosome at different loci. pTA159 contains homology from the *bgaHa* locus whereas pTA168 contains homology from the *leuB* locus. Differences between these loci could mean that RadB is required for efficient recombination at the *leuB* locus but that suppression by RadA-A196V in the absence of RadB is sufficient at the *bgaHa* locus. In chapter 4, it was proposed that the *bgaHa* locus might represent a recombination hotspot since, in strains used in this laboratory, *bgaHa* is located on the main chromosome and not on the mini-chromosome, pHV4, as it is in the wildtype strain. This translocation could implicate the *bgaHa* locus as a recombination hotspot and might explain the difference in recombination frequencies.

Sensitivity to mitomycin C

As demonstrated in chapter 3, Δ*radB* strains are exquisitely sensitive to the DNA cross-linking agent, mitomycin C. This phenotype was presumed to be a result of defects in recombination that prevent the efficient repair of crosslinked DNA. H724 (*radA-A196V* Δ*radB*) was exposed to mitomycin C present in Hv-YPC+Thy plates at varying concentrations to determine whether RadA-A196V was able to suppress sensitivity to this chemical.

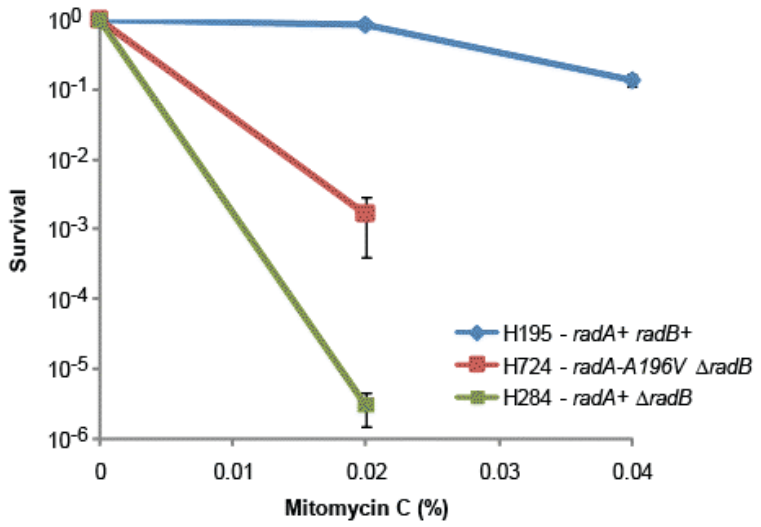

Figure 5.10 Survival of H195 (*radA+ radB+*), H724 (*radA-A196V* Δ*radB*) and H284 (*radA+* Δ*radB*) following exposure to varying concentrations of mitomycin C, present in agar plates. Only relevant genotypes are shown. Data points are calculated as the mean value of three trials. Error bars are calculated as standard error.

RadA-A196V partially suppresses the mitomycin C sensitivity phenotype of ΔradB

Figure 5.10 above shows that H724 (*radA-A196V* Δ*radB*) is more resistant to the crosslinking agent mitomycin C than H284 (*radA*+ Δ*radB*) demonstrating that RadA-A196Vpartially suppresses sensitivity. However, unlike with UV damage and recombination defects, suppression is minor in comparison. At a dose of 0.02% mitomycin C, nearly 90% of H195 (*radA*+ *radB*+) cells survive, whereas only ~0.2% of H724 cells survive. Only ~ 0.0001% of H284 cells survive at this dose. A possible reason for suppression only being partial could be due to the manner in which cells are exposed to mitomycin C. Unlike UV survival assays, where cells are transiently exposed to damage and then allowed to recover, in mitomycin C assays cells are constantly exposed to DNA damaging agents

RadB may possess a secondary role independent of recombination

It was presumed that the extreme sensitivity of Δ*radA* and Δ*radB* strains to mitomycin C was attributable to recombination defects. However, it has been demonstrated in this chapter that RadA-A196V complements the recombination defects associated with Δ*radB* almost completely. Thus, it would be expected that if crosslinked DNA lesions are repaired by recombination, the presence of RadA-A196V in a Δ*radB* strain would exhibit resistance approaching H195 (*radA*+ *radB*+) levels. As this is not the case, this implies a second role for RadB, independent of recombination, which RadA-A196V can not suppress. Alternatively, RadA-A196V may be able to compensate for the absence of RadB, but RadA-A196V itself may be less efficient or slower at the repair of crosslinked DNA lesions. These possibilities are discussed further later in this chapter.

Summary

RadA-A196V suppresses defects associated with ΔradB

In this chapter, it has been demonstrated that a mutation present in *radA* (*radA-A196V*) suppresses defects associated with Δ*radB*. Crossover recombination defects are restored to *radB*+ frequencies at the *bgaHa* locus, and almost completely at the *leuB* locus, as are non-crossover recombination defects. The exquisite sensitivity to UV irradiation is also completely suppressed by *radA-A196V*, and partial suppression of the mitomycin C sensitivity phenotype is observed. Finally, growth rates are partially restored to *radB*+ rates in the presence of RadA-A196V.

Observed suppression is solely due to RadA-A196V

When this suppressor of Δ*radB* (*srbA*) was discovered and characterised in H188 (*radB*Δ*b/b* Δ*hjc srbA*), it was unknown whether suppression was due to the mutation in *radA* or additional mutations. Furthermore, it was not known whether Δ*hjc* or the partial (instead of complete) deletion of *radB* contributed to the suppressor phenotype. By replacing *radA* with *radA-A196V* in H284 (*radA*+ Δ*radB*), a strain from a different strain background to H188, it has been demonstrated that suppression of the Δ*radB* phenotype is equivalent in both strains, indicating that the observed suppression is solely due to *radA-A196V*.

Complete suppression by RadA-A196V

As mentioned, several phenotypes associated with Δ*radB* are completely suppressed by *radA-A196V*. Crossover recombination frequencies at the *bgaHa* locus (pTA159) are restored to H195 frequencies (*radA*+ *radB*+) suggesting that in the presence of the mutant RadA protein, RadB is not required at all for crossover recombination at this locus (Figure 5.8).

UV sensitivity of Δ*radB* is abolished and resistance is restored to H195 levels by *radA-A196V* (Figure 5.6). However, colonies developed significantly slower than expected after irradiation. Although this is partially due to the slower growth rate of H724 (*radA-A196V* Δ*radB*), it could also be due to the repair of UV induced lesions proceeding more slowly in the absence of RadB. I.e., RadA-A196V catalyses the repair of the lesions but perhaps more slowly than in H195 (*radA*+ *radB*+). This could possibly be due to the mutant RadA protein competing with other repair processes such as nucleotide excision repair, the major UV damage repair pathway. Such competition between processes might not occur when wildtype RadA and RadB is present. Alternatively, RadB might function to coordinate the repair of DNA damage by recombination. Recombination is relevant to UV induced lesions, as UV induced nicks in DNA can lead to double strand DNA breaks if encountered by a replication fork which can be repaired through recombination. While RadA-A196V appears to overcome the Δ*radB* phenotype, the repair process might not be efficiently coordinated and thus proceed more slowly, whereas RadB might catalyse the repair of such damage faster The consequence of slower repair would be slower DNA synthesis and cell division, therefore slower colony growth might be expected.

Partial suppression by RadA-A196V

Other phenotypes associated with Δ*radB* are only partially suppressed by RadA-A196V. Growth rates of H724 (*radA-A196V* Δ*radB*) are nearly twice as fast than H284 (*radA*+ Δ*radB*) (3 hours 27 minutes generation time for H724 compared with 6 hour 10 minutes generation

time in H284 (Figure 5.5), indicating that RadA-A196V can partially overcome the slow growth phenotype characteristic of Δ*radB* strains. However, H724 growth rates are significantly slower than H195 (*radA*+ *radB*+) (2 hours 40 minutes generation time).

During recombination, replication forks often stall and sometimes collapse, and can be restarted by homologous recombination in a process called break induced replication (BIR). Thus, RadA-A196V might improve growth rates by increasing the efficiency of replication restart through homologous recombination, which might be much less efficient in H284 (*radA*+ Δ*radB*). Additionally, RadB might possess a secondary role in DNA synthesis independent of recombination that RadA-A196V can not suppress. Alternatively, collapsed replication forks might be restarted effectively by RadA-A196V in the absence of RadB, but restart might proceed slower. The consequence of this would be slower replication and growth rates.

Unlike crossover recombination frequencies at the *bgaHa* locus, crossover and non-crossover recombination frequencies at the *leuB* locus (pTA168) in H724 (*radA-A196V* Δ*radB*) are only partially restored (Figure 5.9). This could be due to locus specific effects such as *bgaHa* potentially being a recombination hotspot, and that recombination at this locus is less dependent on RadB. However, previous results reported in chapter 4 show that RadB appears to have a more significant effect at the *bgaHa* locus. An alternative explanation is that there is less substrate for recombination on pTA168 and that recombination at lower substrate lengths might be more dependent on RadB than recombination at longer substrate lengths, a factor that RadA-A196V might not be able to suppress fully.

Finally, sensitivity to the DNA crosslinking agent, mitomycin C is only partially suppressed by RadA-A196V (Figure 5.10). It is presumed that such suppression occurs through restoration of recombination, therefore crosslinks can be repaired more efficiently. A possible reason for suppression only being partial could be due to the manner in which cells are exposed to mitomycin C. Unlike UV survival assays, where cells are transiently exposed to damage and then allowed to recover, in mitomycin C assays cells are constantly exposed to DNA damaging agents. If H724 (*radA-A196V* Δ*radB*) is slower at repairing lesions than H195 (*radA*+ *radB*+) it would be expected that significantly more cell death would occur if cells are constantly exposed to toxins.

In summary, RadA-A196V appears to suppress many of the phenotypes associated with the deletion of *radB*. As RadA-A196V renders RadB redundant, the question of the effect of having both RadB and RadA-A196V present was raised. Such a strain might be hyper-recombinogenic and/or hyper-resistant to UV damage. Conversely, and more likely, such a combination of both RadB and RadA-A196V might be detrimental to the cell, with more

defective phenotypes than observed in H724 (*radA-A196V* Δ*radB*) . In the following section, the effects of having both RadA-A196V and RadB are analysed, to determine whether such a genotype is detrimental to the cell.

5.2.6 Generation of a *radA-A196V radB*+ strain

Instead of replacing *radA* with *radA-A196V* in H195 (*radA*+ *radB*+), it was decided that an alternative strategy of reintroducing *radB* into H724 (*radA-A196V* Δ*radB*) would be adopted instead. The reason for this is that it is highly probably that a *radA-A196V radB*+ genotype is likely to be significantly slower growing *radA*+ *radB*+. Thus, the chances of obtaining a colony with *radA* replaced with *radA-A196V* would be reduced. Conversely, a *radA-A196V radB*+ strain is more likely to be comparable to *radA-A196V* Δ*radB* strain than a *radA*+ *radB*+ strain, in terms of growth rate. Therefore it would be more likely to obtain a desired colony, than using the previous approach.

H724 (*radA-A196V* Δ*radB*) was transformed with pTA693 (*radB*+ *pyrE2*+) and a *pyrE2*+ integrant transformant was encouraged to recombine the plasmid from the chromosome to leave behind *radB* at the *radB* locus. Details of how this was achieved are in Materials and Methods Section. Following serial propagation for 2 days, cells were plated on media containing 5-FOA to select against cells with the integrated *pyrE2* marked plasmid. Colonies were used for colony PCR analysis. Primers RBXF and RBXR that flank the *radB* locus were used to determine whether *radB* had been reintroduced into the Δ*radB* strain, based on the amplification product size following gel electrophoresis (0.4 kb for Δ*radB* and 1.1 kb for *radB*+). A *radB*+ colony was identified and designated H769 (*radA-A196V* Δ*radB*). Normally, PCR analysis is not deemed sufficiently reliable for confirming strains as smaller amplification products are favoured over larger ones. This would not be a problem in organisms with a single copy of its chromosome. However, *H.volcanii* has multiple copies of its genome per cell, therefore some copies could be *radB*+ and others could be Δ*radB* (meridiploid) Thus, by using PCR in this situation will determine whether all copies of the chromosome contain *radB,* as even one copy of Δ*radB* would be preferentially amplified and therefore easily noticed.

5.2.7 Phenotypic analysis of H769 (*radA-A196V radB*+)

H769 was subjected to the same analyses carried out on previous strains, i.e., Sensitivity to UV irradiation and to the chemical toxin mitomycin C. Other phenotypic features were analysed by determination of growth and cell division rate, crossover recombination frequencies, using pTA159, and non-crossover recombination frequencies, using pTA168.

Results

Growth Rates

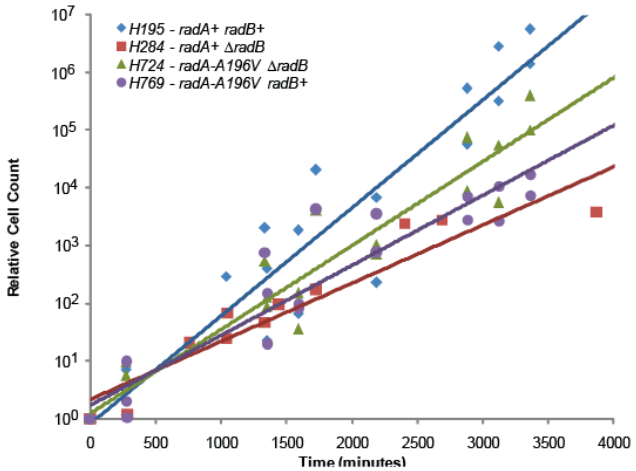

Figure 5.11 Growth rates of H195 (*radB*+ *hjc*+), H284 (Δ*radB hjc*+), H724 (*radA-A196V* ΔradB) and H769 (*radA-A196V radB*+). Cultures were grown continuously at 45°C with rotation (8 rpm) and spotted onto complex media (Hv-YPC) at several time intervals. Relative cell count is calculated as the relative number of cells compared to time = 0 minutes. All data points are a consolidation of data obtained from three trials.

Strain	H195	H284	H724	H769
Generation Time (mins)	160	310	207	248

Table 5.4 Calculated generation times for tested strains H195 (*radA*+ *radB*+), H284 (*radA*+ Δ*radB*), H724 (*radA-A196V* Δ*radB*) and H769 (*radA-A196V radB*+).

RadB is detrimental to growth rates in the presence of RadA-A196V

It has been previously shown in this chapter that H195 (*radA*+ *radB*+) grows at a faster rate than H724 (*radA-A196V* Δ*radB*) and that both of these strains grow at a faster rate than H284 (*radA*+ Δ*radB*) (Figure 5.11 and Table 5.4). Thus, RadA-A196V partially suppresses the slow growth phenotype of Δ*radB*. Figure 5.11, above, shows that the growth rates in strains containing both RadB and RadA-A196V (H769 - *radA-A196V radB*+) are faster than H284 (*radA*+ Δ*radB*) but significantly slower than H195 and H724. This is a clear indication that RadB exerts a negative effect on growth rates when the mutant RadA-A196V protein is present.

UV sensitivity

It has previously been shown that H724 (*radA-A196V* Δ*radB*) exhibits the same survival frequencies as H195 (*radA+ radB+*) following UV irradiation, demonstrating that RadA-A196V compensates for the absence of RadB, in this regard. To determine whether RadB exerts an effect on UV survival frequencies in the presence of RadA-A196V, H769 (*radA-A196V radB+*) was exposed to varying doses of UV irradiation on Hv-YPC + Thy plates and incubated in the dark for 5 days at 45°C.

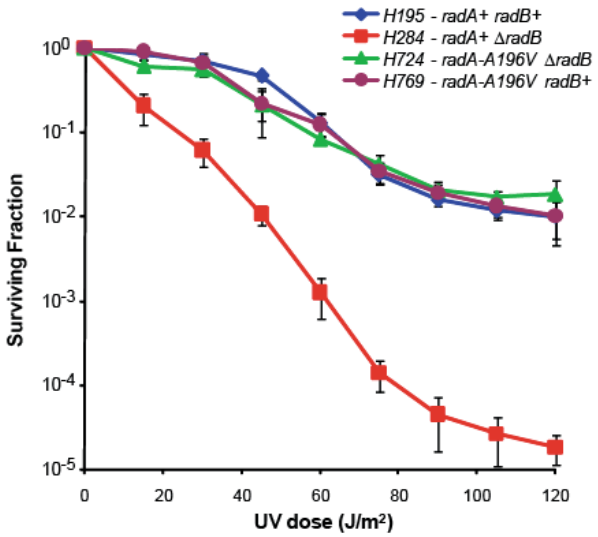

Figure 5.12 Comparison of UV sensitivity of H195 (*radA+ radB+*), H284 (*radA+* Δ*radB*), H724 (*radA-A196V* Δ*radB*) and H769 (*radA-A196V radB+*). All data points are calculated as the mean of at least three trials. Error bars are calculated as standard error.

RadA-A196V restores UV survival to H195 levels regardless of RadB

Figure 5.12 shows that H195 (*radA+, radB+*), H724 (*radA-A196V,* Δ*radB*) and H769 (*radA-A196V, radB+*) display virtually identical phenotypes with regards to survival following UV irradiation. All three strains survive at a higher frequency than H284 (Δ*radB, radA+*). Therefore, regardless of the presence of RadB, strains containing RadA-A196V are as resistant to UV irradiation as H195 (*radA+ radB+*).

Strains with RadA-A196V and RadB might repair UV induced damage slower

It should be noted that although survival following UV irradiation was equal for strains H195 (*radA+ radB+*), H724 (*radA-A196V* Δ*radB*) and H769 (*radA-A196V radB+*), there was a

significant difference in the size of the colonies following five days of incubation at 45˚C. H195 colonies were larger than H724 colonies and H769 colonies. This could either be due to the difference in growth rates between strains and/or because in H724 and H769, the repair of the DNA lesions may be slower and therefore replication and cell growth could be impeded until the less efficient repair process is completed and the lesions removed. The fact that H769 and H724 appear equally slow to recover following UV irradiation suggests that RadB is redundant in the presence of RadA-A196V

Crossover recombination

It has previously been shown that H724 (*radA-A196V* Δ*radB*) exhibits crossover recombination frequencies comparable to H195 (*radA*+ *radB*+), demonstrating that RadA-A196V compensates for the absence of RadB. To determine whether RadB exerts an effect on crossover recombination frequencies in the presence of RadA-A196V, H769 (*radA-A196V radB*+) was transformed with pTA159, containing *pyrE2* and the *bgaHa-Kp* allele with homology to the chromosomal *bgaHa-Bb* locus. Cells that integrate pTA159 at the *bgaHa* locus become ura+ (Figure 4.2 chapter 4).

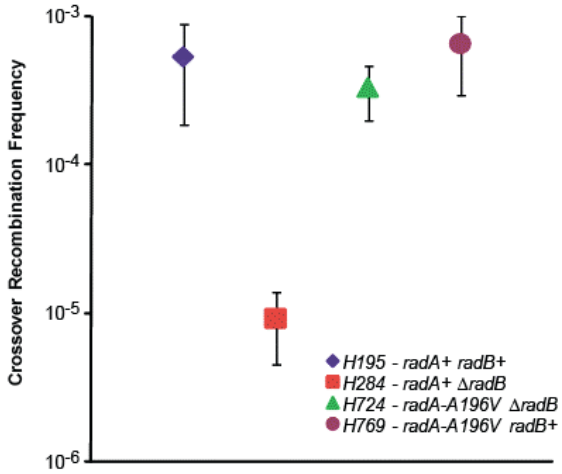

Figure 5.13 Comparison of the crossover recombination frequencies observed in H195 (*radA*+ *radB*+), H284 (*radA*+ Δ*radB*), H724 (*radA-A196V* Δ*radB*) and H769 (*radA-A196V* Δ*radB*) as calculated by the frequency of pTA159 transformed ura+ integrants as a proportion of total viable cells (ura+ and ura-). All data points are calculated as the mean of at least three trials. Error bars are calculated as standard error.

RadA-A196V restores crossover recombination frequencies to H195 levels regardless of RadB

Figure 5.13 shows that H195 (*radA+ radB+*), H724 (*radA-A196V* Δ*radB*) and H769 (*radA-A196V radB+*) share virtually identical frequencies of cross-over recombination. In comparison, H284 (*radA+* Δ*radB*) displaying a greatly reduced frequency. The results suggest that the suppression of the UV sensitivity and recombination defects of a Δ*radB* strain conferred by RadA-A196V is dominant, and will occur regardless of the presence of RadB.

Non-crossover recombination frequencies

It has been shown previously that H724 (*radA-A196V* Δ*radB*) restores non-crossover recombination frequencies to near H195 (*radA+ radB+*) frequencies, demonstrating that RadA-A196V can compensate almost completely for the absence of RadB, in this respect. To determine whether the presence of RadB exerts an effect on the frequency of non-crossover recombination in the presence of RadA-A196V, H769 (*radA-A196V radB+*) was transformed with pTA168, containing *pyrE2* and the *leuB-Aa2* allele with homology to the chromosomal *leuB-Ag1* allele. Crossover recombinants are characterised as those that integrate the plasmid becoming ura+ and leu+ and non-crossover recombinants are those that gene convert the chromosomal *leuB-Ag1* allele, becoming ura- and leu+ (Figure 4.5 chapter 4).

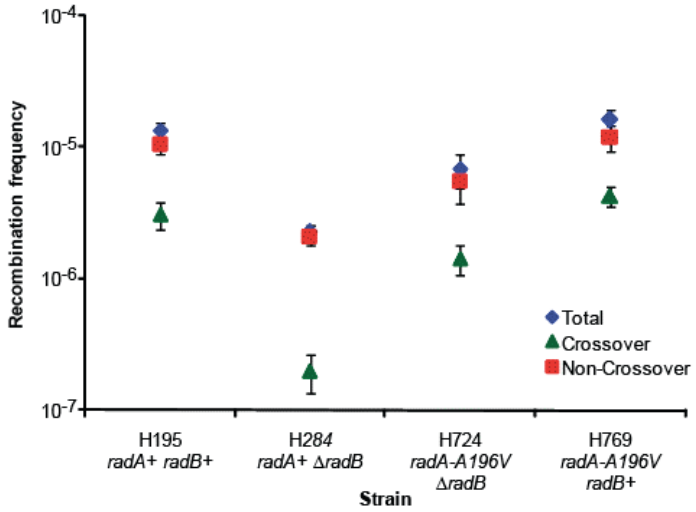

Figure 5.14 Total, crossover and non-crossover (gene conversion) recombination frequencies for strains H195 (*radA+, radB+ hjc+*), H284 (*radA+,* Δ*radB, hjc+*), and H724 (*radA-A196V,* Δ*radB*) and H769 (*radA-A196V radB+*), as assayed by counting leu+ (total), leu+ ura- (non-crossover) and leu+ ura+ (crossover) colonies following transformation with pTA168. All data points are calculated as the mean value of at least three trials. Error bars are calculated as standard error.

Frequency of Recombination	H195 *radA+ radB+*	H284 *radA+* Δ*radB*	H724 *radA-A196V* Δ*radB*	H769 *radA-A196V radB+*
Total	$1.4x10^{-5}$	$2.3x10^{-6}$ (16.7%)	$6.9x10^{-6}$ (50.9%)	$1.6x10^{-5}$ (120%)
Crossover	$3.1x10^{-6}$	$2.0x10^{-7}$ (6.5%)	$1.4x10^{-6}$ (46.6%)	$4.3x10^{-6}$ (139%)
Non-Crossover	$1.0x10^{-5}$	$2.1x10^{-6}$ (19.8%)	$5.5x10^{-6}$ (52.1%)	$1.2x10^{-5}$ (114%)
Crossover/Total	**22.7%**	**8.8%**	**21.3%**	**26.4%**

Table 5.5 Crossover, non-crossover and total recombination frequencies between pTA168 and the chromosomal leuB locus. Percentages in parentheses represent the frequency of the type of recombination compared to the H195 frequency

Recombination frequencies are elevated in the presence of RadB at the leuB *locus*

Figure 5.14 show that non-crossover recombination frequencies appear comparable between H195 (*radA+ radB+*) and H769 (*radA-A196V radB+*), as are crossover recombination frequencies. However, Table 5.5 suggests that both non-crossover and crossover recombination are slightly elevated above H195 levels in H769. Unpaired, one-tailed T-test analysis shows that the differences in recombination frequencies are not significant, however (total recombination p=0.35, crossover recombination p=0.19, non-crossover recombination p=0.49). Both crossover and non-crossover recombination frequencies at the *leuB* locus are significantly higher in H769 (*radA-A196V radB+*) than H724 (*radA-A196V* Δ*radB*) as evidenced by the results of a non-pairwise, one-tailed T-test (Total recombination p=0.007, Crossover recombination p=0.001, Non-crossover recombination p=0.012, i.e. $p<0.05$). This demonstrates that RadB exerts a positive effect on recombination at the *leuB* locus in the presence of RadA-A196V.

In the crossover recombination assay, utilising pTA159, which contains ~3.4 kb of substrate homology with the *bgaHa* chromosomal locus, this significant difference in crossover recombination frequencies between H724 (*radA-A196V* Δ*radB*) and H769 (*radA-A196V radB+*) was not observed (Figure 5.13), nor was the significant difference between H724 and H195 (*radA+ radB+*) in crossover recombination frequencies (Figure 5.8). These differences

in frequencies were only observed when utilising pTA168, with ~0.5 kb of substrate length for recombination to become leu+. This could imply locus specific effects at the *leuB* or *bgaHa* locus. As discussed, *bgaHa* might represent a recombination hotspot, by virtue of it having translocated from pHV4 to the main chromosome. In the laboratory strains used in this study. Such mobility might be due to the new *bgaHa* locus being a recombination hotspot. Recombination might occur more readily with less dependence on RadB, whereas recombination at the *leuB* locus appears to be more dependent on RadB, even if RadA-A196V is present.

Mitomycin C

As demonstrated earlier in this chapter, RadA-A196V can partially suppress the exquisite mitomycin C sensitivity of a Δ*radB* strain (H724 – *radA-A196V* ΔradB) To determine whether RadB would exert a phenotypic effect in the presence of RadA-A196V, H769 (*radA-A196V radB*+) was exposed to mitomycin C present in agar plates at varying concentrations and incubated for 5 days at 45°C.

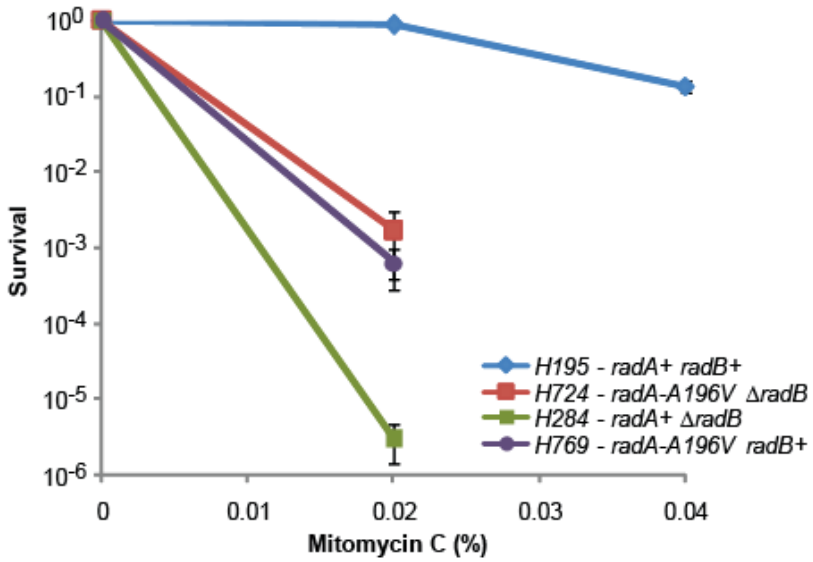

Figure 5.15 Survival of H195 (*radA*+ *radB*+), H724 (*radA-A196V* Δ*radB*), H284 (*radA*+ Δ*radB*) and H769 (*radA-A196V radB*+) following exposure to varying concentrations of mitomycin C, present in agar plates. Only relevant genotypes are shown. Data points are calculated as the mean value of three trials. Error bars are calculated as standard error

RadA suppresses mitomycin C sensitivity regardless of RadB

Figure 5.15 shows that, regardless of the presence of RadB, resistance to mitomycin C is equivalent in both H724 (*radA-A196V* Δ*radB*) and H769 (*radA-A196V radB*+). This suggests that RadA-A196V does in fact suppress the mitomycin C sensitivity phenotype associated with Δ*radB* completely, but that RadA-A196V itself is less effective at repair than wildtype RadA. This also shows that RadB function is made redundant by the presence of RadA-A196V as H769 sensitivity is not restore to H195 levels.

Summary

The data described in this section demonstrate that it is more beneficial for a *radA-A196V* strain of *Haloferax volcanii* to also be Δ*radB* rather than *radB*+. The most significant observed differences between the two strains H724 (*radA-A196V* Δ*radB*) and H769 (*radA-A196V radB*+) is that H724 grows faster. Therefore, the presence of RadB in a strain expressing RadA-A196V has a detrimental effect on its growth phenotype. Furthermore, the very slow growth phenotype following UV irradiation of H724 is accentuated in H769, suggesting that repair of lesions may be slower if both RadA-A196V and RadB are present. Thus, RadA and RadB act in concert to bring about the rapid repair of these lesions.

RadA residue alanine-196 is highly conserved.

A multiple sequence alignment of *radA* sequences from other archaea was carried out. Additionally, *rad51* and *recA* sequences from various eukaryotes and bacteria were aligned. The purpose of this multiple sequence alignment was to determine the level of conservation of alanine-196 and whether conservation extends to other domains of life:

Conserved residues and domains are suggestive of an importance in the proteins function, therefore if the alanine residue is conserved, it would indicate that the residue is important for the function of the protein and that any substitution may alter the functionality of RadA *in vivo* and potentially cause suppression of the Δ*radB* phenotype in *Haloferax volcanii*. *radA* sequences from both the euryarchaeota and the crenarchaeota were used for the alignment. ClustalW was utilised and *radA, rad51 and recA* sequences were obtained from the National Center for Biotechnology Information (NCBI) website (www.ncbi.nlm.nih.gov). Protein accession numbers are listed and the results of this alignment are displayed in Figure 5.16.

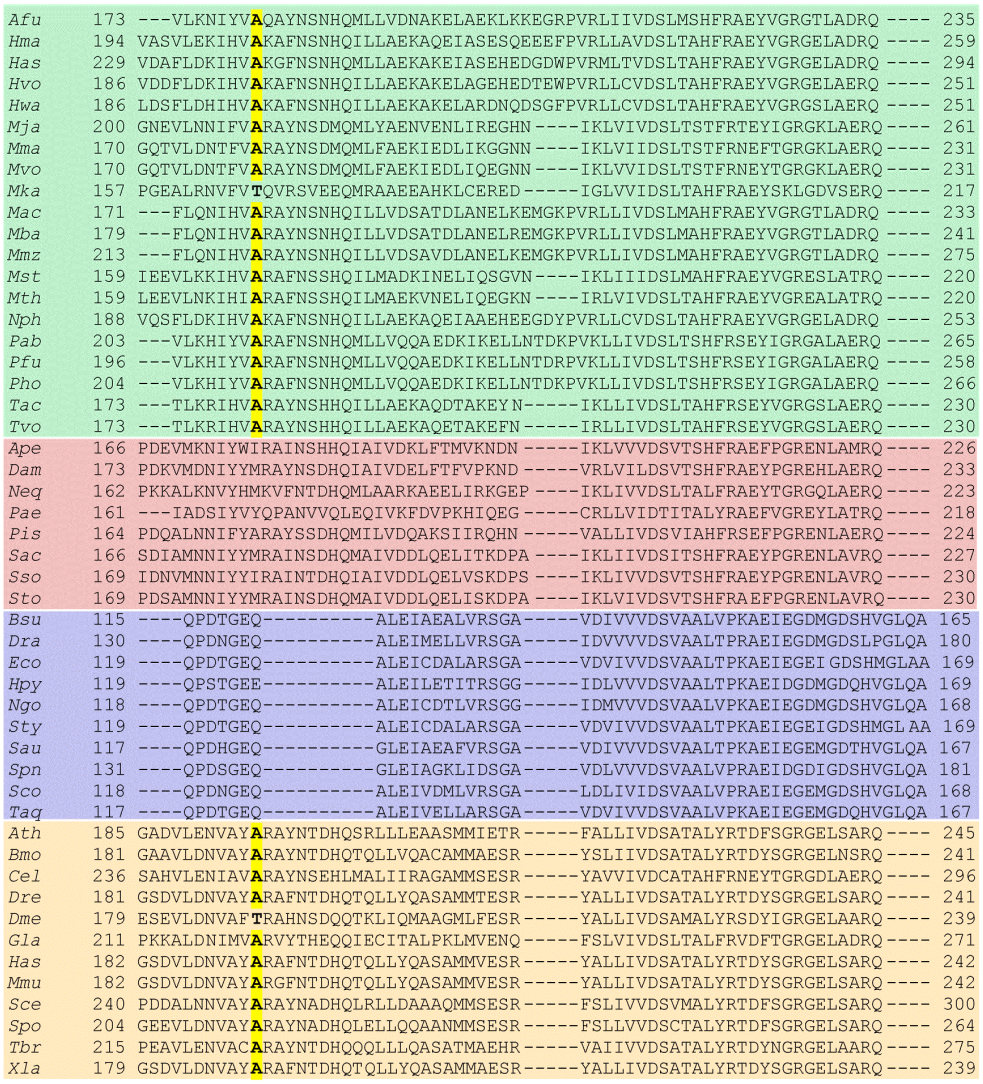

Figure 5.16 Multiple sequence alignment of recombinases RadA, RecA and Rad51 from eury/nano/crenarchaea, bacteria and eukaryotes, respectively. Euryarchaea are highlighted in green, crenarchaea and nanoarchaea in red, bacteria in blue and eukaryotes in orange. Conservation of *Hvo*-RadA-A196 is highlighted in yellow.

Euryarchaeal RadA: *Archaeoglobus fulgidus* (NP_069826), *Haloarcula marismortui* (YP_137357), *Halobacterium salinarum* (AAD16062), *Haloferax volcanii* (Q48328), *Haloquadratum walsbyi* (CAJ53526), *Methanocaldococcus jannaschii* (AAC44122), *Methanococcus maripaludis* (AAL26913), *Methanococcus voltae* (AAC23499), *Methanopyrus kandleri* (NP_614725), *Methanosarcina acetivorans* (NP_618427), *Methanosarcina barkeri* (YP_305841), *Methanosarcina mazei* (Q8PZN5), *Methanosphaera stadtmanae* (YP_448501), *Methanothermobacter thermautotrophicus* (O27436), *Natronomonas pharaonis* (YP_326099), *Pyrococcus abyssi* (NP_125934), *Pyrococcus furiosus* (O74036), *Pyrococcus horikoshii* (NP_142255), *Thermoplasma acidophilum* (NP_394563), *Thermoplasma volcanium* (NP_110976). **Nanoarchaeal RadA:** *Nanoarchaeum equitans* (NP_963710). **Crenarchaeal RadA:** *Aeropyrum pernix* (NP_146978), *Desulfurococcus amylolyticus* (AAD33955), *Pyrobaculum aerophilum* (AAL73354), *Pyrobaculum islandicum* (BAA88984), *Sulfolobus acidocaldarius* (AAD16074), *Sulfolobus solfataricus* (NP_341799), *Sulfolobus tokodaii* (NP_376158)**. Bacterial RecA:** *Bacillus subtilis* (AAB47709), *Deinococcus radiodurans* (BAA21330), *Escherichia coli* (AAQ91336), *Helicobacter pylori* (AAG16545), *Neisseria gonorrhoeae* (AAB49193), *Salmonella enterica* (ABG34230), *Staphylococcus aureus* (AAK15276), *Streptococcus pneumoniae* (CAA78955), *Streptomyces coelicolor* (CAA15875), *Thermus aquaticus* (ABS00959). **Eukaryotic Rad51:** *Arabidopsis thaliana* (CAA04529), *Bombyx mori* (NP_001037484), *Caenorhabditis elegans* (AAD10194), *Danio rerio* (NP_998371), *Drosophila melanogaster* (BAA04580), *Giardia lamblia* (XP_779349), *Homo sapiens* (BAA03189), *Mus musculus* (BAA02718), *Saccharomyces cerevisiae* (CAA45563), *Schizosaccharomyces pombe* (P36601), *Trypanosoma brucei* (AAD51713), *Xenopus laevis* (NP_001080559)

Hvo-*RadA-A196 is highly conserved in the euryarchaeota and eukaryotic Rad51*

The alignment of RadA/RecA/Rad51 sequences (Figure 5.16) shows clearly that the alanine residue mutated in the *srbA* strain H188, is highly conserved throughout the euryarchaeota, suggesting an importance of the residue for RadA function.

Interestingly, this residue is also conserved in all eukaryotic Rad51 sequences used for the multiple sequence alignment, except for in *Drosophila melanogaster* Rad51 (*Dme*-Rad51). RadA and Rad51 are very similar proteins in terms of structural and functional domains (Sandler et al., 1999; Shin et al., 2003), therefore such conservation of this alanine residue could suggest a functional important in both euryarchaeota and eukaryotes.

Hvo-RadA-A196 is not conserved in the crenarchaeota or bacteria

As illustrated in Figure 5.16, the alanine at position 196 of *Haloferax volcanii* RadA is not conserved in the bacterial RecA. While both Walker A and Walker B motifs of the recombinase proteins (RadA, Rad51 and RecA) share high conservation, RadA and Rad51 contain long N-terminal domains that share homology with each other, but no such domain is present in RecA. Conversely, RecA has a long C-terminal domain, not present in either Rad51 or RadA. Therefore, this lack of conservation of the alanine residue is not especially surprising given the pattern of conservation between RadA/Rad51 and RecA.

More surprisingly is that the alanine at position 196 of *Haloferax volcanii* RadA is not conserved in the crenarchaeota. While nearby residues show good conservation, no such conservation is observed at the position of this alanine, suggesting a functional/structural difference between euryarchaeal and crenarchaeal RadA.

Hvo-RadA-A196 could be important in organisms with recombinase paralogues.

The absence of this alanine residue from bacteria and especially crenarchaeotes and its high conservation in both eukaryotes and euryarchaeotes implies a functional similarity between euryarchaeal RadA and eukaryotic Rad51. This correlates with the presence of Rad51/RadA paralogues. Eukaryotes have a large number of Rad51 paralogues that are implicated in HR. Euryarchaea contain a single RadA paralogue, RadB, but this is not present in crenarchaeotes. Both eukaryotes and euryarchaeotes have the conserved alanine residue present in their respective recombinases, whereas species lacking recombinase paralogues, i.e. bacteria and crenarchaeotes, do not possess the conserved alanine residue. It is therefore possible that this conserved residue is important in species that require paralogous proteins for efficient recombination, hence the absence of the residue in crenarchaeota that may have different

requirements for efficient homologous recombination. Furthermore, *Methanopyrus kandleri* does not have the conserved alanine residue, despite being a euryarchaeote. However, unlike other euryarchaeotes, this organism also does not encode RadB

5.2.8 Rationale for the suppression of the Δ*radB* phenotype by *radA-A196V*

To further analyse the potential importance of this conserved alanine residue and its mutation to a valine residue, the crystal structure of RadA was analysed using MacPyMOL to determine the location of the residue in the protein.

At present, the crystal structure of *Haloferax volcanii* RadA (*Hvo*RadA) has not been solved. For this reason, the structure of the euryarchaeal hyperthermophile *Pyrococcus furiosus* (*Pfu*) was analysed instead. Although the crystal structure of *Sulfolobus solfataricus* RadA has been solved (Ariza et al., 2005), it was not used for this analysis due to the absence of the conserved alanine residue, present in virtually all euryarchaeal RadA proteins. The *Pfu*-RadA sequence was obtained from the Research Collaboratory for Structural Bioinformatics Protein Data Bank (http://www.rcsb.org/pdb/) with accession number 1PZN (Shin et al., 2003). Figure 5.17 shows two interacting *Pfu*-RadA proteins.

Suppression of ΔradB *results from mutation of a RadA polymerisation domain*

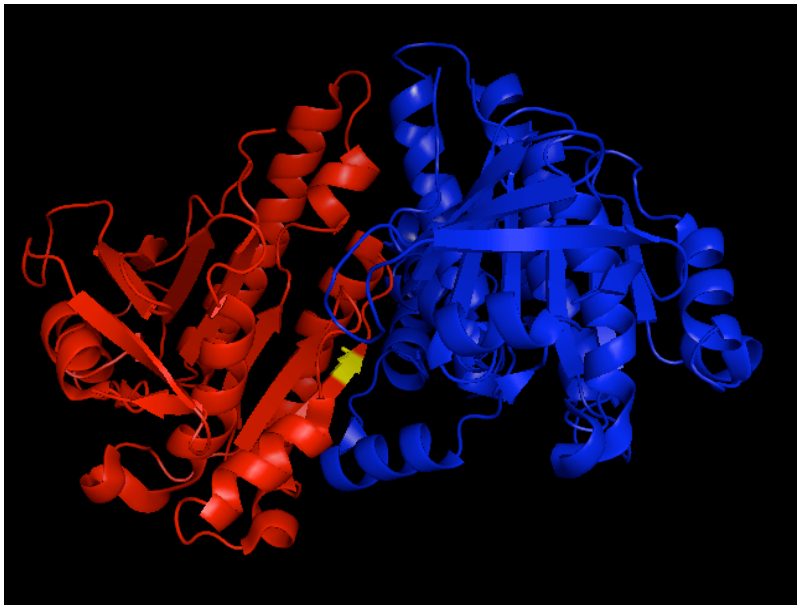

Figure 5.17 Two *Pfu*-RadA interacting monomers, coloured blue and red. Alanine-203 is coloured yellow, the equivalent of the conserved alanine-196 in *Haloferax volcanii* RadA.

Figure 5.17 shows a dimer of two interacting *Pfu*- RadA monomers and the positioning of the equivalent residue of *Hvo*-RadA alanine-196, alanine-203 (shown in yellow). From the model, it is clear that this conserved alanine is at, or close to, the interface between monomers suggesting that it could be important for RadA polymerisation and consequently, efficient nucleoprotein filament formation. The crystal structure of *Pfu*-RadA was solved by Shin *et al.* (Shin et al., 2003) and based on this structure, they proposed key residues that are important for RadA monomer interactions and consequently, RadA filament formation. This interaction relies on a socket comprising seven key hydrophobic residues on one monomer and an invariant hydrophobic phenylalanine (Phe-97 in *Pfu*-RadA) of a neighbouring monomer that slots into the hydrophobic socket. The seven residues that are implicated in the formation of this hydrophobic socket in *Pfu*-RadA are Ile-169, Ile-171, Tyr-201, Ala-203, Leu-214, Ala-218 and Lys-221 (Figure 5.18). As *Pfu*-RadA-Ala-203 is equivalent to *Hvo*-RadA-Ala-196, this shows that the mutation present in RadA-A196V is located in this hydrophobic socket. Work presented here on the RadA-A196V suppressor mutant shows that mutation of this hydrophobic socket in *Hvo*-RadA suppresses the requirement for RadB *in vivo*.

5.2.9 Conservation of RadA/Rad51 polymerisation motif

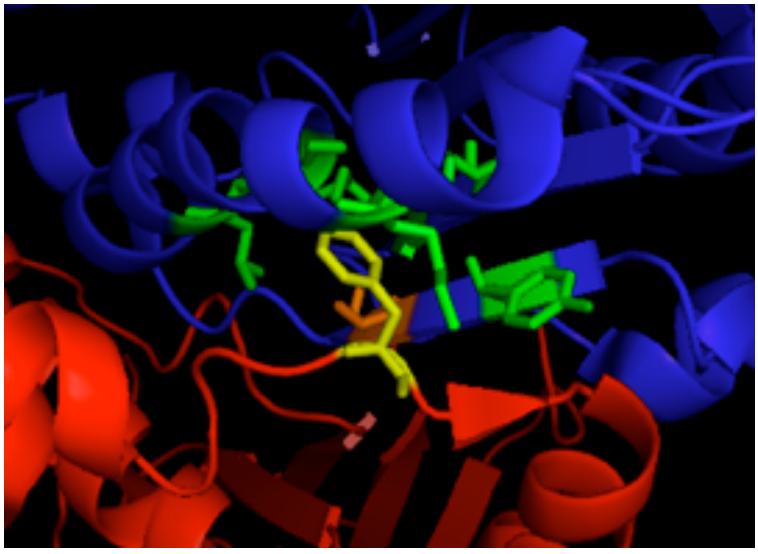

Figure 5.18 Polymerisation motifs of two *Pfu*-RadA monomers as described by Shin *et al* (2003). One polymerisation motif is an invariant phenylalanine residue, shown in yellow, that slots into the second polymerisation motif, a hydrophobic socket, of a neighbouring RadA monomer. The residues important for the function of the hydrophobic socket (Ile-169, Ile-171, Tyr-201, Leu-214, Ala-203, Ala-218, Lys-221) are coloured green except for Ala-203 that is coloured orange. Ala-203 is the equivalent residue to Ala-196 of *Hvo*-RadA.

Shin *et al* (2003) found that the RadA polymerisation motif is also present in eukaryotic Rad51 indicating a common mechanism of interaction for both RadA and Rad51. Earlier in this chapter, it was shown that *Hvo*-RadA-Ala196 (*Pfu*-RadA-Ala203) is highly conserved throughout euryarchaeal RadA and eukaryotic Rad51, but not in crenarchaeal RadA (Figure 5.16). If other socket residues are not conserved, this could suggest that RadA polymerisation occurs through a different mechanism in the crenarchaeota. To determine whether this is true, and whether the hydrophobic socket is conserved in *H. volcanii*, residues implicated in the hydrophobic socket of RadA from euryarchaeal and crenarchaeal species in the previous sequence alignment (Figure 5.16) were examined (Figure 5.19).

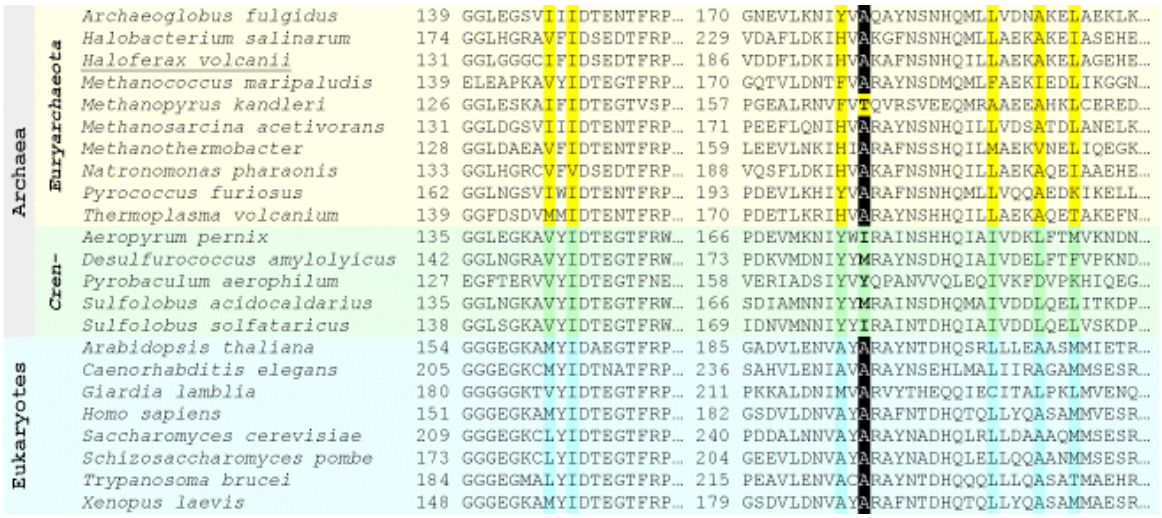

Figure 5.19 Alignment of key residues implicated in the functionality of the hydrophobic socket of RadA and Rad51. Key residues are highlighted and the conserved alanine residue mutated in *Hvo*-RadA-A196V is in bold.

The RadA polymerisation motif is conserved in archaea and eukaryotes

Figure 5.19 shows that the general structure of the hydrophobic socket implicated in RadA/Rad51 polymerisation is conserved in *Haloferax volcanii* and in crenarchaea, with the exception of the highly conserved alanine residue of euryarchaeal RadA proteins. Although residues in this socket are less well conserved than the near invariant alanine residue mutated in RadA-A196V, substitutions tend to be conservative with most residues being hydrophobic. This suggests a common mechanism of RadA polymerisation in all archaea, despite the absence of the near invariant alanine residue in the crenarchaea. As discussed previously, crenarchaea do not encode RadB, or RadA paralogues, with the exception of *Sulfolobus solfataricus* that encodes a single RadA paralogue. Organisms that possess RadA/Rad51 paralogues all possess this conserved alanine residue whereas those that don't encode paralogues do not possess this

residue. This might suggest a role for recombinase paralogues, e.g. RadB in the modulation of RadA polymerisation. This correlation is reinforced by *Methanopyrus kandleri* not encoding RadB and *Mka*-RadA not containing the conserved alanine in its hydrophobic socket.

5.2.10 Consequences of RadA-A196V mutation

It has been shown that a mutation in the RadA polymerisation motif suppresses the Δ*radB* phenotype in *H.volcanii*. As yet, it is uncertain as to how this mutation could result in greater resistance to DNA damage, faster growth rates and elevated frequencies of recombination in the absence of RadB. In this section, ideas of how suppression might arise are discussed

Hydrophobicity

One possible consequence of the alanine to valine mutation in *Hvo*-RadA could be that the hydrophobicity of the socket, formed by the seven residues suggested by Shin *et al* 2003, increases. This increase in hydrophobicity might result in stronger RadA monomer:monomer interactions and an increase in the stability of RadA nucleoprotein filaments on ssDNA or a higher binding affinity for DNA. This idea is discussed later in this section.

While alanine itself is a hydrophobic amino acid, valine is more hydrophobic and due to the similar size of the two residues, valine would be a prime candidate to substitute for an alanine. Valine is identical to alanine bar an additional methyl group thus disruptions to the hydrophobic socket are less likely to occur, while still increasing the hydrophobicity of the socket itself. (Figure 5.20)

To model the effects of the valine to alanine mutation on hydrophobicity, predicted hydrophobicity plots for the seven residues contained within the socket of RadA were

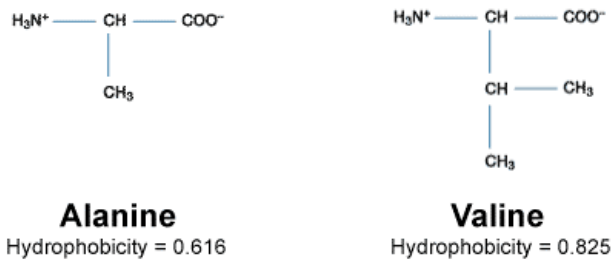

Figure 5.20 Comparison of alanine and valine, with hydrophobicity values. The hydrophobicities given are derived from values from computational *log(P)* determinations by the "Small Fragment Approach" (Black and Mould, 1991)

generated using residues from various eurarchaeal and crenarchaeal RadA proteins, and eukaryotic Rad51. RecA was omitted from these analyses because the hydrophobic socket is not conserved in bacteria (Figure 5.16). The plots were calculated on MacVector with the Sweet/Eisenberg scale and a window size of 3. (Figure5.21)

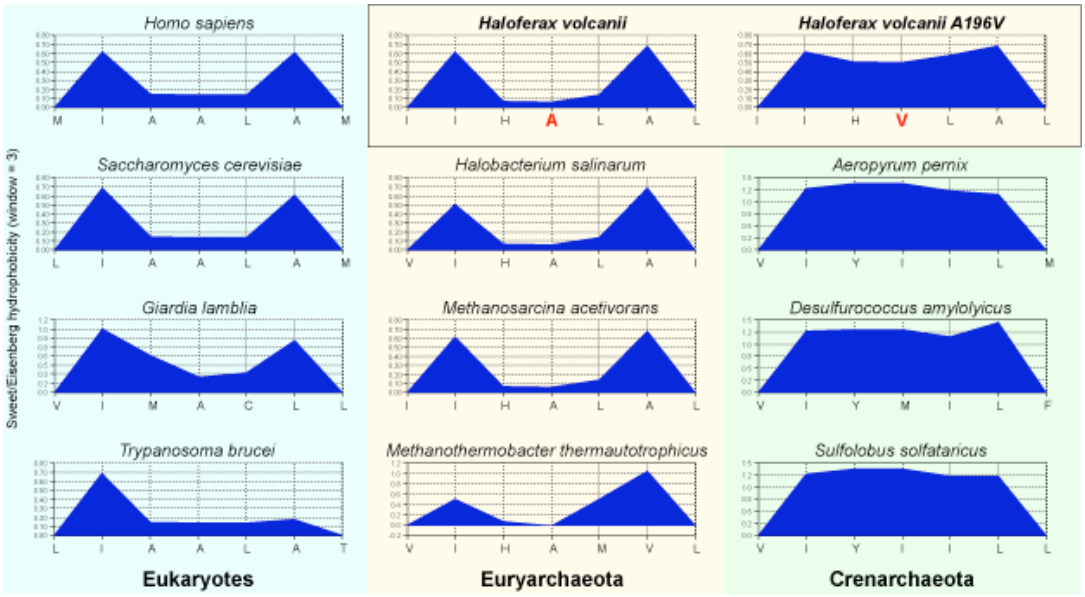

Figure 5.21 Sweet/Eisenberg predicted hydrophobicity plots of key residues of the hydrophobic socket of euryarchaeal and crenarchaeal RadA and eukaryotic Rad51. The predicted hydrophobicity plot for *Hvo*-RadA-A196V is displayed in the top-right of the figure. Plots for *Mka*-RadA and *Pfu*-RadA are displayed at the base of the figure.

Predicted hydrophobicity differs between crenarchaea and euryarchaea

The hydrophobicity plots in Figure 5.21 above show a significant difference in predicted hydrophobicity of crenarchaeal and euryarchaeal RadA sockets. Euryarchaeal proteins are predicted to show two distinct peaks of hydrophobicity whereas crenarchaeal RadAs appear to be more uniformly hydrophobic. Interestingly, the hydrophobicity of the Rad51 socket appears to be of the same pattern as that observed in euryarchaeal RadA.

RadA-A196V socket is more hydrophobic than RadA socket

Figure 5.21 shows that the mutation of *Hvo*-Ala-196 to Val-196 (RadA-A196V) increases the hydrophobicity of the socket implicated in RadA polymerisation, as predicted. Such an increase in hydrophobicity might lead to stronger RadA monomer:monomer interactions involving hydrophobic socket and phenylalanine peg. If true, the consequences of this could be that RadA nucleoprotein filaments form more readily *in vivo*. As RadA-A196V suppresses the Δ*radB* phenotype, this suggests that RadB might act to promote or enhance RadA filament formation *in vivo*. This concept is discussed further later in this section.

RadA-A196V exhibits hydrophobicity similar to crenarchaeal RadA

The plot of *Hvo*-RadA-A196V (Figure 5.21- top right) shows that upon mutation of the alanine-196 to a valine residue, the hydrophobicity plot changes significantly no longer resembling a typical euryarchaeal RadA-socket or Rad51-socket plot and instead being much more similar to crenarchaeal RadA. This observation further reinforces the hypothesis that the conservation of Ala-196 of *Hvo*-RadA and the equivalent residues in other archaeal and eukaryotic recombinases might depend on whether the species has RadA/Rad51 paralogues. In the absence of RadB, strains of *Haloferax volcanii* show a great reduction in recombination frequencies, growth rate and survival following UV irradiation. If the RadA present in these strains is mutated to be 'crenarchaeal', by mutation of the conserved alanine-196 with a valine residue causing a change in hydrophobicity of one of its interaction domains, the strain appears to be independent of the presence of RadB - growth rates and mitomycin C sensitivity are partially complemented and UV damage repair and recombinational defects appear to be almost fully suppressed. In fact, the presence of RadB in strains expressing *radA-A196V* leads to a more severe phenotype than if RadB was not present at all.

Structural alterations

RadA-A196V might have a structurally different hydrophobic socket

An alternative explanation for how the substitution of the near invariant alanine residue in the hydrophobic socket of RadA with a valine residue could lead to suppression of the Δ*radB* phenotype could be due to structural, as opposed to hydrophobicity changes in the socket. While an alanine to valine substitution is conservative, it is conceivable that the methyl side chain of a valine residue could alter the conformation of the socket. Such a change is unlikely to obstruct the entry of the phenylalanine residue of a neighbouring RadA monomer, as evidenced by RadA-A196V being recombinogenic and therefore able to form filaments. Furthermore, residues at this position in crenarchaeal RadA are larger than valine (e.g.

methionine or isoleucine) and the presence of these amino acids does not disrupt monomer:monomer interactions. However, it is possible that the alanine to valine substitution might alter the angle at which the phenylalanine residue enters the socket. A change such as this might lead to more rigid filaments being formed on ssDNA *in vivo*. A further consequence of more rigid RadA filaments might be that disassembly of filaments following recombination is less efficient. This might be the cause of the partial suppression of Δ*radB* slow growth rates, rather than complete suppression. RadB might act to mediate RadA:RadA interactions, possibly by inducing conformational changes in RadA that lead to alterations in the structure of the socket. RadA-A196V might already be primed for filament formation due to a structural alteration of the socket, hence RadB is not required, or to a lesser extent.

RadA-A196V might have structural differences outside the hydrophobic socket

Alternatively, instead of the structure of the socket being altered, it is possible that a protein-wide structural alteration may be observed in RadA-A196V. RadA might exist in an inactive form when not required and become activated when needed. RadA-A196V might already be in an active form and therefore might not need activation. If this is true, it is conceivable that RadB could be required for RadA activation. In the absence of RadB, recombination defects, slow growth and DNA damage sensitivity are exhibited. In the absence of RadB but in the presence of RadA-A196V, these phenotypes are largely suppressed, therefore RadB might act to activate RadA, via structural changes in the latter.

5.3 Discussion

A suppressor of the DNA repair, recombination and growth defect phenotypes associated with a Δ*radB* strain of *Haloferax volcanii* has been identified and characterised. The suppressor was identified as a point mutation in the coding sequence of *radA* causing a residue change from an alanine to a valine at position 196 of the protein. It has also been demonstrated that in many respects, RadA-A196V is a dominant suppressor - whether or not the strain containing the mutant protein is Δ*radB* or *radB*+ the observed DNA repair and recombination phenotypes appear the same. The exceptions to this are that growth rates of *radA-A196V* Δ*radB* are faster than *radA-A196V radB*+ strains, and that recombination frequencies are elevated in *radA-A196V radB*+ strains when compared to *radA-A196V* Δ*radB* strains.

Alanine-196 (Ala-196) of *Hvo*-RadA is highly conserved throughout the euryarchaea and eukaryotic (Rad51) recombinases, but absent from bacterial RecA and crenarchaeal RadA (Figure 5.16). The significance of this could be attributed to the presence of RecA/Rad51/RadA paralogues. To date, no paralogues of RadA have been documented in any crenarchaeal species, with the exception of a non-RadB paralogue in *Sulfolobus solfataricus* - RadB is exclusive to the euryarchaea. Conversely, a number of Rad51 paralogues exist in eukaryotes but their functions are, in general, not well understood. Euryarchaeal species contain one known paralogue of RadA - RadB. These observations correlate with the presence or absence of the conserved alanine residue that is mutated in RadA-A196V: Species that have one or more paralogues of their respective recombinase also have the conserved alanine residue (with the exception of *Sulfolobus solfataricus*) whereas organisms lacking paralogues also lack the conserved residue. This correlation includes *Methanopyrus kandleri,* which does not encode RadB, or possess the conserved alanine residue in its RadA. Both RadA and Rad51 have been shown to interact with their respective paralogues therefore it is possible that this residue is important for recombinase-paralogue interactions, whether physical and/or functional.

The alanine to valine mutation in *Hvo*-RadA was mapped to the equivalent residue in *Pyrococcus furiosus* RadA (*Pfu*-RadA), which has a solved crystal structure (Shin et al., 2003).Ala-196 of *Hvo* is equivalent to Ala-203 of *Pfu*-RadA. The crystal structure of *Pfu*-RadA was then analysed using MacPyMOL. The residue is solvent exposed (Figure 5.18) and within a 'socket' on the surface of RadA. Shin *et al* (Shin et al., 2003), report a number of hydrophobic residues comprise this socket, namely Ile-169, Ile-171, Tyr-201, Leu-214, Ala-218, Lys-221 and Ala-203, the residue responsible for Δ*radB* phenotype suppression in *Haloferax volcanii*. (Figure 5.18) This socket is responsible for RadA monomer-monomer

interaction - a highly conserved, solvent exposed phenylalanine residue (residue 97 in *Pfu*-RadA) of RadA fits into the hydrophobic socket.

The residues that form the hydrophobic socket are conserved throughout all euryarchaeal, crenarchaeal and eukaryotic recombinases. Where a residue is not identical, a similar, hydrophobic residue tends to be present, for example, isoleucine and leucine. This strongly suggests that the same basic mechanism of RadA interface interaction exists in all eukaryotes and archaea. (Figure 5.19). Suggestions of how RadA-A196V suppresses the Δ*radB* phenotype have been briefly discussed and will be discussed further in the following section.

RadB is not a recombinase

Δ*radB* strains of *Haloferax volcanii* can recombine but cannot do so efficiently unless suppressed by encoding *radA-A196V*. One possible conclusion to draw from such a phenotype would be that RadB is a recombinase and that RadA and RadB function on different recombination substrates. In the absence of RadB, RadA cannot compensate unless it is the mutant form of the protein, RadA-A196V. However, *in vitro* strand-exchange assays show that RadB possesses no strand-exchange activity, nor does it hydrolyse ATP at the rate expected of previously identified recombinases (Komori et al., 2000b). However, the purified RadB protein used for these biochemical assays was over-expressed in *E.coli* and not natively from *Pyrococcus furiosus*, therefore any post-translational modification of the protein would be absent and could reduce or abolish some or all of RadB's catalytic activities. Despite this possibility, RadB is a smaller protein than RadA, lacking both N- and C- terminal domains, suggesting that it is unlikely to be a genuine recombinase. Additionally, reported intracellular levels of RadB are two hundred-fold lower than RadA (Komori et al., 2000b; Reich et al., 2001), therefore it is likely that RadB possesses a mediator role rather than one as a strand exchange protein.

RadB might be a RadA mediator protein

The Δ*radB* phenotype implies that RadB might be necessary to assist and regulate RadA filament formation on ssDNA, and in its absence, recombination proceeds much less efficiently. From the crossover recombination data presented here and data obtained by Woods *et al* (Woods and Dyall-Smith, 1997), it is evident that RadA is essential for recombination to proceed, while RadB has an important role in recombination, but not essential.

If RadB acts to regulate RadA activity and/or facilitate RadA filament formation, and RadA-A196V does not require RadB activity to function efficiently, this would explain several of the observed phenotypes of H724 (*radA-A196V* Δ*radB*). Recombination frequencies in this strain

are restored to near H195 (*radA+ radB+*) frequencies, consistent with RadA-A196V being capable of forming nucleoprotein filaments without RadB. In turn, this would restore UV survival levels to H195 levels also as they could be repaired by recombination.

Growth rates could be slower in the *radA-A196V* mutant, because RadB might possess a secondary role in replication that RadA-A196V can not suppress. Alternatively, if RadB is required to control RadA filament formation and RadA-A196V overcomes this requirement for RadB, the mutant RadA protein might form nucleoprotein filaments aberrantly, thus interfering with other DNA metabolic processes such as replication and transcription. It is also possible that disassembly of mutant RadA filaments might proceed more slowly. This in turn could slow down cell division and growth rates. It is notable that H769 (*radA-A196V radB+*) has a slower growth rate than H724 (*radA-A196V* Δ*radB*). RadB might function to recruit RadA to regions where it is required. However, as RadA-A196V appears to suppress the requirement for RadB, making it redundant, RadB might not be able to recruit the mutant protein and may remain bound to DNA, further interfering with DNA metabolic processes.

The importance of mediator proteins

In bacteria and eukaryotes, RecA/Rad51 nucleoprotein filament assembly does not occur readily without the presence of mediator proteins, which act to load the recombinase onto the DNA substrate. This is required due to the presence of other proteins that prevent access of Rad51/RecA to DNA. Both SSB (Single Strand Binding protein) and RPA (Replication Protein A), from bacteria and eukaryotes respectively, are examples of such proteins and coat naked ssDNA. They are referred to as single strand binding proteins (ssbs). Both SSB and RPA interact with a range of proteins involved in DNA repair, replication and recombination, including RecA and Rad51, respectively. Both ssbs have a higher binding affinity to ssDNA than their respective recombinases and compete for DNA binding, meaning that additional mechanisms are necessary to remove SSB/RPA from the DNA before the recombinase can bind *in vivo*.

Paradoxically, ssbs stimulate the assembly of nucleoprotein filaments on ssDNA as well as prevent it. This stimulation activity is consistent with a role in the removal of secondary structures from ssDNA permitting the assembly of contiguous RecA/Rad51 nucleoprotein filaments. Secondary structures in ssDNA have been demonstrated to inhibit the growth of Rad51/RecA filaments, and single strand binding proteins act to hold the DNA in a conformation more accessible to recombinases. However, as mentioned, once SSB or RPA are DNA-bound, RecA/Rad51 is not able to bind. Inhibition of filament formation by ssbs must be overcome through the activities of mediator proteins.

Mediator proteins from bacteria and eukaryotes

In *E.coli*, DNA ends are processed by RecBCD, which then loads RecA onto the single stranded DNA. Specifically, it has been proposed that the 30kDa C-Terminal domain of RecB is responsible for the loading of RecA (Arnold and Kowalczykowski, 2000; Churchill and Kowalczykowski, 2000). In *recBC* strains of *E.coli*, RecA can still be loaded to single stranded regions but only when facilitated by RecFOR. RecO binds the single stranded DNA coated with SSB, implying a specific protein:protein interaction between the two. RecF and RecR are then required for efficient presynaptic complex formation at single stranded/double stranded DNA junctions.

In eukaryotes, a similar process exists whereby Rad51 is not able to efficiently load itself onto RPA-bound ss-DNA. Rad52 and Rad55/57 are both required to promote Rad51 assembly during meiosis, and either Rad52 or Rad55/57 alone are sufficient to promote filament assembly following cell irradiation (Gasior et al., 2001). Rad52 functions in a similar manner to RecO, binding RPA coated ss-DNA. Rad52 also binds Rad51 and RPA, and by displacing the latter, it can then load the recombinase onto the naked single-stranded DNA. Rad55/57 possesses similar activities to Rad52 yet the two complexes are very different. Rad55 and Rad57 share homology with Rad51 whereas Rad52 does not. Additionally, Rad55/57 forms a heterodimer (Sung, 1997b) whereas Rad52 forms heptameric rings (Stasiak et al., 2000).

Archaeal ssb's and recombination mediator proteins

A conserved homologue of the RPA gene exists in all sequenced archaeal genomes and like eukaryotic RPA, the *Pyrococcus furiosus* protein forms a hetero-oligomeric complex consisting of three subunits (RPA41, RPA14 and RPA32) and has a high affinity for ssDNA (Komori and Ishino, 2001). In addition to these features, it has also been shown to interact with RadA and Hjc, as well as replication proteins such as DNA polymerases, primase and PCNA, all characteristic of RPA (Komori and Ishino, 2001). It is likely that archaeal RPA would also need to be displaced from single stranded DNA before efficient presynaptic complex formation can occur. It is therefore possible that RadB fulfils this role.

1) RadB might displace RPA

RadB might displace RPA by binding to DNA

The binding affinity of RadB to DNA is higher than that for RadA (Komori et al., 2000b), therefore it is possible that RadB directly competes with RPA binding to ssDNA. This could occur either by binding DNA before RPA or by binding DNA that is coated in RPA then

displacing the latter, allowing RadA to be recruited to the naked ssDNA through a subsequent or prior RadB:RadA interaction. Eukaryotic Rad52, but not bacterial RecO, is capable of binding DNA substrates that are already coated with RPA (Gasior et al., 2001), therefore it is feasible that RadB may possess a similar activity.

Due to the low protein concentrations of RadB *in vivo,* this displacement of RPA by RadB might occur in a stepwise reaction rather than by an 'all at once' approach: Upon successful binding of ssDNA and displacement of RPA, RadB then recruits RadA to the binding site. After recruitment of the recombinase, RadB dissociates ssDNA and could then bind to the next region of ssDNA that is bound by RPA. Alternatively, RadB might displace sufficient RPA for RadA to initially bind ssDNA. Once RadA is bound, cooperative binding of RadA protomers and subsequent filament formation might be sufficient to displace remaining RPA.

In the absence of RadB, RadA would be less able to compete with the more tightly bound RPA, nucleoprotein filaments would fail to assemble efficiently or spontaneously abort, and recombination would be less efficient. Additionally, if part of the function of RadB is to recruit RadA to its DNA substrate then the binding and subsequent filamentation of RadA would be anticipated to be significantly slower if RadB is absent. RadA-A196V, likely to possess stronger monomer:monomer interactions due to increased hydrophobicity of the polymerization motif, or due to alteration of the socket shape, might be able to overcome RPA inhibition without the need for RadB.

RadB might interact with RPA directly

Rad52, but not Rad55/57, has been shown to directly interact with RPA and catalyse the displacement of the ssb by Rad51. This is in addition to another proposed method of displacing RPA from ssDNA through a stimulatory interaction on Rad51. Therefore, RadB might directly interact with RPA causing the displacement of the DNA binding protein and/or subsequent recruitment of RadA. No *in vitro* or *in vivo* interaction between RadB and RPA has been detected either in the presence or absence of ATP. However, *Pfu*-RadB used for these assays was over-expressed in *E.coli* rather than natively. If *Pfu*-RadB undergoes post-translational modification, such modification would not occur under these circumstances and consequently a number of protein:protein interactions may not be observed with recombinant RadB.

Finally, RadB might stimulate RadA-dependent displacement of RPA, as has been observed in the case of Rad52 and Rad51: When interacting with Rad52, Rad51 can displace ssDNA bound RPA, but not in the absence of Rad52. If RadB is required to stimulate RadA-dependent displacement of RPA, RadA in Δ*radB* strains might not be able to readily displace RPA.

However, RadA-A196V might already be in a state capable of displacing RPA without requiring stimulation by RadB, therefore recombination can still proceed efficiently.

2) RadB might activate RadA

Another possible mediator function could be that upon interacting with RadB, RadA adopts an active state by induction of a conformational change in the recombinase by RadB. If RadA can exist in two states and an active form of RadA is necessary for efficient recombination, it would be expected that Δ*radB* strains would contain less or no active RadA, depending on whether other proteins besides are also capable of activating RadA.

This active form of RadA could manifest itself as a restructuring of the hydrophobic socket thereby strengthening the interactions between RadA monomers. This strengthening of interactions would result in increased stability of the RadA nucleoprotein filament therefore preventing spontaneous abortion of filament assembly, or it could be sufficient to allow the nucleoprotein filament to displace ssDNA-bound RPA as it assembles on its substrate. Thus, the mutant RadA-A196V protein may already exist in an active form and not require RadB for activation.

Alternatively, a conformational change from the inactive and active form of RadA may result in a higher affinity of the protein for ssDNA through changing the structure of the DNA binding domains of RadA. This too might allow the protein to compete for ssDNA substrates with already bound ssDNA-bound RPA. Again, RadA-A196V might already be in this active state.

The hypothesis that RadB might activate RadA is compatible with the previously observed difference in intracellular levels of the two proteins. While high concentrations of RadA would be necessary due to the nature of the long nucleoprotein filaments it forms on DNA, RadB would only be required in low concentrations: Conversely, if the stoichiometry of RadA to RadB is 1:1, a maximum of 0.5% of intracellular RadA would be activate at any given time (i.e. one in two hundred, as indicated by the levels of each protein). However, the active RadA might be recruited to the DNA substrate by RadB rather than binding by chance. Even if RadB does not recruit RadA to ssDNA structures and binding of RadA:RadB complex relies on chance, it might be sufficient for filament formation.

3) RadB might seed RadA nucleoprotein filaments on ssDNA

Although intracellular levels of RadB are lower than those of RadA, it is possible that RadB could initiate RadA nucleoprotein filament either as a monomer or short oligomer: RadB might bind to regions of RPA-coated ssDNA where RadA itself is unable to bind, RadA could then

interact with RadB in a manner that, either due to specific RadA:RadB monomer interactions or because of a RadB induced RadA conformational change, overcomes the inhibition of RPA and efficient assembly of the RadA nucleoprotein filament would proceed. Though significantly diverged from RadA, RadB retains the central core characteristic of the recombinase and one of the two solved crystal structures of RadB suggests that it is capable of forming RecA/Rad51/RadA-like helices. RadB helices have a pitch of 113.4Å containing 6.57 monomers/turn and RecA/Rad51/RadA helices have a pitch of 76-100Å containing 6.1-6.6 monomers/turn (Akiba et al., 2005).

It is unlikely that RadA:RadB interactions are similar to the peg:socket interactions observed in RadA:RadA interactions, as the solved crystal structure indicates that RadB:RadB interactions are mediated by an interaction between a positively charged and a negatively charged patch of neighbouring monomers rather than through hydrophobic interactions. RadB also lacks the C- and N- terminal domains responsible for monomer interactions in Rad51/RadA and therefore does not contain a hydrophobic socket or conserved, surface exposed phenylalanine peg. Thus, if RadB does seed RadA filaments, it would be expected that the RadA:RadB interaction differs from RadA:RadA interactions.

Summary

Several possible functions for RadB have been outlined above: 1) Either interacting with RadA or on its own, RadB might directly remove RPA from ssDNA allowing RadA to bind to its substrate. 2) The interaction between RadA and RadB might activate RadA and while active, the recombinase might be able to overcome the DNA binding inhibition imposed by RPA and/or promote nucleoprotein filament formation. 3) RadB might constitute the initiating section of RadA nucleoprotein filaments that may be necessary to stimulate extended filament formation either by activating RadA, by removing RPA from the DNA or both.

In all cases, the absence of RadB would lead to a decrease in the efficiency of strand exchange and consequently, the observed *in vivo* reduction in recombination frequencies, hypersensitivity to DNA damage and the slow growth phenotypes of Δ*radB* strains. Suppression of this phenotype by the mutant recombinase encoded by *radA-A196V* is reconcilable with the above hypotheses of the function of RadB.

Evolutionary conservation of RadB

It has been shown in this chapter that RadB is only present in the euryarchaea and not the crenarchaea. The reason why a potential regulator of RadA activity would be present in one archaeal kingdom but not another is unknown. One possible explanation could be due to the

environments in which the euryarchaea and crenarchaea tend to inhabit. Crenarchaeal species tend to live at high temperatures, whereas most euryarchaeal species tend to live at more normal temperatures. Crenarchaeal species are likely to suffer more DNA damage due to the high temperatures, therefore repair by homologous recombination is likely to occur more often. For this reason, regulation of RadA by mediator proteins might have been lost as active RadA might be required constantly. Conversely, in the euryarchaea where less DNA damage from environmental factors might occur, it might not be desirable for RadA to be unregulated, as uncontrolled filament formation might lead to sub-optimal growth and survival rates. This is consistent with slow growth phenotype and mitomycin C sensitivity phenotypes of *radA-A196V* strains. Thus, RadB might be functioning as a regulator of RadA activity ensuring its polymerisation proceeds only when desirable.

Chapter 6: Concluding remarks and future perspectives

6.1 Overview

The process of homologous recombination is essential for the efficient repair of DNA double strand breaks, and underpins replication by restoring stalled and collapsed replication forks. Recombinases are central to homologous recombination and catalyse the homology search and subsequent strand exchange reactions. Recombinases are ubiquitous and recombinase mutants tend to exhibit high sensitivity to DNA damage, recombination defects and slower growth rates or lethality, due to the inability to efficiently restore replication forks (Cunningham et al., 1979; Shibata et al., 1979; Woods and Dyall-Smith, 1997).

Eukaryotes and archaea encode paralogues of Rad51 and RadA , respectively. Those that have been characterised have been implicated in genome maintenance and DNA repair (Komori et al., 2000b; Liu et al., 2004a; O'Regan et al., 2001; Sigurdsson et al., 2001; Sung, 1997b; Ward et al., 2007) . These paralogue proteins do not possess strand exchange or homologous pairing activity like their respective recombinases, and their specific functions remain elusive.

The single archaeal RadA paralogue is RadB. RadB shares core features with RadA and is present in nearly all euryarchaeal species but absent from crenarchaea. Crenarchaea do not encode RadA paralogues, with the exception of a putative RadA-like protein in *Sulfolobus solfataricus*. *In vitro* studies have shown that RadB binds both double and single stranded DNA, with a higher affinity than RadA (Komori et al., 2000b). RadB also binds ATP but only possesses a very weak ATPase activity (Komori et al., 2000b). Furthermore, it possesses no strand exchange activity. In yeast two hybrid and immunoprecipitation assays, RadB has been shown to interact with proteins involved in DNA repair and replication.(Hayashi et al., 1999; Komori et al., 2000b) , These proteins are Hjc, an archaeal Holliday junction resolvase (Bolt et al., 2001; Dorazi et al., 2006; Komori et al., 1999), Dp1, the proofreading subunit of the archaeal DNA polymerase, PolD (Jokela et al., 2004; Tang et al., 2004; Uemori et al., 1997), and RadA, the archaeal recombinase (Sandler et al., 1999; Sandler et al., 1996; Seitz et al., 1998; Woods and Dyall-Smith, 1997). These interactions suggest that the function of RadB is intimately linked with DNA replication and recombination.

The crystal structure of *Thermococcus kodakaraensis* RadB was solved in 2005 (Akiba et al., 2005) and a putative DNA binding motif ($^{K}/_{R}$HR) has been identified (Guy et al., 2006).

Mutation of H206A, part of this basic patch of residues implicated in DNA binding, results in a 10-fold decrease in the DNA binding activity of RadB and it is proposed that this mutation disrupts interactions between H206 and the DNA backbone(Guy et al., 2006).

6.2 Genetic analysis of RadB

Until the studies described in this thesis, no genetic data for RadB existed. By deletion and mutation of *Haloferax volcanii radB* in combination with deletions of *radA* and *hjc*, genetic data on the *in vivo* function has been obtained. Δ*radB* strains of *H.volcanii* are slow growing, sensitive to UV irradiation and mitomycin C, and deficient for crossover recombination and to a lesser extent, non-crossover recombination. The same analyses of Δ*radA* strains showed that cells lacking RadA are phenotypically similar to cells lacking RadB, with the exception that Δ*radA* strains are unable to carry out recombination, confirming previous observations (Woods and Dyall-Smith, 1997). Furthermore, the growth rates, DNA damage sensitivity and recombination defects of Δ*radA* Δ*radB* strains are identical to those observed in Δ*radA* strains, demonstrating that RadA is epistatic to RadB. These data demonstrate that RadB functions during homologous recombination. Mutational analysis of the putative ATP binding domain of RadB showed that ATP binding is essential for RadB function. It has previously been shown that RadB undergoes a conformational change upon ATP binding (Guy et al., 2006), suggesting that this alteration of RadB conformation is essential for the function of the protein. Cells encoding RadB-H206A, a mutant of the putative DNA binding motif, exhibit normal sensitivity to UV irradiation, suggesting that the observed *in vitro* reduction in DNA binding of this mutant does not affect the function of RadB *in vivo*.

Quantitation of *radA* and *radB* mRNA transcript levels following UV irradiation showed that transcription of *radA*, but not *radB*, is induced in response to DNA damage. RadB might not be upregulated transcriptionally in response to DNA damage, and instead be regulated by other means, such as post-translational modification. This concept is reinforced by the conformational change of RadB following ATP binding and mutational analysis of a ATP binding mutant. RadB requires ATP to function and this suggests a mean of regulating the protein *in vivo*.

Finally, a suppressor of the slow growth, DNA damage sensitivity and recombination defect phenotype of Δ*radB* was isolated and characterised. This mutation is manifested as a single amino acid substitution in the polymerisation domain of RadA. RadA polymerisation occurs through hydrophobic interaction between a phenylalanine 'peg' of one RadA monomer with a socket, comprising of seven hydrophobic residues, present on another adjacent RadA monomer (Shin et al., 2003). Mutation of an alanine residue in this socket to a valine, in *H.volcanii*

RadA-A196V confers suppression of Δ*radB*. This suppression might be due to stronger protein:protein interactions between RadA-A196V monomers, due to an increase in hydrophobicity. Alternatively, or additionally, the structure of the hydrophobic socket might be altered in the mutant protein, altering the interface monomers and tightening nucleoprotein filaments on DNA.

The alanine mutated in RadA-A196V is invariant in euryarchaeal RadA and eukaryotic Rad51, but not conserved in crenarchaeal RadA. This reveals a strong correlation between the presence of RadA /Rad51 paralogues and the conservation of this alanine residue. This correlation is further reinforced by the fact that the only sequenced euryarchaeal species that does not possess this alanine residue, *Methanopyrus kandleri* is the only euryarchaeota not to encode RadB. Furthermore, analysis of the hydrophobicity of the RadA hydrophobic socket shows a similar profile for euryarchaeal and eukaryotic species, with two distinct peaks of hydrophobicity. Conversely, crenarchaeal species show uniform hydrophobicity across the socket. Mutation of *H.volcanii* RadA to RadA-A196V changes the hydrophobicity and resembles the uniform pattern seen in crenarchaeal RadA.

Δ*radB* cells expressing RadA-A196V are completely suppressed for UV damage sensitivity and recombination deficiencies, and growth rates and resistance to mitomycin C are partially restored. Cells expressing both RadA-A196V and RadB proteins are equally resistant to DNA damage and equally efficient at recombination as strains encoding RadA-A196V but lacking RadB, indicating that RadA-A196V renders RadB redundant. Furthermore, the presence of both proteins results in slower growth rates than when RadA-A196V is present in the absence of RadB, indicating that the presence of both proteins is detrimental to the cell.

These data strongly suggest that RadB functions as a RadA mediator protein. Cells lacking RadB exhibit reduced recombination frequencies and are otherwise nearly phenotypically identical to cells deleted for RadA, suggesting that RadA can not function efficiently without RadB. The suppression of Δ*radB* by a mutation in the RadA polymerisation motif strongly suggests that RadA-A196V is able to function efficiently in the absence of RadB, much like crenarchaeal RadA.

Eukaryotes and bacteria both encode proteins that facilitate Rad51/RecA filament formation. Recombinases generally can not bind to ssDNA *in vivo* without mediator proteins due competition with single strand binding proteins (ssbs). Eukaryotic RPA (Replication Protein A) and bacterial SSB (Single Strand Binding protein) are ssbs and are important for virtually all forms of DNA processing, and are believed to prevent the formation of secondary structures formed in ssDNA, thus promoting Rad51/RecA nucleoprotein filament formation.

Paradoxically, ssbs compete with recombinases for ssDNA binding sites and also have a higher binding affinity meaning that recombinases can not displace ssbs alone. Thus, proteins that assist Rad51/RecA binding to RPA-coated ssDNA are required for efficient homologous recombination.

In *E.coli*, DNA ends are processed by RecBCD, which then loads RecA onto the single stranded DNA (Arnold and Kowalczykowski, 2000; Churchill and Kowalczykowski, 2000). In *recBC* strains of *E.coli*, RecA can still be loaded to single stranded regions but only when facilitated by RecFOR. RecO binds the single stranded DNA coated with SSB. RecF and RecR are then required for efficient presynaptic complex formation at single stranded/double stranded DNA junctions.

Rad52 and Rad55/57 are both required to promote eukaryotic Rad51 filament assembly during meiosis, and either Rad52 or Rad55/57 alone are sufficient to promote filament assembly following cell irradiation (Gasior et al., 2001). Rad52 functions in a similar manner to RecO, by binding RPA coated ss-DNA. Rad52 also binds Rad51 and RPA, and by displacing the latter, permits loading of the recombinase onto the naked single-stranded DNA. Rad55/57 possesses similar activities to Rad52 yet the two complexes are very different. Rad55 and Rad57 share homology with Rad51 whereas Rad52 does not. Rad55/57 forms a heterodimer (Sung, 1997b) whereas Rad52 forms heptameric rings (Stasiak et al., 2000).

While no mediators of RadA are known, archaeal species encode ssbs. Euryarchaea encoded homologues of eukaryotic RPA, and it has been shown that RadA interacts with archaeal RPA (Komori and Ishino, 2001). Thus, it is likely that RadA requires the function of an archaeal mediator protein to overcome the RPA inhibition of ssDNA binding by RadA. RadB is a candidate for this role, and data presented in this thesis reinforces the concept that RadB might act to overcome RPA-inhibition of ssDNA binding by RadA. Like other mediator proteins, RadB interacts with its respective recombinase. Also, the suppressor protein RadA-A196V is likely to possess stronger monomer:monomer interactions due to an increased hydrophobicity of the polymerization socket. Furthermore, RadA-A196V filaments might be more rigid and tightly bound to DNA through an alteration of the interaction between RadA monomers. These potential alterations in RadA filament formation might result in RadA-A196V being able to overcome RPA-inhibition of ssDNA binding. It has been shown that mutations in Rad51 can lead to suppress the requirement for RAD55 and RAD57 (Fortin and Symington, 2002), therefore it follows that mutations in RadA might suppress the requirement for RadA mediators, such as candidates like RadB. Another possibility is that RadA might be present in an inactive form until required, e.g. following DNA damage. When RadA is required, it might

undergo a RadB-induced conformational change, and become active. RadA-A196V might be in a constitutively active form and therefore not require activation by RadB. Finally, work presented here has shown that crossover recombination frequencies are more severely affected than non-crossover recombination frequencies in Δ*radB* strain. Crossover frequencies are reduced to ~6.5% and non-crossover frequencies are reduced to ~20% of *radB*+ frequencies. This, and RadBs proposed interaction with RadA, implies an early and late role for RadB in recombination. RadB might function as a RadA mediator early in recombination, and if it is not present, RadA can not catalyse strand exchange as efficiently (~20% frequency of *radB*+). This is the observed relative frequency of non-crossover recombination in Δ*radB* strains. If a second strand exchange event occurs, as it does in crossover recombination, it would be expected that this event would proceed at ~20% frequency also. The multiplicative effect of these two deficiencies together would result in a total reduction of frequencies to 4% of *radB*+ levels (0.2 x 0.2 = 0.04). This value correlates with the observed relative frequency of crossover recombination in Δ*radB* strains. This further reinforces the concept that RadB acts to promote RadA catalysed strand exchange and implicates RadB as a recombination mediator protein.

6.3 Genetic analysis of Hjc

As discussed, Hjc is a Holliday junction resolvase present in all archaeal species. However, work presented in this thesis indicate that it is not the primary archaeal resolvase in *H.volcanii* as crossover recombination frequencies are unaffected by its absence. Furthermore, Δ*hjc* strains do not display any sensitivity to DNA damage beyond that exhibited by *hjc*+ strains. Finally, growth rates are the same, regardless of the presence or absence of RadB. In fact, the only observed phenotype for Δ*hjc* is in a Δ*radB* background, where crossover recombination frequencies are slightly reduced and growth rates are slower than those observed in Δ*radB hjc*+ strains. Thus, it is likely that a second archaeal Holliday junction resolvase is present in *H.volcanii* that can compensate for the absence of Hjc, or is itself the primary Holliday junction resolvase.

6.4 Future perspectives

While it has been demonstrated that *radB* is required for efficient recombination and that it might be a recombination mediator protein, the genetic data presented here does not conclusively demonstrate this. Several options are available for further investigation of the role of RadB in RadA-dependent recombination. First, it would be informative to demonstrate whether RadB interacts with RadA *in vivo*, as it does *in vitro*. A *H.volcanii* two-hybrid system is currently in development and if successful, this could be used to demonstrate potential RadB

interactions *in vivo*. RadB might act to overcome RPA inhibition of RadA-DNA binding through binding to RPA, in an analogous manner to Rad52 and RecO mediation of recombination. No *in vitro* interaction between RadB and RPA was observed in immunoprecipitation or yeast-two hybrid assays (Hayashi et al., 1999; Komori et al., 2000b). However, RadB protein used in these assays was not natively expressed and therefore any post-translational modification of RadB would not occur, possibly abrogating other interactions. By utilising a native two hybrid system, further RadB:protein interactions might be elucidated.

While it has been demonstrated that a mutation in RadA suppresses the Δ*radB* phenotype, it would be informative to elucidate any other non-RadA suppressors of Δ*radB*. Additional suppressors of Δ*radB* could be selected for by repeated exposure of Δ*radB* cells to DNA damage to enrich any suppressors that confer resistance to DNA damage or that improve growth rates. However, strains containing suppressors would be hard to characterise as it would not be known where the suppressor was located in the genome. A more directed method would be to use mutagenic PCR to amplify genes that encode proteins associated with RadB, followed by replacement of chromosomal wild type genes with a library of mutant alleles. Any transformed cells that exhibited signs of suppression could then be sequenced to determine the nature of the mutation. Prime candidate genes for random mutagenesis are *H.volcanii dp1* and the *rpa* genes. The *Pyrococcus furiosus dp1* protein product has been shown to interact with RadB *in vitro*(Hayashi et al., 1999) and *rpa* is a good candidate to test the idea that RadB functions to overcome the inhibition of DNA binding to ssDNA imposed by RPA. *rpa* mutants that encode RPA lower binding affinity for ssDNA might be viable, and might partially suppress the *radB* phenotype, if RadB is a mediator of RadA-dependent recombination.

It has been demonstrated that over-expression of Rad51 can cause partial suppression of Rad52 and Rad55 mutants (Asleson et al., 1999; Johnson and Symington, 1995). It would be informative to carry out phenotypic analyses of a Δ*radB* strain with elevated expression of *radA* to determine whether elevated levels of RadA are able to suppress Δ*radB*. RadA and eukaryotic Rad51 are structurally and functionally very similar (Shin et al., 2003). Generation of a mutant of Rad51, equivalent to RadA-A196V and studying its effects in Rad52 and Rad55/Rad57 mutants might result in suppression of the DNA damage sensitivity and recombination defect phenotypes associated with these strains. If suppression was observed, this would suggest that RadB is a RadA mediator protein, analogous to Rad52 and Rad55-57. Finally, biochemical analysis of RadA-A196V would be very useful in characterizing the effects of such a mutation on DNA binding affinity and strand exchange. Such studies would provide a clearer view of the function of RadB *in vivo*, as evidenced by the altered activities of a protein that suppresses the phenotypes associated with Δ*radB*.

References

Aihara, H., Ito, Y., Kurumizaka, H., Terada, T., Yokoyama, S. and Shibata, T. (1997) An interaction between a specified surface of the C-terminal domain of RecA protein and double-stranded DNA for homologous pairing. *J Mol Biol*, **274**, 213-221.

Aihara, H., Ito, Y., Kurumizaka, H., Yokoyama, S. and Shibata, T. (1999) The N-terminal domain of the human Rad51 protein binds DNA: structure and a DNA binding surface as revealed by NMR. *J Mol Biol*, **290**, 495-504.

Akiba, T., Ishii, N., Rashid, N., Morikawa, M., Imanaka, T. and Harata, K. (2005) Structure of RadB recombinase from a hyperthermophilic archaeon, Thermococcus kodakaraensis KOD1: an implication for the formation of a near-7-fold helical assembly. *Nucleic Acids Res*, **33**, 3412-3423.

Albala, J.S., Thelen, M.P., Prange, C., Fan, W., Christensen, M., Thompson, L.H. and Lennon, G.G. (1997) Identification of a novel human RAD51 homolog, RAD51B. *Genomics*, **46**, 476-479.

Allers, T. and Lichten, M. (2001) Differential timing and control of noncrossover and crossover recombination during meiosis. *Cell*, **106**, 47-57.

Allers T, Mevarech M (2005) Archaeal genetics - the third way. *Nat Rev Genet* **6:** 58-73

Allers, T., Ngo, H.P., Mevarech, M. and Lloyd, R.G. (2004) Development of additional selectable markers for the halophilic archaeon Haloferax volcanii based on the leuB and trpA genes. *Appl Environ Microbiol*, **70**, 943-953.

Aravind, L. and Koonin, E.V. (1999) DNA-binding proteins and evolution of transcription regulation in the archaea. *Nucleic Acids Res*, **27**, 4658-4670.

Ariza, A., Richard, D.J., White, M.F. and Bond, C.S. (2005) Conformational flexibility revealed by the crystal structure of a crenarchaeal RadA. *Nucleic Acids Res*, **33**, 1465-1473.

Arnold, D.A. and Kowalczykowski, S.C. (2000) Facilitated loading of RecA protein is essential to recombination by RecBCD enzyme. *J Biol Chem*, **275**, 12261-12265.

Asleson, E.N., Okagaki, R.J. and Livingston, D.M. (1999) A core activity associated with the N terminus of the yeast RAD52 protein is revealed by RAD51 overexpression suppression of C-terminal rad52 truncation alleles. *Genetics*, **153**, 681-692.

Barns SM, Delwiche CF, Palmer JD, Pace NR (1996) Perspectives on archaeal diversity, thermophily and monophyly from environmental rRNA sequences. *Proc Natl Acad Sci U S A* **93:** 9188-9193

Barry, E.R. and Bell, S.D. (2006) DNA replication in the archaea. *Microbiol Mol Biol Rev*, **70**, 876-887.

Bashkirov, V.I., Herzberg, K., Haghnazari, E., Vlasenko, A.S. and Heyer, W.D. (2006) DNA damage-induced phosphorylation of Rad55 protein as a sentinel for DNA damage checkpoint activation in S. cerevisiae. *Methods Enzymol*, **409**, 166-182.

Bashkirov, V.I., King, J.S., Bashkirova, E.V., Schmuckli-Maurer, J. and Heyer, W.D. (2000) DNA repair protein Rad55 is a terminal substrate of the DNA damage checkpoints. *Mol Cell Biol*, **20**, 4393-4404.

Bell, S.D. and Jackson, S.P. (2001) Mechanism and regulation of transcription in archaea. *Curr Opin Microbiol*, **4**, 208-213.

Bennett, R.J. and West, S.C. (1995) RuvC protein resolves Holliday junctions via cleavage of the continuous (noncrossover) strands. *Proc Natl Acad Sci U S A*, **92**, 5635-5639.

Benson, F.E., Stasiak, A. and West, S.C. (1994) Purification and characterization of the human Rad51 protein, an analogue of E. coli RecA. *Embo J*, **13**, 5764-5771.

Bhattacharyya, A., Ear, U.S., Koller, B.H., Weichselbaum, R.R. and Bishop, D.K. (2000) The breast cancer susceptibility gene BRCA1 is required for subnuclear assembly of Rad51 and survival following treatment with the DNA cross-linking agent cisplatin. *J Biol Chem*, **275**, 23899-23903.

Bishop, D.K. (1994) RecA homologs Dmc1 and Rad51 interact to form multiple nuclear complexes prior to meiotic chromosome synapsis. *Cell*, **79**, 1081-1092.

Bitan-Banin, G., Ortenberg, R. and Mevarech, M. (2003) Development of a gene knockout system for the halophilic archaeon *Haloferax volcanii* by use of the *pyrE* gene. *J Bacteriol*, **185**, 772-778.

Black, S.D. and Mould, D.R. (1991) Development of hydrophobicity parameters to analyze proteins which bear post- or cotranslational modifications. *Anal Biochem*, **193**, 72-82.

Bolt, E.L., Lloyd, R.G. and Sharples, G.J. (2001) Genetic analysis of an archaeal Holliday junction resolvase in Escherichia coli. *J Mol Biol*, **310**, 577-589.

Boucher, Y., Kamekura, M. and Doolittle, W.F. (2004) Origins and evolution of isoprenoid lipid biosynthesis in archaea. *Mol Microbiol*, **52**, 515-527.

Braybrooke, J.P., Spink, K.G., Thacker, J. and Hickson, I.D. (2000) The RAD51 family member, RAD51L3, is a DNA-stimulated ATPase that forms a complex with XRCC2. *J Biol Chem*, **275**, 29100-29106.

Briggs, G.S., Mahdi, A.A., Weller, G.R., Wen, Q. and Lloyd, R.G. (2004) Interplay between DNA replication, recombination and repair based on the structure of RecG helicase. *Philos Trans R Soc Lond B Biol Sci*, **359**, 49-59.

Brown, J.R. and Doolittle, W.F. (1997) Archaea and the prokaryote-to-eukaryote transition. *Microbiol Mol Biol Rev*, **61**, 456-502.

Bugreev, D.V., Mazina, O.M. and Mazin, A.V. (2006) Rad54 protein promotes branch migration of Holliday junctions. *Nature*, **442**, 590-593.

Catlett, M.G. and Forsburg, S.L. (2003) Schizosaccharomyces pombe Rdh54 (TID1) acts with Rhp54 (RAD54) to repair meiotic double-strand breaks. *Mol Biol Cell*, **14**, 4707-4720.

Chang, Y.C., Lo, Y.H., Lee, M.H., Leng, C.H., Hu, S.M., Chang, C.S. and Wang, T.F. (2005) Molecular visualization of the yeast Dmc1 protein ring and Dmc1-ssDNA nucleoprotein complex. *Biochemistry*, **44**, 6052-6058.

Chedin, F. and Kowalczykowski, S.C. (2002) A novel family of regulated helicases/nucleases from Gram-positive bacteria: insights into the initiation of DNA recombination. *Mol Microbiol*, **43**, 823-834.

Chen, J., Silver, D.P., Walpita, D., Cantor, S.B., Gazdar, A.F., Tomlinson, G., Couch, F.J., Weber, B.L., Ashley, T., Livingston, D.M. and Scully, R. (1998) Stable interaction between the products of the BRCA1 and BRCA2 tumor suppressor genes in mitotic and meiotic cells. *Mol Cell*, **2**, 317-328.

Chen, Y.K., Leng, C.H., Olivares, H., Lee, M.H., Chang, Y.C., Kung, W.M., Ti, S.C., Lo, Y.H., Wang, A.H., Chang, C.S., Bishop, D.K., Hsueh, Y.P. and Wang, T.F. (2004) Heterodimeric

complexes of Hop2 and Mnd1 function with Dmc1 to promote meiotic homolog juxtaposition and strand assimilation. *Proc Natl Acad Sci U S A*, **101**, 10572-10577.

Chrysogelos, S., Register, J.C., 3rd and Griffith, J. (1983) The structure of recA protein-DNA filaments. 2 recA protein monomers unwind 17 base pairs of DNA by 11.5 degrees/base pair in the presence of adenosine 5'-O-(3-thiotriphosphate). *J Biol Chem*, **258**, 12624-12631.

Churchill, J.J. and Kowalczykowski, S.C. (2000) Identification of the RecA protein-loading domain of RecBCD enzyme. *J Mol Biol*, **297**, 537-542.

Clark, A.J. and Margulies, A.D. (1965) Isolation and Characterization of Recombination-Deficient Mutants of Escherichia Coli K12. *Proc Natl Acad Sci U S A*, **53**, 451-459.

Constantinou, A., Chen, X.B., McGowan, C.H. and West, S.C. (2002) Holliday junction resolution in human cells: two junction endonucleases with distinct substrate specificities. *Embo J*, **21**, 5577-5585.

Cortes-Ledesma, F., Malagon, F. and Aguilera, A. (2004) A novel yeast mutation, rad52-L89F, causes a specific defect in Rad51-independent recombination that correlates with a reduced ability of Rad52-L89F to interact with Rad59. *Genetics*, **168**, 553-557.

Cox, M.M. (2007) Regulation of bacterial RecA protein function. *Crit Rev Biochem Mol Biol*, **42**, 41-63.

Cunningham, R.P., Shibata, T., DasGupta, C. and Radding, C.M. (1979) Single strands induce recA protein to unwind duplex DNA for homologous pairing. *Nature*, **281**, 191-195.

Date, O., Katsura, M., Ishida, M., Yoshihara, T., Kinomura, A., Sueda, T. and Miyagawa, K. (2006) Haploinsufficiency of RAD51B causes centrosome fragmentation and aneuploidy in human cells. *Cancer Res*, **66**, 6018-6024.

Deans, B., Griffin, C.S., O'Regan, P., Jasin, M. and Thacker, J. (2003) Homologous recombination deficiency leads to profound genetic instability in cells derived from Xrcc2-knockout mice. *Cancer Res*, **63**, 8181-8187.

DeLange, R.J., Williams, L.C. and Searcy, D.G. (1981) A histone-like protein (HTa) from Thermoplasma acidophilum. II. Complete amino acid sequence. *J Biol Chem*, **256**, 905-911.

Dillingham, M.S., Spies, M. and Kowalczykowski, S.C. (2003) RecBCD enzyme is a bipolar DNA helicase. *Nature*, **423**, 893-897.

Dixon, D.A. and Kowalczykowski, S.C. (1993) The recombination hotspot chi is a regulatory sequence that acts by attenuating the nuclease activity of the E. coli RecBCD enzyme. *Cell*, **73**, 87-96.

Doolittle, W.F. (1998) You are what you eat: a gene transfer ratchet could account for bacterial genes in eukaryotic nuclear genomes. *Trends Genet*, **14**, 307-311.

Dorazi, R., Parker, J.L. and White, M.F. (2006) PCNA activates the Holliday junction endonuclease Hjc. *J Mol Biol*, **364**, 243-247.

Dosanjh, M.K., Collins, D.W., Fan, W., Lennon, G.G., Albala, J.S., Shen, Z. and Schild, D. (1998) Isolation and characterization of RAD51C, a new human member of the RAD51 family of related genes. *Nucleic Acids Res*, **26**, 1179-1184.

Dresser, M.E., Ewing, D.J., Conrad, M.N., Dominguez, A.M., Barstead, R., Jiang, H. and Kodadek, T. (1997) DMC1 functions in a Saccharomyces cerevisiae meiotic pathway that is largely independent of the RAD51 pathway. *Genetics*, **147**, 533-544.

Dyall-Smith, M.L. and Doolittle, W.F. (1994) Construction of composite transposons for halophilic Archaea. *Can J Microbiol*, **40**, 922-929.

Enomoto, R., Kinebuchi, T., Sato, M., Yagi, H., Kurumizaka, H. and Yokoyama, S. (2006) Stimulation of DNA strand exchange by the human TBPIP/Hop2-Mnd1 complex. *J Biol Chem*, **281**, 5575-5581.

Essers, J., Hendriks, R.W., Swagemakers, S.M., Troelstra, C., de Wit, J., Bootsma, D., Hoeijmakers, J.H. and Kanaar, R. (1997) Disruption of mouse RAD54 reduces ionizing radiation resistance and homologous recombination. *Cell*, **89**, 195-204.

Essers, J., van Steeg, H., de Wit, J., Swagemakers, S.M., Vermeij, M., Hoeijmakers, J.H. and Kanaar, R. (2000) Homologous and non-homologous recombination differentially affect DNA damage repair in mice. *Embo J*, **19**, 1703-1710.

Fogel, S. and Mortimer, R.K. (1970) Fidelity of gene conversion in yeast. *Molecular and General Genetics*, 177-185.

Fogel, S. and Mortimer, R.K. (1974) Gene Conversion and mismatched base repair in hybrid DNA. *Genetics*, 522.

Formosa, T. and Alberts, B.M. (1986) DNA synthesis dependent on genetic recombination: characterization of a reaction catalyzed by purified bacteriophage T4 proteins. *Cell*, **47**, 793-806.

Forterre, P. and Philippe, H. (1999) Where is the root of the universal tree of life? *Bioessays*, **21**, 871-879.

Fortin, G.S. and Symington, L.S. (2002) Mutations in yeast Rad51 that partially bypass the requirement for Rad55 and Rad57 in DNA repair by increasing the stability of Rad51-DNA complexes. *Embo J*, **21**, 3160-3170.

Game, J.C. and Mortimer, R.K. (1974) A genetic study of x-ray sensitive mutants in yeast. *Mutat Res*, **24**, 281-292.

Gasior, S.L., Olivares, H., Ear, U., Hari, D.M., Weichselbaum, R. and Bishop, D.K. (2001) Assembly of RecA-like recombinases: distinct roles for mediator proteins in mitosis and meiosis. *Proc Natl Acad Sci U S A*, **98**, 8411-8418.

Gilbertson, L.A. and Stahl, F.W. (1996) A test of the double-strand break repair model for meiotic recombination in Saccharomyces cerevisiae. *Genetics*, **144**, 27-41.

Golub, E.I., Gupta, R.C., Haaf, T., Wold, M.S. and Radding, C.M. (1998) Interaction of human rad51 recombination protein with single-stranded DNA binding protein, RPA. *Nucleic Acids Res*, **26**, 5388-5393.

Gregory, T.R. (2005) *The Evolution of the Genome*. Academic Press Inc.,U.S.

Gruver, A.M., Miller, K.A., Rajesh, C., Smiraldo, P.G., Kaliyaperumal, S., Balder, R., Stiles, K.M., Albala, J.S. and Pittman, D.L. (2005) The ATPase motif in RAD51D is required for resistance to DNA interstrand crosslinking agents and interaction with RAD51C. *Mutagenesis*, **20**, 433-440.

Guy, C.P. and Bolt, E.L. (2005) Archaeal Hel308 helicase targets replication forks in vivo and in vitro and unwinds lagging strands. *Nucleic Acids Res*, **33**, 3678-3690.

Guy, C.P., Haldenby, S., Brindley, A., Walsh, D.A., Briggs, G.S., Warren, M.J., Allers, T. and Bolt, E.L. (2006) Interactions of RadB, a DNA repair protein in archaea, with DNA and ATP. *J Mol Biol*, **358**, 46-56.

Haber, J.E. and Heyer, W.D. (2001) The fuss about Mus81. *Cell*, **107**, 551-554.

Hall, S.D. and Kolodner, R.D. (1994) Homologous pairing and strand exchange promoted by the Escherichia coli RecT protein. *Proc Natl Acad Sci U S A*, **91**, 3205-3209.

Halpern, D., Gruss, A., Claverys, J.P. and El-Karoui, M. (2004) rexAB mutants in Streptococcus pneumoniae. *Microbiology*, **150**, 2409-2414.

Handa, N., Bianco, P.R., Baskin, R.J. and Kowalczykowski, S.C. (2005) Direct visualization of RecBCD movement reveals cotranslocation of the RecD motor after chi recognition. *Mol Cell*, **17**, 745-750.

Hartman, A.L., et al., The genome of Haloferax volcanii: comparative, historical and novel perspectives on a model archaeon. In preparation.Haseltine, C.A. and Kowalczykowski, S.C. (2002) A distinctive single-strand DNA-binding protein from the Archaeon Sulfolobus solfataricus. *Mol Microbiol*, **43**, 1505-1515.

Hayashi, I., Morikawa, K. and Ishino, Y. (1999) Specific interaction between DNA polymerase II (PolD) and RadB, a Rad51/Dmc1 homolog, in Pyrococcus furiosus. *Nucleic Acids Res*, **27**, 4695-4702.

Hays, S.L., Firmenich, A.A. and Berg, P. (1995) Complex formation in yeast double-strand break repair: participation of Rad51, Rad52, Rad55, and Rad57 proteins. *Proc Natl Acad Sci U S A*, **92**, 6925-6929.

Heijden, T.V., Seidel, R., Modesti, M., Kanaar, R., Wyman, C. and Dekker, C. (2007) Real-time assembly and disassembly of human RAD51 filaments on individual DNA molecules. *Nucleic Acids Res*.

Herzberg, K., Bashkirov, V.I., Rolfsmeier, M., Haghnazari, E., McDonald, W.H., Anderson, S., Bashkirova, E.V., Yates, J.R., 3rd and Heyer, W.D. (2006) Phosphorylation of Rad55 on serines 2, 8, and 14 is required for efficient homologous recombination in the recovery of stalled replication forks. *Mol Cell Biol*, **26**, 8396-8409.

Hinz, J.M., Tebbs, R.S., Wilson, P.F., Nham, P.B., Salazar, E.P., Nagasawa, H., Urbin, S.S., Bedford, J.S. and Thompson, L.H. (2006) Repression of mutagenesis by Rad51D-mediated homologous recombination. *Nucleic Acids Res*, **34**, 1358-1368.

Hobbs, M.D., Sakai, A. and Cox, M.M. (2007) SSB protein limits RecOR binding onto single-stranded DNA. *J Biol Chem*, **282**, 11058-11067.

Holliday, R. (1964) A mechanism for gene conversion in fungi. *Genet. Res. Camb.*, **5**, 282-304.

Holmes, M.L. and Dyall-Smith, M.L. (1990) A plasmid vector with a selectable marker for halophilic archaebacteria. *J Bacteriol*, **172**, 756-761.

Holmes, M.L. and Dyall-Smith, M.L. (2000) Sequence and expression of a halobacterial beta-galactosidase gene. *Mol Microbiol*, **36**, 114-122.

Holzen, T.M., Shah, P.P., Olivares, H.A. and Bishop, D.K. (2006) Tid1/Rdh54 promotes dissociation of Dmc1 from nonrecombinogenic sites on meiotic chromatin. *Genes Dev*, **20**, 2593-2604.

Honda, M., Inoue, J., Yoshimasu, M., Ito, Y., Shibata, T. and Mikawa, T. (2006) Identification of the RecR Toprim domain as the binding site for both RecF and RecO. A role of RecR in

RecFOR assembly at double-stranded DNA-single-stranded DNA junctions. *J Biol Chem*, **281**, 18549-18559.

Hornback, M.L. and Roop, R.M., 2nd. (2006) The Brucella abortus xthA-1 gene product participates in base excision repair and resistance to oxidative killing but is not required for wild-type virulence in the mouse model. *J Bacteriol*, **188**, 1295-1300.

Huet, J., Schnabel, R., Sentenac, A. and Zillig, W. (1983) Archaebacteria and eukaryotes possess DNA-dependent RNA polymerases of a common type. *Embo J*, **2**, 1291-1294.

Inwood, W., Kane, S., DiRuggiero, J., Robb, F. and Clark, A.J. (2001) The RadB protein from Pyrococcus does not complement E. coli recA mutations in vivo. *Mol Genet Genomics*, **265**, 683-686.

Ivanov, E.L., Sugawara, N., Fishman-Lobell, J. and Haber, J.E. (1996) Genetic requirements for the single-strand annealing pathway of double-strand break repair in Saccharomyces cerevisiae. *Genetics*, **142**, 693-704.

Jain, S.K., Cox, M.M. and Inman, R.B. (1994) On the role of ATP hydrolysis in RecA protein-mediated DNA strand exchange. III. Unidirectional branch migration and extensive hybrid DNA formation. *J Biol Chem*, **269**, 20653-20661.

Jinks-Robertson, S., Michelitch, M. and Ramcharan, S. (1993) Substrate length requirements for efficient mitotic recombination in Saccharomyces cerevisiae. *Mol Cell Biol*, **13**, 3937-3950.

Johnson, R.D. and Symington, L.S. (1995) Functional differences and interactions among the putative RecA homologs Rad51, Rad55, and Rad57. *Mol Cell Biol*, **15**, 4843-4850.

Jokela, M., Eskelinen, A., Pospiech, H., Rouvinen, J. and Syvaoja, J.E. (2004) Characterization of the 3' exonuclease subunit DP1 of Methanococcus jannaschii replicative DNA polymerase D. *Nucleic Acids Res*, **32**, 2430-2440.

Jones, N.J., Cox, R. and Thacker, J. (1987) Isolation and cross-sensitivity of X-ray-sensitive mutants of V79-4 hamster cells. *Mutat Res*, **183**, 279-286.

Kaine, B.P., Gupta, R. and Woese, C.R. (1983) Putative introns in tRNA genes of prokaryotes. *Proc Natl Acad Sci U S A*, **80**, 3309-3312.

Kelly, T.J., Simancek, P. and Brush, G.S. (1998) Identification and characterization of a single-stranded DNA-binding protein from the archaeon Methanococcus jannaschii. *Proc Natl Acad Sci U S A*, **95**, 14634-14639.

Kim, J.I., Cox, M.M. and Inman, R.B. (1992) On the role of ATP hydrolysis in RecA protein-mediated DNA strand exchange. I. Bypassing a short heterologous insert in one DNA substrate. *J Biol Chem*, **267**, 16438-16443.

King, S.R. and Richardson, J.P. (1986) Role of homology and pathway specificity for recombination between plasmids and bacteriophage lambda. *Mol Gen Genet*, **204**, 141-147.

Klein, H.L. (1984) Lack of association between intrachromosomal gene conversion and reciprocal exchange. *Nature*, **310**, 748-753.

Komori, K. and Ishino, Y. (2001) Replication protein A in Pyrococcus furiosus is involved in homologous DNA recombination. *J Biol Chem*, **276**, 25654-25660.

Komori, K., Miyata, T., Daiyasu, H., Toh, H., Shinagawa, H. and Ishino, Y. (2000a) Domain analysis of an archaeal RadA protein for the strand exchange activity. *J Biol Chem*, **275**, 33791-33797.

Komori, K., Miyata, T., DiRuggiero, J., Holley-Shanks, R., Hayashi, I., Cann, I.K., Mayanagi, K., Shinagawa, H. and Ishino, Y. (2000b) Both RadA and RadB are involved in homologous recombination in Pyrococcus furiosus. *J Biol Chem*, **275**, 33782-33790.

Komori, K., Sakae, S., Shinagawa, H., Morikawa, K. and Ishino, Y. (1999) A Holliday junction resolvase from Pyrococcus furiosus: functional similarity to Escherichia coli RuvC provides evidence for conserved mechanism of homologous recombination in Bacteria, Eukarya, and Archaea. *Proc Natl Acad Sci U S A*, **96**, 8873-8878.

Kooistra, J., Vosman, B. and Venema, G. (1988) Cloning and characterization of a Bacillus subtilis transcription unit involved in ATP-dependent DNase synthesis. *J Bacteriol*, **170**, 4791-4797.

Korangy, F. and Julin, D.A. (1993) Kinetics and processivity of ATP hydrolysis and DNA unwinding by the RecBC enzyme from Escherichia coli. *Biochemistry*, **32**, 4873-4880.

Kowalczykowski, S.C. (1991) Biochemistry of genetic recombination: energetics and mechanism of DNA strand exchange. *Annu Rev Biophys Biophys Chem*, **20**, 539-575.

Kowalczykowski, S.C. (2000) Initiation of genetic recombination and recombination-dependent replication. *Trends Biochem Sci*, **25**, 156-165.

Kowalczykowski, S.C., Clow, J., Somani, R. and Varghese, A. (1987) Effects of the Escherichia coli SSB protein on the binding of Escherichia coli RecA protein to single-stranded DNA. Demonstration of competitive binding and the lack of a specific protein-protein interaction. *J Mol Biol*, **193**, 81-95.

Kraus, E., Leung, W.Y. and Haber, J.E. (2001) Break-induced replication: a review and an example in budding yeast. *Proc Natl Acad Sci U S A*, **98**, 8255-8262.

Kurumizaka, H., Aihara, H., Ikawa, S., Kashima, T., Bazemore, L.R., Kawasaki, K., Sarai, A., Radding, C.M. and Shibata, T. (1996) A possible role of the C-terminal domain of the RecA protein. A gateway model for double-stranded DNA binding. *J Biol Chem*, **271**, 33515-33524.

Kushner, S.R., Nagaishi, H. and Clark, A.J. (1972) Indirect suppression of recB and recC mutations by exonuclease I deficiency. *Proc Natl Acad Sci U S A*, **69**, 1366-1370.

Kushner, S.R., Nagaishi, H., Templin, A. and Clark, A.J. (1971) Genetic recombination in Escherichia coli: the role of exonuclease I. *Proc Natl Acad Sci U S A*, **68**, 824-827.

Kuzminov, A. (1999) Recombinational repair of DNA damage in Escherichia coli and bacteriophage lambda. *Microbiol Mol Biol Rev*, **63**, 751-813, table of contents.

Kuznetsov, S., Pellegrini, M., Shuda, K., Fernandez-Capetillo, O., Liu, Y., Martin, B.K., Burkett, S., Southon, E., Pati, D., Tessarollo, L., West, S.C., Donovan, P.J., Nussenzweig, A. and Sharan, S.K. (2007) RAD51C deficiency in mice results in early prophase I arrest in males and sister chromatid separation at metaphase II in females. *J Cell Biol*, **176**, 581-592.

Kvaratskhelia, M., Wardleworth, B.N. and White, M.F. (2001) Multiple Holliday junction resolving enzyme activities in the Crenarchaeota and Euryarchaeota. *FEBS Lett*, **491**, 243-246.

Kvaratskhelia, M. and White, M.F. (2000) Two Holliday Junction Resolving Enzymes in *Sulfolobus solfataricus*. *J Mol Biol*, **297**, 923-932.

Lake, J.A. (1988) Origin of the eukaryotic nucleus determined by rate-invariant analysis of rRNA sequences. *Nature*, **331**, 184-186.

Lee, M.H., Chang, Y.C., Hong, E.L., Grubb, J., Chang, C.S., Bishop, D.K. and Wang, T.F. (2005) Calcium ion promotes yeast Dmc1 activity via formation of long and fine helical filaments with single-stranded DNA. *J Biol Chem*, **280**, 40980-40984.

Li, Z., Golub, E.I., Gupta, R. and Radding, C.M. (1997) Recombination activities of HsDmc1 protein, the meiotic human homolog of RecA protein. *Proc Natl Acad Sci U S A*, **94**, 11221-11226.

Lichten, M. and Goldman, A.S. (1995) Meiotic recombination hotspots. *Annu Rev Genet*, **29**, 423-444.

Lim, D.S. and Hasty, P. (1996) A mutation in mouse rad51 results in an early embryonic lethal that is suppressed by a mutation in p53. *Mol Cell Biol*, **16**, 7133-7143.

Lio, Y.C., Mazin, A.V., Kowalczykowski, S.C. and Chen, D.J. (2003) Complex formation by the human Rad51B and Rad51C DNA repair proteins and their activities in vitro. *J Biol Chem*, **278**, 2469-2478.

Little, J.W., Edmiston, S.H., Pacelli, L.Z. and Mount, D.W. (1980) Cleavage of the Escherichia coli lexA protein by the recA protease. *Proc Natl Acad Sci U S A*, **77**, 3225-3229.

Liu, J., Xu, L., Sandler, S.J. and Marians, K.J. (1999) Replication fork assembly at recombination intermediates is required for bacterial growth. *Proc Natl Acad Sci U S A*, **96**, 3552-3555.

Liu, L., Maguire, K.K. and Kmiec, E.B. (2004a) Genetic re-engineering of Saccharomyces cerevisiae RAD51 leads to a significant increase in the frequency of gene repair in vivo. *Nucleic Acids Res*, **32**, 2093-2101.

Liu, N., Lamerdin, J.E., Tebbs, R.S., Schild, D., Tucker, J.D., Shen, M.R., Brookman, K.W., Siciliano, M.J., Walter, C.A., Fan, W., Narayana, L.S., Zhou, Z.Q., Adamson, A.W., Sorensen, K.J., Chen, D.J., Jones, N.J. and Thompson, L.H. (1998) XRCC2 and XRCC3, new human Rad51-family members, promote chromosome stability and protect against DNA cross-links and other damages. *Mol Cell*, **1**, 783-793.

Liu, Y., Masson, J.Y., Shah, R., O'Regan, P. and West, S.C. (2004b) RAD51C is required for Holliday junction processing in mammalian cells. *Science*, **303**, 243-246.

Liu, Y. and West, S.C. (2004) Happy Hollidays: 40th anniversary of the Holliday junction. *Nat Rev Mol Cell Biol*, **5**, 937-944.

Lloyd, R.G. and Buckman, C. (1985) Identification and genetic analysis of sbcC mutations in commonly used recBC sbcB strains of Escherichia coli K-12. *J Bacteriol*, **164**, 836-844.

Lloyd, R.G. and K.B. Low, Homologous recombination, in Escherichia coli and Salmonella: cellular and molecular biology, F.C. Neidhardt, et al., Editors. 1996, ASM Press: Washington, D.C. p. 2236-2255. Lovett, S.T. and Mortimer, R.K.

Lusetti, S.L., Drees, J.C., Stohl, E.A., Seifert, H.S. and Cox, M.M. (2004) The DinI and RecX proteins are competing modulators of RecA function. *J Biol Chem*, **279**, 55073-55079.

Lusetti, S.L., Hobbs, M.D., Stohl, E.A., Chitteni-Pattu, S., Inman, R.B., Seifert, H.S. and Cox, M.M. (2006) The RecF protein antagonizes RecX function via direct interaction. *Mol Cell*, **21**, 41-50.

Lydeard, J.R., Jain, S., Yamaguchi, M. and Haber, J.E. (2007) Break-induced replication and telomerase-independent telomere maintenance require Pol32. *Nature*, **448**, 820-823.

Masson, J.Y., Davies, A.A., Hajibagheri, N., Van Dyck, E., Benson, F.E., Stasiak, A.Z., Stasiak, A. and West, S.C. (1999) The meiosis-specific recombinase hDmc1 forms ring structures and interacts with hRad51. *Embo J*, **18**, 6552-6560.

Masson, J.Y., Stasiak, A.Z., Stasiak, A., Benson, F.E. and West, S.C. (2001) Complex formation by the human RAD51C and XRCC3 recombination repair proteins. *Proc Natl Acad Sci U S A*, **98**, 8440-8446.

McGlynn, P., Al-Deib, A.A., Liu, J., Marians, K.J. and Lloyd, R.G. (1997) The DNA replication protein PriA and the recombination protein RecG bind D-loops. *J Mol Biol*, **270**, 212-221.

Meselson, M.S. and Radding, C.M. (1974) A General Model for Genetic Recombination. *Proceedings of the National Academy of Science USA*, **72**, 358-361.

Modesti, M., Ristic, D., van der Heijden, T., Dekker, C., van Mameren, J., Peterman, E.J., Wuite, G.J., Kanaar, R. and Wyman, C. (2007) Fluorescent human RAD51 reveals multiple nucleation sites and filament segments tightly associated along a single DNA molecule. *Structure*, **15**, 599-609.

Morimatsu, K. and Kowalczykowski, S.C. (2003) RecFOR proteins load RecA protein onto gapped DNA to accelerate DNA strand exchange: a universal step of recombinational repair. *Mol Cell*, **11**, 1337-1347.

Mortier-Barriere, I., Velten, M., Dupaigne, P., Mirouze, N., Pietrement, O., McGovern, S., Fichant, G., Martin, B., Noirot, P., Le Cam, E., Polard, P. and Claverys, J.P. (2007) A Key Presynaptic Role in Transformation for a Widespread Bacterial Protein: DprA Conveys Incoming ssDNA to RecA. *Cell*, **130**, 824-836.

Moynahan, M.E., Chiu, J.W., Koller, B.H. and Jasin, M. (1999) Brca1 controls homology-directed DNA repair. *Mol Cell*, **4**, 511-518.

Moynahan, M.E., Cui, T.Y. and Jasin, M. (2001) Homology-directed dna repair, mitomycin-c resistance, and chromosome stability is restored with correction of a Brca1 mutation. *Cancer Res*, **61**, 4842-4850.

Mueller, J.E., Kemper, B., Cunningham, R.P., Kallenbach, N.R. and Seeman, N.C. (1988) T4 endonuclease VII cleaves the crossover strands of Holliday junction analogs. *Proc Natl Acad Sci U S A*, **85**, 9441-9445.

Neitz, M. and Carbon, J. (1987) Characterization of a centromere-linked recombination hot spot in Saccharomyces cerevisiae. *Mol Cell Biol*, **7**, 3871-3879.

New, J.H., Sugiyama, T., Zaitseva, E. and Kowalczykowski, S.C. (1998) Rad52 protein stimulates DNA strand exchange by Rad51 and replication protein A. *Nature*, **391**, 407-410.

Nishino, T., Komori, K., Ishino, Y. and Morikawa, K. (2001) Dissection of the regional roles of the archaeal Holliday junction resolvase Hjc by structural and mutational analyses. *J Biol Chem*, **276**, 35735-35740.

Noirot, P., Gupta, R.C., Radding, C.M. and Kolodner, R.D. (2003) Hallmarks of homology recognition by RecA-like recombinases are exhibited by the unrelated Escherichia coli RecT protein. *Embo J*, **22**, 324-334.

Noll, K.M. and Wolfe, R.S. (1986) Component C of the methylcoenzyme M methylreductase system contains bound 7-mercaptoheptanoylthreonine phosphate (HS-HTP). *Biochem Biophys Res Commun*, **139**, 889-895.

Norais, C., Hawkins, M., Hartman, A.L., Eisen, J.A., Myllykallio, H. and Allers, T. (2007) Genetic and physical mapping of DNA replication origins in *Haloferax volcanii*. *PLoS Genetics*, **3**, e77.

O'Regan, P., Wilson, C., Townsend, S. and Thacker, J. (2001) XRCC2 is a nuclear RAD51-like protein required for damage-dependent RAD51 focus formation without the need for ATP binding. *J Biol Chem*, **276**, 22148-22153.

Ogawa, T., Yu, X., Shinohara, A. and Egelman, E.H. (1993) Similarity of the yeast RAD51 filament to the bacterial RecA filament. *Science*, **259**, 1896-1899.

Orr-Weaver, T.L. and Szostak, J.W. (1983) Yeast recombination: the association between double-strand gap repair and crossing-over. *Proc Natl Acad Sci U S A*, **80**, 4417-4421.

Ortenberg, R., Rozenblatt-Rosen, O. and Mevarech, M. (2000) The extremely halophilic archaeon Haloferax volcanii has two very different dihydrofolate reductases. *Mol Microbiol*, **35**, 1493-1505.

Paques, F. and Haber, J.E. (1999) Multiple pathways of recombination induced by double-strand breaks in Saccharomyces cerevisiae. *Microbiol Mol Biol Rev*, **63**, 349-404.

Parsons, C.A., Stasiak, A., Bennett, R.J. and West, S.C. (1995) Structure of a multisubunit complex that promotes DNA branch migration. *Nature*, **374**, 375-378.

Passy, S.I., Yu, X., Li, Z., Radding, C.M., Masson, J.Y., West, S.C. and Egelman, E.H. (1999) Human Dmc1 protein binds DNA as an octameric ring. *Proc Natl Acad Sci U S A*, **96**, 10684-10688.

Patel, K.J., Yu, V.P., Lee, H., Corcoran, A., Thistlethwaite, F.C., Evans, M.J., Colledge, W.H., Friedman, L.S., Ponder, B.A. and Venkitaraman, A.R. (1998) Involvement of Brca2 in DNA repair. *Mol Cell*, **1**, 347-357.

Petalcorin, M.I., Galkin, V.E., Yu, X., Egelman, E.H. and Boulton, S.J. (2007) Stabilization of RAD-51-DNA filaments via an interaction domain in Caenorhabditis elegans BRCA2. *Proc Natl Acad Sci U S A*, **104**, 8299-8304.

Petalcorin, M.I., Sandall, J., Wigley, D.B. and Boulton, S.J. (2006) CeBRC-2 stimulates D-loop formation by RAD-51 and promotes DNA single-strand annealing. *J Mol Biol*, **361**, 231-242.

Petukhova, G., Sung, P. and Klein, H. (2000) Promotion of Rad51-dependent D-loop formation by yeast recombination factor Rdh54/Tid1. *Genes Dev*, **14**, 2206-2215.

Petukhova, G.V., Pezza, R.J., Vanevski, F., Ploquin, M., Masson, J.Y. and Camerini-Otero, R.D. (2005) The Hop2 and Mnd1 proteins act in concert with Rad51 and Dmc1 in meiotic recombination. *Nat Struct Mol Biol*, **12**, 449-453.

Pittman, D.L., Cobb, J., Schimenti, K.J., Wilson, L.A., Cooper, D.M., Brignull, E., Handel, M.A. and Schimenti, J.C. (1998a) Meiotic prophase arrest with failure of chromosome synapsis in mice deficient for Dmc1, a germline-specific RecA homolog. *Mol Cell*, **1**, 697-705.

Pittman, D.L., Weinberg, L.R. and Schimenti, J.C. (1998b) Identification, characterization, and genetic mapping of Rad51d, a new mouse and human RAD51/RecA-related gene. *Genomics*, **49**, 103-111.

Plessis, A. and Dujon, B. (1993) Multiple tandem integrations of transforming DNA sequences in yeast chromosomes suggest a mechanism for integrative transformation by homologous recombination. *Gene*, **134**, 41-50.

Prangishvilli, D., Zillig, W., Gierl, A., Biesert, L. and Holz, I. (1982) DNA-dependent RNA polymerase of thermoacidophilic archaebacteria. *Eur J Biochem*, **122**, 471-477.

Puhler, G., Leffers, H., Gropp, F., Palm, P., Klenk, H.P., Lottspeich, F., Garrett, R.A. and Zillig, W. (1989) Archaebacterial DNA-dependent RNA polymerases testify to the evolution of the eukaryotic nuclear genome. *Proc Natl Acad Sci U S A*, **86**, 4569-4573.

Radding, C.M. (1991) Helical interactions in homologous pairing and strand exchange driven by RecA protein. *J Biol Chem*, **266**, 5355-5358.

Rao, B.J., Chiu, S.K. and Radding, C.M. (1993) Homologous recognition and triplex formation promoted by RecA protein between duplex oligonucleotides and single-stranded DNA. *J Mol Biol*, **229**, 328-343.

Rao, B.J., Jwang, B. and Dutreix, M. (1991) Production of triple-stranded recombination intermediates by RecA protein, in vitro. *Biochimie*, **73**, 363-370.

Rao, B.J. and Radding, C.M. (1993) Homologous recognition promoted by RecA protein via non-Watson-Crick bonds between identical DNA strands. *Proc Natl Acad Sci U S A*, **90**, 6646-6650.

Rashid, N., Morikawa, M. and Imanaka, T. (1996) A RecA/RAD51 homologue from a hyperthermophilic archaeon retains the major RecA domain only. *Mol Gen Genet*, **253**, 397-400.

Rashid, N., Morikawa, M., Kanaya, S., Atomi, H. and Imanaka, T. (1999) A unique DNase activity shares the active site with ATPase activity of the RecA/Rad51 homologue (Pk-REC) from a hyperthermophilic archaeon. *FEBS Lett*, **445**, 111-114.

Rashid, N., Morikawa, M., Nagahisa, K., Kanaya, S. and Imanaka, T. (1997) Characterization of a RecA/RAD51 homologue from the hyperthermophilic archaeon Pyrococcus sp. KOD1. *Nucleic Acids Res*, **25**, 719-726.

Reeve, J.N. (2003) Archaeal chromatin and transcription. *Mol Microbiol*, **48**, 587-598.

Register, J.C., 3rd and Griffith, J. (1985) The direction of RecA protein assembly onto single strand DNA is the same as the direction of strand assimilation during strand exchange. *J Biol Chem*, **260**, 12308-12312.

Reich, C.I., McNeil, L.K., Brace, J.L., Brucker, J.K. and Olsen, G.J. (2001) Archaeal RecA homologues: different response to DNA-damaging agents in mesophilic and thermophilic Archaea. *Extremophiles*, **5**, 265-275.

Resnick, M.A. (1976) The repair of double-strand breaks in DNA; a model involving recombination. *J Theor Biol*, **59**, 97-106.

Rockmill, B., Sym, M., Scherthan, H. and Roeder, G.S. (1995) Roles for two RecA homologs in promoting meiotic chromosome synapsis. *Genes Dev*, **9**, 2684-2695.

Roman, L.J. and Kowalczykowski, S.C. (1986) Relationship of the physical and enzymatic properties of Escherichia coli recA protein to its strand exchange activity. *Biochemistry*, **25**, 7375-7385.

Saeki, T., Machida, I. and Nakai, S. (1980) Genetic control of diploid recovery after gamma-irradiation in the yeast Saccharomyces cerevisiae. *Mutat Res*, **73**, 251-265.

Sandler, S.J., Hugenholtz, P., Schleper, C., DeLong, E.F., Pace, N.R. and Clark, A.J. (1999) Diversity of radA genes from cultured and uncultured archaea: comparative analysis of putative RadA proteins and their use as a phylogenetic marker. *J Bacteriol*, **181**, 907-915.

Sandler, S.J., Satin, L.H., Samra, H.S. and Clark, A.J. (1996) recA-like genes from three archaean species with putative protein products similar to Rad51 and Dmc1 proteins of the yeast Saccharomyces cerevisiae. *Nucleic Acids Res*, **24**, 2125-2132.

Sanger, F., Nicklen, S. and Coulson, A.R. (1977) DNA sequencing with chain-terminating inhibitors. *Proc Natl Acad Sci U S A*, **74**, 5463-5467.

Schild, D., Lio, Y.C., Collins, D.W., Tsomondo, T. and Chen, D.J. (2000) Evidence for simultaneous protein interactions between human Rad51 paralogs. *J Biol Chem*, **275**, 16443-16449.

Schmid, G. and Bock, A. (1981) Immunological comparison of ribosomal proteins from archaebacteria. *J Bacteriol*, **147**, 282-288.

Schnabel, R., Thomm, M., Gerardy-Schahn, R., Zillig, W., Stetter, K.O. and Huet, J. (1983) Structural homology between different archaebacterial DNA-dependent RNA polymerases analyzed by immunological comparison of their components. *Embo J*, **2**, 751-755.

Schwacha, A. and Kleckner, N. (1994) Identification of joint molecules that form frequently between homologs but rarely between sister chromatids during yeast meiosis. *Cell*, **76**, 51-63.

Scully, R., Chen, J., Plug, A., Xiao, Y., Weaver, D., Feunteun, J., Ashley, T. and Livingston, D.M. (1997) Association of BRCA1 with Rad51 in mitotic and meiotic cells. *Cell*, **88**, 265-275.

Sehorn, M.G., Sigurdsson, S., Bussen, W., Unger, V.M. and Sung, P. (2004) Human meiotic recombinase Dmc1 promotes ATP-dependent homologous DNA strand exchange. *Nature*, **429**, 433-437.

Seitz, E.M., Brockman, J.P., Sandler, S.J., Clark, A.J. and Kowalczykowski, S.C. (1998) RadA protein is an archaeal RecA protein homolog that catalyzes DNA strand exchange. *Genes Dev*, **12**, 1248-1253.

Sharan, S.K. and Kuznetsov, S.G. (2007) Resolving RAD51C function in late stages of homologous recombination. *Cell Div*, **2**, 15.

Sharan, S.K., Pyle, A., Coppola, V., Babus, J., Swaminathan, S., Benedict, J., Swing, D., Martin, B.K., Tessarollo, L., Evans, J.P., Flaws, J.A. and Handel, M.A. (2004) BRCA2 deficiency in mice leads to meiotic impairment and infertility. *Development*, **131**, 131-142.

Sharples, G.J. (2001) The X philes: structure-specific endonucleases that resolve Holliday junctions. *Mol Microbiol*, **39**, 823-834.

Shen, P. and Huang, H.V. (1986) Homologous recombination in Escherichia coli: dependence on substrate length and homology. *Genetics*, **112**, 441-457.

Shibata, T., DasGupta, C., Cunningham, R.P. and Radding, C.M. (1979) Purified Escherichia coli recA protein catalyzes homologous pairing of superhelical DNA and single-stranded fragments. *Proc Natl Acad Sci U S A*, **76**, 1638-1642.

Shim, K.S., Schmutte, C., Tombline, G., Heinen, C.D. and Fishel, R. (2004) hXRCC2 enhances ADP/ATP processing and strand exchange by hRAD51. *J Biol Chem*, **279**, 30385-30394.

Shin, D.S., Chahwan, C., Huffman, J.L. and Tainer, J.A. (2004) Structure and function of the double-strand break repair machinery. *DNA Repair (Amst)*, **3**, 863-873.

Shin, D.S., Pellegrini, L., Daniels, D.S., Yelent, B., Craig, L., Bates, D., Yu, D.S., Shivji, M.K., Hitomi, C., Arvai, A.S., Volkmann, N., Tsuruta, H., Blundell, T.L., Venkitaraman, A.R.

and Tainer, J.A. (2003) Full-length archaeal Rad51 structure and mutants: mechanisms for RAD51 assembly and control by BRCA2. *Embo J*, **22**, 4566-4576.

Shinohara, A., Ogawa, H. and Ogawa, T. (1992) Rad51 protein involved in repair and recombination in S. cerevisiae is a RecA-like protein. *Cell*, **69**, 457-470.

Shinohara, A., Shinohara, M., Ohta, T., Matsuda, S. and Ogawa, T. (1998) Rad52 forms ring structures and co-operates with RPA in single-strand DNA annealing. *Genes Cells*, **3**, 145-156.

Shinohara, M., Shita-Yamaguchi, E., Buerstedde, J.M., Shinagawa, H., Ogawa, H. and Shinohara, A. (1997) Characterization of the roles of the Saccharomyces cerevisiae RAD54 gene and a homologue of RAD54, RDH54/TID1, in mitosis and meiosis. *Genetics*, **147**, 1545-1556.

Siaud, N., Dray, E., Gy, I., Gerard, E., Takvorian, N. and Doutriaux, M.P. (2004) Brca2 is involved in meiosis in Arabidopsis thaliana as suggested by its interaction with Dmc1. *Embo J*, **23**, 1392-1401.

Sigal, N. and Alberts, B. (1971) Genetic Recombination : The Nature of a Crosssed Strand-exchange between Two Homologous DNA Molecules. *Journal of Molecular Biology*, **71**, 789-793.

Sigurdsson, S., Van Komen, S., Bussen, W., Schild, D., Albala, J.S. and Sung, P. (2001) Mediator function of the human Rad51B-Rad51C complex in Rad51/RPA-catalyzed DNA strand exchange. *Genes Dev*, **15**, 3308-3318.

Singleton, M.R., Dillingham, M.S., Gaudier, M., Kowalczykowski, S.C. and Wigley, D.B. (2004) Crystal structure of RecBCD enzyme reveals a machine for processing DNA breaks. *Nature*, **432**, 187-193.

Smith, J. and Rothstein, R. (1999) An allele of RFA1 suppresses RAD52-dependent double-strand break repair in Saccharomyces cerevisiae. *Genetics*, **151**, 447-458.

Soppa, J. (2001) Basal and regulated transcription in archaea. *Adv Appl Microbiol*, **50**, 171-217.

Spies, M., Dillingham, M.S. and Kowalczykowski, S.C. (2005) Translocation by the RecB motor is an absolute requirement for {chi}-recognition and RecA protein loading by RecBCD enzyme. *J Biol Chem*, **280**, 37078-37087.

Stahl, F.W. (1994) The Holliday junction on its thirtieth anniversary. *Genetics*, **138**, 241-246.

Stasiak, A.Z., Larquet, E., Stasiak, A., Muller, S., Engel, A., Van Dyck, E., West, S.C. and Egelman, E.H. (2000) The human Rad52 protein exists as a heptameric ring. *Curr Biol*, **10**, 337-340.

Sugawara, N., Wang, X. and Haber, J.E. (2003) In vivo roles of Rad52, Rad54, and Rad55 proteins in Rad51-mediated recombination. *Mol Cell*, **12**, 209-219.

Sugiyama, T., Kantake, N., Wu, Y. and Kowalczykowski, S.C. (2006) Rad52-mediated DNA annealing after Rad51-mediated DNA strand exchange promotes second ssDNA capture. *Embo J*, **25**, 5539-5548.

Sugiyama, T., Zaitseva, E.M. and Kowalczykowski, S.C. (1997) A single-stranded DNA-binding protein is needed for efficient presynaptic complex formation by the Saccharomyces cerevisiae Rad51 protein. *J Biol Chem*, **272**, 7940-7945.

Sun, H., Treco, D., Schultes, N.P. and Szostak, J.W. (1989) Double-strand breaks at an initiation site for meiotic gene conversion. *Nature*, **338**, 87-90.

Sun, J.Z., Julin, D.A. and Hu, J.S. (2006) The nuclease domain of the Escherichia coli RecBCD enzyme catalyzes degradation of linear and circular single-stranded and double-stranded DNA. *Biochemistry*, **45**, 131-140.

Sung, P. (1997a) Function of yeast Rad52 protein as a mediator between replication protein A and the Rad51 recombinase. *J Biol Chem*, **272**, 28194-28197.

Sung, P. (1997b) Yeast Rad55 and Rad57 proteins form a heterodimer that functions with replication protein A to promote DNA strand exchange by Rad51 recombinase. *Genes Dev*, **11**, 1111-1121.

Sung, P. and Robberson, D.L. (1995) DNA strand exchange mediated by a RAD51-ssDNA nucleoprotein filament with polarity opposite to that of RecA. *Cell*, **82**, 453-461.

Symington, L.S. (2002) Role of RAD52 epistasis group genes in homologous recombination and double-strand break repair. *Microbiol Mol Biol Rev*, **66**, 630-670, table of contents.

Szostak, J.W., Orr-Weaver, T.L., Rothstein, R.J. and Stahl, F.W. (1983) The double-strand-break repair model for recombination. *Cell*, **33**, 25-35.

Takata, M., Sasaki, M.S., Sonoda, E., Fukushima, T., Morrison, C., Albala, J.S., Swagemakers, S.M., Kanaar, R., Thompson, L.H. and Takeda, S. (2000) The Rad51 paralog Rad51B promotes homologous recombinational repair. *Mol Cell Biol*, **20**, 6476-6482.

Takata, M., Sasaki, M.S., Tachiiri, S., Fukushima, T., Sonoda, E., Schild, D., Thompson, L.H. and Takeda, S. (2001) Chromosome instability and defective recombinational repair in knockout mutants of the five Rad51 paralogs. *Mol Cell Biol*, **21**, 2858-2866.

Tang, X.F., Shen, Y., Matsui, E. and Matsui, I. (2004) Domain topology of the DNA polymerase D complex from a hyperthermophilic archaeon Pyrococcus horikoshii. *Biochemistry*, **43**, 11818-11827.

Tarsounas, M., Munoz, P., Claas, A., Smiraldo, P.G., Pittman, D.L., Blasco, M.A. and West, S.C. (2004) Telomere maintenance requires the RAD51D recombination/repair protein. *Cell*, **117**, 337-347.

Taylor, A.F. and Smith, G.R. (1985) Substrate specificity of the DNA unwinding activity of the RecBC enzyme of Escherichia coli. *J Mol Biol*, **185**, 431-443.

Taylor, A.F. and Smith, G.R. (1995) Strand specificity of nicking of DNA at Chi sites by RecBCD enzyme. Modulation by ATP and magnesium levels. *J Biol Chem*, **270**, 24459-24467.

Taylor, A.F. and Smith, G.R. (2003) RecBCD enzyme is a DNA helicase with fast and slow motors of opposite polarity. *Nature*, **423**, 889-893.

Thompson, J.D., Higgins, D.G. and Gibson, T.J. (1994) CLUSTAL W: improving the sensitivity of progressive multiple sequence alignment through sequence weighting, position-specific gap penalties and weight matrix choice. *Nucleic Acids Res*, **22**, 4673-4680.

Tsukamoto, M., Yamashita, K., Miyazaki, T., Shinohara, M. and Shinohara, A. (2003) The N-terminal DNA-binding domain of Rad52 promotes RAD51-independent recombination in Saccharomyces cerevisiae. *Genetics*, **165**, 1703-1715.

Uemori, T., Sato, Y., Kato, I., Doi, H. and Ishino, Y. (1997) A novel DNA polymerase in the hyperthermophilic archaeon, Pyrococcus furiosus: gene cloning, expression, and characterization. *Genes Cells*, **2**, 499-512.

Umezu, K., Chi, N.W. and Kolodner, R.D. (1993) Biochemical interaction of the Escherichia coli RecF, RecO, and RecR proteins with RecA protein and single-stranded DNA binding protein. *Proc Natl Acad Sci U S A*, **90**, 3875-3879.

Wadsworth, R.I. and White, M.F. (2001) Identification and properties of the crenarchaeal single-stranded DNA binding protein from Sulfolobus solfataricus. *Nucleic Acids Res*, **29**, 914-920.

Ward, J.D., Barber, L.J., Petalcorin, M.I., Yanowitz, J. and Boulton, S.J. (2007) Replication blocking lesions present a unique substrate for homologous recombination. *Embo J*, **26**, 3384-3396.

Webb, B.L., Cox, M.M. and Inman, R.B. (1997) Recombinational DNA repair: the RecF and RecR proteins limit the extension of RecA filaments beyond single-strand DNA gaps. *Cell*, **91**, 347-356.

Weinert, B.T. and Rio, D.C. (2007) DNA strand displacement, strand annealing and strand swapping by the Drosophila Bloom's syndrome helicase. *Nucleic Acids Res*, **35**, 1367-1376.

West, S.C. (1997) Processing of recombination intermediates by the RuvABC proteins. *Annu Rev Genet*, **31**, 213-244.

Whittaker, R.H. (1959) On the broad classification of organisms. *Q Rev Biol*, **34**, 210-226.

Whittaker, R.H. and Margulis, L. (1978) Protist classification and the kingdoms of organisms. *Biosystems*, **10**, 3-18.

Williams, E., Lowe, T.M., Savas, J. and DiRuggiero, J. (2007) Microarray analysis of the hyperthermophilic archaeon Pyrococcus furiosus exposed to gamma irradiation. *Extremophiles*, **11**, 19-29.

Witkin, E.M. (1969) The mutability toward ultraviolet light of recombination-deficient strains of Escherichia coli. *Mutat Res*, **8**, 9-14.

Woese, C.R. (1987) Bacterial evolution. *Microbiol Rev*, **51**, 221-271.

Woese, C.R. and Fox, G.E. (1977) Phylogenetic structure of the prokaryotic domain: the primary kingdoms. *Proc Natl Acad Sci U S A*, **74**, 5088-5090.

Woese, C.R., Kandler, O. and Wheelis, M.L. (1990) Towards a natural system of organisms: proposal for the domains Archaea, Bacteria, and Eucarya. *Proc Natl Acad Sci U S A*, **87**, 4576-4579.

Woese, C.R. and Olsen, G.J. (1986) Archaebacterial phylogeny: perspectives on the urkingdoms. *Syst Appl Microbiol*, **7**, 161-177.

Wolner, B., van Komen, S., Sung, P. and Peterson, C.L. (2003) Recruitment of the recombinational repair machinery to a DNA double-strand break in yeast. *Mol Cell*, **12**, 221-232.

Wong, A.K., Pero, R., Ormonde, P.A., Tavtigian, S.V. and Bartel, P.L. (1997) RAD51 interacts with the evolutionarily conserved BRC motifs in the human breast cancer susceptibility gene brca2. *J Biol Chem*, **272**, 31941-31944.

Woods, W.G. and Dyall-Smith, M.L. (1997) Construction and analysis of a recombination-deficient (radA) mutant of Haloferax volcanii. *Mol Microbiol*, **23**, 791-797.

Wu, Y., He, Y., Moya, I.A., Qian, X. and Luo, Y. (2004) Crystal structure of archaeal recombinase RADA: a snapshot of its extended conformation. *Mol Cell*, **15**, 423-435.

Xu, X., Weaver, Z., Linke, S.P., Li, C., Gotay, J., Wang, X.W., Harris, C.C., Ried, T. and Deng, C.X. (1999) Centrosome amplification and a defective G2-M cell cycle checkpoint induce genetic instability in BRCA1 exon 11 isoform-deficient cells. *Mol Cell*, **3**, 389-395.

Yang, H., Li, Q., Fan, J., Holloman, W.K. and Pavletich, N.P. (2005) The BRCA2 homologue Brh2 nucleates RAD51 filament formation at a dsDNA-ssDNA junction. *Nature*, **433**, 653-657.

Yeeles, J.T. and Dillingham, M.S. (2007) A dual-nuclease mechanism for DNA break processing by AddAB-type helicase-nucleases. *J Mol Biol*, **371**, 66-78.

Yokoyama, H., Sarai, N., Kagawa, W., Enomoto, R., Shibata, T., Kurumizaka, H. and Yokoyama, S. (2004) Preferential binding to branched DNA strands and strand-annealing activity of the human Rad51B, Rad51C, Rad51D and Xrcc2 protein complex. *Nucleic Acids Res*, **32**, 2556-2565.

Yoshida, K., Kondoh, G., Matsuda, Y., Habu, T., Nishimune, Y. and Morita, T. (1998) The mouse RecA-like gene Dmc1 is required for homologous chromosome synapsis during meiosis. *Mol Cell*, **1**, 707-718.

Yu, M., Souaya, J. and Julin, D.A. (1998) The 30-kDa C-terminal domain of the RecB protein is critical for the nuclease activity, but not the helicase activity, of the RecBCD enzyme from Escherichia coli. *Proc Natl Acad Sci U S A*, **95**, 981-986.

Yu, V.P., Koehler, M., Steinlein, C., Schmid, M., Hanakahi, L.A., van Gool, A.J., West, S.C. and Venkitaraman, A.R. (2000) Gross chromosomal rearrangements and genetic exchange between nonhomologous chromosomes following BRCA2 inactivation. *Genes Dev*, **14**, 1400-1406.

Zahradka, K., Slade, D., Bailone, A., Sommer, S., Averbeck, D., Petranovic, M., Lindner, A.B. and Radman, M. (2006) Reassembly of shattered chromosomes in Deinococcus radiodurans. *Nature*, **443**, 569-573.

Zillig, W., Stetter, K.O. and Janekovic, D. (1979) DNA-dependent RNA polymerase from the archaebacterium Sulfolobus acidocaldarius. *Eur J Biochem*, **96**, 597-604.